PN-ACS-356
M18-054

# Transboundary Air-Quality Effects from Urbanization

11941Y

Report No. 2

for the period of

March 2001-August 2002

Award No.: M18-054

prepared by

Prof. R. Bornstein

San Jose State University (SJSU)
San Jose, CA, USA

Prof. Jamal Safi and Dr. Yasser El-Nahhal

Environmental Protection Research Institute (EPRI)
Gaza City, Palestinian Territories

Prof. Jad Isaac and Mr. Khaldoun Rishmawi

Applied Research Institute–Jerusalem (ARIJ)
Bethlehem, Palestinian Territories

Prof. Menachem Luria, Prof. Yitzhak Mahrer,
Dr. Dean Ranmar, and Mr. Erez Weinroth

Hebrew University of Jerusalem (HUJI)
Jerusalem and Rehovot, Israel

RECEIVED
MAR 06 2003
Per.....

September 2002

Table of contents


| Section | Page |
|---|---|
| I. Technical Progress | 3 |
| A. Research Objectives | 3 |
| B. Research Accomplishments | 4 |
| C. Scientific Impacts | 8 |
| D. Project Impacts | 12 |
| E. Strengthening Institutions | 13 |
| F. Future Work | 15 |
| II. Management and Cooperation | 18 |
| A. Managerial | 18 |
| B. Special Concerns | 19 |
| C. Cooperation, Travel, Training, and Publication | 19 |
| D. Requests for USAID Actions | 28 |
| E. List of support documentation | 28 |

Appendices

A. ARIJ contributions
B. EPRI contributions
C. Ali Rahmah (ARIJ) Ph.D. work to date at DRI
D. Dean Ranmar (HUJI) Ph.D. thesis
E. Erez Weinroth (HUJI) Ph.D. thesis work to date
F. Ramar et al. (2002a,b) journal article page proofs
G. Bornstein et al. (2003a,b) and Weinroth (2002) submitted conference abstracts
H. Bornstein et al. (2001a,b, 2002) preprint volume papers

## I. Technical Progress

### A. Research Objectives

The overall aim of the proposed effort is to generate the information required by government planning agencies in Israel and West Bank/Gaza to develop strategies for the socially and environmentally sustainable development of their coastal areas.

The four main specific research objectives instrumental to achievement of the above overall aim (as stated in the original proposal) are:

**Statement of Objective 1: Data Bases**

The main objectives of this task are: (1) installation of three new environmental monitoring sites in Gaza and the West Bank and (2) preparation of a comprehensive environmental data base and climatology of the study area.

**Statement of Objective 2: Field Studies**

The main objective of this task is the execution of short-term intensive field observational campaigns during meteorological conditions producing poor regional air quality. Such campaigns should involve measurement of both meteorological and air quality parameters by Israeli and Palestinian scientists and students.

**Statement of Objective 3: Modeling Current Conditions**

The main objective of this task is the adaptation and application of appropriate meteorological and air quality model to the study area to increase understanding of air quality problems associated with current levels of regional urbanization. Meteorological, air quality, geographic, and emission data collected to satisfy Objectives 1 and 2 will be used to initialize and evaluate the accuracy of these simulations of current emission patterns. Verification of model results against available meteorology-

ical and air quality data will provide confidence limits of the ability of the selected models to carry out the planning simulations using input based on a variety of possible development strategies.

**Statement of Objective 4: Modeling Possible Future Conditions**

The main objective of this task is the simulation of possible future regional meteorological and air quality patterns using validated models of Objective 3. The models will be applied to a variety of potential urban growth and emission scenarios associated with various urban/industrial development plans supplied by government planning agencies. Results will aid governmental development agencies concerned with regional air quality trends of societal (health and economic) air pollution impacts.

## B. Research Accomplishments

Additional progress has been made since the first Report in March 2001 towards achievement of the overall aim of the proposed effort: generation of information required by government planning agencies in Israel and West Bank/Gaza for planning the socially and environmentally sustainable urbanization/industrialization of their coastal areas. Additional progress has been achieved in each of the four specific research objectives instrumental for the achievement of the above overall aim, as follows:

### B.1. Accomplishments for Objective 1: Data Bases

**B-1.a With respect to the new environmental monitoring sites for Gaza and the West Bank,** the following has been accomplished:

1. The instruments have remained in storage at the HUJI
2. As Palestinian technicians were unable to train at HUJI for the technical skills necessary to install and operate them at the approved West Bank/Gaza sites, arrangements were made to bring three technicians to the US to obtain training at a week-long EPA sponsored course

at Rutgers University. The first attempt in March 2002 was unsuccessful, as the waiting period for visas in Israel was increased and they thus could not be issued in time for any of the three technicians. The second attempt in July 2002 was only partly successful, as the waiting period was again increased. Only one of the three (Dr. Yasser El-Nahhal of EPRI) was thus able to attend the course. After the course, he came to SJSU for a second week, during which he received practical training in the operation and maintenance of the instruments at a site operated by the Bay Area Air Quality Management District (BAAQMD). He also presented a seminar at SJSU on his research efforts at EPRI.

3. The next version of the EPA class at Rutgers will be held in January or March 2003, and this time the visa process will begin early enough to ensure that the two ARIJ technicians will be able to attend. They will also visit SJSU and the BAAQMD sites.

**B.1.b With respect to preparation of a comprehensive environmental database and climatology of the study area,** the following has been accomplished:

1. The ongoing analysis of the required (for modeling) meteorological, air quality, emissions, and geographic (GIS) parameters was continued as follows:
   a. SPOT satellite images of the West Bank were purchased by ARIJ and GIS analyses carried out
   b. Emission inventories were compiled by EPRI for Gaza, ARIJ for the West Bank, and HUJI for Israel, with techniques, sources, and factors continually updated. Techniques developed at HUJI were shared with the EPRI and ARIJ groups.
2. Data bases were established at EPRI, HUJI and ARIJ, but have not yet been merged.

### B-1.c With respect to the preparation of the climatology of the study area

Discussions have been held with Prof. Uri Dyan of HUJI to publish his project paper (included in Report 1) on the air-pollution climatology of Israel and the Palestinian Territories as a monograph for distribution to air pollution scientists in the Middle East.

## B-2 Accomplishments for Objective 2: Field Studies

With respect to the execution of short-term intensive field observational campaigns during periods conducive to the existence of periods with poor regional air quality, the following were carried out (as discussed in Report 1):

1. Feb 2000: A successful preliminary field observational study was carried out to estimate the flux of pollutants from Gaza into Israel. Results showed that all systems worked properly, and analyzed results have appeared in journal publications.
2. June 2000: Another successful similar preliminary field observational study was carried out to estimate the flux of pollutants from Israel into the West Bank. Again the systems worked well, and these results will also appear in future publications.

The two above preliminary field studies were carried out in preparation for this main study, and collected data are being analyzed by an M.S. student at the HUJI. It has not been possible, however, to carry out the larger study during the last period, and thus it has again been postponed to the next regional ozone period, i.e., June 2003. This final campaign will involve measurements of meteorological and air quality parameters by Israeli and Palestinian scientists and students, as well as by a number of visiting international meteorological and chemical measurement groups who have expressed an interest in joining the study.

## B-3 Accomplishments for Objective 3: Modeling Current Conditions

With respect to the adaptation and application of appropriate meteorological and air quality models to the study area to gain an increased understanding of the air quality problems associated with current levels of regional urbanization, the following has been accomplished since the last report:

1. RAMS and MM5 modeling has been/is being carried out as follows:
    a. Mr. Dean Ranmar, an Israeli student at Prof. Mahrer's Lab at the HUJI, has run RAMS as part of his Ph.D. research effort for the current project. He completed his degree in mid-2002
    b. Mr. Erez Weinroth, an Israeli student at Prof. Luria's Lab at the HUJI, is currently running RAMS as part of his Ph.D effort for the current project. His expected completion is at the end of 2002.
    c. Mr. Ali Abu-Rahmah, an ARIJ Palestinian student at Prof. Gertler Lab at the DRI in Reno, is currently running MM5 as part of his Ph.D. He is supported equally by this project and by DRI, where he also works with Prof. Luria who visits DRI several times a year. His expected completion is at the end of 2005.
2. HYPACT Lagrangian particle modeling: Mr. Dean Ranmar ran it as part of his Ph.D. research to study regional air pollutant transport paths.
3. CAMX photochemical modeling is currently being carried out by
    a. Mr. Abu-Rahmah at DRI as part of his Ph.D. on a project on the impacts of coastal operations on urban scale air quality
    b. Mr. Weinroth at the HUJI as part of his Ph.D. work for the current project.
4. Prof. Bornstein's group at SJSU has continued to work on the urbanization of meteorological models, updating the PAVE graphics package (based on the NCAR package) and

the MAPS statistical evaluation package. The first effort, was carried out by visiting Israeli Post-Doc (Natalie Perlin) has expand the capabilities of MM5 (and will next be applied to RAMS) to better simulate the effects of urban areas on regional flow patters. The latter two packages, supplied by Mr. Jim Wilkinson of Alpine Geophysics, Inc., who is working with the SJSU group, have improved the graphical presentation and statistical evaluation opportunities, respectively, for output fields generated by MM5 (and will next be applied for RAMS) and CAMX. MAPS was expanded under this project, and can now carry out statistical evaluations on arbitrary specified sub-domains. PAVE has likewise been expanded, and is now able to construct vertical cross-sections in arbitrary directions, so that model output can be directly compared to observations. The updated software will be made available to Israeli and West Bank/Gaza scientists through visits to SJSU by Palestinian and Israeli scientists.

### B-4 Objective 4: Modeling Possible Future Conditions

With respect to the final objective (scheduled for final year of project, i.e., simulations of possible future regional meteorological and air quality patterns using the validated models of Objective 3, discussions have been carried out with Dr. Eran Feitelson of HUJI. He is the transportation planner who will identify mechanisms for determination of the emission scenarios to be tested in the models.

## C. Scientific Impact of Cooperation

### 1. During the period of Report 1:

Prof. Bornstein was in Gaza, West bank, and Israel during both February to April 2000 and June to July 2000, during which he met with all project participants and with a number of other Israeli and Palestinian scientists and administrators. He traveled to:

a. EPRI in Gaza to meet with Dr. Safi and his group
b. ARIJ in Bethlehem to meet twice with Dr. Issac and his group and with a representative of the Ministry of the Environment of the Palestinian Authority
c. HUJI in Jerusalem to meet with Dr. Luria and his group
d. HUJI in Rehovat to meet with Dr. Mahrer and his group
e. Tel Aviv University to meet with Dr. Bitan and his group
f. Israel Meteorological Service to meet with Dr. Seter and his group
g. HUJI in Jerusalem to meet with Dr. Feitelson
h. HUJI with a representative of the Israeli Ministry of the Environment.

All of the above groups were represented twice at project meetings at Dr. Luria's Lab at the HUJI, at which the following was discussed:

- project overview
- communication channels
- assignment of prime and secondary responsibilities for each task
- identification of potential students
- project schedules.

**2. Since the period of Report 1**

After Prof. Bornstein's return to SJSU after his Spring-Summer 2000 sabbatical at the HUJI, the following visits have occurred:

a. Mr. Erez Weinroth of HUJI visited ARIJ in late Summer 2000 to discuss emission inventories

b. Mr. Erez Weinroth of HUJI visited SJSU, Prof.. Mark Jacobson at Stanford University, and Mr. Chris Emery of Environ Inc. to study cutting edge photochemical modeling during April-May 2001

c. Dr. Bornstein and a group of his SJSU students visited Prof. Alan Getler of DRI in Fall 2001 to discuss how DRI scientists could work with the current project

d. Mr. Ali Abu-Rahmah of ARIJ thus started his Ph.D. in Atmospheric Sciences at DRI under Profs. Gertler (of DRI) and Luria (of HUJI) in Fall 2001

e. Mr. Ali Abu-Rahmah of ARIJ and DRI visited SJSU to discuss his project efforts in Winter 2001

f. Nidal Abukubie of ARIJ and his wife and two children came to start a M. S. in Meteorology SJSU in May 2002, but family stresses caused him to resign and return to the West bank after a few weeks

g. Dr. Yasser El-Nahhal of EPRI took the week long EPA instrument class at Rutgers and then came to SJSU for a week in July 2002

h. Dr. Jamal Safi of EPRI and his wife visited SJSU for a week in August 2002 to discuss the project

i. Dr. Menachem Luria of the HJUJI and his wife will visit SJSU from DRI for several day at the end of September 2002 to discuss the project

j. Ms. Shoukri Kasakseh of ARIJ has received an I-20 and will start a M. S. in Meteorology SJSU in October 2002

k. Mr. Khalil El_Khateeb of EPRI has received an I-20 and will start a M. S. in Environmental Sciences and GIS at SJSU in October 2002

l. Dr. Jad Isaac of ARIJ and his wife will visit SJSU for a week in October 2002 to discuss the project.

The regional cooperative approach used in this project thus resulted in a series of

- visits in the West Bank and Gaza by U. S. embassy personnel and Prof. Bornstein to select the three new fixed air quality/meteorological observational sites
- telephone contacts between Palestinian and Israeli project scientists after the end the last visit of Prof. Bornstein to the region
- meetings between Palestinian and Israeli project scientists right after the end of the last visit of Prof. Bornstein to the region.

The meetings and conversations focused on

- appropriate measurement site selection, in terms of representative pollutant levels, security, power, and communications, so that the new measured data can be joined with those already collected in Israel
- selection, purchase, and delivery of the US made air quality and meteorological instrumentation for the three new West bank and Gaza sites
- joint efforts on selection of hardware, software, and images for the required regional GIS analyses
- joint activities on development of complete regional pollutant source emission inventories
- joint activities on development and application of regional mesometeorological and photochemical models

- identification of appropriate (with respect to academic background and current interest) Palestinian students, who have/will start graduate studies in English at DRI or SJSU and who will then finish (when possible) at HUJI and Tel Aviv University.

## D. Description of Project Impacts

The above cooperative efforts have the following anticipated regional uses

- The new monitoring sites will provide measurements that can be joined with those already made in Israel to provide the only international environmental monitoring network in the region, with which other neighboring countries could join in the future
- The air quality and meteorological instrumentation for the three new West bank and Gaza sites will provide data for the first international environmental data-base in the region. Other neighboring countries in the region could make use of the data and will be invited in the future to add their measurements to the data
- The GIS hardware, software, and images provide the tools for the first regional land use analyses in the area
- The regional pollutant emission inventories are a first in the region, and again neighboring countries will be invited to add their emission data to the database.
- The meteorological and air quality models provide analysis and planning tools for the future sustainable development of the region, beyond the lifetime of the current project

- The Palestinian and Israeli graduate students who will receive M. S. or Ph.D. degrees as part of this project will provide the core of the photochemical air quality groups involved in future studies in the two areas
- Palestinian and Israeli scientists and students have strengthened old research and personal ties and have formed new ones that should make it possible for them to work together beyond the lifetime of this project.

## E. Strengthening Middle Eastern Institutions

Project investments include:

- Purchase of instrumentation for the three new air quality West Bank and Gaza observational sites, which will provide essential data for the current project and for many future environmental projects in Gaza and the West bank
- Purchase of SPOT images by ARIJ provides essential data for the current project and for future environmental projects in Gaza and the West bank

New research skills include:

- The application of GIS to regional atmospheric studies at ARIJ represents a new application of their extensive environmental GIS background
- Emission inventory construction at the HUJI, EPRI, and ARIJ represents development of a new urban planning skill that will be useful in a variety of future environmental projects
- The visit of HUJI Ph.D. student Erez Weinroth to SJSU, Stanford University, and Environ to study cutting edge photochemical modeling represented the first effort in the study region in this research area

- The Environmental Sciences group at the HUJI (Jerusalem), which has an international reputation in air quality measurements, has had the opportunity to expand its capabilities into photochemical air quality modeling
- The Air Quality Modeling group at the HUJI (Rehovot), which has an international reputation in mesoscale meteorological modeling, has had the opportunity to expand its capabilities into Lagrangian particle modeling
- The September 2001 enrolment of a Palestinian Ph.D. student at DRI and the October 2002 enrolment of two Palestinian students at SJSU will help educate the next generation of Palestinian atmospheric environmental scientists.

Institutional constraints that have been overcome include:

- While both the ARIJ and EPRI groups consist of numerous well-trained (Ph.D.s from the U.S., Canada, Israel, etc.) environmental scientists (with specialties in water quality management, GIS, and biology), both groups are just starting to work in air quality management. During the first phase of the project, senior researchers at EPRI and ARIJ interested in expanding their skills into air quality were identified, as were a number of qualified (based on previous undergraduate achievement) new graduate students.
- Palestinian students expressed some hesitancy at beginning their studies in the Hebrew language, as had been planned in the original proposal. This was overcome by having them begin their studies in English at SJSU.
- An initial hesitancy of the part of the Israeli government to supply specific emission values for industrial sources was overcome by a promise not to identify those sources by name.

- Ever lengthening visa wait periods were overcome by ever earlier submission of applications.

## F. Future Work

### F.1 By Objective

The overall aim of the proposed effort (the generation of information required by government planning agencies in Israel and West Bank/Gaza to develop strategies for the socially and environmentally sustainable development of their coastal areas) will be advanced in the final year of the project. The four main specific research objectives instrumental for the achievement of this overall aim will thus be advanced, as follows:

**With respect to Objective 1: Data Bases**

With respect to the three new environmental monitoring sites in Gaza and the West Bank, the following additional efforts are anticipated:

- The final two Palestinian technicians will train at Rutgers University and the BAAQMD, and not at HUJI (as in the original proposal)
- The three monitoring sites will be prepared (i.e., with respect to security, power supply, communications, etc.) for the installation of the instruments
- The instruments in storage at HUJI will be installed and made operational at the three West Bank/ Gaza sites. The process has begun under coordination with US embassy personnel.

With respect to the preparation of a comprehensive environmental database and climatology of the study area, the following will be accomplished:

- meteorological, air quality, emissions, and geographic data required for modeling will continue to be collected
- database construction at HUJI and ARIJ will continue, and their merging will be initiated.

Construction of the environmental database will be lead by:

- ARIJ will lead the GIS analyses tasks, while Dr. Bitan's group at TAU will also contribute to this effort
- Dr. Jad Isaac of ARIJ and Dr. Yasser El-Nahhal of EPRI will obtain required data from the Palestinian meteorological and air quality networks and databases
- Mr. Erez Weinroth of the HUJI, Mr. Kaldoun Rishmawi of ARIJ, and Dr. Yasser El-Nahhal of EPRI will blend the regional pollutant inventories.

**With respect to Objective 2: Field Studies**

Execution of short-term intensive field observational campaigns during periods conducive to the existence of poor regional air quality should be implemented during June 2003 to measure regional transboundary pollutant fluxes. This (final) campaign will involve measurement of both meteorological and air quality parameters by project scientists and students.

**With respect to Objective 3: Modeling Current Conditions**

With respect to application of meteorological and air quality models to the study area to increase understanding of air quality problems associated with current levels of regional urbanization, the following will continue:

>the RAMS (at HUJI) and MM5 (at DRI and SJSU) meteorological models will continue to be used to simulate additional flow cases

> the HYPACT Lagrangian particle model at HUJI will be continued to used to simulate additional transport patterns

> the CAMX photochemical model will be continued to be used at HUJI and DRI with output from the above RAMS and MM5 simulations

> the SJSU/Alpine Geophysics urbanization, PAVE graphics, and MAPS statistical evaluation packages will be used to improve the graphical presentation and statistical evaluation capabilities for outputs from the RAMS, MM5, CAMX, and HYPACY models

**With respect to Objective 4: Modeling Possible Future Conditions**

With respect to the simulation of possible future regional meteorological and air quality patterns using the validated models of Objective 3, the following will been done:

> discussions will continue with transportation planner Dr. Eran Feitelson to identify various possible future regional emission scenarios to be tested in the models during the final year of the project

> the planning simulations will study the environmental impacts from projected population conditions during the years 2010 and 2020 (when the regional population will have doubled from its present value).

## F.2 Project Schedule

The project is not on schedule in all areas, due to the following factors

- normal delays associated with starting an international project of this size and complexity
- institutional delays (now overcome) in obtaining U S. Embassy approval for the (i) three new Palestinian monitoring stations (given the dual use listing for the required

sulfur dioxide monitors) and (ii) visas for the new Palestinian technicians and students.

- the joint Israeli-Palestinian field study could not be carried out under the current circumstances

Because of these issues, the original project work schedule should be revised as follows:

- tasks originally scheduled for completion the second year were stretched out and completed during the third year
- the original three year project will be extended into a fourth year
- the original third year tasks will become fourth year tasks.

## II. Project Management and Cooperation

### A. Managerial Issues

- There have been no major staff changes or research site changes, except that the Palestinian students have started their course work in English at SJSU and not in Hebrew at Israeli universities. This has involved the shifting money from both the Palestinian and Israeli budgets (earmarked in both budgets for Palestinian student stipends) to the SJSU budget, so that the students at SJSU and DRI can be paid in a timely manner.
- The original funding for the three-year project will be sufficient to last during the requested fourth "stretch out" year of the project (see revised Budget in Report 1).
- When Prof. Bornstein was in the area during February to April 2000 and June to July 2000, he met with all project participants and with a number of other Israeli

and Palestinian scientists and administrators. After his return to the U.S., however, bilateral meetings in the area between Palestinian and Israeli project scientists have ceased (although phone and e-mail contacts have occurred). This still remains as the only significant current administrative barrier. It has, however, been mitigated by the visits of both Israeli and Palestinian scientists and students to SJSU and DRI. It can also been over come in the future by having the group meet at international technical conferences, e.g., in Tsukuba (Japan) in March 2003, Istanbul in May 2003, and Seattle in January 2004.

## B. Special concerns

No special concerns (of the type listed in the USAID Report Preparation Guidelines) exist.

## C. Cooperation, Travel, Training, and Publications

### m. Areas of completed cooperation include

- Prof. Bornstein was in Gaza, West Bank, and Israel during February to April 2000 and June to July 2000, when he held a series of joint planning meetings with all project participants. He also held separate meetings with each project group, and met with a number of other Israeli and Palestinian scientists and administrators.
- Telephone contacts between Palestinian and Israeli project scientists have continued after the end of his visits, while meetings in the region between Palestinian and Israeli project scientists ceased at the end of the Summer 2000. Meet-

ings in the US at DRI and SJSU, however, have continued between Palestinian, Israeli, and/or US scientists.

- Requirements for the new Gaza and West Bank instrument sites were determined in 2000 via joint efforts between U.S., Palestinian, and Israeli project personnel. Three sites fulfilling the criteria were identified by the group and certified by U. S. embassy personnel.
- The locations of the future joint shared databases were determined by Palestinian and Israeli scientists, and joint discussions begun on how to construct them.
- Discussions were held between ARIJ and TAU scientists on the GIS analysis tasks.
- HUJI, ARIJ, and EPRI scientists have discussed how to integrate Israel, West Bank, and Gaza inventory information into a single data set.

**n. Completed travel**

- Prof. Bornstein traveled to Israel, Gaza, and the West Bank during February to April 2000 and June to July 2000, when he held a series of meetings with all project participants
- Mr. Erin Tass, HUJI atmospheric chemist and Ph.D. student, visited Dr. S. T. Rao at the State University of Albany to study chemical mechanisms during July-August 2000
- Mr. Erez Weinroth of HUJI visited ARIJ in late Summer 2000 to discuss emission inventories
- Mr. Erez Weinroth, HUJI Ph.D. student, visited SJSU, Stanford University, and Environ Inc. to study photochemical modeling during April-May 2001

- Dr. Bornstein and a group of his SJSU students visited Prof. Alan Getler of DRI in Fall 2001 to discuss how DRI scientists could work with the current project
- Mr. Ali Abu-Rahmah of ARIJ thus started his Ph.D. in Atmospheric Sciences at DRI under Profs. Gertler (of DRI) and Luria (of HUJI) in Fall 2001
- Mr. Ali Abu-Rahmah of ARIJ and DRI visited SJSU to discuss his project efforts in Winter 2001
- Nidal Abukubie of ARIJ came to SJSU in May 2002
- Dr. Yasser El-Nahhal of EPRI took the week long EPA instrument class at Rutgers and then came to SJSU for a week in July 2002
- Dr. Jamal Safi of EPRI and his wife visited SJSU for a week in August 2002 to dis-cuss the project
- Dr. Menachem Luria of the HJUJI will visit SJSU from DRI for several day at the end of September 2002 to discuss the project
- Ms. Shoukri Kasakseh of ARIJ will start a M. S. in Meteorology SJSU in October 2002
- Mr. Khalil El_Khateeb of EPRI will start a M. S. in Environmental Sciences and GIS at SJSU in October 2002
- Dr. Jad Isaac of ARIJ will visit SJSU for a week in October 2002 to discuss the project

o. **Training in progress or finished**

- Mr. Dean Ranmar, HUJI meteorology student, carried out both HYPACT Lagrangian particle transport modeling and RAMS meteorological modeling as part of his Ph.D. effort (awarded 2001)

- Mr. Erez Weinroth, HUJI air quality chemistry student, has compiled the first emission inventory in the study area and has carried out RAMS meteorological and CAMX photochemical modeling as part of his Ph.D. research (should finish 2002)
- Dr. Yasser El-Nahhal took the week long EPA Air Quality Instrumentation course at Rutgers University in July 2002
- Mr. Ali Abu-Rahmah, an ARIJ Palestinian student at DRI, is currently running MM5 and CAMX as part of his Ph.D research (should finish 2004).

**p. Publications and presentations achieved**

- HUJI prepared Emissions Report (appended Report 1)
- HUHI prepared Regional Air Pollution Climatology Report (appended Report 1)
- Stanford University prepared Chem Mechanisms Report (appended Report 1)
- Israeli Ministry of Environment prepared Monitoring Network Report (appended Report 1)
- TAU prepared List of References of Middle-East Modeling Studies (appended Report 1)
- Bornstein, R., M. Luria, Y. Mahrer, M. Peleg, D. Rammar, E. Weinroth, E. Tas, V. Matziev, E. Feitelson, J. Kaplan, U. Dayan, J. Issac, H. Maoh, M. Ghanayem, J. Safi, Y. El-Nahhal, A. Bitan, E. Ben-Dor, I. Benenson, Setter, and Y. Levi, 2001: Preliminary results from the middle-east transboundary pollutant transport study. Preprint Volume, Second International Symposium on Air Quality Management, 25-28 Sept. 2001, Istanbul, Turkey, 8 pp.

- Bornstein, R., M. Luria, Y. Mahrer, M. Peleg, D. Rammar, E. Weinroth, E. Tas, V. Matziev, E. Feitelson, J. Kaplan, U. Dayan, J. Issac, H. Maoh, M. Ghanayem, J. Safi, Y. El-Nahhal, A. Bitan, E. Ben-Dor, I. Benenson, Setter, and Y. Levi, 2001: Middle-east transboundary pollutant transport study. Preprint Vol., Third IAHR, Symposium on Environmental Hydraulics, 5-8 Dec. Tempe, AZ, 6 pp.
- Bornstein, R., M. Luria, Y. Mahrer, M. Peleg, D. Rammar, E. Weinroth, E. Tas, V. Matziev, E. Feitelson, J. Kaplan, U. Dayan, J. Issac, H. Maoh, M. Ghanayem, J. Safi, Y. El-Nahhal, A. Bitan, E. Ben-Dor, I. Benenson, Setter, and Y. Levi, 2002: Middle-east transboundary pollutant trans-port project. Preprint Vol., 12th Joint AMS/AWMA Conference on the Applications of Air Pollution Meteor., Norfolk, VA, 55-56, 2pp.
- Ranmar, D., 1999: Utilization and integration of interdisciplinary computer models as a tool for analyzing ozone production from transportation sources. Presented, 7th International Conf., Israeli Society for Ecology and Environmental-Quality Sciences, 13-18 June, Jerusalem.
- Ranmar, D., 1999: Utilization and integration of interdisciplinary computer models as a tool for analyzing ozone production from transportation sources. Poster, 6th International Conf. on Harmonization within Atm. Dispersion Modelling for Regulatory Purposes, 11-14 Oct., Rouen, France.
- Ranmar, D., 1999: Utilization and integration of interdisciplinary computer models as a tool for analyzing ozone production from transportation sources. Poster, 2nd Research Workshop on the Interactions between Chemistry, Physics, and Dynamics in the Troposphere, 24-29 Oct., Nazareth, Isreal.

- Ranmar, D., 2000: Utilization and integration of interdisciplinary computer models as a tool for analyzing ozone production from transportation sources. Poster, Millennium NATO/CCMS International Tech. Meeting on Air Pollution Modelling and its Application, 15-19 May, Boulder, CO.
- Ranmar, D., 2001: Ozone production from transportation sources: Utilization and integration of inter-disciplinary computer models as a tool for environmental-oriented-improvement of transportation planning. Ph.D. dissertation, Graduate School of Applied Sciences and Technology, Dept. of Atmospheric Sciences, HUJI, 220 pp.
- Ranmar, D., M. Luria, J. Kaplan, and Y. Mahrer, 2002: Utilization and integration of interdisciplinary computer models as a tool for analyzing ozone production from transportation sources. To appear *International J. of Environ. And Pollution.*
- Ranmar, D., V. Matveev, U. Dayan, M. Peleg, J. Kaplan, A. Gertler, M. Luria, G. Kallos, P. Katsafados, and Y. Mahrer, 2002: Impact of coastal transportation emissions on inland air pollution over Israel: Utilizing numerical simulations, airborne measurements, and synoptic analyses. To appear *J. of Geophysical Research*, **107**.
- Weinroth, E., A, Ben-Nun, C. Emery, M. Luria, and Y. Mahrer, 2002: Model simulations of ozone formation over Israel, the West Bank, and Jordan. Presented at the RAMS Modelers Workshop.

q. **Planned areas of cooperation (with SJSU as intermediary) include**

- New Gaza and West Bank instruments should be given by the HUJI to EPRI and ARIJ during Fall 2002.
- Work will continue on the regional databases at EPRI, ARIJ, and HUJI.
- Work will continue on the regional GIS analyses at ARIJ and TAU.
- Work will continue on regional emissions inventories at HUHI, EPRI, and ARIJ.
- Work will continue on RAMS modeling at HUJI, MM5 modeling at DRI and SJSU, and CAMX modeling at DRI and HUJI

r. **Anticipated travel**

- Dr. Menachem Luria of HJUJI will visit SJSU from DRI for several day at the end of September 2002 to discuss the project
- Ms. Shoukri Kasakseh of ARIJ will start a M. S. in Meteorology at SJSU in October 2002
- Mr. Khalil El_Khateeb of EPRI will start a M. S. in Environmental Sciences and GIS at SJSU in October 2002
- Dr. Jad Isaac of ARIJ will visit SJSU for a week in October 2002 to discuss the project.
- Prof. Bornstein plans to travel to the area during December 2002 to help plan a special session for the October 2004 Clean Air Congress (in Israel, organized by Prof. Luria) on this project and to hold planning meetings with all project participants.

- Mr. Erez Weinroth (HUJI student) and Ali Rathman (ARIJ student at DRI) will both come to SJSU during the summer 2003 to teach MM5 and CAMX to the SJSU project students and Dr. Yasser El-Nahhal of EPRI.
- Prof. Bornstein will attend the 8th International ASAAQ Conference in Tsukuba, Japan on 11-13 March 2003, as he is on the International Organizing Committee
- Profs. Luria and Bornstein will attend the 26th NATO/CCMS/ITM Meeting in Istanbul, Turkey on 26-30 May 2003
- Prof. Bornstein will attend the AMS Annual Meeting in Seattle in January 2004, as he is organizing its Urban Symposium

**s. Anticipated training**

- Mr. Erin Tass, HUJI atmospheric chemistry student, will continue to study chemical mechanisms as part of his Ph.D. research
- Mr. Erez Weinroth, HUJI air quality chemistry student, will continue to carry out RAMS and CAMX photochemical modeling as part of his Ph.D. research and should finish at the end of 2002
- Mr. Ali Abu-Rahmah, an ARIJ Palestinian student at DRI will continue running MM5 and CAMX as part of his Ph.D research and should finish in 2004
- Ms. Shoukri Kasakseh of ARIJ will start a M. S. in Meteorology at SJSU in October 2002 and should finish in August 2004
- Mr. Khalil El-Khateeb of EPRI will start a M. S. in Environmental Sciences and GIS at SJSU in October 2002 and should finish in August 2004
- Mr. Ali Abu-Rahmah, the ARIJ Palestinian student at DRI, will come to train the new Palestinian students in MM5 in December 2002

- Mr. Ali Abu-Rahmah (ARIJ Palestinian student at DRI) and Mr. Erez Weinroth (HUJI student) will both come to train Dr. Yasser El-Nahhal and the new Palestinian students in CAMEX in Summer 2003

t. **Planned publications and presentations (jointly when possible)**

- HUJI report on the history of past, present, and future environmental regulations in the region (by January 2003)
- Joint SJSU, EPRI, ARIJ, and HUJI journal submission on preliminary project results (prepared by SJSU) for a special journal issue for papers from the Second International Symposium on Air Quality Management, 25-28 Sept. 2001, Istanbul, Turkey (due by end of October 2002)
- Bornstein, R., M. Luria, Y. Mahrer, M. Peleg, D. Rammar, E. Weinroth, E. Tas, V. Matziev, E. Feitelson, J. Kaplan, U. Dayan, J. Issac, H. Maoh, M. Ghanayem, J. Safi, Y. El-Nahhal, A, 2003: Observations and RAMS/CAMEX Results from the Middle-East Transboundary Pollutant Transport Study. Submitted to the 26th NATO/CCMS International Tech. Meeting on Air Pollution Modelling and its Application in May 2003 in Istanbul, Turkey
- Prof. Luria plans to present a paper at the 26th NATO/CCMS International Tech. Meeting on Air Pollution Modelling and its Application in May 2003 in Istanbul, Turkey.
- Bornstein, R., M. Luria, Y. Mahrer, M. Peleg, D. Rammar, E. Weinroth, E. Tas, V. Matziev, E. Feitelson, J. Kaplan, U. Dayan, J. Issac, H. Maoh, M. Ghanayem, J. Safi, Y. El-Nahhal, A, 2003: Observations and RAMS/CAMEX Results from

the Middle-East Transboundary Pollutant Transport Study. Submitted to the 8th International ASAAQ Conference, 11-13 March 2003, Tsukuba, Japan.

- Prof. Bornstein plans to present and publish a paper co-authored by all project participants for the; preprint volume of the Urban Symposium at the AMS Annual Meeting in Seattle, WA in Jan. 2003
- M. S. and Ph.D. theses from all students in 2003-2004 will be submitted for journal publication

**D. Request for USAID Actions**

During previous conversations with USAID/MERC administrators, it was advised that the current lack of regional bilateral contacts be overcome by Prof. Bornstein, who would provide the information that each group required for successful completion of their current research efforts. Additional suggestions and help from USAID to facilitate the blending of the two efforts into regional environmental solutions that will benefit mideast regional air quality would be useful.

**E. Support Documentation**

Following is a list of attached appendices, their authors, and technical content:

- Appendix A: Mr. K. Rishmawi summary of ARIJ's contributions with respect to site selection, data collection, data analysis, emission inventories, and GIS data bases.
- Appendix B: Dr. Y. El-Nahhal summary of EPRI's contributions with respect to site selection, data collection, and data analysis
- Appendix C: Mr. Ali-Rahmah of ARIJ summary of his Ph.D. work at DRI

- Appendix C: Mr. Ali-Rahmah of ARIJ summary of his Ph.D. work at DRI
- Appendix D: Dr. D. Ranmar HUJI Ph.D. thesis, including his papers

  > Impact of coastal transportation emissions on inland air pollution over Israel: Utilizing numerical simulations, airborne measurements, and synoptic analyses. To appear *J. of Geophysical Research*, **107**

  > Utilization and integration of interdisciplinary computer models as a tool for analyzing ozone production from transportation sources. To appear in *Intenational J. of Environ. and Pollution.*
- Appendix E: Mr. Erez Weinroth HUJI Ph.D. thesis (preliminary chapters only) including his work on emission inventories, and RAMS and CAMEx modeling
- Appendix F: Rammar et al. (2002a,b) page proofs
- Appendix G: Three submitted conference abstracts by Bornstein et al. and Weinroth et al.
- Appendix H: Three preprint conference papers by Bornstein et al.

Appendix A: ARIJ contributions

MERC Proposal No M18-054

# TRANBOUNDARY AIR-QUALITY EFFECTS FROM THE URBANIZATION OF ISRAELI-GAZA MEDITERRANEAN COAST

Annual Progress Report

**Khaldoun Rishmawi**

Water and Environment Research Unit
Applied Research Institute - Jerusalem
P.O.Box 860, Caritas St., Bethlehem
Tel: +972-(0)2-274-1889
Fax: +972-(0)2-2776966
e-mail: khaldoun@arij.org

**June 2002**

Applied Research Institute - Jerusalem

EXECUTIVE SUMMARY 3

1 SCIENTIFIC SYNTHESIS 4

2 RESEARCH TASKS UNDERTAKEN & METHODOLOGIES 5

2.1 SELECTION OF SITES FOR THE INSTALLATION OF AIR QUALITY AND METEOROLOGICAL MONITORING EQUIPMENT 5
2.2 COLLECTION OF SURFACE METEOROLOGICAL DATA 5
2.3 PREPARATION OF AN EMISSION INVENTORY 5
*2.3.1 Energy Sector* 6
2.3.1.1 Estimating CO2 emissions 6
2.3.1.2 Estimating non-CO2 emissions 10
2.4 PREPARATION OF A COMPREHENSIVE GEOGRAPHIC DATA BASE AND ANALYSIS OF SATELLITE IMAGES 13
2.5 GIS DATA HARMONIZATION AND INTEGRATION 17
2.6 ASSESSING THE COLLECTED AND/OR ANALYZED DATA FOR SPATIAL ACCURACY 21
2.7 ESTABLISHMENT OF A METADATABASE 21
2.8 INCOMPLETE DATA SETS 24
2.9 RE-DISTRIBUTION OF DIGITAL DATA 24
2.10 ARIJ RESPONSIBILITIES DURING THE NEXT PHASE (THIRD YEAR) OF PROJECT IMPLEMENTATION 24

3 DIFFICULTIES ENCOUNTERED 25

2.11 DATA AVAILABILITY AND RELIABILITY 25
2.12 COOPERATION BETWEEN PROJECT PARTNERS 25
2.13 MOVEMENT WITHIN THE WEST BANK 25
2.14 DELAYS DUE TO CURFEW OR CLOSURE 25

ANNEX 1: HARMONIZED DATA SETS: ARIJ METADATABASE 26

# EXECUTIVE SUMMARY

The overall aim of the project is to generate information required by government planning agencies in Israel and Palestine for the socially and environmentally sustainable urbanization of their coastal areas.

This report summarizes the activities carried out by the Applied Research Institute – Jerusalem during the first two years of project implementation. The specific objectives of the two work years were to establish and maintain comprehensive environmental databases and climatologies of the area, to install two new continuously operated (climatological) dial-up regional air quality and meteorological stations in the West Bank, to execute a short term intensive field observational campaign during periods of poor regional air quality in order to measure meteorological and air quality parameters and to integrate the data into a sound geographic data management system.

The following results have been achieved:

- Collection of environmental databases and climatologies that include meteorological, air quality, precursor emission rates and geographic parameters.
- Assessment of data consistency
- Collection of supplementary data to fill data gaps (e.g. remote sensing data)
- Establishment of a project metadatabase
- Integration of collected data into homogenous geographic layers
- Selection of two sites for the climatological dial-up regional air quality and meteorological stations

The following activities were not carried out:

- The climatological stations were not installed.
- Field observational campaigns were not executed.
- Overall harmonization of data between project partners was not established.
- Local meetings, the semi-annual Mideast project meeting and the annual Mideast project meeting were not carried out.

The aforementioned activities were not carried out mainly due to the current political situation: Palestinian scientists are virtually unable to travel out of their confined areas. Consequently, the whole training program and human resource development has to be changed in light of the prevailing political constraints. The monitoring stations arrived in the Hebrew University a year a half ago but were not delivered to the Palestinian partners. Regrettably, the Israeli scientists were contacted to facilitate the delivery of equipment and other project activities but no action was made. Several contacts were made with AID to transfer the monitoring stations but so far, no progress has been made. The success of the project depends on the monitoring of air quality in the three specified locations in the Palestinian areas as well as those in Israel where such data will be shared and analyzed. Failure of fulfilling this task so far will jeopardize the successful implementation of the project objectives. Consequently, options were made for a training session for Palestinian technicians to take place in the US; however, it was impossible to acquire the visas due to the fat that Bethlehem was under curfew by the Israeli army for 40 days. Another training session was scheduled for July 2002 but again Bethlehem is under curfew and leaving the Palestinian areas abroad is now severely restricted. The Palestinian project team hopes for an improvement of the present political situation and alleviation of the restrictions of movement on Palestinians imposed by Israel. Under such conditions, ARIJ decided to continue to work in this project and exchange knowledge and data through electronic means (e.g. electronic mail and FTP sites). ARIJ has been able to construct a harmonized climatological and environmental database for the West Bank. The harmonized database will provide a blueprint for the development of a more sustainable urbanization in the region.

# 1 SCIENTIFIC SYNTHESIS

This report documents the activities of the Applied Research Institute – Jerusalem during the first year of implementing the MERC project *"Transboundary Air Quality Effects from Urbanization"* that included the collection, processing, harmonization and integration of comprehensive environmental databases and climatologies into a spatial database. The platform for the integration was ArcView GIS and was selected for its versatility and widespread availability. More specifically, the activities of the Applied Research Institute Jerusalem (ARIJ) included:

- Selection of two appropriately-located sites for the installation of air quality and meteorological monitoring equipment.
- Collection of surface meteorological data from disparate sources (precipitation, humidity, wind speed, min and max temperatures and atmospheric pressure).
- Preparation of an emission database for key anthropogenic and natural emission sources.
- Using monitoring data (i.e. LANDSAT ETM+, SPOT XIS) from the present and the recent past to extract land use/cover detailed maps.
- Preparation of a comprehensive geographic database of the West Bank including topographic, detailed land use/cover and air pollutant sources.
- Assessing the collected and/or analyzed data for consistency and accuracy
- Establishment of a project metadatabase

The GIS-based database has been established in ArcView format, which is an established standard. The grid-based layers are established in ArcInfo grid format, readable via ArcView Spatial Analyst. The scientific challenge was to develop the means that allows integrating the emission data inventory into geographic information.

# 2 RESEARCH TASKS UNDERTAKEN & METHODOLOGIES

## 2.1 Selection of sites for the installation of air quality and meteorological monitoring equipment

The objective involved the installation of two new continuously operated (climatological) dial-up regional air quality and meteorological stations in the West Bank to measure air quality parameters (CO2, NOx, O3, and SO2 concentrations in the atmosphere, while simultaneously measuring meteorological parameters such as wind, temperature, humidity, precipitation, and pressure. Unfortunately, and due to security reasons, the two monitoring stations were not transferred from the Hebrew university to their new selected sites in Bethlehem and Nablus. The Applied research Institute in Bethlehem will be the site for installing the first station whereas Najah university in Nablus will be the site for the second site. Bethlehem is located in the mid-southern part of the West Bank and is in close proximity to Jerusalem, whereas Nablus is located in the Northern part of the West Bank at distance of 48km from Tel Aviv (north eastern direction) and at a distance of approximately 40km to the east of Natanya. Jerusalem, Tel – Aviv and Natanya are busy centers that produce large volumes of green house gases.

## 2.2 Collection of surface meteorological data

Precipitation: The precipitation data are needed to calculate the spatial distribution of rainfall within the region. ARIJ has produced the necessary data sets, namely time series with precipitation sums per for 80 rain monitoring and Meteorological stations. The temporal resolution of the data varies from one station to another, but for most stations the recorded precipitation data goes back to the year 1965. Precipitation data was processed in time series of monthly sums.

Temperature: The temperature data are recorded by 13 meteorological stations distributed over the West Bank. The spatial density of the data is variable and decreases gradually as we move southwards. Monthly time series of minimum, maximum and average recorded temperature data were generated for the thirteen stations. The temporal resolution of the data is variable and is dependent on the date each corresponding meteorological station became operational.

Humidity: Monthly time series of average recorded relative humidity data were generated for thirteen stations.

Pressure: Monthly time series of average recorded atmospheric pressure data were generated for thirteen stations.

Wind Speed and Direction: Monthly time series of average wind speed were generated for the thirteen meteorological stations. The temporal resolution of the data spans 20-30 years of historic data. However, no information as regards to wind direction was available for the aforementioned period. Meteorological data available from the Palestinian Metrological office contains recent daily wind speed and direction data (1996-2002).

## 2.3 Preparation of an emission inventory

Introduction:

The structure of the green house gas inventory follows the order established in the "Revised 1996 IPCC Guidelines-Greenhouse Gas Inventory Workbook, Volume 2", which has identified six major economic sectors, as follows:

- Energy
- Industrial processes
- Solvent and other product use
- Agriculture
- Land use change and forestry
- Waste

Data on the following greenhouse gases were collected:

| | |
|---|---|
| CO2: | carbon dioxide |
| CO: | carbon monoxide |
| NOx: | nitrogen oxides |
| N2O: | nitrous oxide |
| SO2: | sulfur dioxide |
| CH4: | Methane |
| NMVOCs | non methane volatile organic compounds |
| HFCs: | Hydro fluorocarbons |
| PFCs: | Per fluorocarbons |
| SF6: | sulfur hexafluoride |

In this report, each section starts with an introduction presenting the state of each sector in Palestine, followed by the methodology adopted in order to compute emissions of greenhouse gases by sources. It should be noted that the computation of emissions was done in accordance with the IPCC guidelines. Finally the IPCC Sectoral tables, which portray the results obtained in each sector are presented.

### *2.3.1 Energy Sector*

The aim of this section is to report the results of the greenhouse gas (GHG) emission inventory for all available years. The following GHG are of interest in the energy sector: carbon dioxide $CO_2$, methane $CH_4$, nitrous oxide $N_2O$, oxides of nitrogen NOx, carbon monoxide CO, sulphur dioxide $SO_2$ and non-methane volatile organic compounds (NMVOCs). The inventory has focused on the following GHG related sources:

1. Electricity generation.
2. Manufacturing industries and construction
3. Transport
4. Energy use in the residential sector.
5. Economical activities.

The fuel types taken into consideration are: gasoline, kerosene, gas oil, diesel oil, LPG, lubricating oil, coal, and wood. The amount of GHG released to the atmosphere has been estimated using the IPCC methodology and emission factors [1].

#### *2.3.1.1 Estimating CO2 emissions*

Data sources:

-PCBS (Palestinian Central Bureau of Statistics)

-General Petroleum Corporation

The provided data are trustable due to the fact that these data are complied by comprehensive enumeration of data, but it is worth mentioning the following notes:

- Data excludes those parts of Jerusalem annexed by Israel in 1967.
- Data excludes the quantity entered the Palestinian territory in illegal cases.

- The data sources consider the following geographical classification of Palestine:
  - A- West bank and includes:

    West bank north: including Jenin, Tubas, Tulkarm, Qalqilya, Nablus and Salfit governorates.

    West bank middle: including Jerusalem, Ramallah and Jericho governorates

    West bank south: including Bethlehem and Hebron governorates.
  - B- Gaza strip

*Estimating CO2 emissions using the Reference Approach*

Methodology and calculations:

The following method was used to calculate CO2 emissions using the reference approach:

- The quantity of apparent consumption of all fuels was calculated by subtracting fuel import from the fuel re-exported and adding the resultant value to the fuel stock exchange (equation 1).

  Apparent consumption = import - (re-export – stock change) ... *1*
- Apparent consumption was multiplied by the conversion factors (TJ/ unit) in order to get the apparent consumption in Tera Joule (Tj). Energy conversion factors were obtained from PCBS [2].
- Apparent consumption was multiplied by the carbon emission factors specific for each fuel type. The carbon emission factors were obtained from the IPCC guidelines [1]. This resulted in the carbon content in tones of carbon, which was latter multiplied by $10^{-3}$ in order to convert it into gigagrams of carbon (Gg C).
- As carbon stored was set to zero, then net carbon emissions is equal to carbon content. The former was multiplied by the fraction of carbon oxidized which was obtained from the IPCC guidelines [1]. This resulted in the actual emissions of carbon (Gg C).
- Actual carbon emissions were multiplied by 44/12 in order to get the actual emissions of CO2 in (Gg CO2).

The obtained results of CO2 emissions are summarized in table 1.

| Region | 1996 | 1997 | 1998 | 1999 |
|---|---|---|---|---|
| West bank north | 250.6475 | 339.949 | NA | 415.9029 |
| West bank middle | 155.0706 | 191.9458 | NA | 238.4559 |
| West bank south | 282.6336 | 417.9807 | NA | 316.9661 |
| Total | 688.3517 | 949.8755 | 1382.798 | 971.3249 |

**Table 1.** Actual CO2 emissions from 1966-1999 in (Gg CO2) for each geographical region.

It should be noted that in 1998 the emission value is for the whole West Bank plus Gaza strip, as the available data for consumption of fuels are provided for the region as a whole

*Estimating CO2 emissions using the Sectoral Approach*

This section reports the greenhouse gases emitted from various sectors, namely, electrical generation, residential consumption, economical activities, manufacturing and industries . The conversion and carbon emission factors as well as the fraction of carbon oxidized used for all fuel types are those recommended by the IPCC methodology.

Methodology and calculations:

The following method was used to calculate CO2 emissions using the sectoral approach:

- The quantity of each fuel consumed in the various above mentioned sectors were collected in Metric ton and thousand liters.
- Consumption was multiplied by the conversion factors (TJ/ unit) in order to get the consumption in Tera Joule (TJ). Energy conversion factors were obtained from PCBS [2].
- Consumption was multiplied by the carbon emission factors specific for each fuel type. The carbon emission factors were obtained from the IPCC guidelines [1]. This resulted in the carbon content in tones of carbon, which was latter multiplied by $10^{-3}$ in order to convert it into gigagrams of carbon (Gg C).
- As Fraction of carbon stored was set to zero, then net carbon emissions is equal to carbon content (Gg C). The former was multiplied by the fraction of carbon oxidized, which was obtained from the IPCC guidelines [1]. This resulted in the actual emissions of carbon (Gg C).
- Actual carbon emissions were multiplied by 44/12 in order to get the actual emissions of CO2 in (Gg CO2).

Electricity generation sub-sector:

The types of fuel used in this sector are gasoline, diesel, kerosene, LPG, lubricates and coal. Table 2 shows the CO2 emissions generated from electricity generation.

| Region | 1996 | 1997 | 1998 | 1999 |
|---|---|---|---|---|
| West bank north | NA | 11.84269 | NA | 63.00247 |
| West bank middle | NA | 0.109956 | NA | 25.03402 |
| West bank south | NA | 15.78792 | NA | 4.728355 |
| total | NA | 27.740566 | 48.67854 | 92.764845 |

**able 2.** Actual CO2 emissions generated from the electrical generation sector in (Gg CO2) for each geographical region.

It should be noted that in 1998 the emission value is for the whole West Bank plus Gaza strip, as the available data for consumption are provided for the region as a whole

Residential Consumption sub-Sector:

The types of fuel used in this sector are gasoline, diesel, kerosene, LPG, lubricates and coal. These fuels used for heating and cooking purposes. Table 3 shows the CO2 emissions from residential consumption sector

| Region | 1996 | 1997 | 1998 | 1999 |
|---|---|---|---|---|
| West bank north | 121.9849 | 158.3694 | NA | NA |
| West bank middle | 130.9557 | 160.9082 | NA | NA |
| West bank south | 84.43806 | 128.4577 | NA | NA |
| Total | 337.37866 | 447.7353 | NA | NA |

**Table 3.** Actual CO2 emissions from residential sector in (Gg CO2) for each geographical region .

Manufacturing and Industry sub-Sector:

This section estimates the emission of CO2 from the consumption of fuel in manufacturing and industry. The types of manufacturing and industry in Palestine are:

- Mining and quarrying
- Manufacturing
- Electricity and water supply

Table 4 shows the CO2 emissions from Manufacturing and industry sector by region

| Region | 1996 | 1997 | 1998 | 1999 |
|---|---|---|---|---|
| West bank north | 56.66657 | 76.84673 | 101.0752 | 207.6445 |
| West bank middle | 25.49437 | 42.92882 | 50.77831 | 90.91745 |
| West bank south | 63.68809 | 82.21739 | 109.0808 | 23.63154 |
| Total | 145.848903 | 201.99294 | 260.93431 | 322.19349 |

**Table 4.** Actual CO2 emissions from manufacture and industry in (Gg CO2) for each geographical region.

Economical activities sub-sector:

This section estimates the emission of gases from the economical activities (except industry). In Palestine these activities are:

- Construction
- Services
- Internal trade
- Transport, storage & communications

Table 5 shows the CO2 emissions from Economical Activities sector by region.

| Region | 1996 | 1997 | 1998 | 1999 |
|---|---|---|---|---|
| West bank north | 40.04981 | 90.20992 | 116.1639 | 194.2954 |
| West bank middle | 53.22503 | 93.41434 | 121.3747 | 85.54498 |
| West bank south | 32.51203 | 78.32642 | 101.9616 | 41.52101 |
| Total | 125.78687 | 261.95068 | 339.5002 | 321.36139 |

**Table 5.** Actual CO2 emissions from economical activities in (Gg CO2) for each geographical region.

Transport sub-sector

Since there is no data available for the consumption of fuels in the transport sector yet from our data sources, it is proposed to subtract the known emissions from energy sectors (generating electricity, residential consumption, economical activities , manufacturing and industry) from the emissions from the carbon content of fuels supplied to the country as a whole( the reference approach), so the result will be the emissions for the remaining sector which is the transport sector.

Table 6 shows the CO2 emissions from transport sector for all regions

| | 1996 | 1997 | 1998 | 1999 |
|---|---|---|---|---|
| Total | | 10.456014 | | |

**Table 6.** Actual CO2 emissions from transport sector in (Gg CO2) for each geographical region.

It should be noted that in 1996, there is no available data for electricity generation, and for the years 1997.1998 there is no available data for residential consumption sector, so the results in table 6 for year 1996 shows the emissions for transport plus electricity generation sectors, and years 1998,1999 shows the emissions for transport plus residential consumption sectors.

*2.3.1.2 Estimating non-CO2 emissions*

The aim of this section is to estimate non-CO2 greenhouse gas from manufacturing and industry, electrical generation, residential consumption, and economic activities into the atmosphere.

The non-CO2 gasses which are of interest are methan (CH4), nitrouse oxide (N2O), nitrogen dioxide (Nox), carbon monoxide (CO), sulphur dioxide (SO2) and non-methan volatile organic compounds (NMVOC).

Methodology and calculations:

- Consumption of different fuels used in the different energy sectors in (TJ) was multiplied by non-CO2 emission factors specific for each fuel type and for each gas (Kg/TJ) [3], this resulted in emissions by fuel in Kg.
- Emissions by fuel were divided by $10^6$ in order to get the total emissions in Gg.

The obtained results of non-CO2 emissions were summarized in table 7

| Gas | 1996 | 1997 | 1998 | 1999 |
|---|---|---|---|---|
| Carbon monoxyde | 0.728738 | 0.865933 | 0.213599 | 0.195745 |
| Methane | 0.058694 | 0.063786 | 0.018909 | 0.016154 |
| Nitrogen dioxide | 1.218419 | 3.233181 | 2.901919 | 2.7519 |
| Nitrous oxide | 0.015119 | 0.023796 | 0.021343 | 0.019518 |
| Nmvoc | 0.066568 | 0.085611 | 0.054253 | 0.052152 |
| Sulphur dioxide | 0.1935681 | 0.229285 | 0.269179 | 0.235025 |
| Total | 2.2811061 | 4.501592 | 3.481976 | 3.270494 |

Table 7. Non-CO2 emissions from all energy sectors in (Gg CO2).

It should be noted that the non- CO2 emissions outlined in table 7 are based only on the data available for the consumption of different fuels in the different sectors, i.e the consumption of electricity generation for the year 1996, and the consumption for the residential sector for the years 1998,1999 are not still available.

Tables 8-13 summarize emissions for each non-CO2 gas by type of activity and fuel type for all the available years.

| Type of Activity | Coal &Wood | Gasoline | Diesel | Kerosene | LPG | Lubricate |
|---|---|---|---|---|---|---|
| Manufacturing and industry | 0.006625211 | 0.011215 | 0.231973 | 0.001836 | 0.00903 | 0 |
| Generating electricity | 1.72538E-09 | 9.91E-11 | 4.49E-08 | 2.99E-10 | 1.68E-11 | 0 |
| Economic activities | 1.07823E-08 | 1.83E-08 | 2.58E-07 | 3.7E-09 | 8.83E-09 | 0 |
| Residential consumption | 1.14367E-06 | 1.12E-07 | 9.35E-09 | 2.25E-08 | 1.09E-07 | 0 |
| Transport | 0 | 0 | 0 | 0 | 0 | 0 |
| Total | 0.006626367 | 0.011216 | 0.231973 | 0.001836 | 0.00903 | 0 |

Table 8. Carbon monoxide emissions in (Gg CO2) for the years 1996,1997,1998,1999

| Type of activity | Coal &Wood | Gasoline | Diesel | Kerosene | LPG | Lubricate |
|---|---|---|---|---|---|---|

41

| | | | | | | |
|---|---|---|---|---|---|---|
| Manufacturing industry | 0.001002 | 0.002835 | 0.01871 | 0.000502 | 0.000621 | 0 |
| Generating electricity | 0.000552 | 2.73E-05 | 0.00388 | 7.47E-05 | 0 | 0 |
| Economic activities | 0.001589 | 0.004619 | 0.02008 | 0.00076 | 0 | 0 |
| Residential consumption | 0.059387 | 0.03222 | 0 | 0.007139 | 0.003545 | 0 |
| Transport | 0 | 0 | 0 | 0 | 0 | 0 |
| Total | **0.06253** | **0.039701** | **0.042669** | **0.008475** | **0.004167** | **0** |

**Table 9.** Methane emissions in (Gg CO2) for the years 1996,1997,1998,1999

| Type of activity | Coal &Wood | Gasoline | Diesel | Kerosene | LPG | Lubricate |
|---|---|---|---|---|---|---|
| Manufacturing industry | 2.893273 | 1.117449 | 0.044091 | 0.031273 | 0 | 0 |
| Generating electricity | 0.697949 | 0.188363 | 0.00079 | 0 | 0 | 0 |
| Economic activities | 2.812369 | 1.499631 | 0.006404 | 0 | 0 | 0 |
| Residential Consumption | 0.021013 | 0.047737 | 0.350793 | 0 | 0 | 0 |
| Transport | 0 | 0 | 0 | 0 | 0 | 0 |
| Total | **6.424603** | **2.853179** | **0.402078** | **0.031273** | **0** | **0** |

**Table 10.** Nitrogen dioxide emissions in (Gg CO2) for the years 1996,1997,1998,1999

| Type of activity | Coal &wood | Gasoline | Diesel | Kerosene | LPG | Lubricate |
|---|---|---|---|---|---|---|
| Manufacturing industry | 0.000193272 | 0.001797 | 0.022468 | 0.000303 | 0.000695 | 3.92E-05 |
| Generating electricity | 5.17614E-05 | 1.65E-05 | 0.004493 | 4.98E-05 | 0 | 0 |
| Economic activities | 0.000317611 | 0.002948 | 0.025533 | 0.000608 | 2.92E-05 | 1.35E-05 |
| Residential consumption | 0.000294987 | 0.010695 | 0.00088 | 0.0021 | 0.004356 | 6.43E-06 |
| Transport | 0 | 0 | 0 | 0 | 0 | 0 |
| Total | **0.000857631** | **0.015456** | **0.053374** | **0.003061** | **0.00508** | **5.91E-05** |

**Table 11.** Nitrous oxide emissions in (Gg CO2) for the years 1996,1997,1998,1999

| Type of activity | Coal &wood | Gasoline | Diesel | Kerosene | LPG | Lubricate |
|---|---|---|---|---|---|---|
| Manufacturing industry | 0.000994 | 0.004673 | 0.057993 | 0.000765 | 0.001459 | 0 |
| Generating electricity | 0.000259 | 4.13E-05 | 0.011232 | 0.000125 | 0 | 0 |
| Economic activities | 0.001617 | 0.007644 | 0.064557 | 0.000911 | 0.001427 | 0 |
| Residential consumption | 0.06862 | 0.016789 | 0.001403 | 0.003379 | 0.009147 | 0 |
| Transport | 0 | 0 | 0 | 0 | 0 | 0 |
| Total | **0.07149** | **0.029148** | **0.135185** | **0.005179** | **0.012033** | **0** |

**Table 12.** NMVOC emissions in (Gg CO2) for the years 1996,1997,1998,1999

| Type of activity | Coal & wood | Gasolin | Diesel | Kerosen | LPG | Lubricate |
|---|---|---|---|---|---|---|

| | | | | | | |
|---|---|---|---|---|---|---|
| **Manufacturing industry** | 0.0433482 | 0.004725 | 0.286882 | 0.000837 | 0 | 0 |
| **Generating electricity** | 0.0123192 | 4.56E-05 | 0.059493 | 0.000125 | 0 | 0 |
| **Economic activities** | 0.0687638 | 0.007699 | 0.307888 | 0.001266 | 0 | 0 |
| **Residential consumption** | 0.0963557 | 0.023014 | 0.009197 | 0.005099 | 0 | 0 |
| **Transport** | 0 | 0 | 0 | 0 | 0 | 0 |
| **Total** | **0.2207869** | **0.035483** | **0.66346** | **0.007326** | **0** | **0** |

**Table 13.** Sulfur dioxide emissions in (Gg CO2) for the years 1996,1997,1998,1999

### 2.4 Preparation of a comprehensive geographic data base and Analysis of Satellite images

A. Basic topographic information

Borders: All necessary base data to define the official administrative units, and the borders of the study area were digitized from base maps at ARIJ.

Jordan River and Dead Sea: Data showing the spatial extent of the Dead Sea and the Jordan River were digitized from LANDSAT ETM+ images. Both files are in ArcView format.

Road network: The road network was digitized from a combination of different sources. LANDSAT ETM+ and SPOT panchromatic and IKONOS images were used to digitize the road network, whereas maps were used to differentiate between main roads, secondary roads, and by-pass roads. The later are exclusively used by Israeli colonists residing in the West Bank. Data on traffic density for the year 1999 is available at ARIJ. This information is important to estimate the emissions from transportation which is a non-point source of pollution.

Built-up areas and population: Binary logistic regression modeling was used to classify the LANDSAT and IKONOS image pixels into two categories, built-up and other. Binary logistic regression predicts a dichotomous response variable from a set of explanatory variables. The logistic equation, which gives the quantitative relationship between the dependent response variable and the independent explanatory variables, can be expressed in the equation below (Mendehall and Sincich, 1996):

$$E(y) = \frac{\exp(b_0 + b_1X_1 + b_2X_2 + \ldots + b_kX_k)}{1 + \exp(b_0 + b_1X_1 + b_2X_2 + \ldots + b_kX_k)} \quad (2.1)$$

where,

$$y = \begin{cases} 1 \text{ if category A occurs} \\ 0 \text{ if category B occurs} \end{cases}$$

$E(y)$ is equal to $P$ (Category A occurs) = •

$X_1, X_2, \ldots, X_k$ are quantitative or qualitative independent explanatory variables

$b_0, b_1, \ldots, b_k$ are estimated coefficients

The output of the logistic regression model forms a realistic probability surface (Narumalini et al., 1997), with a minimum of 0 and a maximum of 1. Koutsias and Karteris (2000) identified binary logistic regression as an alternative classification technique to discriminant analysis and multiple regression, both of which pre-assume univariate and multivariate normality in the explanatory variables (Afifi and Clarck, 1990; Norusis, 1990; Mendenhall and Sincich, 1996), conditions that are not necessarily satisfied when using multispectral satellite images (Koutsias and Karteris, 2000). In the case of built-up area mapping, the explanatory variables in the model are the radiometric values of the original spectral channels of the satellite images (Chuvieco, 1999). Using the appropriate set of explanatory variables, the logistic regression models can be structured for estimating the

probability of whether or not a pixel is a built-up area. The criterion used to classify an individual pixel into one of the two groups depends on the value of E ($y$). The pixels with a probability value less than 0.5 are classified as a non-built area, and those greater than the value 0.5 are classified as built-up.

To ensure the successful development of the logistic regression models, the sampling criteria provided by Koutsias and Karteris (1998) were followed:

- first, the sampling areas for the built-up and non-built-up cases were accurately located on the satellite image;
- second, the sampling size regarding both cases was about the same to avoid bias in the sampling process; and
- third, a satisfactory absolute sampling size of 11,900 pixels was obtained to represent all the spectral variability occurring on the satellite image within and outside the built-up area.

The non-built-up pixels represented water, forests, bare surfaces, agricultural lands, and shade. Built-up areas were assigned the value zero, whereas non-built-up areas were assigned the value one to create the dependent variable in the modeling process.

The logistic regression equations were structured using (1) the radiometrically corrected bands of the LANDSAT TM image as the explanatory variables and the radiometrically corrected IKONOS data. Following the construction of the equations, the performance of each was evaluated by calculating the percentage of correct classified observations (built-up, non-built-up and overall).

*LANDSAT ETM+ DATA*

The mathematical formulation of the logistic regression model was built into the ERDAS graphical model maker and applied to the entire dataset. This resulted in a new continuous data layer with a minimum of 0 and a maximum of 1. All pixels with a value greater than 0.5 were classified as built, otherwise as non-built.

Results from the accuracy assessment showed that the built-up areas were accurately mapped using binary logistic regression modeling. The comparison of the classification with the base maps using 256 points is reported in Table 2.5.1. The classification error matrix shows the commission and emission errors in the classification. Of the 128 pixels predicted by the logistic model to be built-up, only three pixels were erroneously classified as non-built-up (commission error). The omission error was almost equal to the commission error where 4 pixels were erroneously classified as non-builtup. The overall classification accuracy was estimated to be 97.3%. The landcover types confused with the built-up areas were bare/low vegetated areas.

| Classified Data | Reference Data | | Reference Totals | Classified Totals | Number Correct | Producers Accuracy | Users Accuracy |
|---|---|---|---|---|---|---|---|
| | NB | B | | | | | |
| Non-Built Areas (NB) | 124 | 4 | 127 | 128 | 124 | 97.6% | 96.9% |
| Built Areas (B) | 3 | 125 | 129 | 128 | 125 | 96.9% | 97.6% |
| Column Total | 127 | 129 | 256 | 256 | 249 | | |
| **Overall Classification Accuracy = 97.3%** | | | | | | | |

**Table 2.5.1 Accuracy assessment**

*IKONOS DATA*

The mathematical formulation of the logistic regression model was built into the ERDAS graphical model maker and applied to the entire dataset. This resulted in a new continuous data layer with a minimum of 0 and a maximum of 1. All pixels with a value greater than 0.5 were classified as built, otherwise as non-built.

Results of the binary logistic classification and the accuracy assessment showed that built-up areas can be mapped with IKONOS data with a reasonable degree of accuracy. The comparison of the classification with aerial photos using 256 points is reported in Table 2.5.2. The classification error matrix shows the commission and emission errors in the classification. Of the 128 pixels predicted by the logistic model to be built-up areas, only eight pixels were erroneously classified as non-built-up. However, the commission error was slightly higher where 12 pixels were erroneously classified as built-up. The overall classification accuracy was estimated to be

92.2%. The landcover types that were confused with the built-up areas were seawater, bare/low vegetated areas and shaded understory vegetation.

| Classified Data | Reference Data | | Reference Totals | Classified Totals | Number Correct | Producers Accuracy | Users Accuracy |
|---|---|---|---|---|---|---|---|
| | NB | B | | | | | |
| Non-Burned Areas (NB) | 116 | 12 | 124 | 128 | 116 | 93.55% | 90.63% |
| Burned Areas (B) | 8 | 120 | 132 | 128 | 120 | 90.91% | 93.75% |
| Column Total | 124 | 132 | 256 | 256 | 236 | | |
| Overall Classification Accuracy = 92.19% | | | | | | | |

**Table 2.5.2 Accuracy assessment**

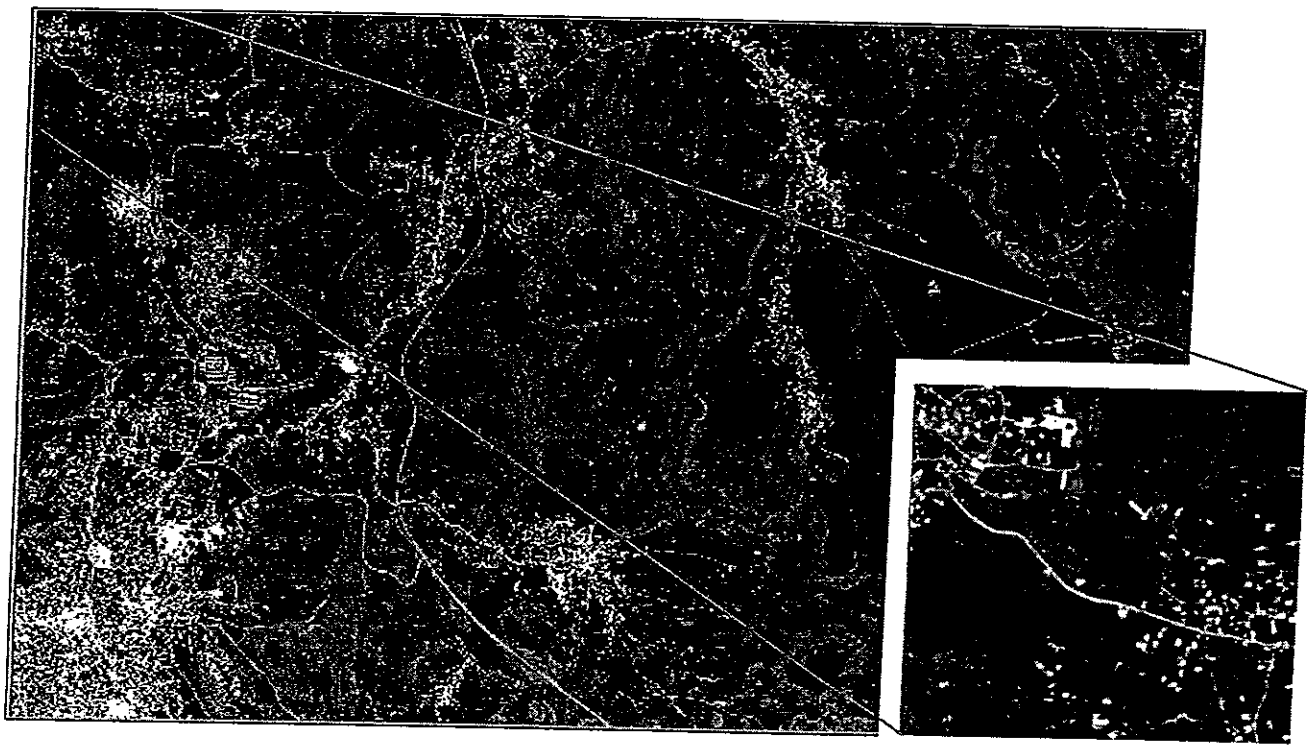

**Figure 2.5.1 Built-up area map of northern Ramallah obtained using binary logistic regression**

The binary layer of the built-up and non-builtup layer was converted into vector data in ArcView GIS. Data attributes such as population and solid waste generation was associated with each built-up area. Figure 2.5.2 shows the built-up areas in vector format.

Palestinian Built-up Areas: With the spatial extent of the built-up area mapped from satellite images, the Palestinian built-up areas were identified and separated from the Israeli colonies. Attributes such as town/village name and district name were associated with Palestinian builtup areas from topographic maps.

Israeli Colonies in the west Bank: Data attributes such as colony name and population were associated with the spatial data.

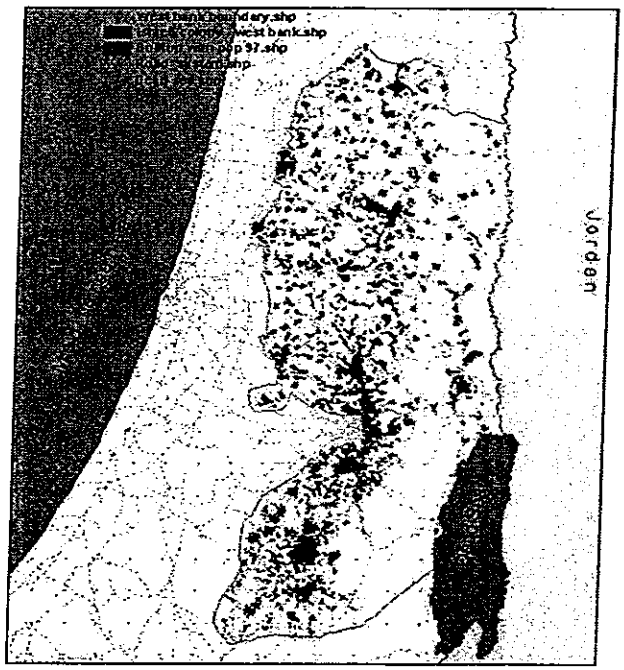


**Figure 2.5.2 Palestinian built-up areas and Israeli Colonies in the West bank.**

Digital elevation model: A 10-meter digital terrain model (DTM) was purchased. The DTM was extracted from a SPOT stereo pair captured over the West Bank in 1997 (Figure 2.5.3). Accuracy assessment performed on the DTM using 30 ground truth point collected using a differential Global Positioning System (dGPS) has shown that the elevation shift is within the range of ± 15 m.

Land use/cover: Multinomial Logistic Regression was used to classify two recent LANDSAT Images. The first image was captured on October 2000 (hereinafter referred to as the fall image) and the second was captured on early May 2001 (hereinafter referred to as the spring image). The reason for using two LANDSAT images is to provide the opportunity to differentiate between rainfed and irrigated crops on one hand and between fruit trees and natural/semi-natural areas. Multinomial Logistic Regression is similar to logistic regression, but it is more general because the dependent variable is not restricted to two categories. Multinomial logistic regression was used to classify the fall image into 5 main classes, namely, rocks and soil with little or no vegetation, urban fabric, fruit trees and irrigated crops, rainfed crops, and a mixture of crop lands and fruit trees (figure 2.5.3), whereas the spring images was mainly used to separate irrigated crops from fruit trees.

**Figure 2.5.3 Digital Terrain Model extracted from a SPOT Stereo pair.**

Man-made and natural forests: Since it was difficult to separate forests from fruit trees by using LANDSAT data, land use/cover maps and IKONOS images were used to digitize the boundaries of man-made and natural forests.

Agricultural greenhouses: The spatial distribution of greenhouses in the West Bank was digitized from aerial photos captured in the year 1996 with a scale of 1:20,000. Information was updated using a combination of SPOT Panchromatic and IKONOS images.

Military bases: Israeli military bases act as potential sources for air pollution. The spatial distribution of the military bases is available; however, no information is available as regards to the number of forces and the machines they use.

Restricted usage areas: Nature reserves and Israeli closed military areas are areas of restricted usage for the Palestinian people. Nature reserves and Israeli closed military areas were provided to serve as supplementary information to identify areas tbat are excluded from cultivation and urbanization activities. Moreover, closed (military) areas are useful as additional information for areas that are (presently) excluded from usage but would make sense that after achieving full peace to clean it from mines and open it for agricultural utilization as there is suitable soil for cultivation.

B. Emission sources:

Dumping sites: Data about dumping sites have been collected by ARIJ as point locations; however no information is available on the spatial extent of each site. The Palestinian Ministry of Environment provided waste quantity data. Missing data on waste quantities for some dumping sites were estimated using the population number served by each dumping site and the average per capita solid waste generation. It should be noted however that most of the dumping sites in the West Bank are uncommissioned (illegal) open dumping sites and the accumulated waste is periodically burned. However, the exact amounts of gases released into the atmosphere through the burning process cannot be accurately calculated due to the fact that there are no studies describing the exact composition of solid waste in the West Bank.

Gasoline seepage: Gas stations were thought to be another source of Gas emissions. Data about gas stations have been collected by ARIJ as point locations. The PCBS and the General Petroleum Corporation provide a rough estimate of the amounts of petroleum lost due to seepage. Insofar the percentage of lost fuel that evaporates into the atmosphere has not been determined. Project partners should agree on a standard formulation that allows a coherent estimation of evaporating fuels under different climatic conditions.

Olive mills: Olive mills are potential sources for air pollution, as the produced olive cake is left to decompose in open dumps. Data about olive mills have been collected by ARIJ as point locations. Information on the amounts of olive cake produced was estimated from geo statistical data showing the distribution of olive orchards in the West Bank and the yearly yield of olive fruit. The later is available from the ministry of agriculture, whereas the former is available from ARIJ GIS database.

Stone Quarries: Stone quarries are potential sources for air pollution. Data about olive mills have been collected by ARIJ as point locations.

Palestinian Industrial Sites: This data set provides additional information to assess the amounts of gases emitted from the different industrial sites. Data about Industrial sites have been collected by ARIJ as point locations. Currently, ARIJ is collecting information about type, extent, production or gas generation of the industries.

Israeli Industrial Sites: Data about Industrial sites have been collected by ARIJ as point locations. However and for clear reasons, ARIJ cannot obtain data on type, extent, production or gas generation of the industries in the Israeli Industrial Sites.

Open wastewater streams: This information is important for identifying a non-point source of gas emissions into the atmosphere. The generated waste water in the cities of the West Bank is dumped into open waste water streams without any treatment. Several major waste water streams were detected and mapped using LANDSAT TM images. Major waste water streams are easily detected as the banks of the waste water streams appear dense bright red in a 4-3-2 LANDSAT band combination. Other main wastewater streams – including the important Wadi An-Nar wastewater stream collects waste water from Israeli cities and stretches from Jerusalem to the Dead Sea. The amount of waste water running through each stream was estimated from the respective population that dumps it waste water into that particular

stream. Project partners should agree on a standard formulation that allows a coherent estimation of gases emitted from waste water streams under different climatic conditions.

Fertilizer usage: Fertilizer data have been estimated from the landuse/cover map. These data have been estimated using the recommended fertilizer application rates for different crops. ARIJ has calculated the nitrogen input from fertilizers by using average fertilization requirements by various crops, and using cropping patterns from the land use classification.

Wastewater treatment: The major wastewater treatment facilities are not functional at the moment. However ARIJ has provided point locations of the wastewater treatment sites for the West bank.

Husbandry and livestock: Information on the number and spatial distribution of livestock in the West Bank were obtained from the Ministry of Agriculture. The location of the major Israeli farming units is available; however little is know as regards to the number and type of animals in the Israeli farming units.

## 2.5 GIS data harmonization and integration

The GIS-based database has been established in ArcView format, which is an established standard. The grid-based layers are established in ArcInfo grid format, readable via ArcView Spatial Analyst. The scientific challenge was to develop the means that allows the integration of climatological data and emission inventory data into the geographic database.

Climatological data: The collected climatological data included precipitation, temperature, humidity, wind speed and atmospheric pressure data. The aforementioned statistical data was integrated into the GIS database as follows:

Precipitation Data: Time series with monthly precipitation sums per for 80-rain monitoring and Meteorological stations were linked to their respective point locations in the GIS database. The join function available in ArcView was used in the process. The joined table included the geographic coordinates per for each meteorological station as well as its respective monthly sum precipitation data. The joined table was then converted into a point type shapefile.

Temperature data: Temperature data included three time series with monthly average of maximum, minimum and average recorded temperatures by each of the thirteen meteorological stations. Temperature data were linked to the geographical location of their respective meteorological station by using the Join function available in ArcView. This has resulted in three shapefiles for minimum, maximum and average monthly temperatures.

Humidity data: Time series with monthly humidity average data per for 13 Meteorological stations were linked to their respective point locations in the GIS database. The join function available in ArcView was used in the process. The joined table included the geographic coordinates per for each meteorological station as well as its respective monthly average humidity data. The joined table was then converted into a point type shapefile.

Wind speed data: Time series with monthly average wind speed data per for 13 Meteorological stations were linked to their respective point locations in the GIS database using the same methodology outlined for humidity data.

Atmospheric pressure data: Time series with monthly average atmospheric pressure data per for 13 Meteorological stations were linked to their respective point locations in the GIS database using the same methodology outlined for humidity data.

Average annual precipitation:

Time series with monthly precipitation sums per for a number of stations was linked to the GIS database as point locations. ARIJ has combined the data sets for ~80 sites with the monthly precipitation with the data sets for (few) stations with long-term annual averages to produce a data set that shows average annual rainfall in the study area. The generated average annual rainfall dataset along with an isoarea precipitation map of average annual precipitation for the last thirty years in Palestine were used in an interpolation technique (Kriging interpolation) to generate an average annual precipitation map (2.5.4).

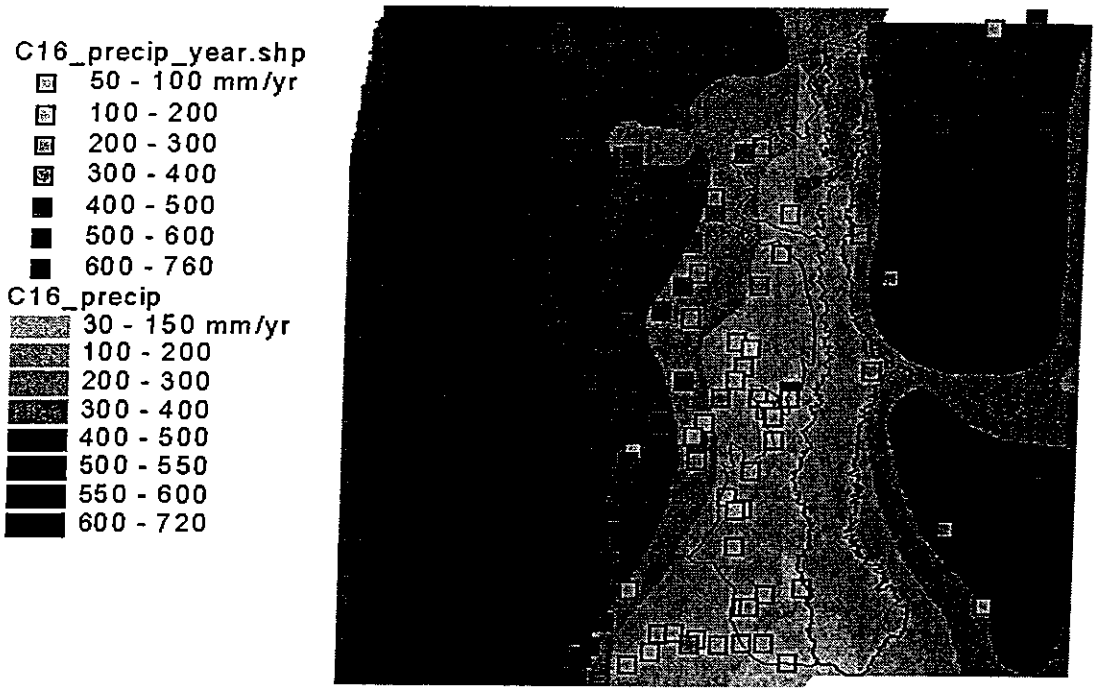


**Figure 2.5: Precipitation in and around study area**

Emission inventory data: The structure of the green house gas inventory follows the order established in the "Revised 1996 IPCC Guidelines-Greenhouse Gas Inventory Workbook, Volume 2", which has identified six major economic sectors, namely, energy, industrial processes, solvent and other product use, agriculture, Land use change and forestry, and waste. So far, the collected gas emission data included emissions from energy sector (electricity generation sector, residential Consumption Sector, manufacturing and industry sector, economical activities sector and transport sector). The aforementioned statistical data was integrated into the GIS database as follows:

Electricity generation sector: Most of the electricity utilized in the West Bank is imported from Israel, however, 458.2 Terra J. were generated in the Palestinian territories in the year 2000 using privately owned generators. Most of this generated electricity was used in the industrial sector (85.7%), whereas 9.4% was used in the constructions sector. Therefore, it is reasonable to assume that 85.7% of gas emissions from the electricity generation sector are generated at the industrial locations and stone quarries whereas the remaining is generated in residential areas. Therefore, 85.7% of the calculated CO2 and non-CO2 gas emissions generated from the electrical generation sector were spatially linked to the industrial sites in the northern, middle and southern West Bank. The amounts of gas emissions attributed to each industrial site were a function of the location of the industrial site (Northern, or middle or southern West Bank) and on the spatial extent of the industrial site. On the other hand 14.3% of gas emissions from this sector were linked to the centers of the cities. The amounts of gas emissions attributed to each city were a function of the location of the city (Northern, or middle or southern West Bank) and on its spatial extent.

Residential Consumption Sector: Most of the fuel in the residential sector is used for the purposes of heating and cooking. In the marginalized communities of Palestine, coal and wood are still used in preparing food. Data from the PCBS regarding fuel consumption for residential purposes divides the West Bank into three consumption areas, namely, the northern, middle and southern West Bank. However, it is not possible to assume that fuel consumption per city is only a function of the population of that city, because:

- The fuel needed for heating is a function of the climate which significantly changes over short distances in the West Bank.
- Coal and wood are rarely used for cooking purposes in the main cities

Therefore, fuel consumption and their relevant emission gases are a function of average temperature in winter months, location of the city in one of the three parts of the West Bank (northern, middle and southern), the population in that city and the classification of the city as urban or rural. Based on the above the distribution of fuel consumption over the cities was estimated and the relevant emission of CO2 and non-CO2 gases was estimated and attributed to the built-up area geographical database layer.

Manufacturing and industry sector: Data from the PCBS regarding fuel consumption for manufacturing and industry divides the West Bank into three consumption areas, namely, the northern, middle and southern West Bank. The geographic data base contains information on the location and spatial extent of each industrial and stone quarries area in the West Bank. Currently, fuel consumption in each industrial location was estimated on the bases of the area of each industrial site and its location in one of the three parts in the West Bank (North, middle and south). However, if data becomes available on the types and size of industries in each industrial area, better estimates of gas emission from each industrial areas can be calculated.

Economical activities sector: Data from the PCBS regarding fuel consumption for the economical activity sector (construction, services, internal trade, transport, storage and communications) divides the West Bank into three consumption areas, namely, the northern, middle and southern West Bank. Fuel consumption in the construction and services sub-sectors will be spatially linked to the built-up area in the West Bank. Therefore, fuel consumption and their relevant emission gases are a function of the location of the built-up areas in either northern, middle or southern West bank and the spatial extent of each city. Fuel consumption and their relevant gas emissions from internal trade, transport, storage and communications will be added to gas emissions from the transport sector and spatially linked to the road network.

Transport sector: Currently, gas emissions from the transport sector for the years 1996 and 1997 were estimated using the methodology outlined in section *2.3.1.1.2.* Traffic counts on major road intersections for the year 1998 were used to estimate traffic density on the roads of the West Bank. With this information in hand, it was possible to distribute fuel consumption by the transport sector, the internal trade and the transport-communications sub-sectors over the road network in a way that reflects the traffic density. The relevant gas emissions from the road network were then calculated and spatially linked to the road network.

It should be noted that there are data gaps in the emission inventory of the energy sector. Fuel consumption data is missing for some years or for some sub-sectors (e.g. transportation). Moreover, the Israeli army has destroyed the statistical databases at the PCBS and the national petroleum cooperation. The aforementioned institutions are in the process of digitally re-establishing their databases. Once that is accomplished, gas emissions will be estimated and the emission inventory of the energy sector will be completed.

ARIJ is in the process of estimating gas emissions from the other sectors. So far the following has been achieved:

Agricultural sector: The objective of this sector is to link methane and nitrous oxide emissions from the agricultural sector to the spatial database. Relevant to the agricultural sector are the emissions from the domestic livestock sub-sector and the net N2O emissions from agricultural soils. The net N2O emissions from agricultural soils are dependent on the amounts of fertilizer usage, areas cultivated with nitrogen fixing crops, non-nitrogen fixing crops and organic agriculture.

Animal husbandry (livestock): This data is important to estimate methane and nitrous oxides emissions from two sources, namely, enteric fermentation and manure management. Emissions are calculated by applying an emission factor to the number of animals of each livestock type in the country to produce a total for enteric fermentation. The same methodology is applied to estimate emissions from manure management. The emission factor provided by the IPCC guideline is dependent upon the climatic regime. Livestock data was collected for two districts in the West Bank, namely, Tubas and Jericho. ARIJ is currently collecting livestock data for the other districts of the West Bank. Livestock in the West Bank is raised in rural areas mostly as small enterprises. There are no major farming units. Therefore, the estimated emissions from livestock have been spatially linked to village locations.

Table 11: Animal husbandry in the Target Area.

| Animals Unit | ARIJ-Jericho | ARIJ-Tubas | methane | nitrous oxides |
|---|---|---|---|---|
| Dairy Cattle | No (head) | 1030 | | |

| | | |
|---|---|---|
| Other Cattle | No (head) | 1072 |
| Goat + Sheep | No (1000 head) | 67 |
| Chicken No (1000 head) | 940 | 240 |
| Other No (head) | 320 | 20 |

Agricultural soils: This data set is important to estimate N2O emissions from agricultural systems including (1) direct emissions from agricultural soils (2) direct soil emissions of N2O from animal production and (3) indirect N2O emissions from nitrogen used in agriculture. The data required to calculate the abovementioned emissions are:

- Total use of synthetic fertilizer
- Number of Livestock in country per category
- Dry pulses and soybeans produced
- Dry production of other crops
- Area of cultivated organic soils

Total use of synthetic fertilizer: A fraction of synthetic soil fertilizer is directly emitted into the atmosphere. In order to calculate the nitrous oxide emitted into the atmosphere, it is necessary to estimate the total use of synthetic fertilizer. ARIJ has based its estimation of the amount of fertilizer input on the irrigated agricultural areas (citrus trees, date palms, vineyards, bananas, and field crops). The amount of N fertilizer input was estimated by multiplying the rates of "typical" fertilizer usage per hectare for the various crops. It should be noted that irrigated agricultural areas were identified using remote sensing techniques. Fertilizer input data was collected for two districts in the West Bank, namely, Tubas and Jericho. ARIJ is currently collecting N-input data for the other districts of the West Bank. Fertilizer input data and Nitrogen oxides emissions has been linked as attributes to irrigated agricultural fields.

Table 10: Nitrogen input through usage of fertilizers.

| Fertilizer Type | Crop type (t N/yr) | Tubas and Jericho |
|---|---|---|
| Chem Fertilizer | Citrus | 653 |
| Chem Fertilizer | Date Palm | 691 |
| Chem Fertilizer | Vineyards | 595 |
| Chem Fertilizer | Banana | 1182 |
| Chem Fertilizer | Field Crops/Vegetables | 3451 |
| Chem Fertilizer | Non-Citrus fruit | 10 |
| Chem Fertilizer | Other crops | 0 |
| Chem Fertilizer | Greenhouses | 12 |

Nitrogen from animal waste: Number of animals per category has been collected for Tubas and Jericho. Once the data is available for all districts, the fraction of Nitrogen released into the atmosphere from animal waste will be calculated using the IPC guidelines.

No data is yet available as regards to the net production of dry pulses and soybeans, dry production of other crops, and area of cultivated organic soils. If this data is not available at the ministry of agriculture, the net dry production will be estimated from the areas cultivated with theses crops. However, such estimates will not be very accurate as it difficult to accurately differentiate between crops using remote sensing techniques.

## 2.6 Assessing the collected and/or analyzed data for spatial accuracy

Validation of maps through GPS-readings

To ensure the spatial accuracy of the data, ARIJ has collected ground truthing points using a differential Global Positioning System of major map reference points (such as confluences, road junctions, bridges, roads crossings, waterways, pipelines) with a description of the reference point, the longitude/latitude readings, and the location of the point in the relevant map set. The ground truth points were used to

geometrically rectify the LANDSAT, IKONOS and SPOT satellite image into the UTM system (UTM, WGS 84) using a first order polynomial transformation. The same ground truth points were used to reproject the maps used in this project from the Palestinian coordinate system to the UTM system. The reason for reprojecting the maps into the UTM system is to allow spatial harmonization of the datasets collected between the partners. Project partners are recommended to reproject their data into the standard, well established UTM projection system.

### 2.7 Establishment of a metadatabase

ARIJ has established an appropriate project metadatabase. This was essential to organize the wealth of data that the project has generated so far. Meanwhile, the metadatabase has become a central feature for data documentation and updating.

The metadatabase consists of the following fields:

- Data set ID (Text, 10):
  This field contains the project partner acronym plus an internal ID for the data set
- Contents (Text, 100):
  This field contains a short description of data set: e.g. secondary roads, built-up area
- Purpose (Text, 100):
  This field contains a description of purpose or intended use of data set. This is important to assess the usability and to avoid improper use of data
- DataType (Text, 50):
  This field contains a description of the data type (statistical, polygon, point, line, grid, image etc.)
- DataFormat (Text, 50):
  This field contains a description of the data format (document, spreadsheet, raster data, vector data etc.)
- MapExtent (Text, 50):
  This field contains a verbal description of the spatial reference of data
- MapScale (Number Long, 4):
  This field contains a number that refers to the 1/Scale ratio (e.g. the number 50000 refers to a scale of 1:50000).
- Accuracy (Number Long, 4):
  This field contains a number that indicates the estimated spatial accuracy in meters (suggested numbers are >1000 - 1000 - 300 - 100 - 30 - 10 - 3 - 1)
- Projection (Text, 50):
  This field contains the projection type (UTM, PalGrid, Lambert etc.) & projection parameters (spheroid, datum)
- DataHolder (Text, 50):
  This field contains the institute and person who actually hold the data physically.
- Source (Text, 100):
  This field contains a description of the original data source(s). It is important to document these sources (such as original maps, books, statistics, surveys) to follow up on accuracy and errors.
- TemporalExtent (Text, 50):
  This field contains a description of temporal extent of data that refer to regular time series (e.g. yearly, weekly, daily, one-off).
- ProductionDate (Text, 50):
  This field should exactly document the production date or the last revision date of the data set
- DataAttributes (Memo)
  This field contains a description of the data attributes. Data attributes are parameters of data or the distribution of data classes. Also, all data coding should be documented here. If necessary, a separate file should be generated and documented in the "FileName" data field.
- FileName (Text, 200):
  This field documents the exactly full name of the file or files that make up the data set. File-names should refer to the nomenclature or should be self-explaining.
- UpdateHistory (Memo):
  This field contains a documentation of all changes in the data holdings (e.g. "*dd-mm-yy: all names corrected*"; "*dd-mm-yy: new georeferencing in UTM-WGS4 format*"; "*dd-mm-yy: extended data base*").
  If there are many updates, the update history should be documented an extra file which then should be referenced in the SharedFiles data field as well as in the UpdateHistory field.

- Comments (Memo):
  Comments on personal observations, reservations, trustworthiness, resolution of raster data, restrictions of use.

The metadatabase has been defined in both MS Access and MS Excel formats. However, because of the better possibilities for documentation and data harmonization the Access format has been given preference.

At present, the metadatabase documents 50 records. Figure 1 shows an example of a metadatabase record.

Figure 1: Example of a data set from the metadatabase

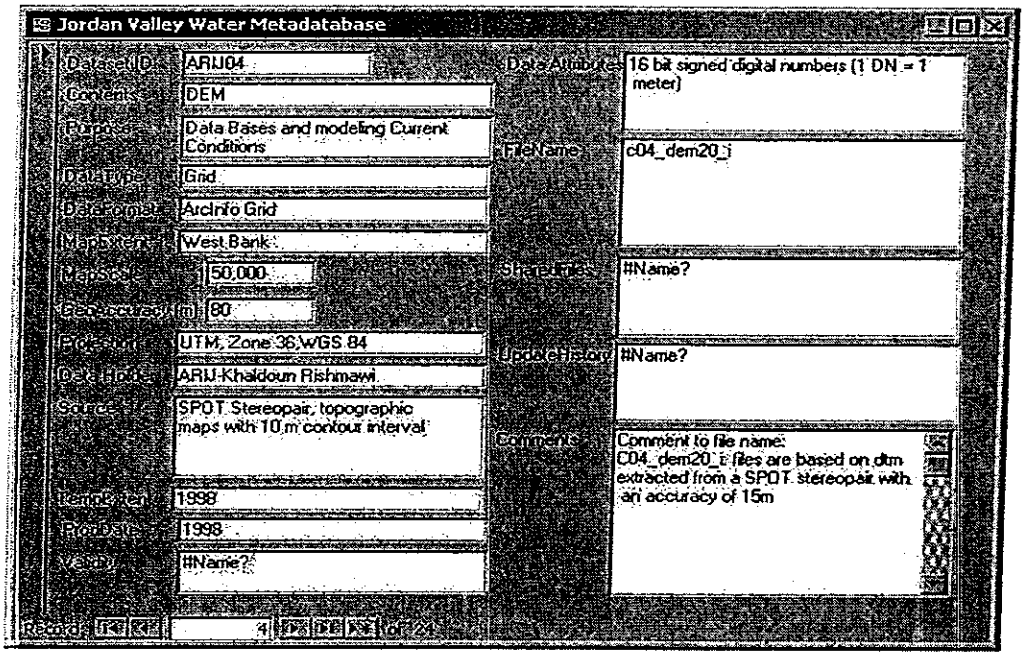


53

### 2.8 Incomplete data sets

Several data sets that have been collected by ARIJ contain data gaps. Several other data sets have not been collected yet. The following will be collected during the next phase of project implementation:

Land use/cover data: The land use/cover data needs to be refined. In particular more detailed information as regards to the types of agricultural crops should be extracted from RS images. A detailed landuse/cover map has been generated for the Jericho and tubas districts. The same will be generated for the remaining districts in the West Bank. The reason for the delays in accurately mapping the agricultural patterns in the West Bank is the inability of the project team to move within the West Bank to collect a sufficient number of ground truth points necessary to extract detailed and accurate information from satellite images. However, if the project team cannot travel within the West Bank during the coming few months, aerial photos from the year 1996 will be used as reference points in the detailed classification of the satellite images.

Roughness length and Albedo: Data will be generated by the Applied Research Institute.

Climatological data: information on historical records of wind speed was not available. ARIJ contacted the National Authority Metrological offices to provide the required data. Moreover, cloudiness data is not available. A potential solution is to use AVHRR data from the NOAA orbiting satellites. Other datasets required by the project such as data on the upper level meteorological conditions are not available in Palestine.

Emission inventory data: Data on gas emissions from the energy sector still contain data gaps. The PCBS and other national authority agencies has been contacted to provide statistical data. Data from the other sectors are largely dependent on the generation of the detailed landuse map.

Animal Husbandry: Data on livestock by category in the West Bank has been collected but not yet integrated into GIS. ARIJ is currently calculating the methane and Carbon dioxide emissions from the livestock. The emission data will then be integrated into GIS.

Installation of the Monitoring stations: The two monitoring stations have not been installed yet due to security concerns. Israeli scientists and technicians are not permitted to visit their Palestinian counterparts and Palestinian scientists and technicians are not permitted to travel to Israel. The two stations are now at the Hebrew University Jerusalem. Following the course to be held at Rutgers University, Palestinian scientists and technicians will acquire the knowledge necessary to run and maintain the stations. Consequently, the American embassy will facilitate the transfer of equipment from Israel to Palestine.

### 2.9 Re-distribution of digital data

Following the completion of the data sets, project partners should agree upon which data sets will be shared among partners. Data sets will both be GIS data layers and excel spreadsheets. The redistribution should be made through electronic media such as CD-ROMs. Harmonization of GIS datasets between project partners is important to facilitate the other activities of the project.

### 2.10 ARIJ responsibilities during the next phase (Third Year) of project implementation

The following will be done during the third year of project implementation:

- Filling the data gaps listed under section 2.9
- Training two technicians from ARIJ on the running and the maintenance of the meteorological stations
- Installation of the two meteorological and air quality monitoring stations
- Execution of three short term intensive field observational campaigns that will involve measurements of both meteorological and air quality parameters
- Modeling current and past meteorological and pollutant conditions

# 3 DIFFICULTIES ENCOUNTERED

The data collection activities have experienced considerable delays. The reasons for this will be discussed in the following sections in order to facilitate "lessons to learn" for both the project team and the USAID. It should be noted, however, that following discussion of difficulties should not overshadow the accomplishments of the project team.

In order to emphasize the aggregated nature of this section, names from partners are generally not mentioned here. This section is not about accusations of partners or "passing the buck". This section should document the generic nature of difficulties that might be inherent in projects like this one. The summary of the difficulties should help to learn on how to best deal with such difficulties or how such problems can (or can't) be prevented.

## 3.1 Data availability and reliability

The scarcity of reliable data about fuel consumption, waste generation, and fertilizer usage in the West Bank posed a major problem in this project. Many data were simply estimated (even if using logical assumptions).

For instance, it was very difficult to access data for the Israeli settlements in the West Bank. For security concerns, the ARIJ in whose domain these settlements are located could not collect the required data directly. On the other hand, even if data existed, it was sometimes difficult or impossible to collect. The Palestinian authority digital databases were destroyed or confiscated by the Israeli army.

One problem that had not been anticipated at the project preparation is that some of the excellent existing data on water resources and the water supply system would be available only if the project partners would pay for data. As in most countries government data on natural resources would be publicly available, funding for "buying data" has not been sufficiently been considered in this project. Thus, in many cases, ARIJ had to use surrogate data or even own estimates to fill the data gaps.

Lessons to learn for future projects are to be aware that the collection of data is an important part of such projects that must not be underestimated during project planning. Even if common sense (and proposal evaluators) says: "all data are available" this does not necessarily mean that they can be easily accessed.

## 3.2 Cooperation between project partners

The nature of this project, which deals with transboundary pollutants, requires cooperation and collaboration between project partners during and after the implementation of the project; cooperation in the following tasks is important:

Training of Palestinian technicians on the meteorological and air quality monitoring instruments: Currently the Palestinian scientists are prohibited to travel into Israel to receive training; therefore the training was replaced to take place in the United States. Delays in issuing the United States Visa has already made it impossible twice for the trainees to travel to the United States in time for training.

Transfer of the meteorological and air quality monitoring instruments: The instruments were purchased and are now at the Hebrew University Jerusalem (HUJ). Several contacts were made with the HUJ to transfer the equipment but to no avail.

Local meetings, the semi-annual Mideast project meeting and the annual Mideast project meeting: The objectives of theses meetings are to agree on the type and format of the database as well as the temporal and spatial resolution of each data set. These meetings are also brainstorm meetings at which the difficulties encountered by each project partner can be discussed to the point of jointly concluding appropriate solutions.

## 3.3 Movement within the West Bank

Field trips and surveys necessary to collect current meteorological and air quality parameters as well as for the purpose of assessing the accuracy of data obtained from the analysis of RS data were not accomplished due to the restrictions on movement imposed on the Palestinian scientists even between the districts of the West Bank. Alternative measures such as the use of very high resolution satellite data and aerial photos were used for assessing the accuracy of the Land use/cover map obtained from the RS images. However, detailed land use/cover maps require extensive field trips in order to identify the different agricultural practices and patterns.

55

### 3.4 Delays due to curfew or closure

During the last year, Bethlehem was invaded several times by Israeli forces, which imposed a curfew on the district for a sum of around 80 working days. This, in addition to the restriction on movement within and to the outside of the West Bank has caused a considerable delay in implementing the work schedule aforethought at the launch of the project.

## ANNEX 1: Harmonized Data Sets: ARIJ Metadatabase

| | |
|---|---|
| ***Dataset ID*** | ***ARIJ01*** |
| ***Contents*** | Road network |
| ***Purpose*** | Data Bases and modeling Current Conditions |
| Data Type | Line |
| Data Format | ArcView Shape |
| Map Extent | West Bank |
| Map Scale | 10,000 |
| Accuracy | 5 |
| Projection | UTM, Zone 36, WGS 84 |
| Data Holder | ARIJ-Khaldoun Rishmawi |
| | Source Combination of LandSat ETM+, Spot images, and IKONOS images |
| Temporal Extent | Continuously updated |
| Production Date | 2002 |
| Data Attributes | Codes: 1 main roads, 2 secondary roads, 3 bypass roads, Traffic, (CO2, N-oxides, Methane, Non-Methane volatile organic compounds, Sulfur |
| File Name | Main road.shp, Secondary road.shp, existing by pass road.shp, |

| | |
|---|---|
| ***Dataset ID*** | ***ARIJ02*** |
| Contents | Built-up areas |
| Purpose | Data Bases and modeling Current Conditions |
| Data Type | Point |
| Data Format | ArcView Shape |
| Map Extent | West Bank |
| Map Scale | 50,000 |
| Accuracy | 25 |
| Projection | UTM, Zone 36, WGS 84 |
| Data Holder | ARIJ-Khaldoun Rishmawi |
| Source | Combination of LandSat ETM+, Spot images, and |

| | |
|---|---|
| | IKONOS images |
| Temporal Extent | Continuously updated |
| Production Date | 2002 |
| Data Attributes | Population, households, solid waste generation, waste water generation |
| File Name | Built-up with pop 97.shp |
| Comments | |

| ***Dataset ID*** | ***ARIJ03*** |
|---|---|
| Contents | Background image |
| Purpose | Visualization |
| Data Type | Image |
| Data Format | TIFF |
| Map Extent | West Bank |
| Map Scale | 0 |
| Accuracy | 25 |
| Projection | UTM, Zone 36, WGS 84 |
| Data Holder | ARIJ-Khaldoun Rishmawi |
| Source | ARIJ |
| Temporal Extent | 2001 |
| Production Date | 03. 05. 2001 |
| Data Attributes | 8 bit digital numbers |
| File Name | c03_9005sub.tif |
| Comments | TM bands used: 4/R -3/G - 2/B; |

| ***Dataset ID*** | ***ARIJ04*** |
|---|---|
| Contents | DEM |
| Purpose | Data Bases and modeling Current Conditions |
| Data Type | Grid |
| Data Format | ArcInfo Grid |
| Map Extent | West Bank |
| Map Scale | 50,000 |
| Accuracy | 80 |
| Projection | UTM, Zone 36, WGS 84 |
| Data Holder | ARIJ-Khaldoun Rishmawi |
| | Source SPOT Stereo pair, topographic maps with 10 m Contour interval |
| Temporal Extent | 1998 |
| Production Date | 1998 |

| | |
|---|---|
| Data Attributes | 16 bit signed digital numbers (1 DN = 1 meter) |
| File Name | c04_dem20_i |
| Comments | file is based on DTM extracted from a SPOT stereo pair with an accuracy of 15m |

| | |
|---|---|
| ***Dataset ID*** | ***ARIJ05*** |
| Contents | Administrative units |
| Purpose | Visualization |
| Data Type | Polygons |
| Data Format | ArcView shape |
| Map Extent | West Bank |
| Map Scale | 50,000 |
| Accuracy | 100 |
| Projection | UTM, Zone 36, WGS 84 |
| Data Holder | ARIJ-Khaldoun Rishmawi |
| Source | Geopolitical maps |
| Temporal Extent | 1995-1999 |
| Production Date | 1999 |
| Data Attributes | District Borders |
| File Name | c05_admin_ply.shp |
| Comments | This data set is only for relating statistical data with Geographic entities. It does not have any political significance. |

| | |
|---|---|
| ***Dataset ID*** | ***ARIJ06*** |
| Contents | Land use/cover |
| Purpose | Data Bases and modeling Current Conditions |
| Data Type | Grid |
| Data Format | ArcInfo Grid |
| Map Extent | West Bank |
| Map Scale | 10,000 |
| Accuracy | 5 |
| Projection | UTM, Zone 36, WGS 84 |
| Data Holder | ARIJ-Khaldoun Rishmawi |
| | Source Analysis of a Combination of LandSat ETM+, Spot images, IKONOS images and Aerial Photos |
| Temporal Extent | 2001 |
| Production Date | 2001 |
| Data Attributes | Land Use/Cover ID, Land Use/Cover - text, emission rates (CO2, N-oxides, Methane, Non-Methane volatile organic compounds and Sulfur oxides) |

| | |
|---|---|
| File Name | c07_landuse |
| Comments | |

| | |
|---|---|
| ***Dataset ID*** | ***ARIJ07*** |
| Contents | Boundaries of Target Research Area |
| Purpose | Data Bases and modeling Current Conditions |
| Data Type | Polygons |
| Data Format | ArcView Shape |
| Map Extent | West Bank |
| Map Scale | 50,000 |
| Accuracy | 100 |
| Projection | UTM, Zone 36, WGS 84 |
| Data Holder | ARIJ-Khaldoun Rishmawi |
| Source | Geopolitical maps |
| Temporal Extent | 2001 |
| Production Date | 2001 |
| Data Attributes | Area, perimeter |
| File Name | c08_bound_ta.shp |
| Comments | |

| | |
|---|---|
| ***Dataset ID*** | ***ARIJ08*** |
| Contents | Nature reserves |
| Purpose | Data Bases and modeling Current Conditions |
| Data Type | Polygon |
| Data Format | ArcView Shape |
| Map Extent | West Bank |
| Map Scale | 50,000 |
| Accuracy | 70 |
| Projection | UTM, Zone 36, WGS 84 |
| Data Holder | ARIJ-Khaldoun Rishmawi |
| Source | Israeli - Palestinian agreements |
| Temporal Extent | 2000 |
| Production Date | 2000 |
| Data Attributes | Area, perimeter |
| File Name | c11_natreserv.shp |
| Comments | |

| | |
|---|---|
| ***Dataset ID*** | ***ARIJ09*** |
| Contents | Israeli Closed Military Areas |

59

| | |
|---|---|
| Purpose | Data Bases and modeling Current Conditions |
| Data Type | Polygon |
| Data Format | ArcView Shape |
| Map Extent | West Bank |
| Map Scale | 20,000 |
| Accuracy | 70 |
| Projection | UTM, Zone 36, WGS 84 |
| Data Holder | ARIJ-Khaldoun Rishmawi |
| Source | Israeli Maps |
| Temporal Extent | 1993 |
| Production Date | 1993 |
| Data Attributes | Area, perimeter |
| File Name | c12_closedmil.shp |
| Comments | |

| ***Dataset ID*** | ***ARIJ10*** |
|---|---|
| Contents | location of olive mills |
| Purpose | Point location of pollutant sources |
| Data Type | Point |
| Data Format | ArcView Shape |
| Map Extent | West Bank |
| Map Scale | 0 |
| Accuracy | 300 |
| Projection | UTM, Zone 36, WGS 84 |
| Data Holder | ARIJ-Khaldoun Rishmawi |
| Source | Field Surveys using Ordinary GPS (No differential correction) |
| Temporal Extent | 1995 |
| Production Date | 1995 |
| Data Attributes | Olive Cake, CO2 emissions, Methane and Non-Methane Volatile Organic compounds) |
| File Name | c13_olivemills.shp |
| Comments | derived from non-differential GPS. Data can have range between 0 - 300 m. |

| ***Dataset ID*** | ***ARIJ11*** |
|---|---|
| Contents | military bases |
| Purpose | Point location of pollutant sources |
| Data Type | Polygon |
| Data Format | ArcView Shape |
| Map Extent | West Bank |
| Map Scale | 50,000 |
| Accuracy | 70 |
| Projection | UTM, Zone 36, WGS 84 |
| Data Holder | ARIJ-Khaldoun Rishmawi |
| Source | Aerial Photos |
| Temporal Extent | Continuously Updated |
| Production Date | 2002 |
| Data Attributes | area, perimeter, name, source |
| File Name | c17_milbases.shp |
| Comments | |

| ***Dataset ID*** | ***ARIJ12*** |
|---|---|
| Contents | Location of industrial zones |
| Purpose | Point location of pollutant sources |
| Data Type | Point |
| Data Format | ArcView Shape |
| Map Extent | West Bank |
| Map Scale | 0 |
| Accuracy | 300 |
| Projection | UTM, Zone 36, WGS 84 |
| Data Holder | ARIJ-Khaldoun Rishmawi |
| Source | Field Surveys using ordinary GPS (No differential correction) |
| Temporal Extent | Continuously updated |
| Production Date | 2002 |
| Data Attributes | join_id, source, name, x/y-coordinate, emissions |
| File Name | c19_industry.shp |
| Comments | |

| ***Dataset ID*** | ***ARIJ13*** |
|---|---|
| Contents | Gas Stations Locations |
| Purpose | Point location of pollutant sources |
| Data Type | Point |

| | |
|---|---|
| Data Format | ArcView Shape |
| Map Extent | West Bank |
| Map Scale | 0 |
| Accuracy | 300 |
| Projection | UTM, Zone 36, WGS 84 |
| Data Holder | ARIJ-Khaldoun Rishmawi |
| Source | Field Surveys using ordinary GPS (No differential correction) |
| Temporal Extent | Continuously updated |
| Production Date | 2002 |
| Data Attributes | source, location, emissions |
| File Name | c21_gas_station.shp |
| Comments | |

| ***Dataset ID*** | ***ARIJ14*** |
|---|---|
| Contents | Greenhouses |
| Purpose | Data Bases and modeling Current Conditions |
| Data Type | Polygon |
| Data Format | ArcView Shape |
| Map Extent | West Bank |
| Map Scale | 20,000 |
| Accuracy | 50 |
| Projection | UTM, Zone 36, WGS 84 |
| Data Holder | ARIJ-Khaldoun Rishmawi |
| Source | Analysis of Aerial Photos |
| Temporal Extent | 1995 |
| Production Date | 1995 |
| Data Attributes | source, emissions |
| File Name | c22_greenhouses.shp |
| Comments | derived from non-differential GPS. Data can have range between 0 - 300 m. |

| ***Dataset ID*** | ***ARIJ15*** |
|---|---|
| Contents | Israeli Colonies |
| Purpose | Modeling and Planning |
| Data Type | Polygon |
| Data Format | ArcView Shape |
| Map Extent | West Bank |
| Map Scale | 50,000 |

| | |
|---|---|
| Accuracy | 70 |
| Projection | UTM, Zone 36, WGS 84 |
| Data Holder | ARIJ-Khaldoun Rishmawi |
| Source | Analysis of a combination of LandSat ETM+, Spot Images and Aerial Photos |
| Temporal Extent | Continuously updated |
| Production Date | 2002 |
| Data Attributes | Population, households, solid waste generation, waste water generation |
| File Name | c24_colonies.shp |
| Comments | |

| | |
|---|---|
| ***Dataset ID*** | ***ARIJ16*** |
| Contents | Solid Waste Open Dumping Sites |
| Purpose | Point location of pollutant sources |
| Data Type | Point |
| Data Format | ArcView Shape |
| Map Extent | West Bank |
| Map Scale | 0 |
| Accuracy | 300 |
| Projection | UTM, Zone 36, WGS 84 |
| Data Holder | ARIJ-Khaldoun Rishmawi |
| | Source Field Surveys using ordinary GPS (No differential correction) |
| Temporal Extent | Continuously updated |
| Production Date | 2002 |
| Data Attributes | emission rates (CO2, N-oxides, Methane, Non-Methane volatile organic compounds and Sulfur Oxides Dioxides) |
| File Name | c25_solid_waste.shp |
| Comments | |

| | |
|---|---|
| ***Dataset ID*** | ***ARIJ17*** |
| Contents | Waste water streams |
| Purpose | Line location of pollutant sources |
| Data Type | Line |
| Data Format | ArcView Shape |
| Map Extent | West Bank |
| Map Scale | 20,000 |

| | |
|---|---|
| Accuracy | 70 |
| Projection | UTM, Zone 36, WGS 84 |
| Data Holder | ARIJ-Khaldoun Rishmawi |
| Source | LandSat ETM+ |
| Temporal Extent | 2001 |
| Production Date | 2001 |
| Data Attributes | emission rates (CO2, N-oxides, Methane, Non-Methane volatile organic compounds and Sulfur Oxides |
| File Name | c27_open_wastewater.shp |
| Comments | |

| ***Dataset ID*** | ***ARIJ18*** |
|---|---|
| Contents | Meteorological Stations |
| Purpose | Data Bases and modeling Current Conditions |
| Data Type | Point |
| Data Format | ArcView Shape |
| Map Extent | West Bank |
| Map Scale | 0 |
| Accuracy | 0 |
| Projection | UTM, Zone 36, WGS 84 |
| Data Holder | ARIJ-Khaldoun Rishmawi |
| Source | ARIJ database |
| Temporal Extent | 1995 |
| Production Date | 2001 |
| Data Attributes | Join_Ids to excel files, x/y location |
| File Name | Meteorological Station.shp |
| Comments | |

| ***Dataset ID*** | ***ARIJ19*** |
|---|---|
| Contents | Rainfall Gauges |
| Purpose | Data Bases and modeling Current Conditions |
| Data Type | Point |
| Data Format | ArcView Shape |
| Map Extent | West Bank |
| Map Scale | 0 |
| Accuracy | 0 |
| Projection | UTM, Zone 36, WGS 84 |
| Data Holder | ARIJ-Khaldoun Rishmawi |
| Source | ARIJ database |

| | |
|---|---|
| Temporal Extent | 1995 |
| Production Date | 2001 |
| Data Attributes | Join_Ids to excel files, x/y location |
| File Name | Rainfall Gauge.shp |
| Comments | |

| ***Dataset ID*** | ***ARIJ20*** |
|---|---|
| Contents | Agricultural Weather Stations |
| Purpose | Data Bases and modeling Current Conditions |
| Data Type | Point |
| Data Format | ArcView Shape |
| Map Extent | West Bank |
| Map Scale | 0 |
| Accuracy | 0 |
| Projection | UTM, Zone 36, WGS 84 |
| Data Holder | ARIJ-Khaldoun Rishmawi |
| Source | ARIJ database |
| Temporal Extent | 1995 |
| Production Date | 2001 |
| Data Attributes | Join_Ids to excel files, x/y location |
| File Name | Agricultural Weather Station.shp |
| Comments | |

| ***Dataset ID*** | ***ARIJ21*** |
|---|---|
| Contents | Proposed Palestinian industrial Zones |
| Purpose | Data Bases and modeling Future Conditions |
| Data Type | Point |
| Data Format | ArcView Shape |
| Map Extent | West Bank |
| Map Scale | 0 |
| Accuracy | 0 |
| Projection | UTM, Zone 36, WGS 84 |
| Data Holder | ARIJ-Khaldoun Rishmawi |
| Source | ARIJ database |
| Temporal Extent | 1995 |
| Production Date | 2001 |
| Data Attributes | X/Y location |
| File Name | Proposed industrial area.shp |
| Comments | |

| | |
|---|---|
| ***Dataset ID*** | ***ARIJ22*** |
| Contents | Jordan River |
| Purpose | Modeling and Planning |
| Data Type | Polygon |
| Data Format | ArcView Shape |
| Map Extent | West Bank |
| Map Scale | 10,000 |
| Accuracy | 25 |
| Projection | UTM, Zone 36, WGS 84 |
| Data Holder | ARIJ-Khaldoun Rishmawi |
| Source | Recent TM images |
| Temporal Extent | 2000 |
| Production Date | 2001 |
| Data Attributes | Length |
| File Name | E_Jordan.shp |
| Comments | |

| | |
|---|---|
| ***Dataset ID*** | ***ARIJ23*** |
| Contents | Israeli Industrial Zones |
| Purpose | Point location of pollutant sources |
| Data Type | Polygon |
| Data Format | ArcView Shape |
| Map Extent | West Bank |
| Map Scale | 10,000 |
| Accuracy | 25 |
| Projection | UTM, Zone 36, WGS 84 |
| Data Holder | ARIJ-Khaldoun Rishmawi |
| Source | Field Surveys |
| Temporal Extent | 1999 |
| Production Date | 2000 |
| Data Attributes | Area, perimeter |
| File Name | Israeli Industrial Zone.shp |
| Comments | |

| | |
|---|---|
| ***Dataset ID*** | ***ARIJ24*** |
| Contents | Dead Sea |
| Purpose | Modeling and Planning |
| Data Type | Polygon |

| | |
|---|---|
| Data Format | ArcView Shape |
| Map Extent | West Bank |
| Map Scale | 10,000 |
| Accuracy | 25 |
| Projection | UTM, Zone 36, WGS 84 |
| Data Holder | ARIJ-Khaldoun Rishmawi |
| Source | Recent TM images |
| Temporal Extent | 2000 |
| Production Date | 2001 |
| Data Attributes | Area, Perimeter |
| File Name | Dead Sea.shp |
| Comments | |

| **Dataset ID** | **ARIJ25** |
|---|---|
| **Contents** | monthly precipitation |
| **Purpose** | Modeling |
| **Data Type** | Point |
| **Data Format** | Point shape file |
| **Map Extent** | WB |
| **Map Scale** | 0 |
| **Accuracy** | 0 |
| **Projection** | UTM, Zone 36, WGS 84 |
| **Data Holder** | ARIJ-Rania Rishmawi |
| **Source** | ARIJ weather database,meteorological office of ministry of transport,agricultural departments,PHG, |
| **Temporal Extent** | 1953-1999 |
| **Production Date** | 2002 |
| **Data Attributes** | monthly average rainfall from Jan-Dec for the specified years |
| **File Names** | (Dah,arro,heb,tarq,yatta,idna,dura,baninaim,beitola),( arraba,maithaloun,yabad,tammoun,beitqad,,jenin,qaba |
| **Comments** | Data are based on the files:ARIJ:(Hebron,Jenin,Nablus,Bethlehem,Tulkarm, jericho, jerusalem,ramallah).xls |

| **Dataset ID** | **ARIJ26** |
|---|---|
| **Contents** | monthly temperature |
| **Purpose** | Modeling |
| **Data Type** | Point |

| | |
|---|---|
| **Data Format** | Point shape file |
| **Map Extent** | WB |
| **Map Scale** | 0 |
| **Accuracy** | 0 |
| **Projection** | UTM, Zone 36, WGS 84 |
| **Data Holder** | ARIJ-Rania Rishmawi |
| **Source** | ARIJ weather database, meteorological office of ministry of transport, agricultural departments, PHG, |
| **Temporal Extent** | 1968-1992 |
| **Production Date** | 2002 |
| **Data Attributes** | monthly minimum and maximum temperature from Jan-Dec for the specified years |
| **File Names** | (hebron, nablus, jericho, tiratzvi,, jerusalem)-max-temp,-min-temp.dbf |
| **Comments** | Data are based on the files: ARIJ:(Hebron, Jenin, Nablus, Bethlehem, Tulkarm, jericho, jerusalem, ramallah).xls |

| | |
|---|---|
| **Dataset ID** | ARIJ40 |
| **Contents** | CO2 gas-emissions-Energy Sector |
| **Purpose** | inventory |
| **Data Type** | Point |
| **Data Format** | Excel spreadsheet file |
| **Map Extent** | WB |
| **Map Scale** | 0 |
| **Accuracy** | 0 |
| **Projection** | 0 |
| **Data Holder** | ARIJ-Rania Rishmawi |
| **Source** | Palestinian Central Bureau of Statistics(PCBS),IPCC Guidelines tables, general petroleum corporation |
| **Temporal Extent** | 1996-1999 |
| **Production Date** | 2002 |
| **Data Attributes** | consumption(TJ),carbon emission factor,carbon content(Gg C),Net Carbon emissions(GgC),fraction of carbob oxidized,Actual carbon emissions(Gg C),actual CO2 emissions(GgCO2) |
| **File Names** | Reference Approach(1996-1999).xls,generating Electricity (1997-1999).xls,resedintial(1996- |
| **Comments** | in generating electricity there is missing data in year 1996 |

| | |
|---|---|
| **Dataset ID** | ARIJ41 |
| **Contents** | Non-CO2 gas-emissions-Energy sector |
| **Purpose** | inventory |
| **Data Type** | Point |
| **Data Format** | Excel spreadsheet file |
| **Map Extent** | WB |
| **Map Scale** | 0 |
| **Accuracy** | 0 |
| **Projection** | 0 |
| **Data Holder** | ARIJ-Rania Rishmawi |
| **Source** | Palestinian Central Bureau of Statistics(PCBS),IPCC Guidelines tables,general petroleum corporation |
| **Temporal Extent** | 1996-1999 |
| **Production Date** | 2002 |
| **Data Attributes** | consumption(TJ),emission factor for each fuel type(Kg/Tj),,emissions of non-CO2 gases from the activities in Gg |
| **File Names** | Carbon monoxide(1996-1999).xls,methane(1996-1999).xls,nitrogen dioxide(1996-1999).xls nitrous |
| **Comments** | in non co2 files there is still missing data in the consumption in transportation sector |

| | |
|---|---|
| **Dataset ID** | ARIJ47 |
| **Contents** | Non-CO2 gas emissions-Waste sector |
| **Purpose** | inventory |
| **Data Type** | Point |
| **Data Format** | Excel spreadsheet file |
| **Map Extent** | WB |
| **Map Scale** | 0 |
| **Accuracy** | 0 |
| **Projection** | 0 |
| **Data Holder** | ARIJ-Rania Rishmawi |
| **Source** | interviews with municipilities Engineers,IPCC Guidelines tables |
| **Temporal Extent** | 1996-1999 |
| **Production Date** | 2002 |
| **Data Attributes** | total annual municipal solidwaste(Gg),methane correction factor,fraction of DOC which actually degrades,fraction of carbon released as methane, |

| | |
|---|---|
| | potential methanr generation rate(Gg), Realised rate, gross annual methane generation(Gg CH40, net annual methanet annual methane emissions(GgCH4) |
| **File Names** | |
| **Comments** | there is still missing data about jaiyus dumping site |

| | |
|---|---|
| **Dataset ID** | ARIJ42 |
| **Contents** | CO2 emission-Industrial processes sector |
| **Purpose** | inventory |
| **Data Type** | Point |
| **Data Format** | Excel spreadsheet file |
| **Map Extent** | WB |
| **Map Scale** | 0 |
| **Accuracy** | 0 |
| **Projection** | 0 |
| **Data Holder** | ARIJ-Rania Rishmawi |
| **Source** | Palestinian Central Bureau of Statistics(PCBS),IPCC Guidelines tables |
| **Temporal Extent** | 1996-1999 |
| **Production Date** | 2002 |
| **Data Attributes** | quantity of specific industry produced, emission factor, CO2 emitted(Gg) |
| **File Names** | |
| **Comments** | Data to be collected |

| | |
|---|---|
| **Dataset ID** | ARIJ43 |
| **Contents** | non-CO2 emissions-industrial processes sector |
| **Purpose** | inventory |
| **Data Type** | Point |
| **Data Format** | Excel spreadsheet file |
| **Map Extent** | WB |
| **Map Scale** | 0 |
| **Accuracy** | 0 |
| **Projection** | 0 |
| **Data Holder** | ARIJ-Rania Rishmawi |
| **Source** | Palestinian Central Bureau of Statistics(PCBS),IPCC Guidelines tables |
| **Temporal Extent** | 1996-1999 |

| | |
|---|---|
| **Production Date** | 2002 |
| **Data Attributes** | quantity of specific industry produced, emission factor, non-CO2 gases emitted(Gg) |
| **File Names** | |
| **Comments** | Data to be collected |

| | |
|---|---|
| **Dataset ID** | ARIJ44 |
| **Contents** | non-CO2 emissions- Agriculture sector |
| **Purpose** | inventory |
| **Data Type** | Point |
| **Data Format** | Excel spreadsheet file |
| **Map Extent** | WB |
| **Map Scale** | 0 |
| **Accuracy** | 0 |
| **Projection** | 0 |
| **Data Holder** | ARIJ-Rania Rishmawi |
| **Source** | Palestinian Central Bureau of Statistics(PCBS),IPCC Guidelines tables, Ministry of agriculture |
| **Temporal Extent** | 1996-1999 |
| **Production Date** | 2002 |
| **Data Attributes** | methane and nitrous oxide emissions from domestic livestock, field burning of agricultural residue, agricultural soils |
| **File Names** | |
| **Comments** | Data to be collected |

| | |
|---|---|
| **Dataset ID** | ARIJ45 |
| **Contents** | CO2 emissions-Land-Use Change and Forestry sector |
| **Purpose** | inventory |
| **Data Type** | Point |
| **Data Format** | Excel spreadsheet file |
| **Map Extent** | WB |
| **Map Scale** | 0 |
| **Accuracy** | 0 |
| **Projection** | 0 |
| **Data Holder** | ARIJ-Rania Rishmawi |
| **Source** | ARIJ land use database, Palestinian Central Bureau of Statistics (PCBS),IPCC Guidelines tables |
| **Temporal Extent** | 1996-1999 |

| | |
|---|---|
| **Production Date** | 2002 |
| **Data Attributes** | CO2 emissions from changes of forests, impacted soils, managed soils |
| **File Names** | |
| **Comments** | Data to be collected |
| **Dataset ID** | ARIJ46 |
| **Contents** | Non-CO2 emissions- Land- Use Change and Forestry sector |
| **Purpose** | inventory |
| **Data Type** | Point |
| **Data Format** | Excel spreadsheet file |
| **Map Extent** | WB |
| **Map Scale** | 0 |
| **Accuracy** | 0 |
| **Projection** | 0 |
| **Data Holder** | ARIJ-Rania Rishmawi |
| **Source** | ARIJ land use database, Palestinian Central Bureau of Statistics (PCBS), IPCC Guidelines tables |
| **Temporal Extent** | 1996-1999 |
| **Production Date** | 2002 |
| **Data Attributes** | non-CO2 gases from burning biomass |
| **File Names** | |
| **Comments** | Data to be collected |
| **Dataset ID** | ARIJ27 |
| **Contents** | monthly pressure |
| **Purpose** | Modeling |
| **Data Type** | Point |
| **Data Format** | Point shape file |
| **Map Extent** | WB |
| **Map Scale** | 0 |
| **Accuracy** | 0 |
| **Projection** | UTM, Zone 36, WGS 84 |
| **Data Holder** | ARIJ-Rania Rishmawi |
| **Source** | ARIJ weather database |
| **Temporal Extent** | 1964-1992 |
| **Production Date** | 2002 |
| **Data Attributes** | monthly pressure from Jan-Dec for the specified years |

| | |
|---|---|
| **File Names** | Hebron-pressure72-92.dbf, Jericho-pressure70-92.dbf, Jerusalem-pressure64-92,.bf |
| **Comments** | Data are based on the files:ARIJ: Hebron.xls,Jericho.xls,Nablus.xls, Jerusalem.xls , data to be collected for the other istricts |

| | |
|---|---|
| **Dataset ID** | ARIJ28 |
| **Contents** | monthly wind speed |
| **Purpose** | Modeling |
| **Data Type** | Point |
| **Data Format** | Point shape file |
| **Map Extent** | WB |
| **Map Scale** | 0 |
| **Accuracy** | 0 |
| **Projection** | UTM, Zone 36, WGS 84 |
| **Data Holder** | ARIJ-Rania Rishmawi |
| **Source** | ARIJ weather database |
| **Temporal Extent** | 1964-1992 |
| **Production Date** | 2002 |
| **Data Attributes** | monthly wind speed from Jan-Dec for the specified years |
| **File Names** | hebron-wind-knot68-92.dbf, nablus-wind-knot70-92.dbf, jericho-wind-knot68-92.dbf, tiratzvi-wind- |
| **Comments** | Data are based on the files:ARIJ: Hebron.xls,Jericho.xls,Nablus.xls, Jerusalem.xls, data to be collected for the missing districts and years |

| | |
|---|---|
| **Dataset ID** | ARIJ34 |
| **Contents** | annual wind speed |
| **Purpose** | Modeling |
| **Data Type** | Point |
| **Data Format** | Point shape file |
| **Map Extent** | WB |
| **Map Scale** | 0 |
| **Accuracy** | 0 |
| **Projection** | UTM, Zone 36, WGS 84 |
| **Data Holder** | ARIJ-Rania Rishmawi |
| **Source** | meteorological office of ministry of transport, |

| | |
|---|---|
| | Jerusalem meteorological station (Israel) |
| **Temporal Extent** | 1964-1992 |
| **Production Date** | 2002 |
| **Data Attributes** | annual wind speed for the specified years |
| **File Names** | Jericho-wind 68-92.dbf, Jerusalem-wind 64-92.dbf |
| **Comments** | Data are based on the files: ARIJ: Jericho.xls, Jerusalem.xls. data to be collected for the remaining districts and years |

| | |
|---|---|
| **Dataset ID** | ARIJ31 |
| **Contents** | annual precipitation |
| **Purpose** | Modeling |
| **Data Type** | Point |
| **Data Format** | Point shape file |
| **Map Extent** | WB |
| **Map Scale** | 0 |
| **Accuracy** | 0 |
| **Projection** | UTM, Zone 36, WGS 84 |
| **Data Holder** | ARIJ-Rania Rishmawi |
| **Source** | meteorological office of ministry of transport, agricultural departments |
| **Temporal Extent** | 1923-1998 |
| **Production Date** | 2002 |
| **Data Attributes** | annual rainfall for the specified years |
| **File Names** | bethlehem1900-96.dbf, jenin52-95.dbf, jericho23-98.dbf, ramallah74-98.dbf, tulkarm52-95.dbf |
| **Comments** | Data are based on the files: ARIJ: Jericho.xls, ramallah.xls, bethlehem.xls, Jenin .xls, tulkarm.xls. data to be collected for the remaining |

| | |
|---|---|
| **Dataset ID** | ARIJ32 |
| **Contents** | annual temperature |
| **Purpose** | Modeling |
| **Data Type** | Point |
| **Data Format** | Point shape file |
| **Map Extent** | WB |
| **Map Scale** | 0 |
| **Accuracy** | 0 |
| **Projection** | UTM, Zone 36, WGS 84 |

| | |
|---|---|
| **Data Holder** | ARIJ-Rania Rishmawi |
| **Source** | meteorological office of ministry of transport, Jerusalem meteorological station (Israel) |
| **Temporal Extent** | 1964-1992 |
| **Production Date** | 2002 |
| **Data Attributes** | annual temperature for the specified years |
| **File Names** | jericho-temp68-92.dbf, Jerusalem-temp64-92.dbf, nablus-temp70-92.dbf |
| **Comments** | Data are based on the files: ARIJ: Jericho.xls, Jerusalem.xls, Nablus.xls data to be collected for remaining districts and years. |

| | |
|---|---|
| **Dataset ID** | ARIJ33 |
| **Contents** | annual pressure |
| **Purpose** | Modeling |
| **Data Type** | Point |
| **Data Format** | Point shape file |
| **Map Extent** | WB |
| **Map Scale** | 0 |
| **Accuracy** | 0 |
| **Projection** | UTM, Zone 36, WGS 84 |
| **Data Holder** | ARIJ-Rania Rishmawi |
| **Source** | jerusalem meteorological station(israel) |
| **Temporal Extent** | 1964-1992 |
| **Production Date** | 2002 |
| **Data Attributes** | annual pressure for the specified years |
| **File Names** | jerusalem-pressure64-92.dbf |
| **Comments** | Data are based on the file:ARIJ:Jerusalem.xls, data to be collected for the remaining districts and years |

| | |
|---|---|
| **Dataset ID** | ARIJ29 |
| **Contents** | monthly humidity |
| **Purpose** | Modeling |
| **Data Type** | Point |
| **Data Format** | Point shape file |
| **Map Extent** | WB |
| **Map Scale** | 0 |
| **Accuracy** | 0 |
| **Projection** | UTM, Zone 36, WGS 84 |

| | |
|---|---|
| **Data Holder** | ARIJ-Rania Rishmawi |
| **Source** | meteorological office of ministry of transport, agricultural departments, Israel metrological |
| **Temporal Extent** | 1964-1992 |
| **Production Date** | 2002 |
| **Data Attributes** | monthly humidity from Jan-Dec for the specified years |
| **File Names** | hebron-hum68-92.dbf, arro-hum80-84.dbf, Jericho-hum68-92.dbf, tiratzvi-hum64-92.dbf,,jerusalem- |
| **Comments** | Data are based on the files:ARIJ:Jericho.xls,Jerusalem.xls,Nablus.xls, Hebron.xls, data to be collected for the remaining districts and years |

| | |
|---|---|
| **Dataset ID** | ARIJ30 |
| **Contents** | monthly evaporation |
| **Purpose** | Modeling |
| **Data Type** | Point |
| **Data Format** | Point shape file |
| **Map Extent** | WB |
| **Map Scale** | 0 |
| **Accuracy** | 0 |
| **Projection** | UTM, Zone 36, WGS 84 |
| **Data Holder** | ARIJ-Rania Rishmawi |
| **Source** | meteorological office of ministry of transport Israel metrological services |
| **Temporal Extent** | 1970-1992 |
| **Production Date** | 2002 |
| **Data Attributes** | monthly evaporation from Jan-Dec for the specified years |
| **File Names** | jericho-evaporation70-92, tiratzvi-evaporation68-92.dbf, nablus-evaporation81-92 |
| **Comments** | Data are based on the files: ARIJ: Jericho.xls, Nablus.xls. data to be collected for the remaining districts and years |

| | |
|---|---|
| **Dataset ID** | ARIJ35 |
| **Contents** | annual humidity |
| **Purpose** | Modeling |
| **Data Type** | Point |
| **Data Format** | Point shape file |
| **Map Extent** | WB |

| | |
|---|---|
| **Map Scale** | 0 |
| **Accuracy** | 0 |
| **Projection** | UTM, Zone 36, WGS 84 |
| **Data Holder** | ARIJ-Rania Rishmawi |
| **Source** | meteorological office of ministry of transport, Jerusalem meteorological station (Israel) |
| **Temporal Extent** | 1964-1992 |
| **Production Date** | 2002 |
| **Data Attributes** | annual humidity for the specified years |
| **File Names** | jerusalem-hum64-92.dbf, jericho-hum68-92.dbf |
| **Comments** | Data are based on the files: ARIJ: Jericho.xls, Jerusalem.xls data to be collected for the remaining districts and years |

| | |
|---|---|
| **Dataset ID** | ARIJ36 |
| **Contents** | daily precipitation |
| **Purpose** | Modeling |
| **Data Type** | Point |
| **Data Format** | Point shape file |
| **Map Extent** | WB |
| **Map Scale** | 0 |
| **Accuracy** | 0 |
| **Projection** | UTM, Zone 36, WGS 84 |
| **Data Holder** | ARIJ-Rania Rishmawi |
| **Source** | meteorological office of ministry of transport |
| **Temporal Extent** | 1983-1995 |
| **Production Date** | 2002 |
| **Data Attributes** | daily rainfall for the specified years |
| **File Names** | jenin83.dbf,,jenin84.dbf,,jenin85.dbf,jenin86.dbf,jeni n87.dbf,,jenin88.dbf,jenin89.dbf,jenin90.dbf,,jenin91 |
| **Comments** | Data are based on the file:ARIJ:Jenin.xls,data to be collected for the remaining districts and years |

| | |
|---|---|
| **Dataset ID** | ARIJ37 |
| **Contents** | Insolation |
| **Purpose** | Modeling |
| **Data Type** | Point |
| **Data Format** | Point shape file |
| **Map Extent** | WB |

| | |
|---|---|
| **Map Scale** | 0 |
| **Accuracy** | 0 |
| **Projection** | UTM, Zone 36, WGS 84 |
| **Data Holder** | ARIJ-Rania Rishmawi |
| **Source** | meteorological office of ministry of transport |
| **Temporal Extent** | 1980-1995 |
| **Production Date** | 2002 |
| **Data Attributes** | Insolation value for the specified years |
| **File Names** | |
| **Comments** | Data to be collected |

| | |
|---|---|
| **Dataset ID** | ARIJ38 |
| **Contents** | turbulence |
| **Purpose** | Modeling |
| **Data Type** | Point |
| **Data Format** | Point shape file |
| **Map Extent** | WB |
| **Map Scale** | 0 |
| **Accuracy** | 0 |
| **Projection** | UTM, Zone 36, WGS 84 |
| **Data Holder** | ARIJ-Rania Rishmawi |
| **Source** | meteorological office of ministry of transport |
| **Temporal Extent** | 1980-1995 |
| **Production Date** | 2002 |
| **Data Attributes** | turbulence value for the specified years |
| **File Names** | |
| **Comments** | Data to be collected |

| | |
|---|---|
| **Dataset ID** | ARIJ39 |
| **Contents** | mixing height |
| **Purpose** | Modeling |
| **Data Type** | Point |
| **Data Format** | Point shape file |
| **Map Extent** | WB |
| **Map Scale** | 0 |
| **Accuracy** | 0 |
| **Projection** | UTM, Zone 36, WGS 84 |

| | |
|---|---|
| **Data Holder** | ARIJ-Rania Rishmawi |
| **Source** | meteorological office of ministry of transport |
| **Temporal Extent** | 1980-1995 |
| **Production Date** | 2002 |
| **Data Attributes** | mixing height value for the specified years |
| **File Names** | |
| **Comments** | Data to be collected |

## References

[1] The revised 1996 IPCC guidelines for national Green House Gas Inventory. Work book, (Vol. 2)

[2] Palestinian Central Bureau of statistics, dissemination &documentation Dept., division of Users Services, DUS-1 energy conversion factor.

[3] http://www.risoe.dk/sys/esy/emiss_e/emf25082000.xls

Appendix B: EPRI contributions

# Transboundary Air-Quality Effects from Urbanization

Report No. 2

for the period of

March 2001-August 2002

Award No.: M18-054

prepared by

Dr. Yasser El-Hahhal

Environmental Protection Research Institute (EPRI)

Gaza City, Gaza

July 2002

## 1. Introduction

This report summarizes work carried out since Report 1 at EPRI on the USAID/MERC project: Transboundary Air Quality Effects from Urbanization.

## 2. Accomplishments

### a. Meetings

After Prof. Bornstein left the area, meetings continued in the Gaza and West Bank between EPRI, ARIJ, and U. S. Embassy (Tel Aviv) personnel. Topics discussed included future cooperation for the instrumentation site selection, and data collection and analysis tasks.

### b. New observational site selection

An appropriate site was tentatively selected and approved by Mr. David Cohen of the U. S. Embassy in Tel Aviv. The site is located within Gaza City and satisfies all EPA criteria for an urban air quality site. All instruments were thus shipped and temporarily stored at the HJUI to await training of a Gaza scientist in their installation and use.

### c. EPA class

Given the current situation, it was not possible to conduct the instrumentation training at the HUJI, as originally proposed. Thus after some delay, arrangements were made for Dr. Yasser El-Nahhal of EPRI to obtain the instrument training at an EPA sanctioned class at Rutgers University during July 2002. Dr. El-Nahhal then visited SJSU to obtain additional on-site monitoring experience at a facility operated by the San Francisco Bay Area Air Quality Monitoring District (BAAQMD). He also presented a seminar at SJSU on his EPRI research.



82

**d. Student selection**

Mr. Khalil El-Khateeb was selected by EPRI to study for a M.S. in Environmental Studies, with an emphasis in Meteorology, at SJSU starting in October 2002. The student has a B. S. degree in Environmental Sciences in 2002 from the Islamic University of Gaza. His course of study will include an emphasis on environmental planning, GIS analyses, and air pollution meteorology.

**e. Emission inventories**

The following activities were carried out in Gaza to assemble the information necessary to produce the detailed source emission inventories required for future numerical air quality simulations:

i. Several meeting was held with scientists from the main Gaza engineering consulting group to obtain information the operational characteristics of the major non-residential stationary pollutant sources in the Gaza industrial zone

ii. Several meeting was held with the site manager and scientists from the Gaza meteorological station, operated by the Palestinian Ministry of Transportation. Information was obtained in the form of annual reports of fuel usage in the West bank and Gaza. Data were generally segmented by fuel type, geographic distribution, month to month usage, and industrial sector usage.

**f. Meteorological data analysis**

The meeting with the site manager and scientists from the Gaza meteorological station also provided hourly meteorological observations (e.g., temperature, pressure, wind velocity, relative humidity, insolation, and precipitation) from three Gaza sites for 2000.

### g. Ambient concentrations analysis

The meeting with the Gaza engineering consults also provided information concerning 1999-2000 hourly concentrations of gaseous and particulate pollutants at two non-residential sites close to the northeast Gaza industrial zone. Site 1 is located north of the zone, while Site 2 is located southeast of the zone. Data included values of nitrogen dioxide ($NO_2$), carbon monoxide C0), sulfur dioxide ($SO_2$), and hydrogen sulfide ($H_2S$). Analyses were carried out on the raw data to produce average monthly distributions of each pollutant at each site (daily and/or eight hour averages, as well as monthly maximum values).

### h. Results

The monthly variation of CO concentrations (Fig. 1) show Site 1 values normally higher than Site 2 values for all three statistics (daily and eight hour averages, and monthly maximum values). Peak values for all three statistics tend to occur during spring months.

The reverse pattern is true for daily and maximum (8 h values not available) $SO_2$ values, with higher values generally found at Site 2 (Fig. 2). Seasonal trends are clearer for $SO_2$ than for CO, as both sites show again strong spring peaks, but $SO_2$ now shows low summer values.

For 24 h $H_2S$ (only averaging period available), data are only available for the second half of the period. No pattern exists as to which site is more polluted, and no clear monthly pattern is yet shown (Fig. 3). Only limited data (last month of study) are thus far available for $NO_2$ at either site.

An understanding of the processes producing the above variations must include concurrent analyses of available meteorological data, a process that has just begun. Monthly temperature values (Fig. 5) show the expected diurnal (daytime warmer than nighttime) and seasonal (summer peak and winter minimum) variations at both sites. As Site 2 is somewhat south of Site 1, it is generally the warmer of the two.

**i. Future**

Future efforts will focus on

i. installation of the new urban meteorological and air quality Gaza monitoring site

ii. collection of data from the urban new site

iii. comparison of new urban data with that from two existing industrial sites

iv. development of explanations of daily and monthly variations in air quality in terms of observed meteorological patterns

v. completion of Gaza emission inventory

vi. blending of Gaza emissions with those from the rest of the study area

vii. have Mr. Khalil El-Khateeb study environmental management at SJSU

viii. have Dr. Yasser El-Nahhal learn MM5 meteorological and CAMEX photochemical modeling at SJSU.



85

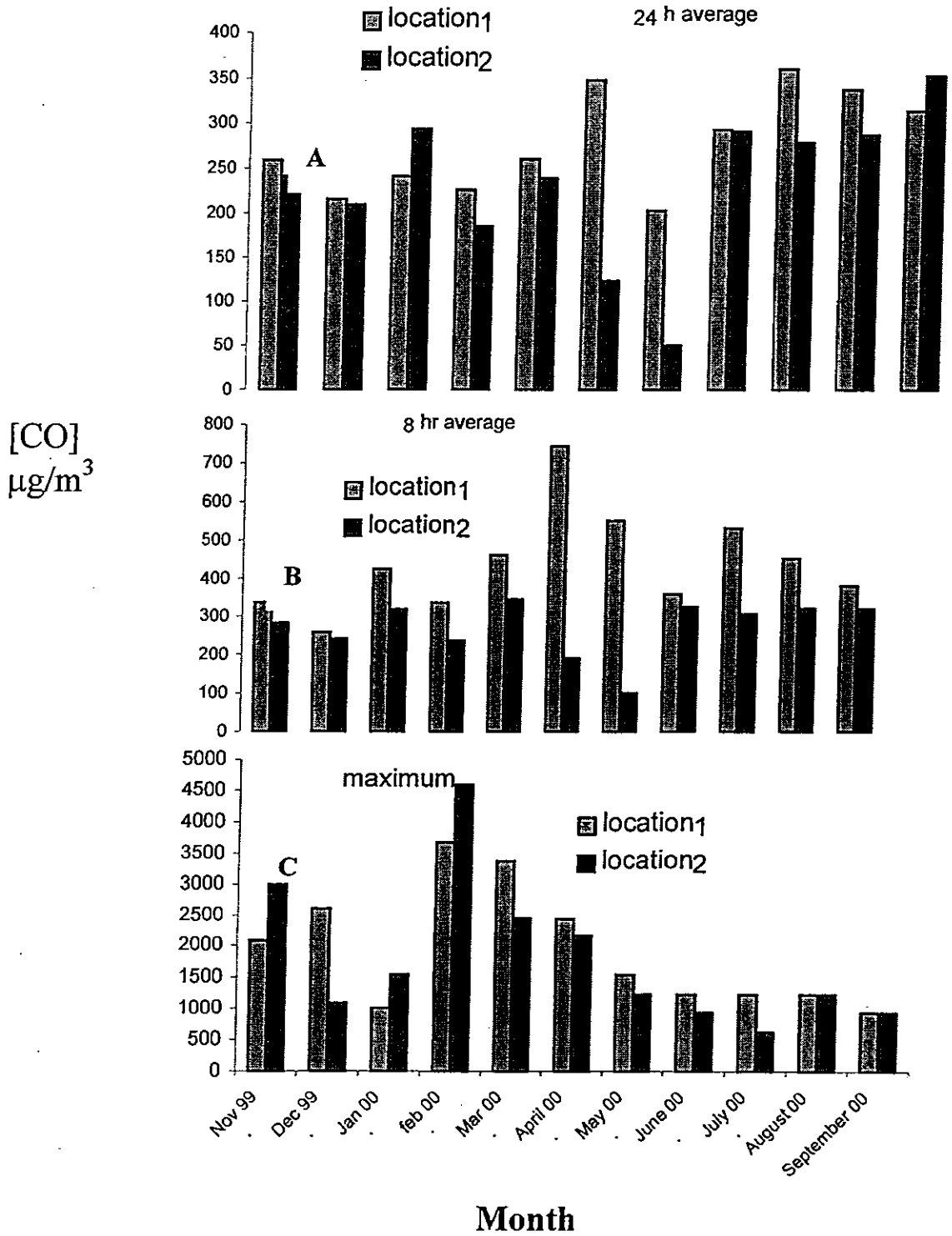


Figure 1. Concentration of carbon monoxide as an avaerage of 24 h (A), as average of 8h (B) and as a maximum concentration (C) in different locations in Gaza strip. The location represins non- residential area.

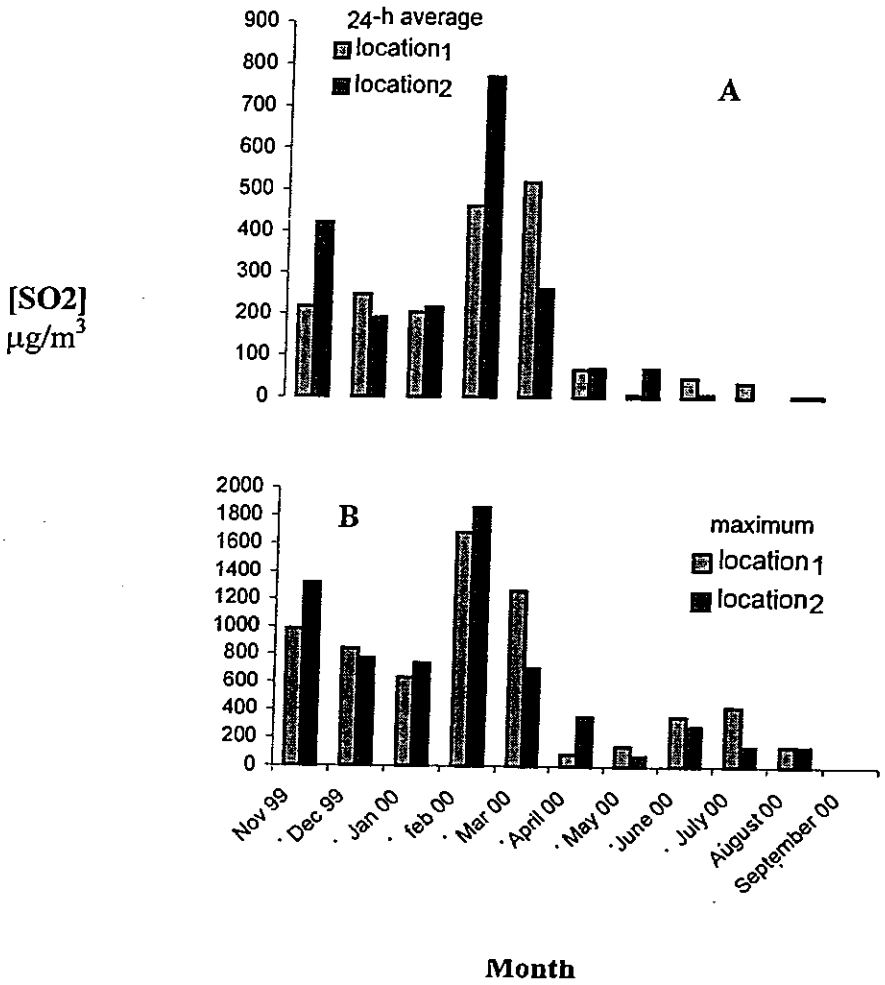


Figure 2 concentration of sulfer dioxide as an average of 24 h (A) and as maximum concentration (B) in different non- residential area distributed along in Gaza strip.

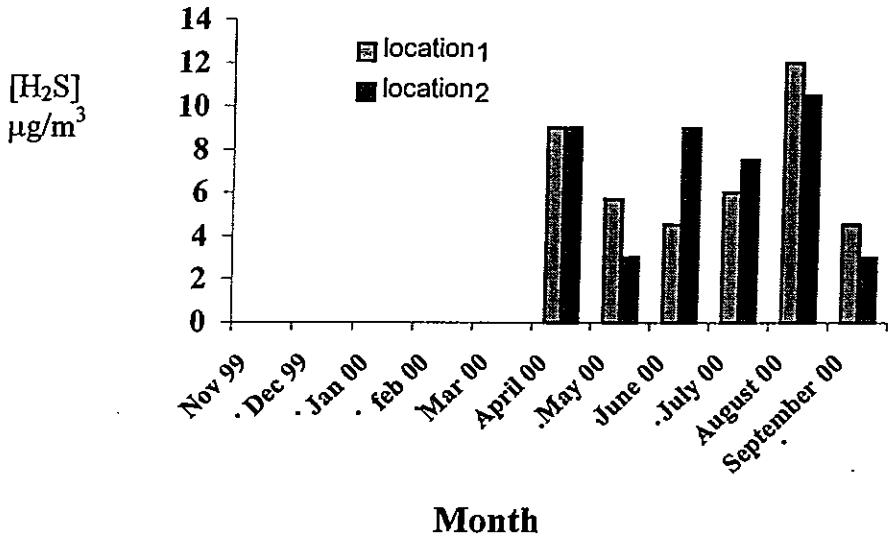


Figure 3. 24 h period concentration of hydrogen sulfide in different non- residential area distributed along in Gaza strip.

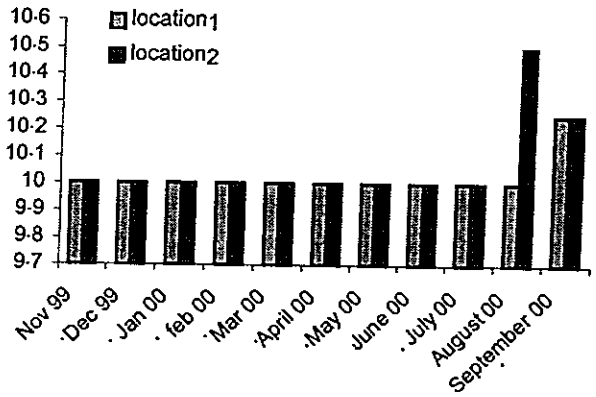


Figure 4. Concentration of nitrogen dioxide in different non- residential area distributed along in Gaza strip.

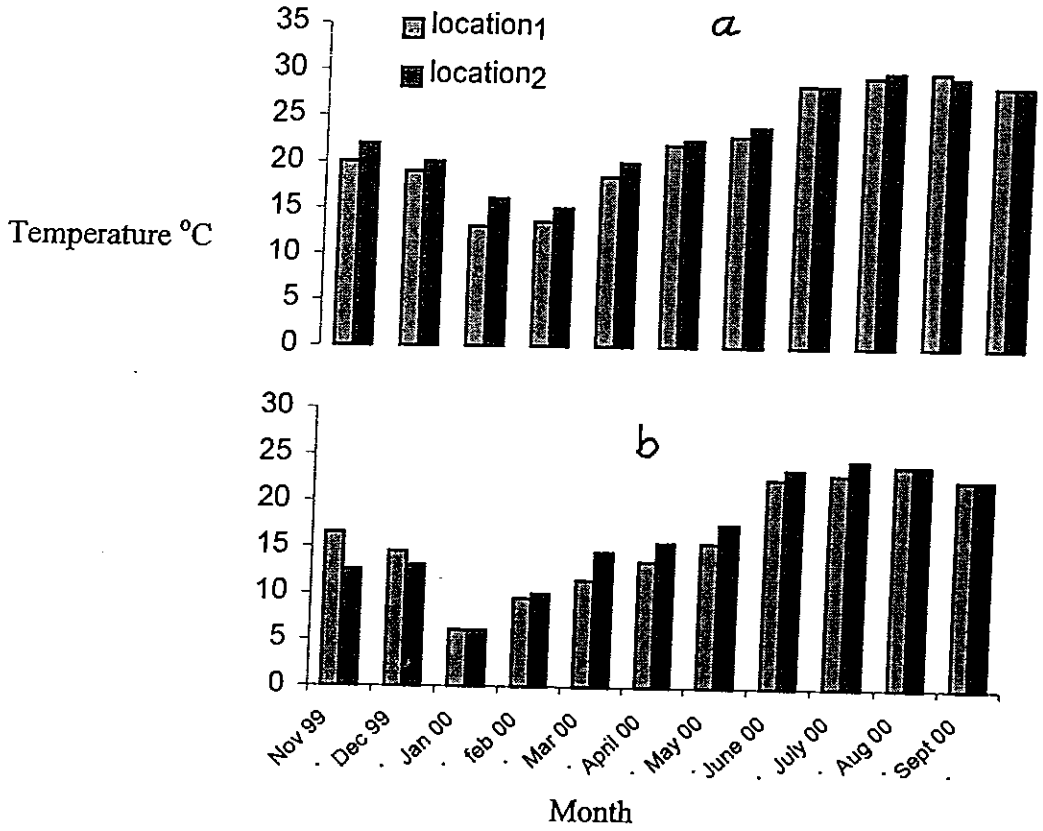


Figure 5. Magnitude of temperature at different non- residential area distributed along in Gaza strip, during the day (a) and during night (b).

Appendix C: Ali Rahmah (ARIJ) Ph.D. work to date at DRI

Desert Research Institute

June 10, 2002

**Memorandum**

To: Bob Bornstein, SJSU

From: Alan Gertler, DRI/UNR

Subject: Ali Abu-Rahmah

Attached is Mr. Ali Abu-Rahmah's summary of his progress to-date. Ali arrived in Reno on February 4. The deadline for registering for classes had already passed; however, he sat in on ATMS 748, Measurements in the Atmosphere and received a grade of B+ on his term paper. This was one of the top grades in the class so I am quite pleased by his performance.

In addition to his studies, Ali has been learning how to use a number of air quality tools, with an emphasis on receptor modeling. While I don't anticipate this will be part of his dissertation research, this will help him in future air quality studies.

This month we are beginning a new study funded by SERDP (Strategic Environmental Research and Defense Program) entitled "Development and Validation of a Predictive Model To Assess The Impact of Coastal Operations On Urban Scale Air Quality." Prof. Menachem Luria from the Hebrew University is a co-investigator on this study and Ali will work closely with him on the chemical modeling component. Ali will play a major role in this study and it will form the basis of his dissertation.

Overall, Ali is making excellent progress. Please don't hesitate to contact me if you have any questions or require additional information.

## Progress Report to the USAID

**Dear Sir/Madam:**

In this report, I would like to summarize my academic performance during the Spring 2002, which represents the first semester of postgraduate study at the University of Nevada, Reno, US. The Ph.D. program in Atmospheric Science consists of both course and research work. I have made progress in both these areas under the supervision of Dr. Alan Gertler.

In terms of course work, I participated in the Measurement in the Atmosphere course taught by Dr. John Hallett. I gained useful training on a wide range of meteorological devices including the Wind Profiler, Radio Acoustic Sounding System (RASS), Net Radiometer and the Radiosonde. I used this up-to-day technology to obtain and analyze data to describe the case study of a temperature inversion that occurred in the Reno basin on the 9$^{th}$ of March 2002. This case study was presented as a term paper, which was submitted in partial fulfillment of the course requirements, for which I received a grade of B$^{+}$. A copy of the term paper can be submitted, if necessary.

In terms of my research, I have received training on the use of the Chemical Mass Balance (CMB) air quality model. I used this model to estimate the fraction of particulate matter emitted from light- and heavy-duty vehicles in a highway tunnel.

In the Fall 2002, two of the Atmospheric Science Program core courses, Introduction to Atmospheric Physics and Mathematical Physics. I plan to attend both classes. Also, I will be involved in a new air quality modeling study that involves the application of a number of air quality models including the Urban Airshed Model (UAM) and the Regional Atmospheric Modeling System (RAMS).

.

Finally, I wish to express my appreciation and thanks to the USAID foundation for funding this study and I hope that the progress reported above is good enough to sustain their financial support.

**Development and Validation of a Predictive Model To Assess The Impact of Coastal Operations On Urban Scale Air Quality - Project CP-1253**

## OBJECTIVES

The primary objective of the proposed study is to develop and validate a prognostic modeling system capable of assessing the impact of coastal DoD operations on air quality. Included in this objective are the determination of primary and secondary pollutant concentrations, as well as their spatial and temporal variation. In order to accomplish this objective, the proposed study will address the following questions:

*What is the chemical composition of the emissions and their associated emission rates?* We propose to account for emission rates of $NO_x$, $SO_2$, and PM from ships, PM and $NO_x$ from on-shore diesel activities, and $NO_x$, CO, speciated hydrocarbons, and PM from other on-shore activities.

*What is the impact of coastal meteorology on air quality?* To answer this question we will model the impact of air mass transport and dispersion, coastal thermodynamics and dynamics (surface winds, on-shore/off-shore flow, temperature, and relative humidity), the presence or absence of liquid water, and changes in mixing height on air quality.

*What is the influence of the land/sea interface on atmospheric chemistry?* The proposed research approach includes the contributions from heterogeneous versus homogeneous reaction pathways, appropriate deposition velocities for estimating the fate of the primary and secondary pollutants, and the affect of land/sea interface on photolysis and reaction rate parameters.

Finally, we hope to provide a tool that can be used to develop and implement effective strategies to reduce the impact of DoD operations on urban scale air quality.

## TECHNICAL APPROACH

In order to achieve the stated objective of the SON we propose four tasks. These tasks include the preparation of an emissions inventory that includes on-shore and off-shore activities, the development of a prognostic modeling system using state-of-the art meteorological, transport, and chemical modules, the use of detailed meteorological data from current DoD coastal operations to drive the meteorological and transport modules of the model, evaluation of the uncertainty in the model predictions, a verification of the model predictions using real-world data, and transitioning and reporting of the results of this study to DoD. We will test and evaluate the model for the San Diego area.

The four tasks and associated approaches are as follows:

Task 1: Emissions Inventory Development

An emission inventory for primary PM emissions, the $O_3$ forming precursors ($NO_x$ and VOC), and PM forming precursors ($SO_2$, $NO_x$, $NH_3$, and VOC), along with carbon monoxide (CO) will be developed for each domain to be modeled. In addition to the county specific emissions inventory that will form the basis of our initial emissions estimate, the development of the emission inventory will include an assessment of the levels of DoD activity in the modeling domain that produces an emission and the emission factor for that operation. This assessment will consist of identification of specific source categories and types (e.g., combustion sources such as diesel and gasoline powered vehicles, aircraft, ships, electrical generation and evaporative sources such as fuel storage, solvent use, painting operations, etc.) and their associated emission factors. Following the evaluation, assessment, and estimation of emission factors for the domain to be modeled (San Diego), an initial emissions inventory taking into account both the civilian (county specific) and DoD related emissions will be developed. The emissions inventory will then be evaluated and compared against other available inventories to check its reliability and a revised inventory will be prepared, if deemed necessary.

Task 2: Prognostic Modeling System Development

As part of this task we will develop a versatile prognostic system that can be used to assess the impact of various military emission sources on mesoscale and regional air quality. The modeling system will be composed of three integrated components:

- An emissions processing system that will allow area sources, stationary sources, and mobile sources to be entered into the model in a user-friendly manner.
- A prognostic meteorological component that uses operationally available forecasts for the domain of interest.
- A prognostic hybrid Lagrangian random particle dispersion component-model coupled with a Eulerian chemical component-model that uses output from the meteorological component to simulate the transport, dispersion, and the chemical transformations of pollutants emanating from specified emission sources.

The area to be modeled, including the military operation region and the metropolitan area, will be specified and an available forecast of atmospheric fields will be accessed from the NPS through the computer network.

Atmospheric Transport and Dispersion Module

In order to accommodate a wide range of types and numbers of possible sources, their positions and displacements, and short-term variations in emission rates, we propose to use a Lagrangian random particle dispersion model that has been developed at the Desert Research Institute (DRI) and evaluated against the tracer experiment data in complex terrain. Besides the advantage of using predicted or analyzed wind fields to track air particles, our Lagrangian particle model can determine turbulence transfer using mean meteorological parameters as input. An innovative approach of scaling vertical randomness with the turbulence kinetic energy values has also been included. The Lagrangian random particle model estimates the dispersion of pollutants by tracking a large number (on the order of millions) of hypothetical particles in the domain. The fate of the particles is determined by the simulated atmospheric fields and a modeled direct link

between the turbulence transfer and dispersion. Since particles are traced in time and space and represents a unique Lagrangian entity for specifying continuous chemical treatment and transformations. In addition, environmental atmospheric parameters at every point of the domain are available from the meteorological model in the Eulerian framework. The Lagrangian random particle dispersion model is capable of simultaneously treating multiple sources (point, line, areal, and volume) without restrictions on position and movement, as well as on prescribed time variation of emission rates. In the case of a known source emission rate, the model can predict the magnitude of concentrations in all three dimensions. In the case of an unknown emission

Chemistry Module and Lagrangian-Eulerian-Lagrangian Translation

One of the key issues in developing the hybrid model is the linking of the Eulerian chemistry module with the Lagrangian random particle dispersion model. The chemistry module consists of a chemical driver (Lagrangian to Eulerian and Eulerian to Lagrangian transformation modules) that includes an emissions module, gas-phase chemistry module, cloud and aqueous phase transformation module, aerosol module, and dry deposition module.

The gas-chemistry will be based on the Regional Acid Deposition Mechanism, version 2 (RADM2) and Regional Atmospheric Chemistry Mechanism (RACM), a highly updated version of RADM2. Both are standard atmospheric chemistry mechanisms that are widely used for the modeling of ozone and aerosol formation. Photolysis rate coefficients will be calculated in accord with an actinic flux computed from episode specific lookup tables. The effect of clouds on the photolysis rate coefficients is included. The chemistry will be implemented within a fast chemical solver.

Clouds play a major role in the production of photochemical air pollution. Aqueous-phase reactions in clouds are major contributors to the production of acids that react with ammonia to produce aerosol. Therefore it is important for both the gas-phase mechanism and the aqueous-phase chemical mechanisms to accurately predict chemical concentrations. Cloud/fog information will be derived from MM5 output.

An aerosol module will be used to calculate the concentrations of secondary aerosol from the concentrations of sulfate and nitric acid as described above. The fraction of sulfuric and nitric acid that combines with ammonia to form particulate ammonium nitrate will be parameterized from simulations made with the model, Simulating Composition of Atmospheric Particles at Equilibrium (SCAPE). Aerosol formation and properties using a mechanism such as that included in Models-3, along with deposition will be included in the aerosol module.

The flux of trace gases and secondary aerosol from the atmosphere to the surface will be calculated by multiplying concentrations in the lowest model layer by the spatially and temporally varying deposition velocity, $v_d$. Following this step the chemical concentrations of each Lagrangian particle are saved and the chemical driver returns control to the Lagrangian particle module.

Task 3: Model Validation

As part of the modeling system development, we will evaluate the effects of emissions inventory and meteorological parameter uncertainty on the model predictions. In addition, we will use real-world data to validate the prognostic model results. An airborne air sampling campaign will be employed. These measurements will enable us to determine the rate of ozone formation and $NO_x$ conversion in plumes from sources such as naval ships, determine the rate of secondary aerosol formation (particulate nitrate and sulfate), determine the relative contribution of emissions from DoD activities to regional air quality, and provide database with spatial and temporal resolution of the various reactive chemical species for model testing, calibration and validation.

The sampling campaign will include 60 to 80 hours of flight time during a period of approximately six-weeks during the summer (most likely July). Measurements will be performed during the morning and afternoon periods. The morning flights will be used to characterize the emissions while he afternoon flights will examine the formation of secondary pollutants. The morning flights will be limited to the near sources region (within ~30 km) while the afternoon flights will cover a wider area of up to 120 km from the sources, which is the typical range over which similar plumes can be detected. An arcing sampling method be utilized to enable us to measure the polluted air parcels in a near Lagrangian manner. This procedure will allow the determination of the rate of the change of the various parameters governing the chemical evolution of the polluted air parcels as they age.

Task 4: Reporting and Transition

Attend In-Progress Reviews (IPRs), SERDP Scientific Advisory Board (SAB) meetings, and the annual SERDP Symposium. Prepare annual reports and the final report for SERDP describing the procedures and results of this study. Prepare three papers for peer-reviewed publication describing preparation of the emissions inventory, development of the prognostic model, and model validation. Develop procedures and model output visualizations for use by DoD personnel or subcontractors responsible for assessing air quality impacts of DoD operations as part of the transitioning of this study to DoD.

Appendix D: Dean Ranmar (HUJI) Ph.D. thesis

# OZONE PRODUCTION FROM TRANSPORTATION SOURCES: UTILIZATION AND INTEGRATION OF INTER-DISCIPLINARY COMPUTER MODELS AS A TOOL FOR ENVIRONMENTAL-ORIENTED-IMPROVEMENT OF TRANSPORTATION PLANNING

A Thesis Presented to

The Faculty of Environmental Sciences

Hebrew University of Jerusalem (HUJI)

Israel

In Partial Fulfillment

Of the Requirements for the Degree

Doctor of Science

by

Dean Ranmar

2001

99

# Curriculum Vitae

## *Personal data*


| | | |
|---|---|---|
| Name: | | Dean Orr Ranmar |
| Place of birth: | | [redacted] |
| Address: | Home: | Moshav Kidron (P.O.Box 290), Israel |
| | Tel: | [redacted] |
| | | Work – 972-3-7519226 |
| | e-mail: | ranmar@agri.huji.ac.il |
| | | dean@imbm.org |


Military service: Served in the IDF, 1984-1987

## *Current Occupation*

2001 - The Institute on Medical BioMathematica (www.imbm.org). Working as a scientist in the development of a numerical model describing the pharmacodynamics of special lineage of the immune system (coding in C++).

## *Academic Education*

1997-2001 - **Ph.D.**, The Graduate School of Applied Sciences and Technology/Dept. of Atmospheric Sciences, The Hebrew University of Jerusalem, Israel. **Thesis:** "*Ozone Production from Transportation Sources: Utilization and Integration of Inter-Disciplinary Computer Models as a Tool for Environmental-Oriented-Improvement of Transportation Planing*".

Supervision: **Prof. Isaac Mahrer**, the Seagram center for Soil & Water Sciences and **Prof. Menahem Luria**, Environmental Science Division, the Graduate School of Applied Sciences and Technology the Hebrew University of Jerusalem.

1995-1996 - **Ph.D.**, The Department of Chemical Immunology, The Weizmann Institute of Science, Rehovot Israel. **Proposal submitted:** "*Extracellular Degrading Enzymes: Regulation of Expression, Secretion and Activity by Migration Immune Cells*".

Supervision: **Prof.. Irun R. Cohen** and **Dr. Ofer Lider.**

April 1996 – *Scientific 'Redirection'. Orienting myself in the Atmospheric Science/Environmental Quality and Preservations discipline.*

1991-1994 - **M.Sc.**, Department of Chemical Biology, The Weizmann Institute of Science, Rehovot, Israel. **Thesis:** "*The Effects of Site-Directed Mutagenesis on the Spectroscopic Properties of the Bacterial Reaction Center*".

Supervisor: **Prof. Avigdor Scherz**. Grades: Thesis-97, Examination-97, Courses-93.6.

1988-1991 - **B.Sc.**, in Soil & Water Sciences, The Hebrew University of Jerusalem, Israel. Grade 92.

## *Complementary studies*

(i) *Parallel computing on High Performance Computers (HPC)*

Spent two month (October – November 2000) at the EPCC (Edinburgh Parallel Computing Center) at the Edinburgh University, Scotland, studying parallel coding for shared and distributed memory architectures under the TRACS (Training and Research on Advanced Computing Systems) Project. The training included studying different parallel coding approaches (MPI, OpenMP and HPF) as well as parallelizing a numerical 3D atmospheric code as part of my Ph.D. research.

(ii) *Computer science*

B.Sc. in computer Sciences the Open University (1998 - continues).

(iii) *Molecular Biology*

Spent 6 months (December 1992 - June 1993) at Argonne National Laboratory, USA, studying the techniques of Recombinant DNA Technology, specializing in the fields of site directed mutagenesis, expression and purification of the photosynthetic reaction center protein complex.

## *Awards and Distinctions*

1989 Rector's award for distinction.
Certificate of honor from the Israeli Parliament for distinction.

1990 Dean's award for distinction.

1991 Dean's list for distinction.

Qualified the M.Sc. degree with distinction.

Received the Rieger Foundation Scholarship for Environmental Sciences.

Received the Rieger Foundation Scholarship for Environmental Sciences.

## *Publications*

(a) **D. O. Ranmar, M. Luria, J. Kaplan, and Y. Mahrer.** "*Utilization and Integration of Interdisciplinary Computer Models as a Tool for Analyzing Ozone production from*

*Transportation Sources".* Accepted for publication by the International Journal of Environment and Pollution. To be published during 2001 (special issue).

(b) **D.O. Ranmar, V. Matveev, U. Dayan, M. Peleg, J. Kaplan, A. W. Gertler, M. Luria, G. Kallos, P. Katsafados and Y. Mahrer.** *"The impact of coastal transportation emission of $NO_x$ and VOC on inland air pollution over Israel - utilizing numerical simulations, airborne measurements and synoptic analyses.* Accepted for publication by the Journal of Geophysical Research, 2001.

## *Conferences*

All the presentations in the following conferences (June 1999 to May 2000) were entitled *"Utilization and Integration of Interdisciplinary Computer Models as a Tool for Analyzing Ozone production from Transportation Sources".*

(i) The 7th International conference of the Israeli Society for Ecology and Environmental quality Sciences, June 13 – 18, 1999, Jerusalem Israel. (*Oral presentation*)

Sixth International Conference on Harmonization within Atmospheric Dispersion Modelling for Regulatory Purposes October 11 - 14, 1999 CORIA, Rouen, France. (*Poster presentation*)

(iii) The 2nd Research Workshop on the interactions between Chemistry, Physics and Dynamics in the Troposphere, October 24 – 29, 1999 Nazareth, Israel. (*Poster presentation*)

(iv) The Millennium NATO/CCMS International Technical Meeting on Air Pollution Modeling and it's Application, May 15 – 19, 2000 Boulder, Colorado, USA. (*Poster presentation*)

# *Table of Contents*:


**Acknowledgments** ii

**Abstract** vi

Part I Introduction

I. *Background*

I.1. General 1

I.2. Air pollutants characteristic of motor vehicle emissions 3

I.3. Chemical pollutants of fossil-fuel origin

I.3.1 Nitrogen oxides 4

I.3.2. Carbon-containing compounds 6

I.3.3. Ozone chemistry and tropospheric photochemistry 8

I.3.4. Ozone-$NO_x$-VOC sensitivity 12

I.4. Synoptic and meteorological factors influencing air pollution 13

I.5. Air pollution models 16

I.6. Air pollution meteorology, state of the science 18

II. *Research Objectives* 21

III. *Research Significance* 22

**Literature cited** 24

Part II Methodology ~~28~~ 30

Part III *"Utilization and Integration of Interdisciplinary Computer Models as a Tool for analyzing Ozone Production from Transportation Sources"* 31

**Abstract** 32

**Introduction** 32

**Modeling System** 34

Transportation model 34

Emission Factor Model 35
Atmospheric Modeling 35
Transport Diffusion Simulation 36
**Synoptic Conditions** 36
**Model Application** 37
**Results and Discussion** 37
**Conclusions** 38
**Acknowledgments** 39
**References** 40

Part IV *"The impact of coastal transportation emissions on inland air pollution over Israel – utilizing numerical simulations, airborne measurements and synoptic analyses"* 41

**Abstract** 42
**1. Introduction** 43
**2. Modeling Systems** 45
2.1. Transportation Model 45
2.2. Emission-Factor Model 46
2.3. Atmospheric Modeling 46
2.4. Emission-Factor Model 47
2.5. Photochemical Model 48
**3. Experimental Design**
3.1. Research Flights 48
3.2. Tunnel Experiment 49
3.3. Ground-Based Measurements and Data Analysis 49
**4. Model Application** 50
4.1. Traffic Flow Simulation 50
4.2. Vehicle Emission Factors Calculation 50
4.3 Atmospheric Modeling Aspects 52
4.4. Rush Hour Determination 53
**5. Results and Discussion** 53
5.1. Model Simulation 53

5.2. Flight and Model Comparison 54
5.3. Relation of Air pollution Scenarios to Weather Conditions 55
5.4. Data Analysis of Ground-Based Monitoring Stations 57
**6. Conclusions** 57
**Acknowledgements** 58
**References** 60
**Figure Captions** 63
**Table 2** 64
**Figures** 65

/ DID NOT PRINT

**Part V** ***"Analyses of urban and rural surface ozone levels in Israel"*** 74
**I. Introduction** 74
**II. Month & Site Dependency** 76
**III. Day of Week Profiles** 81
**IV. Predicting Daily 1-h Maxima, 8-h Averages, and Hourly Ozone Levels** 86
**References** 98

**Summary and Conclusion** 101
**Abstract in Hebrew** ℵ

# Abstract

Air pollution, with ozone-generating processes being of primary importance, coupled with the ever-diminishing natural resources in general and land resources in particular, are among the most significant ecological impacts of the modern-age transportation network. The transportation network and corresponding traffic flow constitute a system which is the most elementary part of a country's infrastructure and a prerequisite for its economic growth. The necessity to protect and preserve our ecosystem, linked to the ongoing need for robust and functional traffic infrastructures, calls for the development and implementation of a modeling system targeting the various factors involved in the transportation-to-ozone formation linkage. The daily dynamics of rush hour traffic emissions to inland air pollution in general and airborne ozone measurements in particular was studied using a newly devised interdisciplinary modeling system. For the purpose of this study, the following models were selected: a transportation model (EMME/2) coupled to the emission-factor model (EFM), the regional atmospheric modeling system (RAMS) and a transport and diffusion model (TDM). The photochemical module was addressed through multiple-regression analysis, which found a correlation between ozone mixing ratios, $NO_y$ levels and air temperature (Olszyna et al., 1994, 1997) in photochemically aged air masses typical of the region under study (Peleg et al., 1994). Explicitly, the modeling system's construction and execution tracked the following path: (i) Execution of a dynamic atmospheric model (RAMS), to obtain the atmospheric windfiled parameters at a predefined resolution; (ii) Combining the output data from (i) with the coupled traffic flow-emission factor models, as input to the transport and diffusion model (TDM), to obtain a traffic-derived time-dependent spatial distribution of the air pollution particles; (iii) Finally, executing a photochemical model on output data from (i) and (ii) to obtain the transportation-originating emission pollution-oriented ozone dispersion. The photochemical module was addressed through a multiple-regression analysis, which found a correlation between ozone-mixing ratios, $NO_y$ levels and air temperature in photochemically aged air masses typical of the region under study. Part II [Ranmar et al., 2001] decribes the modeling flow algorithm, its components and its calibration with an airborne-measured ozone episode detected over central Israel.

The impact of the Tel Aviv metropolitan area as well as the Gaza Strip, as pivotal coastal transportation sources for inland air pollution in general and ozone formation in particular, was addressed in part III [Ranmar et al .,2001]. The modeling results elucidated a spatial and temporal overlap between the ozone precursors and ozone production. The model simulations indicated east to southeasterly dispersion of the pollution cloud. The results agreed well with both spatial and temporal summertime ozone levels as recorded by aircraft over central Israel, as well as with ground-based monitoring stations. The surface observations indicated that ozone levels exhibit a distinct inland scale dependency: peaking at later hours and on average reaching higher levels as we progress inland. These results correspond well with the dynamics of the inland-penetrating plume where an increase in ozone concentrations is attributed to ongoing photochemical transformations while traversing inland. Synoptic analysis identified the conditions prevailing when elevated air pollution, and especially high ozone levels, exist over central Israel during the early, mid and late summer. The analysis showed that this season features a shallow mixed layer and weak zonal flow, which lead to poor ventilation rates and inhibit efficient dispersion of this secondary pollutant. These poor ventilation rates result in the slow transport of ozone precursors originating from urban pollution plumes along the Mediterranean coastline, enabling their photochemical transformation under intense solar radiation during their travel from the coast inland in central Israel. Thus, these findings establish a scenario in which the physical process of inland movement of pollutants in general, and ozone precursors in particular, is established. The Tel Aviv metropolitan area and possibly the Gaza Strip region emit transportation pollutants into the troposphere on a daily basis, initiating their subsequent photochemical transformation as they are transported downwind. Model simulations showed that about 60% of the detected inland ozone concentration is nourished by traffic emissions during the morning rush hours from the Tel Aviv metropolitan area. The work presented here demonstrates the ability of interdisciplinary modeling systems to collectively operate as a prediction tool/tracing device, capable of successfully predicting ozone pollution hotspots.

Ground-level ozone has become a problem of major concern in many metropolitan areas in Israel experiencing recurring high ozone concentrations during the summertime "photochemical smog season". In a study aimed at

complementing the airborne ozone pollution modeling (part II and III), statistical data analyses of urban and rural surface ozone were performed (part IV). The statistical analyses were based upon data collected between June 1 and September 30 for the years 1999 and 2000 from the national air pollution-monitoring network. They targeted the the following objectives: (i) performing preliminary data analyses in order to extract site, month and day-of-week dependencies of ground-level ozone. This study was executed for five cities representing densely populated and industrial areas (Tel aviv and Jerusalem), moderately populated (Be'er Sheva and Modiin) and rural, less populated regions (Ariel); (ii) developing statistical ozone prediction models based on multiple linear regression methods, using meteorological and chemical variables. The mathematical models were set to address the daily 1-h max, 8-h averages and daily 1-h averaged ozone concentration dynamics and were developed for four locations in Israel (Tel Aviv, Ariel, Modiin and Jerusalem).

Realization of (i) was achived by obtaining preliminary characteristics of the ground-level ozone profiles of the aforementioned regions in Israel under different time regimes. The various instances of quantitative ozone phenomena were based upon different time intervals (monthly, daily, 1-h maxima and 8-h (10:00 h – 17:00 h) ozone averages). The presented results reveal a rather site-specific, and to a lesser extent month-specific ozone average concentration spectrum. Additionally, two distinct regimes are suggested, one concerning the time-space dependency of the trans-boundary inland-transported pollution from Tel Aviv to Modiin to Jerusalem (discussed in part III), and the other concerning isolated, "self-sustained" ozone producers, represented by Be'er Sheva and Ariel. Analyses of day-of-week dependency revealed two transportation emission-ozone formation regimes. The first corresponds to the more highly populated urbanized areas (Tel Aviv, Jerusalem and Be'er Sheva) where the weekend decrease (Friday and Saturday) in traffic emissions results in a slight increase in ozone levels. Such a weekday-to-weekend dependency reflects the transition from a VOC-limited regime to a $NO_x$-limited regime found in populated industrial urban areas. The opposite results are encountered in Ariel, in which the low local weekend $NO_x$ emissions by traffic flow inhibit the formation of ozone. Sunday, the first working day in Israel, is found to exhibit on average higher ozone concentrations than mid-week days, even though traffic activities are on par with these days. A possible mechanism for the asymmetrical day-of-week increase in ozone levels is the downward mixing of the ozone reservoir at the inversion base, replenished by the relatively high weekend

concentrations. Objective (ii) was accomplished by utilizing multiple linear regression prediction models for the 1-h max and 8-h average ozone levels were based on 19 explanatory meteorological and chemical variables. The most significant explanatory (highest $R^2$) variables, obtained through stepwise regression and correlation analyses, were site-specific. For 1-h peak ozone levels at the four sites, RMSE model error ranged from 5.7 ppbv to 10.8 ppbv, while the $R^2$ values ($R^2 \cong 0.6$) were site-independent. For the 8-h average the RMSE model error ranged from 4.8 ppbv to 6.7 ppbv, the $R^2$ values from 0.58 to 0.69. The daily 1-h average ozone prediction model aimed at capturing the dynamics of daily ozone evolution incorporated a different set of variables including a polynomial in time as its predictors. The model's statistical attributes ($R^2$ and model RMSE, respectively) were: Tel Aviv (0.78, 7.4 ppbv), Ariel (0.66, 8.8 ppbv), Modiin (0.76, 8.4 ppbv), and Jerusalem (0.64, 10.9 ppbv). In general, the predicted daily 1-h peaks, 8-h averages and daily 1-h averages tracked the observed values at the four stations and generally, the models captured the daily variation reasonably well, but underestimated high concentrations of observed ozone. This occurred particularly on days following days of low observed values and in the case of daily 1-h averages, when a secondary late afternoon-to-late evening peak was established. While the prediction models did not reach the anticipated predictive levels, they provide the first statistical procedures addressing decision-grade forecast levels in Israel.

# PART I

# *Introduction*

## I. Background

### I.1. General

The atmosphere is a complex and dynamic photochemical reactor that exhibits a wide range of temperatures, pressures, compositions and motion. The chemical species found in this heterogeneous multiphase system include the noble gases, neutral molecules, reactive atoms, free radicals and ions. Excluding variable amounts of water vapor, more than 99.9% by volume of the earth's thin gaseous atmosphere consists of molecular nitrogen (78.08%), oxygen (20.95%) and argon (0.93%). The concentrations of these ubiquitous constituents are beyond significant human influence. Most emissions of chemical constituents into the troposphere take place at the earth's surface by natural, mostly biological, processes and to a large, and increasing degree by anthropogenic (agricultural, technological and urban infrastructure) activities. Civilization's expansion and self-sustained demand have increased the concentrations of many less abundant gases, such as volatile organic compounds (VOC), oxides of nitrogen ($NO_x$), and sulfur and $CO_2$, creating an "urban sphere" and urban-dependent "rural sphere" of additional highly complex mixtures of gaseous and particulate components. These chemicals react under the influence of sunlight to create a variety of products, including ozone ($O_3$) and submicrometer aerosols [Finlayson-Pitts and Pitts, 1986; Seinfeld and Pandis, 1998].

Air pollution meteorology may be defined as the process by which gases and particulate matter produced by human activity and emitted into the atmosphere undergo chemical and photochemical transformations during their transport and diffusion. Under atmospheric conditions in which the efficient dispersion of these pollutants in the air is limited, air pollution is manifested, damaging the surroundings, human health and quality of life. Even though the concentration of pollutants is of negligible consequence with regard to the composition of the atmosphere, an overall understanding of air pollution pathway processes, with respect to emission, dispersion, chemical transformation and removal characteristics, is of major importance in terms of their damaging impact on

human health [Dockery et al 1993], agriculture [Selldin and Pleijel 1993] and structures [Peleg et al 1989].

The presented research targets the impact of transportation systems, i.e. traffic flow–road network assembly, on air pollution in general and on ozone formation in particular. Automobiles emit a large fraction of the urban and rural concentrations of volatile hydrocarbons and nitrogen oxides [Kleindienst et al., 1992], and are an increasingly major determinant in local and worldwide environmental air pollution. Mobile sources generate most of the nitric oxide found in urban areas and frequently account for more than 60% of urban loading of nitrogen oxides [Atkinson, 1988]. In the Greater Los Angeles area in 1990, for example, on-road motor vehicles were estimated to contribute 76% of carbon monoxide (CO) emissions, 47% of non-methane organic carbon (NMOC) emissions, and 51% of nitrogen oxides emissions [Harley et al., 1997]. In 1998, there were approximately 1.7 million motor vehicles in Israel, with these numbers forecast to swell to over 2 million by the beginning of the 3rd millenium. Add to this the facts that the number of cars has increased by 72% from 1990 to 1998 and that the total distance traveled by all motor vehicles in the corresponding time span has more than doubled [the Central Bureau of Statistics, Israel Environment Bulletin, Spring 1999], it is obvious that vehicular air pollution is becoming a severe problem in Israel. Scaling the contribution of traffic emissions with regard to point sources embodies their significance with regard to tall stack plumes such as power plants. Unlike tall stack sources however, traffic emissions occur at numerous locations at ground level with reduced dispersion capacity and in proximity to pedestrians and drivers. Furthermore, the composite of motor vehicle chemicals released into the troposphere is more heterogeneous than that emitted by power plants (negligible VOC), rendering it more reactive in terms of atmospheric chemistry and photochemical fog formation. Overall, the traffic fleet is responsible for the lion's share of the country's CO pollution (92%) and for a substantial percentage of nitrogen oxides, particulate matter, VOC emissions and the subsequent photochemical ozone formation.

The following sections present an overview of the components involved in the transportation-to-ozone formation scenario. These include incomplete fossil-fuel combustion byproducts, the physicochemical processes of urban and regional atmospheres characterized by the initiation of ozone production, and the

atmospheric conditions prevailing during the transition seasons and summer, the annual time window favoring air pollution episodes.

## I.2. Air pollutants characteristic of motor vehicle emissions

Vehicles and fuels constitute an assemblage whose emission composite is dependent on both vehicle type and technology, and on the properties of the fuel. Under perfect combustion conditions, oxidation of fossil fuel results in the production of carbon dioxide and water through the fundamental process:

(1) $$C_xH_y + (X + \tfrac{1}{4})O_2 \rightarrow XCO_2 + \tfrac{1}{2}H_2O$$

However, the suboptimal conditions prevailing during fuel combustion result in a complex set of chemical reactions that form various fuel/vehicle system byproducts. The main chemicals formed are:

- Carbon monoxide (CO)
- Nitrogen oxides ($NO_x$)
- Volatile organic compounds (VOC)
- Sulfur dioxide ($SO_2$)
- Particulate matter (TSP)
- Ozone ($O_3$), which is defined as a secondary product formed through chemical processes rather by direct emission.

In general, excess fossil fuel-to-air (high F/A ratio) regarded as a "rich mixture", favors the formation of CO, since there isn't enough air to complete the reaction towards $CO_2$ formation and VOC. Such a composite is characteristic of gasoline engines. Alternatively, "poor mixtures" of fossil fuel (low F/A ratio) are characterized by the interaction of the ubiquitous atmospheric molecular nitrogen ($N_2$) with molecular oxygen ($O_2$) to produce nitrogen oxides.

Sulfur dioxide and particulate matter are not directly involved in the photochemical formation of tropospheric ozone and are therefore excluded from the following description of atmospheric pollution compounds.

## I.3. Chemical pollutants of fossil-fuel origin

### I.3.1 *Nitrogen oxides*

Nitrogen oxides are among the most important molecules in atmospheric chemistry. Two of the most reactive nitrogen species, nitric oxide (NO) and nitrogen dioxide ($NO_2$), play a pivotal role in determining the levels of tropospheric ozone [Carroll and Thompson, 1995; Seinfeld and Pandis, 1998]. They originate mainly from fossil-fuel combustion, soil release (natural and anthropogenic), biomass burning, lightning, $NH_3$ oxidation, aircraft, and transport from the troposphere. Between 40% and 45% of all $NO_x$ ($NO + NO_2 = NO_x$) emissions in the US are estimated to come from transportation, 30 to 35% from power plants and about 20% from industrial sources. High-temperature biomass burning and fossil-fuel combustion are the dominant anthropogenic sources of tropospheric $NO_x$. Under these conditions, the chemical bond of molecular nitrogen ($N_2$) is broken, and the resulting atomic nitrogen reacts endothermally with atomic oxygen:

(2) $$N_2 + O_2 \rightarrow 2NO$$

Most of the resulting products are NO molecules with the minority (~10%) being $NO_2$. NO emitted into the atmosphere is converted into $NO_2$ on a time scale of a few minutes and an equilibrium is rapidly established during daylight hours. An attempt to forecast NO and $NO_2$ concentrations proximal to a heavily traveled street, using statistical methods and a three-layer feed-forward neural network scheme [Perez and Trier, 2001], produced mixed results, mainly due to variations in the vehicle traffic sources and incomplete knowledge of the synoptic conditions during the analyzed period. The main pathways for the conversion of NO to $NO_2$ are via reactions with ozone, hydroperoxyl radical ($HO_2$), and alkyl (R) peroxyradical ($RO_2$):

(3) $$NO + O_3 \rightarrow NO_2 + O_2$$

(4) $$NO + HO_2 \rightarrow NO_2 + HO$$

(5) $$NO + RO_2 \rightarrow NO_2 + RO$$

$NO_2$ is a brownish-red, irritating, corrosive gas, possessing absorption spectra in the visible region, and is a pivotal component of photochemical smog. The combination of a low F/A ratio ("poor mixture") and high temperatures favors the production of $NO_x$, typifying diesel motor vehicles and making them the main

transportation source for $NO_x$ emission. In Israel, nitrogen oxides are monitored by the Israeli National Monitoring Network (24 stations) and by local municipal stations. For example, the annual averages for 1998 (in $\mu g/m^3$), based on the national monitoring network, were: 113 for Tel Aviv, 58 for Jerusalem, 52 for ashdod, 51 for Modiin, 49 for Rehovot, 32 for Hadera, 30 for Haifa and 25 Ashkelon [The Ministry of the Environment, Israel Environment Bulletin, Spring 1999]. It is common (and practical) to define two additional complementary groups of nitrogen oxides:

(a) Reactive nitrogen, denoted $NO_y$, defining the sum of $NO_x$ and all compounds that are products of the atmospheric oxidation of $NO_x$. These include nitric acid ($HNO_3$), nitrous acid (HONO), nitrate radical ($NO_3$), dinitrogen pentoxide ($N_2O_5$), peroxyacetyl nitrate (PAN) and its homologues.

(b) Oxidation products of $NO_x$, denoted $NO_z$.

Thus, $NO_y = NO_x + NO_z$. The partition of the nitrogen oxides into origin ($NO_x$), oxidized ($NO_z$) and overall concentrations ($NO_y$) is advantageous when studying urban vs. rural nitrogen oxides, and the chemical age/oxidation activity of monitored air masses. The conversion of $NO_x$ to $NO_z$ (the subgroups of $NO_y$), reflected by the ratio of $NO_x$ to $NO_y$ (or by the complementary $NO_z/NO_y$ ratio), reflects the chemical processing that occurs in an air mass from and since the release of $NO_x$ into the atmosphere. In the early morning, the freshly introduced traffic $NO_x$ will highly correlate with $NO_y$ in the absence of oxidation products ($NO_z$). As time evolves, photochemical transformation and oxidation processes convert $NO_x$ molecules to $NO_z$ species. Since significant transport and mixing occur simultaneously with the chemical reactions [McKeen et al., 1991; Peleg et al., 1994], formation of $NO_z$ (high $NO_z/NO_y$ ratio) coupled to a decrease in $NO_x$ (low $NO_x/NO_y$ ratio) is characteristic of rural sites downwind of an urban emission source. Oxidation of $NO_x$ to $NO_z$ characteristically takes 4 to 20 h [Seinfeld and Pandis, 1998] and is on the order of several hours in our region [Peleg et al., 1994]. Alternatively, since urban areas accommodate ubiquitous and essentially continuous emission sources of $NO_x$, combined with the fact that it takes several hours to convert $NO_x$ to other $NO_y$ species, $NO_y$ in urban areas is largely dominated by $NO_x$. An air mass is referred to as *photochemical aged* when the $NO_x/NO_y$ ration is less than 0.4, a situation typically encountered at rural sites downwind of urban locations and in inland rural regions in Israel. $NO_y$ and $O_3$ levels have been found to be positively correlated under this regime [Fahely et al., 1986; Doddridge et al.,

1992; Trainer et al., 1993; Olszyna et al., 1994, 1997; Peleg at al., 1994]. Furthermore, under a $NO_x$-limited regime, it was demonstrated that about 12 molecules of ozone are produced for every $NO_x$ molecule consumed. Finally, the main sinks for $NO_x$ are the conversion of $NO_2$ to water-soluble nitric oxide ($HNO_3$) by reaction with OH during the day:

(6) $$NO_2 + OH \cdot + (M) \rightarrow HNO_3 + (M)$$

and via reaction with $O_3$ at night:

(7) $$NO_2 + O_3 \rightarrow NO_3 + O_2$$

(8) $$NO_3 + NO_2 + (M) \rightarrow N_2O_5 + (M)$$

where M is an energy quencher, such as $N_2$ or $O_2$, which removes the excess energy and stabilizes the reaction. The average removal rate of $NO_y$ in the summertime via the deposition pathway, mainly in the form of nitrites, is on the order of 2 to 3 cm/s [Hubert and Robert, 1985]. The deposition rate of $NO_2$ and NO is on the order of 0.1 and 0.01 cm/s, respectively, making them long-distance transporters.

### I.3.2 *Carbon-containing compounds*

The hydrocarbons are a large and diverse group of carbon-containing compounds whose complex nonlinear interactions with $NO_x$ are the driving force of ground-level ozone formation. The main organic species involved in atmospheric chemistry include the classes of alkanes, alkenes, alkynes, aromatics, aldehydes, ketones, acids and alchohols. The term volatile organic compounds (VOC) refers to the entire set of vapor-phase atmospheric organic compounds, excluding CO and $CO_2$. VOC are pivotal to atmospheric chemistry from rural to urban and from local to global scales, with an estimated global anthropogenic emission (excluding methane) of 142 Tg/y [Middleton, 1995]. VOC exhibit a large range of chemical reactivities in general, ozone-forming capacities in particular. The VOC are formed and emitted as a complex mixture, whose exact composition and concentrations, along with the levels of the surrounding $NO_x$, define their ozone-forming potential [Bowman and Seinfeld, 1994; Carter, 1994]. Transportation is the dominant contributor to VOC emissions in the US [Seinfeld and Pandis, 1998] and in Israel [Ministry of the Environment, Israel Environment Bulletin, Summer 1999]. The VOC emitted from motor vehicles are the result of incomplete combustion,

vaporization processes and fossil-fuel leaks, and are the predominant sources for alkane and aromatic emissions. Methane is the most abundant volatile hydrocarbon in the atmosphere, with a global annual emission estimated at 535 Tg($CH_4$)/yr. About 160 Tg($CH_4$)/y is attributed to natural sources, 375 Tg($CH_4$)/yr comes from anthropogenic sources, with the most prominent contribution (100 Tg($CH_4$)/yr) resulting from fossil-fuel combustion (IPCC, 1995). Formation of ozone and formaldehyde $CH_2O$ from $CH_4$ takes the net form:

(9) $$CH_4 + 4O_2 \rightarrow CH_2O + H_2O + 2O_3$$

However, given its slow second-order oxidation rate, and a long life time (about a year), methane levels exhibit negligible time and space variations in the troposphere and are deemed a non-factor in high-ozone level episodes. The level of the rest of the VOC ranges from ppt levels in remote areas to 100 ppb in urban areas [Warneck, 1988; Field et al., 1992; Solberg et al., 1996; Seinfield and Pandis, 1998]. The catalyst of VOC chemistry, manifesting its reactivity potential in driving ozone production, is the hydroxyl radical ($OH\cdot$). This key tropospheric oxidizing species is formed mainly from ozone photolysis, but also from the photochemical dissociation of carbonyl compounds and nitrous acid molecules. Finally, the most abundant air pollutant is CO, whose atmospheric concentrations are in the range of parts per million by volume (ppmv), a factor 10-fold higher than that of other atmospheric pollutants. The main source for CO is incomplete fossil-fuel combustion [Finlayson-Pitts, 1986; Burnett et al., 1998; Israel Ministry of the Environment Bulletin, Spring 1999], mainly from light-duty motor vehicles, as already mentioned. The net production of ozone via the CO pathway is:

(10) $$CO + 2O_2 \rightarrow CO_2 + O_3$$

**B**oth the $CH_4$ and CO pathways require sufficient levels of NO in the atmosphere to drive the reaction towards the formation of ozone. From hereon the term VOC will include the CO molecule. Table 1 displays the differential contribution from anthropogenic energy sources to the to the $NO_x$ and VOC chemical groups.

Table 1. Pollutant partitioning according to energy sources.

| | $NO_x$ ($10^3$t) | CO ($10^3$t) | NMVOC* ($10^3$t) | $SO_2$ ($10^3$t) |
|---|---|---|---|---|
| **Energy** | 215 | 832 | 158 | 260 |
| *Energy Industries* | 86 | 6 | 2 | 191 |
| *Manufacturing Industries* | 23 | 1 | 1 | 46 |
| *Transportation* | 100 | 824 | 155 | 11 |
| *Residential* | 5 | 1 | | 10 |
| *Agriculture* | 1 | | | 3 |

Source: Koch, et al., 2000.

* NMVOC – non-methane VOC.

A few points should be noted in Table 1: (i) transportation is the main source for both $NO_x$ and VOC, (ii) energy industries do not emit the VOC essential for ozone formation as compared to transportation sources, (iii) $SO_2$ is a prominent pollutant of energy industries, thus making it an important fingerprint identifying the origin/source of remote air pollution episodes via the $NO_x/SO_2$ ratio.

### I.3.3 *Ozone chemistry and tropospheric photochemistry*

The dynamic nature of air pollution photochemistry reflects the pivotal role of solar radiation in driving atmospheric chemistry. At the earth's surface, radiation of wavelengths 290 nm and greater – termed the actinic region – is available for inducing photochemical reactions leading to the formation of ozone, as well as of additional oxidizing species such as peroxyacetyl nitrate (PAN; CH3C(O)OONO2), which acts as an important temporary temperature-dependent reservoir for both $NO_2$ and the peroxyacetyl radical, both pivotal in tropospheric ozone formation.

Ozone is one of the most important molecules in the earth's atmosphere. About 90% of the ozone is produced in the stratosphere, where it screens out

most of the UV radiation, preventing it from reaching the earth's surface. In the troposphere, $O_3$ is not emitted directly, but is created from complex interactions between VOC and $NO_x$ in the presence of solar radiation, the chemical transformations being catalyzed by the attack of the hydroxyl radical (OH·) on the hydrocarbons [Seinfeld, 1989; Seinfeld and Pandis, 1998]. Tropospheric ozone, the target of this work, is formed exclusively by reactions between atomic oxygen (O) and $O_2$. In the troposphere, the principal source of atomic oxygen is the photochemical cycle, involving NO, $NO_2$ ($NO_x$) and sunlight:

(11) $$NO_2 \xrightarrow{h\nu} NO + O(^3P) \qquad \text{Rate} = k$$

(12) $$O(^3P) + O_2 + M \rightarrow O_3 + M \qquad \text{Rate} = \text{"instantaneous"}$$

(13) $$NO + O_3 \rightarrow NO_2 + O \qquad \text{Rate} = J_{NO2}$$

where the photon $h\nu$ has a wavelength between 280 and 430 nm, and $O(^3P)$ is the ground triplet state of atomic oxygen. The photolysis of $NO_2$ is the only known anthropogenic source of tropospheric ozone, accounting for about 10% of all the atmospheric ozone. A relatively small quantity of ozone results from the steady-state cycle of reactions (11) – (13), sustained by the continual input of photons. The so-called photostationary state relation gives the ozone concentration at steady state:

(14) $$[O_3] = \frac{J_{NO_2}[NO_2]}{k[NO]}$$

where $J$ is the photolysis rate of $NO_2$, diurnally, seasonally and latitude dependent, and $k$ is the rate constant of reaction (11). For tropospheric ozone to accumulate, a reaction path converting NO to $NO_2$ that bypasses step (13) – without consuming a molecule of ozone – is required. Such a conversion is accomplished through the oxidation of hydrocarbons, initiated by reactive agents such as hydroxyl radicals. Thus, ozone formation takes place as a result of the so-called photooxidation of VOC, which is a chain-reaction process including radical-initiation, radical-propagation, and radical-termination steps. In these reactions, the hydroxyl radical plays a key role as a VOC-oxidizing chemical component to form the peroxy radical ($RO_2$· where R is an alkyl group):

(15) $$VOC + OH\cdot \xrightarrow{O_2} RO_2\cdot + H_2O$$

In particular, peroxy radicals ($RO_2\cdot$) produced during the photooxidation of VOC react with NO to produce $NO_2$, shifting the photostationary state in favor of ozone production:

(16) $$RO_2\cdot + NO \rightarrow NO_2 + RO$$

(17) $$NO_2 \xrightarrow{h\nu} NO + O$$

(18) $$O(^3P) + O_2 + M \rightarrow RO + M$$

the net process being:

(19) $$RO_2\cdot + O_2 \xrightarrow{h\nu} RO + O_3$$

Thus, ozone generation is dependent on the VOC-$NO_x$ reactions, closely related to the rate of $RO_2\cdot$ formation and critically dependent on NO concentrations. While the presence of $NO_x$ is essential for the formation of ozone through the photochemical cycle of reactions (11) – (13), VOC are the real precursors of ozone. The ozone yield strongly depends on the particular VOC as well as on the prevailing VOC/$NO_x$ ratio, where $NO_x$ can be viewed as the catalyst for ozone, and VOC as the fuel [Bowman and Seinfield, 1994].

An additional source of tropospheric $O_3$ is penetration from the stratosphere, which is estimated at a rate of 450 Tg/yr [Collins et al., 1997] by the so-called tropopause folding events. Extensions of stratospheric air invade the troposphere, resulting in a flux of 3 to 8 $10^{10}$ $O_3$ molecules/$cm^2$s in the northern hemisphere [Crutzen, 1995a].

Tropospheric $O_3$ sinks take the following pathways:

(a) Photolysis

(20) $$O_3 \xrightarrow{h\nu} O(^1D) + O_2 \qquad (\lambda = 310 \text{ nm})$$

(21) $$O(^1D) + H_2O \rightarrow 2OH\cdot$$

where $O(^1D)$ corresponds to excited-state molecular oxygen. This reaction is pivotal in the formation of OH· in the troposphere.

(b) Via reaction (13)

Primarily near high NO emitters such as power plants.

(c) Via reaction with the $HO_2$· radical

(22) $$HO_2 \cdot + O_3 \rightarrow OH \cdot + 2O_2$$

(d) Nighttime chemistry

(23) $$NO_2 + O_3 \rightarrow NO_3 + O_2$$

forming the $NO_3$ light-sensitive radical, which is an important nighttime agent.

(e) Dry deposition

At a rate (cm/s) of 0.4 over the continent and 0.07 over the ocean [Hauglustaine et al., 1994].

Overall, at most rural ground-level sites, ozone concentration exhibits a diurnal cycle with a minimum in the early morning hours due to nighttime titration with NO and absence of photochemistry to counter its destruction, and a maximum in the afternoon due to continuous intense daytime photochemistry.

The "trilateral" nonlinear chemical interactions of the lower troposphere, involving heterogeneous biogenic and anthropogenic VOC, anthropogenic $NO_y$ and ozone are very complex in nature and have been addressed through both experimental and modeling research [Luria and Meagher, 1988; Chameides et al., 1992; Bowman and Seinfeld, 1994; Carter, 1994; Derwent and Davies, 1994; Crutzen, 1995b, to name a few].

In Israel, the Ministry of the Environment has provided preliminary results based on air quality monitoring in 1998 underscoring the severity of the air pollution in Israel [Israel Environment Bulletin, Spring 1999]. Highlighted were the nitrogen oxide concentrations, particularly in the Tel Aviv metropolitan area and the ozone levels, primarily in the Jerusalem region. The Tel Aviv metropolitan area exhibited annual concentrations of 113 $\mu g/m^3$ – more than double to quadruple the values detected in other areas of the country. These in turn gave rise to 167 (rooftop measurements) exceedances of the half hour standard (Tel Aviv + Holon) compared to few exceedances in other parts of the country, and 834 (ground-level transportation-monitoring stations) half-hour exceedances and 16 diurnal

exceedances. In Jerusalem, one monitoring station alone recorded 49 half-hour ozone standard exceedances as compared to an overall 53 exceedances in 20 stations across the country and 8 exceedances of the 8-h standards as compared to 9 in the rest of the country. Both the primary ($NO_x$) and secondary ($O_3$) pollutants – the precursors and photochemical transformed molecules, were attributed to ground-level mobile pollution sources, i.e. transportation.

### I.3.4 *Ozone-$NO_x$-VOC sensitivity*

The relative behavior of VOC and $NO_x$ in ozone formation can be viewed in terms of competition for the hydroxyl radical, hydroperoxyl radical ($HO_2$) and alkyl peroxy radicals [Sillman, 1995]:

(24) $$OH\cdot + NO_2 \rightarrow HNO_3$$

(25) $$HO_2 + HO_2 \rightarrow H_2O_2 + O_2$$

(26) $$RO_2 + HO_2 \rightarrow ROOH + O_2$$

The relative extent of reactions (20) - (22), which define *termination steps* for the precursors of ozone production, discerns two different photochemical regimes: a $NO_x$-sensitive regime at high VOC/$NO_x$ ratios and a VOC-sensitive regime at low VOC/$NO_x$ ratios. At high VOC/$NO_x$ ratios, or at sufficiently low $NO_x$ concentrations, the peroxy-peroxy reactions – (21) and (22) – dominate, resulting in ozone-formation retardation due to OH· removal from the system, leading to a $NO_x$-sensitive regime. In this case, the rate of ozone production increases with increasing $NO_x$ and is largely insensitive to changes in VOC. At low VOC/$NO_x$ ratios, OH· reacts predominately with $NO_2$ (reaction 24), removing OH· radicals from the active VOC oxidation cycle and resulting in ozone-formation retardation, thereby forming a VOC-sensitive regime. Under these conditions, the rate of ozone production increases with increasing VOC and decreases with increasing $NO_x$. The significance of the 'regime differentiation' stems from the general transformation from a VOC-sensitive regime in the early morning, when urban traffic emits high concentrations of $NO_x$, resulting in the titration of ozone through reaction (13) [Sillman, 1995], to the $NO_x$-sensitive regime encountered in rural areas as a result of transport of the polluted air mass downwind of the urban sources [Seinfeld, 1995]. The gravity of

the *VOC-sensitive regime* to *$NO_x$-sensitive regime* transformation, coupled to the aforementioned *photochemical aged air mass regime*, centers on the general daily dynamics of the polluted air masses formed in highly populated cities and carried downwind. Based on measurements at different sites in central Israel, Peleg et al., [1994], detected a trend of increasing ozone levels with increasing inland distance (from the seashore eastward). They speculated that the ozone is produced during inland transport (due to NW winds) and that the "ingredients" feeding the photochemical transformations originate from the Tel Aviv metropolitan area. The inland travel of about 3 to 5 h (the estimated time after precursor emission required to reach peak concentrations of ozone [Seinfeld, 1989]) is coupled to $NO_x$-sensitive, photochemical aged air mass processes (unless a local source of $NO_x$ emission exists) taking place mainly in rural areas [Olszyna et al., 1994, 1997; Peleg et al., 1994]. As a secondary pollutant, in a $NO_x$-sensitive regime, ozone production was found to be positively correlated with temperature and $NO_y$, when using multivariate linear regression analysis on air samples measured for primary and secondary pollutants, as well as for meteorological variables, at a rural site [Olszyna et al., 1997].

A recent report by Luria et al., [1998, in Hebrew] based on an airborne-measurements campaign, was aimed at evaluating ozone concentrations over central Israel. The measurements, encompassing the early-to-mid-to-late summertime periods for the years 1994 to 1995 and 1997, showed that out of the 32 flights performed, 19 detected high ozone concentrations of above 120 ppbv, which are above the 1-h exceedance. These findings, coupled with previous ground-level measurements of high ozone concentrations [Peleg et al., 1994] underscore a consistent problem of ozone pollution over central Israel.

The presented research addresses 12 of the 32 airborne measurements conducted in the years 1994 to 1995 and 1997, 10 of which correspond to ozone pollution episodes in central Israel.

## I.4. Synoptic and meteorological factors influencing air pollution

The dominant synoptic conditions prevailing in the eastern Mediterranean Sea from mid-May to mid-September are influenced by three major systems surrounding the region: (i) the Persian trough, (ii) the subtropical high, and (iii) the Azorean high. The interplay between these systems results in overall monotonic weather conditions. From eastern, mid and southern Asia, land warming during the

summer leads to the development of the Monsoon low, resulting in predominant northerly winds in the eastern Mediterranean. One of its centers is located in the Persian Gulf, forming the Persian trough, which extends from the Persian Gulf towards the southern shores of Turkey, and dominates the Mediterranean in the summer. It forms NW winds, influencing the northern and central regions of Israel. Alpert et al. [1992] mirrored the cyclic deepening and withdrawal of the surface Persian trough pressure system with the upper level subtropical high motion/location. The Persian trough is generally bounded to the lower 2 km of the atmosphere capped aloft by the subtropical high-pressure system, which extends in the summer season from the northern part of the African continent to our region. Withdrawal of the subtropical high results in an increase in the surface pressure gradient and augmentation of the western marine winds, forming a weak cold front which penetrates deeper inland. This in turn elevates the mixing layer height (~1000 m), as warm continental air is lifted up by the penetrating heavier marine air. Alternatively, subsidence of the subtropical high, accompanied by adiabatic warming and a decrease in relative humidity, suppresses penetration of the Persian trough, causing its retraction. This results in a weakening and northerly veering of the wind, coupled to a reduction of the mixing layer height (~500 m). Thus, the fluctuations in the penetration of the Persian trough are resolved through the vertical position of the lower boundary of the marine inversion (the interface of these two air masses), which in turn is determined by the motion of the subtropical high. The basis of the inversion forms the upper boundary for the vertical dispersion of air pollutants, rendering a low-level inversion (shallow Persian trough) with reduced ventilation capacity of the mixing layer and increasing the potential for air pollution episodes, and vice versa.

West of this region, the Azorean high influences the area as part of the subtropical belts of highs. The Azorean high is centered over the Atlantic Ocean, near the Azorean islands, and dictates NW air motions.

Coastal breezes resulting from the land/sea circulation combined with mountain slope winds of the Judean Hills, both evolving from extensive daytime heating of the land surface, are an additional important mechanism determining the transport and vertical distribution of pollutants. Such a structural combination of sea-land-topography wind circulation superimposed on synoptic winds was found to be the main driving force in the Los Angeles Basin air pollution [Lu and Turco, 1996]. There, the dynamic/chemical interplay elevated ground-level air pollution,

and injected oxidized pollutants into the inversion layer, forming a reservoir of high-latitude photochemical aged air mass which could mix downward to enhance surface concentrations. Such a mechanism has been speculated to take place in Israel, taking into account the similarities in geography and climate [Dayan and Coch, 1996].

Transition seasons are characterized by the overwhelming influence of the subtropical high-pressure system, leading to frequent subsidence inversions aloft accompanied by well-developed radiative inversions on the ground, introducing hot and dry air initially at the top of the mountains and gradually to lower regions. This situation often leads to a shallow mixed layer accompanied by weak zonal winds. Both these features result in poor ventilation conditions and consequently to rising air pollution concentrations within the stable profile formed [Dayan and Rodnizki, 1999].

Identification and classifications of atmospheric conditions and synoptic systems leading to/correlating with air pollution in general and ozone pollution in particular have been presented previously: over Europe [Davies et al., 1992], in the US [Davis et al., 1998] and over Israel [Dayan and Koch, 1996; Koch and Dayan, 1992; Peleg et al., 1994] these authors found that most of the high ozone levels (≥ 80ppbv) occur during the transition season (April-May), converging with some observations [Monks, 2000] and diverging from others [Vukovich and Fishman, 1986; McKendry, 1994, Ryan, 1995]. They also differentiated the ozone episodes into four main synoptic conditions accounting for 77% of the cases analyzed: a barometric high east of the Mediterranean Sea (28%), a "Yam-Suf" trough with a central axis (22%), a weak Persian trough (15%) and a "Yam-Suf" trough with an eastern axis (11%).

This type of analysis is chiefly diagnostic in nature, providing a qualitative picture of the weather/atmospheric conditions prevailing during episodes of above-average ozone levels at specific locations. It lacks, however, prognostic/quantitative insight into "real-time" assessment of inland air pollution/ozone pollution episodes. Such evaluations are provided by numerical modeling systems, covering the fields of atmospheric dynamics, transport and diffusion, the nature of the emission sources, and atmospheric photochemistry.

## I.5. Air pollution models

Air pollution meteorology, in addition to the nature of the pollutants involved, is categorized according to the meteorological scale it describes. Meteorological scales of motion can be partitioned into:

(i) *Micrometeorology.* Phenomena occurring on a scale on the order of 1 km, such as meandering and dispersion of point sources (chimney plume, stack of a power plant) and the complex flow regime in the wake of a large building. Time scale: minutes to hours.

(ii) *Mesoscale.* Phenomena occurring on a scale of tens to hundreds of kilometers, such as land-sea breeze (thermal circulation), mountain-valley winds, and migratory high- and low-pressure fronts. Time scale: hours to days.

(c) *Synoptic scale.* Phenomena occurring on a scale of thousands of kilometers, such as seasonal high- and low-pressure systems residing over oceans and continents (see the aforementioned Monsoon low, Azorean high), motions of whole weather systems (e.g. Persian trough). Time scale: days to weeks.

(d) *Global scale.* Phenomena occurring on a scale exceeding $5 \times 10^3$ km. Time scale: months to years.

Urban and regional air pollution essentially overlap with the mesoscale category, the geophysical domain addressed in the presented research. Regarding the urban-rural air pollution in our area of interest ($\leq$ 200 km), the atmospheric region governing transport and dispersion corresponds to the so-called planetary boundary layer, roughly 1000 m above ground, reflecting the extent of the earth's surface influence on the wind profile in the troposphere.

Air pollution modeling is based on (i) atmospheric, (ii) transport-diffusion, and (iii) chemical-photochemical attributes.

(i) Atmospheric models. Numerous prognostic atmospheric models have been developed to calculate the meteorological variables necessary for simulating atmospheric motion. These models are based on a set of equations governing motion, thermodynamics, moisture and mass continuity, supplemented by various parameterizations such as categorical variables (soil type, vegetation type),

radiation, cloud microphysics and turbulent kinetic energy (TKE). They usually differ by the numerical scheme used to solve the set of equations, the vertical coordinate system used (geopotential coordinate, terrain-following coordinate, pressure coordinate, for instance), the number of grids used, the nesting capability, horizontal and vertical resolution, the range of the simulated region, turbulent order technique, and so on. It is worth mentioning the well-documented and applied atmospheric models: the MEMO model [Moussiopoulos, 1994], which is the wind field component of the EZM photochemical model, MM5 [Grell et al., 1994], the RAMS (regional atmospheric modeling system) [Pielke et al., 1992, Walko et al., 1995], which is the one used in the present research, and the more recent TVM [Schayes et al., 1996; Thunis and Clappier, 2000].

(ii) **D**ispersion models. Transport and diffusion models are generally based on three dispersion schemes: Eulerian, Lagrangian and their combination. A Eulerian frame of reference such as the CALGRID model [Yamartino et al., 1992] centers on the conservation of pollutant mass (mean concentration) per unit grid cell of the model:

$$\frac{\partial \bar{c}}{\partial t} + \Delta \cdot (\bar{U}\bar{c}) + \Delta \cdot \overline{(U'c')} = R + S + L$$

where $\bar{U}$ and $U'$ are the 3D mean and fluctuation components of the wind vector, respectively, $\bar{c}$ and $c'$ are the mean pollution concentration (in mass of pollutant per unit volume) and the corresponding fluctuation, respectively, $R$ is the net rate of chemical production of the pollutant, $S$ is the emission rate of the pollutant and $L$ is the net removal/sink rate of the pollutant. On the other hand, a Lagrangian dispersion scheme, such as the Lagrangian atmospheric dispersion model (LADM) [Hurley and Physick, 1991], follows each particle's trajectory by updating its position according to the windfield (neglecting precipitation):

$$x_i(t+\Delta t) = x_i(t) + \left(\bar{u}_i(t) + u_i'\right) \cdot \Delta t$$

where $\bar{u}_i$ is the average wind velocity component (i = 1,2,3) and $u_i'$ is the turbulent perturbation velocity. In both cases, an independent atmospheric model is often used to calculate the wind fields upon which the dispersion models derive the particle's motion. A hybrid scheme utilizing a sequential transition from a

Lagrangian-to-Eulerian dispersion scheme was introduced by Walko et al. [1995]. The Lagrangian mode resolves subgrid emission sources and maintains subsequent downwind pollutant concentrations until atmospheric dispersion dictates broadening of the pollution cloud. Once the Lagrangian plume becomes sufficiently developed downstream of the source, it is converted to a well-resolved concentration field and advected using the Eulerian formulation. A comparison between the two approaches can be found in Nguyen et al. [1997] and references therein. This work utilizes the Lagrangian scheme for simulating pollutant dispersion in the atmosphere, the wind fields being provided by the RAMS.

(iii) **P**hotochemical models. The so-called chemical/photochemical solvers simulate the complex nonlinear chemical interactions taking place in the atmosphere. The simulated chemical transformations entail several tens of chemical compounds in some 80 to more than 100 chemical reactions with a wide range of reaction rate constants. Such 3D regional photochemical grid models include the URM [Kumer et al., 1994], UAM-V [System Aplications International (SAI), 1995], CAMx [ENVIRON, 1997], MODELS-3 [US EPA, 1998, 2000], SMOG model [Lu et al., 1997], and EZM (EUMAC ZOOMING MODEL) [Moussiopoulos, 1994], to name a few. These models calculate the concentration of each pollutant for each time step based on different chemical reaction mechanisms involving various organic, inorganic and photochemical reactions [Hess et al., 1992; Hedly et al., 1997; Jiang et al., 1997; Lu et al., 1997a,b; Seinfeld and Pandis, 1998]. These models are full-fledged models containing the windfield and dispersion models.

## I.6. Air pollution meteorology, state of the science

**A**ir pollution episodes have been extensively studied using measurements and numerical meteorological models. These works have addressed metropolitan areas with severe recurring ozone pollution and rural areas with local and transported emissions of air pollution precursors, many of them with the aim of establishing regulatory actions. Perhaps the most intense urban air pollution studies in recent years have focused on summertime in Athens, Greece [Pilinis et al., 1993; Moussiopoulos and Paragrigoriou, 1997; Klemm et al., 1998; Svensson, 1998; Ziomas et al., 1998; Clappier et al., 2000; Grossi et al., 2000 to name a few]. The case studies of Athens, located in a special geophysical basin, bounded from the south by the sea and from the west, north and east by four mountains, enabled

the elucidation of various aspects of air pollution generation. Modeling efforts by Pilinis et al., [1993] for example, using a RAMS-CALGRID hybrid, indicated that the principal source of high $NO_x$ in the main urban area was transportation, and pointed to the significance of the sea breeze in transporting ozone precursors to NNW parts of the city resulting in elevated ozone-mixing ratios. The dynamics of the synoptic sea breeze coupling/decoupling in determining the local spread of air pollution hot spots in the Greater Athens Area was addressed by Clappier et al. [2000] using a combined vorticity mesoscale model and a photochemical module. Klemm et al. [1998], using airborne and ground-level measurements, found that the sea breeze carried air pollution of different origins and of different photochemical ages as determined by the $O_3/NO_y$ ratio. Grossi et al. [2000], using a sort of "factor separation" modeling approach by differentiating between nighttime and daytime emissions in industrial sources vs. urban area sources, showed that ozone production in Athens is essentially a 1-day process. However, recirculation of old pollutants may have an important effect on other sections of the area, including overseas. Zimonas et al. [1998], using the UAM photochemical grid model simulated the impact of different $NO_x$/VOC emission reduction scenarios on ozone formation, concluding that a VOC, rather than $NO_x$ control strategy is desirable. Moving to Atlanta, Georgia, Saylor et al. [1999], using, UAM-IV model, determined that a $NO_x$-sensitive regime exists, necessitating a reduction in $NO_x$ emissions by as much as 75% to achieve both the 1-h (120 ppb) and 8-h (80 ppb) standards. Dabdub et al. [1999] addressed the differential impact of boundary conditions, winds, emissions, and $NO_x$/VOC sensitivity on the nature of ozone formation in the San Joaquin Valley of California using a SAQM photochemical grid model and emission inventory model (SEIM). The simulation was applied to a region that included a major coastal metropolitan area (San Francisco) as well as the influence of the sea breeze from the Pacific Ocean. They showed that significant inflow into the valley imposes a strong dependency on the boundary concentration of pollutants. Additionally, they showed that the region was $NO_x$-sensitive, with the dependency of ozone formation on incoming $NO_x$ greater than that on internally emitted $NO_x$. It is interesting to note that this work has some relevance to our region, when one compares coastal San Francisco with coastal Tel Aviv, the $NO_x$-sensitive regime found to exist in both cases, and the dependency of "inland" ozone formation on boundary input of chemicals rather than local emission. The CALMET-CALGRID model was applied to Milan's highly industrialized and populated metropolitan area [Silibello et al., 1998]. The simulations were based on input of national inventories data corresponding to

traffic, industry and biogenic emissions, where the road traffic sector accounted for 62, 50 and 90% of total $NO_x$, VOC and CO, respectively. The simulations of the summertime ozone-mixing ratio were in good agreement with monitored data, but discrepancies were revealed with measured vs. simulated $NO_x$, particularly at urban stations during the night. Another interesting photochemical modeling of urban air pollution, inputting a database of various sources of emissions centering on current and projected traffic emissions, was carried out during the Urban Air Pollution Athens 2004 Air Quality campaign [Moussiopoulos and Paragrigoriou, 1997]. The campaign addressed present (1994) vs. future (2004) air pollution scenarios corresponding to implementation of strategies to reduce chemical pollutant release into the atmosphere, primarily from transportation in Athens. They used different photochemical grid models, such as the ARDEA-I/UAM hybrid modeling system and the CTC model, as well as a model for evaluating future traffic flow and corresponding emissions. Their simulations revealed an overall reduction in the $NO_x$ and ozone-mixing ratios, even though the ozone patterns were more complex and model-oriented.

In Israel, some experimentally based and modeling-oriented work has been carried out to address local air pollution dynamics. Robinson et al. [1992] for example, analyzed high $SO_2$ concentrations detected over the eastern Mediterranean coast, using a prognostic wind field model. The simulation pointed to a recirculation pattern, where sulfate dioxide emitted from the tall stack of a power plant and from the refinement industries in Ashdod is carried over the sea due to night land breezes, and returned over land with the onset of the morning sea breeze. Recirculation of polluted air masses over the eastern Mediterranean coast was the driving force behind the elevated $NO_x$ and $NO_y$ concentrations and the very high concentration of ozone detected by a coastal observatory in October of 1995 [Alper-Siman Tov et al., 1997]. Using a back trajectory model (developed by the Israeli Meteorological service) and a wind field model [Mahrer and Pielke, 1977], they showed that the high concentration of ozone could be attributed to easterly winds, which swept continental air parcels containing the locally emitted pollution westerly over the sea. The intense photochemical activity that occurred during the air parcel trajectory over the sea, for a relatively extended time, coupled with the low mixing height on the measuring day, gave rise to the abnormally high recorded ozone concentration. Tokar et al. [1993] and Goldstein et al., [1994] developed a Pollution Dispersion and Transport Model based on the MM4 model

[Anthes et al., 1987] and applied it to a region encompassing the Hadera power plant. Weinroth [1997, in Hebrew] used a combined mesoscale wind field model/GIS system to study the transport of pollution clouds from mobile sources. These findings, with those from previously mentioned works [Peleg et al., 1994; Luria et al., 1998 (in Hebrew); Ministry of the Environment, 1999] indicate a highly dynamic air pollution profile in Israel. The pivotal players in determining the destination and characteristics of the polluted air mass over Israel are the coastal area with its sea/land breeze cycling and the coastal Tel Aviv metropolitan area as the major source for precursor emissions.

# II Research Objectives

(i) To develop a reliable, operational, predictive tool for determining, analyzing, and predicting the impact of the transportation system on the spatial evolution and distribution of ozone. The prediction of transportation-to-inland air pollution will couple and interface transportation flow rate, vehicular emission factors, and atmospheric, transport/diffusion and photochemical attributes.

(ii) To perform simulations addressing the *daily* impact of the Tel Aviv metropolitan transportation infrastructure on the subsequent inland air pollution in general and ozone pollution in particular. The simulation will be compared with data derived from airborne measurements and ground-based monitoring stations.

(iii) To perform statistical analyses on data recorded by the National Air Pollution Monitoring Network stations that correspond to locations detected by (ii) with potentially high ozone concentrations. The analysis will address the hourly, daily, and monthly $O_3$ profiles. Furthermore, a multiple regression analysis will be performed for each site in order to construct a prediction tool relating ozone concentration to meteorological and chemical variables associated with its formation.

# III Research Significance

Air pollution, with ozone-generating processes being of primary importance, coupled with the ever-diminishing natural resources, land resources in particular, is among the most significant ecological impacts of the modern age's transportation network. The need to protect and preserve our ecosystem, linked to the ongoing need for a robust and functional traffic infrastructure, calls for the development and implementation of a modeling system targeting the various factors involved in transportation-to-ozone formation. These models should address atmospheric dynamics, geographical location of traffic networks, traffic flow, traffic-related pollution emission, and overall development strategies. The latter are intimately linked to transportation development.

The presented work originated as a trilateral German-Israeli-Palestinian research project and continued as an American-Israeli-Palestinian research project targeting the impact of transportation on the environment. The aim of the research was to map the Israeli-Palestinian transportation infrastructure network and study its subsequent impact on inland air pollution/ozone formation. As part of the project, a new coherently integrated simulation tool to assess transportation-to-ozone formation scenario was developed, integrating atmospheric, dispersion, transportation, emission, and photochemical models. It is important to note that as far as we know, the photochemical module incorporated into the modeling system is the first to be based on multiple-regression statistical analyses rather than heavy-duty, time-consuming chemical solvers.

This research provided the opportunity to address and link individual studies of the airborne measurement campaign [Luria et al., 1998 (in Hebrew)], the emission factor modeling inventory [Yavin Y., 1998 (in Hebrew)], and both trilateral transportation/environmental projects, and to assimilate them into a modeling system as the anthropogenic contribute to air pollution over Israel.

For the first time, an interdisciplinary multifactorial modeling system was used to addressed the air pollution potential over inland areas in Israel in the

context of the pollutants originating *exclusively* from *coastal transportation sources.*

To my knowledge, no other work has dealt with the impact of urban traffic pollution on neighboring areas. Furthermore, zooming in on the ubiquitous *rush hour* traffic emission phenomenon provides an assessment of the "real-time" *daily basis frequency* with which major metropolises pollute their surroundings. Centering on the "concept" of major coastal municipal areas (Tel Aviv metropolitan area and the Gaza Strip), influenced by the superposition of land/sea breeze and synoptic systems, powering through internally produced traffic emissions to their surroundings, is of general geophysical-geopolitical value, and adds additional originality and applicability to the work.

A statistical analysis of areas with high ozone levels, as determined by airborne measurements and modeling, was executed for five cities influenced by the emissions from traffic sources in the Tel Aviv metropolitan area and the Gaza Strip. This research provides the first detailed history of an ozone profile, including site-specific multiple-regression models for calculating ozone concentrations.

The final systematic-integrated modeling product is expected to be able to address the issue of present and future transportation infrastructure shaping where environmental protection and preservation on the one hand, and socioeconomic transportation demands on the other, are to be considered.

# Literature cited


דיין א., מרר י., וא. לוי, היתצרות מזהמים שניוניים ותפרוסתם בזמן ובמרחב, דוח התקדמות חצי שנתי, מוגש למדען הראשי והמשרד לאיכות הסביבה, 34 ע"מ, 2001.

לוריא מ., פלג מ., מטבייב ו., ונגר א., לפידות ע., צחי י., רוזן ד., וד. סימנטוב, התפתחות אוזון בתימרה העירונית של גוש דן, *דו"ח מדעי סופי לקרן בלפר, האוג.* העברית בירושלים, הבי"ס למדע ישומי, המעבדה לחקר איכות האויר, 1998.

ויינרוט א., הערכת תנועות עננים הפליטה של כלי רכב באמצעות מודלים ממוחשבים והשוואתן למדידות, חיבור לשם קבלת תואר "מוסמך", האוניברסיטה העברית ירושלים, 1997.

יבין י., קביעת מקדמי פליטה באמצעות ניסוי במנהרה, חיבור לשם קבלת תואר "מוסמך", האוניברסיטה העברית ירושלים, 1998.

Alper-Siman Tov D., Peleg M., Matveev V., Mahrer Y., Seter I. and M. Luria, Recirculation of polluted air masses over the east Mediterranean coast, *Atmospheric Environment*, 31, 1441-1448, 1997.

Alpert P., Abramsky R. and B. U. Neeman, The prevailing summer synoptic system in Israel – subtropical high, not Persian trough, *Isr. J. Earth Sci.*, 39, 93-102, 1992.

Anthes R. A., Hsie E. –Y. and Y. –H. Kuo, Description of Penn state/NCAR meso scale model version 4 (MM4), *NCAR Technical Note, NCAR/TN-282 +STR*, 1987.

Atkinson R., Atmospheric transformation of automobiles emissions. In *Air Pollution, the Automobile, and Public Health* (Edited by Watson A. Y., Bates R. R and Kennedy D.). National Academy Press, Washington, DC., 99-132, 1988.

Bowman F. M. and J. H. Seinfeld, Ozone productivity of atmospheric organics, *J. Geophys. Res.*, 99, 5309-5324, 1994.

Carroll M. A. and A. M. Thompson, $NO_x$ in the non-urban troposphere. In *Progress and Problems in Atmospheric Chemistry* (Edited by J. R. Barker). Advances Series in Physical Chemistry Vol. 3. World Scientific Publ., London, 198-255, 1995.

Burnet R. T., Cakmak S., Raezenne M. E., Steib D., Vincent R. and D. Krewski, The association between ambient carbon monoxide levels and daily mortality in Toronto, Canad, *J. Air Waste & Manage. Assoc.*, 48, 1998.

Carter W. P. L., Development of ozone reactivity scales for volatile organic compounds, *J. Air Waste & Manage. Assoc.*, 44, 881-899, 1994.

Chameides W. L. et al., Ozone precursor relationships in the ambient atmosphere, *J. Geophys. Res.*, 97, 6037-6055, 1992.

Clappier A. et al., Effect of sea breeze on air pollution in the Greater Athens Area. Part I: Numerical simulations and field observations, *J. Appl. Meteorol.*, 39, 546-562, 2000.

Coch J. and U. Dayan, Synoptic analysis of the Meteorological conditions affecting dispersion of pollutants emitted from tall stacks in the coastal plain of Israel, *Atmospheric Environment*, 26A, 2537-2543, 1992.

Collins W. J., Stevenson D. S., Jonson C. E. and R. G. Derwent, Tropospheric ozone in global-scale three-dimensional Lagrangian model and its response to $NO_x$ emission control, J. *Atmos. Chem.*, 26, 223-274, 1997.

Crutzen P. J., Ozone in the troposphere. In *Composition, Chemistry, and Climate of the Atmosphere* (Edited by H. B. Singh). John Wiley & Sons, New York, 349-393, 1995a.

Crutzen P. J., On the role of ozone in atmospheric chemistry. In *The chemistry of the atmosphere – Oxidants and oxidation in the earth's atmosphere*, (Edited by A. R. Bandy), The Royal Society of Chemistry, London, 3-22, 1995b.

Dabdub D., DaHaan L. L. and L. H. Seinfeld, Analysis of ozobe in the San Joaquine Valley of California, *Atmospheric Environment*, 33, 2501-2514, 1999.

Davies T. D., Kelly P. M., Low P. S. and C. E. Pierce, Surface ozone concentration in Europe: Links with regional-scale atmospheric circulation, *J. Geophys. Res.*, 97, 9819-9832, 1992.

Davis J. M., Eder B. K., Nychka D. and Q. Yang, Modeling the effects of meteorology on ozone in Houston using cluster analysis and generalized additive models, *Atmospheric Environment*, 12, 2505-2520, 1998.

Dayan U. and L. Koch, Ozone concentration profiles in the Los Angeles Basin – A possible similarity in the build-up mechanism of inland surface ozone in Israel, *J. Appl. Meteor.*, 35, 1085-1090, 1996.

Dayan U. and J. Rodnizki, The Temporal Behavior of the Atmospheric Boundary Layer in Israel. *J. Appl. Meteor.*, 38, 830-836, 1999.

Derwent R. G. and T. J. Davies, Modeling the impact of $NO_x$ or hydrocarbon control on photochemical ozone in Europe, *Atmospheric Environment*, 28, 2039-2052, 1994.

Dockery D.W., Pope C.A., Xu X., Spengler J.D., Ware J.H., Fay M.E., Ferris B.G. and F.E. Speizer, An association between air pollution and mortality in six US cities, *Journal of Medicine*, 329, 24, 1753-1808, 1993.

Doddridge B. J., R. R. Dickerson, R. G. Wardell, K. L. Civerolo and L. J. Nunnermacker, Trace gas concentrations and meteorology in rural Virginia, 2, Reactive nitrogen compounds, *J.Geophys. Res.*, 97, 20631-20646, 1992.

Duncan B. N. and W. L. Chameides, Effects of urban emission control strategies on the export of ozone and ozone precursors from the urban atmosphere to the troposphere, *J. Geophys. Res.*, 103, 28159-28179, 1998.

Fahely D. W. et al., Reactive nitrogen species in the troposphere: Measurements of NO, $NO_2$, $HNO_3$, particulate nitrate, peroxyacetyl nitrate (PAN), $O_3$, and total reactive odd nitrogen ($NO_y$) at Niwot Ridge, Colorado, *J.Geophys. Res.*, 91, 9781-9793, 1986.

Field R. A., Goldstone M. E., Lester J. N. and R. Perry, The sources and behavior of tropospheric anthropogenic volitile hydrocarbons, *Atmospheric Environment*, 16, 2983-2996, 1992.

Finlayson-Pitts, Pitts (Eds.). In Atmospheric Chemistry: Fundamentals and Experimental Techniques, A Wiley-Interactive Publication, 1986.

Goldstein J., Tokar Y., Balmor Y., Glaser E. and P. Alpert, Summer episode of pollution dispersion over the coastal area of Israel – a numerical study. In *Air Pollution Modeling and Its Application X* (Edited by Gryning S.E. and Millan M. M.), Plenum Press, NY, 45-52, 1994.

Grell G. A., Dudhia J. and D. Stauffer, A description of the fifth-generation Penn State/NCAR mesoscale model (MM5), *NCAR technical note, NCAR/TN-398 +STR*, 1994.

Grossi P. et al., Effect of sea breeze on air pollution in the Greater Athens Area. Part II: Analysis of different emission scenarios, *J. Appl. Meteorol.*, 39, 563-575, 2000.

Harley R. A., Sawyer R. F. and J. B. Milford, Updated photochemical Modeling for California's south coast air basin: comparison of chemical mechanisms and motor vehicle emission inventories, *Environ. Sci. Technol.*, 31, 2829-2839, 1997.

Hauglustaine D. A., Granier C., Brasseur G. P. and G. Megie, The importance of atmospheric chemistry in the calculation of radiative forcing on the climate system, *J. Geophys. Res.*, 99, 1173-1186, 1994.

Hedley M., McLaren R., Jiang W. and D.L. Singleton, Evaluation of an air quality simulation of the Lower Fraser Valley. 2. Photochemistry, *Atmospheric Environment*, 31, 11, 1617-1630, 1997.

Hess G. D., Carnovale F., Cope M. E. and G. M.Johnson, The evaluation of some photochemical smog reaction-mechanisms. 1. Temperature and initial composition effects, *Atmospheric Environment, Part A – General Topics*, 26, 4, 625-641, 1992.

Hubert B. J. and C. H. Robert, The dry deposition of nitric acid to grass, *J. Geophys. Res.*, 90, 9315-9324, 1985.

Hurley P. and W. Physick, A Lagrangian particle model of fumigation by breakdown of the nocturnal inversion, *Atmospheric Environment*, 25A, 1313-1325, 1991.

Intergovernmental Panel on Climate Change (IPCC), Climate Change 1994: Radiative Forcing of Climate Change and Evaluation of the IPCC IS92 Emission Scenarios. Cambridge University Press, Cambridge, UK, 1995.

Jiang W., Singleton D. L., McLaren R. and M. Hedley, Sensitivity of ozone concentrations to rate constants in a modified SAPRC90 chemical mechanism used for Canadian Lower Fraser Valley ozone studies, *Atmospheric Environment*, 31, 1195-1208, 1997.

Kleindienst T. E., Smith D. F., Hudgens E. E., Snow R. F., Perry E., Claxton L. D., Bufalini J. J., Black F. M. and T. CupittL, The Photo-oxidation of automobiles emissions: measurments of the transformation products and their mutagenic activity, *Atmos. Environ.*, 26A, 3039-3053, 1992.

Klemm O., Ziomas I. C., Balis D., Suppan P., Slemr J., Romero R. and L.G. Vyras, A summer air-pollution study in Athens, Greece, *Atmospheric Environment*, 32, 2071-2087,1998.

Kock J., Dayan U. and A Mey-Marom, Inventory of emissions of green house gases in Israel, *Water, Air & Soil Pollution*, 123, 259-271, 2000.

Kumar N., Odman M. T. and A. G. Russell, Multiscale air quality modeling: application to southern California, *J. Geophys. Res.*, 99, 5385-5397, 1994.

Lu R. and R. P. Turco, Ozone distribution over the Los Angeles Basin: Three-dimensional simulations with the SMOG model, *Atmospheric Environment*, 30, 4155-4176, 1996.

Lu R., Jacobson M. Z. and R. P. Turco, An integrated air pollution modeling system for urban and regional scales: 1. Structure and performance, *J. Geophys. Res.*, 102, 5, 6063-6079, 1997.

Luria M. and J. F. Meagher, Computer simulation of the boundary layer oxidation and removal of atmospheric pollutants over the western Atlantic Ocean, *Atmospheric Environment*, 22, 307-316, 1988.

Mahrer Y. and R. A. Pielke, The effects of topography on sea and land breeze in a two-dimensional numerical model, *Mon .Wea. Rev.*, 105, 1151-1162, 1977.

McKeen S. A., Hsie E.-Y. and S. C. Liu, A study of the dependence of rural ozone on ozone precursors in the Eastern United States, *J. Geophys. Res.*, 96, 15,377-15,394, 1991.

McKendry I. G., Synoptic circulation and summertime ground-level ozone concentration at Vancouver, British Columbia, *J. Appl. Meteor.*, 33, 627-641, 1994.

Middleton P., Sources of air pollutants. In *Composition, Chemistry and Climate of the Atmosphere*, (Edited by H. B. Singh). John Wiley & Sons, New York, 88-119, 1995.

Monks P., Origins and observations of the early spring ozone maximum, *Eurotrac-2 Newsletter*, 22, 17-21, 2000.

Moussiopoulos N. (Ed.), The EUMAC Zooming model – model structure and applications, *EUROTRAC (A EUROTRAK environmental project)*, International Scientific Secretariat Garmisch-Partenkirchen, 1994.

Moussiopoulos N. and S. Paragrigoriou (Eds.), Athens 2004 air quality, *Proceedings of International Scientific Workshop "Athens 2004 air quality"*, 183 pp, 1997.

Nguyen K. C., Noonan J. A., Galbally I. E., and W. L. Physick, Predictions of plume dispersion in complex terrain: Eulerian versus Lagrangian models, *Atmospheric Environment*, 11, 847-958, 1997.

Olszyna K. J., Bailey E. M., Simonaitis R. and J. F. Meagher, $O_3$ and $NO_y$ relationships at a rural site, *J. Geophys. Res.* 99, 14,557-14,563, 1994.

Olszyna K. J., Luria M. and J. F. Meagher, The correlation of temperature and rural ozone levels in southeastern U.S.A. *Atmospheric Environment*, 31, 3011-3022, 1997.

Peleg M., Luria M., Setter I., Perner D. and P. Russel, Ozone levels in Central Israel, *Israel J. of Chemistry*, 34, 375, 1994.

Peleg M., Burla E., Cohen I and M. Luria, Deterioration of Jerusalem limestone from air pollutants. Field observations and laboratory simulation, *Environ. Monitoring and Assessment*, 12, 191-201, 1989.

Perez P. and A. Trier, Prediction of NO and $NO_2$ concentrations near a street with heavy traffic in Santiago, Chile, *Atmospheric Environment*, 35, 1783-1789, 2001.

Pielke R. A., Cotton C. J., Walko R. L., Tremback C. J., Lyons W. A., Grasso L. D., Nicholls M. E., Moran M. D., Wesley D. A., Lee T. J. and J. H. Copeland, A comprehensive meteorological modeling system - RAMS", *Meteor. Atmos. Phys.*, 49, 69, 1992.

Pilinis C., Kassomenos P. and G. Kallos, Modeling of photochemical pollution in Athens, Greece. Application of the RAMS-CALGRID modelling system. *Atmospheric Environment*, 27B, 353-370, 1993.

Robinson J., Mahrer Y. and E. Wakshal, The effect of mesoscale circulation on the dispersion of pollutants ($SO_2$) in the eastern Mediterranean, southern coastal plain of Israel, *Atmosph. Environ.*, 26B, 271-277, 1992.

Ryan W. F., Forcasting severe ozone episodes in the Baltimore metropolitan area. *Atmosph. Environ.*, 29, 2387-2398, 1995.

Saylor R. D., Chameides W. L. and M.E. Chang, Demonstrating attainment in Atlanta using urban airshed model simulations: impact of boundary conditions and alternative forms of the NAAQS, *Atmos. Environ*, 33, 1057-1064, 1999.

Schayes G., Thunis P. and R. Bornstein, Topographic vorticity-mode mesoscale-beta (TVM) model .1. Formulation, *J. Appl. Meteor.*, 35, 1815-1823, 1996.

Seinfeld J. H., Urban air pollution: state of the art, *Science*, 243, 745 – 752, 1989.

Seinfeld J. H., Chemistry of ozone in the urban and regional atmosphere. In *Progress and Problems in Atmospheric Chemistry* (Edited by J. R. Barker). Advances Series in Physical Chemistry Vol. 3, World Scientific Publ., London., 34 – 57, 1995.

Seinfeld J. H. and S. Pandis (Eds.), *Atmospheric Chemistry and Physics: Air Pollution to Climate.* John Wiley & Sons, New York., 1998.

Selldin G. and H.Pleijel, Influence of atmospheric ozone on agricultural crops, (Buxton D.R. et al Eds.). International crop science I., Madison WI, *American society of agronomy Inc., Crop science society of America Inc., Soil science of America Inc.*, pp 315, 1993.

Silibello C., Calori G., Brusasca G., Catenacci G. and G. Finzi, Aplication of photochemical grid model to Milan metropolitan area, *Atmos. Environ*, 25, 2025-2038, 1998.

Sillman S., New developments in understanding the relationship between ozone, $NO_x$ and hydrocarbons in urban atmosphere. in *Progress and problems in atmospheric chemistry* (Edited by J. R. Barker). Advances Series in Physical Chemistry Vol. 3, World Scientific Publ., London, 145-171, 1995.

Solberg S., Dye C., Schimidbauer N., Herzog A. and R. Gehrig, Carbonyls and non methane hydrocarbons at rural European sites from the Mediterranean to the Artic, *J. Atmospheric Chemistry*, 25, 33-66, 1996.

Svensson G., Model simulation of the quality in Athens, Greece, during the Medcaphot-trace campaign. *Atmospheric Environment*, 32, 2239-2268, 1998.

Systems Applications International (SAI), Users guide to the variable grid urban airshad model (UAN-V). *System Applications International*, San Rafael, CA, 131pp, 1995.

Thunis P. and A. Clappier, Formulation and evaluation of a nonhydrostatic mesoscale vorticity model (TVM), *Mon. Weather Rev.*, 128, 3236-3251, 2000.

Tokar Y., Goldstein J., Levin Z. and P. Alpert, The use of meso-gamma scale model for evaluation of pollution concentration over an industrial region in Israel (Hadera), *Boundary-Layer Meteorol.* 62, 185-193, 1993.

Trainer M. et al., Correlation of ozone with $NO_y$ in photochemically aged air, *J. Geophys. Res.*, 98, 2917-2925, 1993.

United States Environmental Protection Agency (US EPA), EPA third-generation air quality modeling system. Models-3 vol. 9B: User manual. EPS-600/R-98/069(a), June 1998, *United States Environmental Protection Agency*, Research Triangle Park, 1998.

United States Environmental Protection Agency (US EPA), Models-3 home page, 2000. Available online at http://www.epa.gov/asmdnerl/model-3.

Vukovich F. M. and J. Fishman, The climatology of summertime $O_3$ and $SO_2$, *Atmospheric Environment*, 20, 2423-2433, 19861986.

Walko R. L., Tremback C. J. and M. J. Bell, HYPACT the HYbrid Particle And Concentration Transport Model, *User's Guide Version 1.0*, Aster Division, 1995.

Warneck P., Chemistry of the natural atmosphere. In *International Geophysical Series* Vol. 41, Academic Press Inc., 1988.

Yamartino R. J., Scire J. S., Carmichael G. R. and Y. S. Chang, The Calgrid mesoscale photochemical model – I. model formulation, *Atmospheric Environment*, 26A, 1493-1512, 1992.

Ziomas I. C. et al., Ozone epizodes in Athens Grees. A modelling approach using data from the MEDCAPHOT-TRACE, *Atmospheric Environment*, 32, 2313-2321, 1998.

# PART II

## *Methodology*

### II.1. *Modeling Systems*

The impact of traffic infrastructure on ozone formation, through the dynamics of the atmosphere, the characteristics of traffic flow, and the nature of the pollution emission, dispersion and photochemistry, was addressed by utilization of modeling techniques, interfacing and linking these disciplines.
For the purpose of this study, the following models were selected: a transportation model (Emme/2, pronounced *em-two*, named after the French letter "emme" for mobility model) coupled to the emission-factor model (EFM), the regional atmospheric modeling system (RAMS) and a transport and diffusion model (TDM). A photochemical module is addressed through a multiple-regression analysis, which found a correlation between ozone mixing ratios, $NO_y$ levels and air temperature (Olszyna et al., 1994, 1997) in photochemically aged air masses typical of the region under study (Peleg et al., 1994).

All the models are described in detail in parts III and IV.

### II.2. *Multivariate statistical analysis*

In part V, a multiple linear regression method is used in order to develop statistical models to predict the 1-h maximum, 8-h average and hourly average of surface ozone. Part V thus, contains a detailed description of the general mathematical form of multiple regression equations, the model development and its use in forecasting ozone levels.

### II.3. *Computer Hardware and Software*

Simulations of ozone air pollution dynamics (Regional Atmospheric Modeling System (RAMS), Transport-Diffusion Model (TDM) and the photochemical multiple regression model) were executed on Pentium II 400 MHz based on a *Linux* platform.

Multivariate statistical analyses were performed using the *SAS* statistical software (SAS release 6.12).

# Part III

## *Utilization and Integration of Interdisciplinary Computer Models as a Tool for analyzing Ozone Production from Transportation Sources*

**D. O. Ranmar**

The Department of Soil & Water Sciences, The Faculty of Agricultural, Food and Environmental Quality Sciences, The Hebrew University of Jerusalem, Rehovot 76100, Israel

**M. Luria**

The Environmental Science Division, the School Applied Sciences and Technology, The Hebrew University of Jerusalem, Jerusalem, 91904, Israel.

**J. kaplan**

The department of Geography, The Hebrew University of Jerusalem, Jerusalem, 91405, Israel.

**Y. Mahrer**

The Department of Soil & Water Sciences, The Faculty of Agricultural, Food and Environmental Quality Sciences, The Hebrew University of Jerusalem, Rehovot 76100, Israel

*Accepted for publication by the* International Journal of Environment and Pollution *November 2000 (special edition),*

# Utilization and Integration of Interdisciplinary Computer Models as a Tool for analyzing Ozone Production from Transportation Sources

D. O. Ranmar[1], M. Luria[2], J. Kaplan[3], and Y. Mahrer[1]

**ABSTRACT**
High ozone levels detected over large inland areas in Israel triggered analysis of air mass back trajectory, which pointed to the coastal Tel-Aviv metropolitan transportation system as the origin of the ozone's precursors. In order to link the transportation emissions to ozone formation interdisciplinary modeling systems were utilized and integrated. The transportation-to-ozone formation simulation, coupled transportation, emission factors, atmospheric and transport/diffusion models. The modeling results elucidated the spatial and temporal overlap between the ozone precursors and ozone production. The model simulations indicated an eastward transport accompanied with a 3D expansion of the pollution cloud. The results agreed well with observed spatial and temporal ozone levels.

**KEYWORDS**
Air pollution, numerical atmospheric modeling, transportation model, emission factors, ozone, advection/diffusion model.

## INTRODUCTION

The transportation network and the traffic flow constitute a system, which is the most elementary part of a country's infrastructure and a prerequisite for its economic growth. The spatial positioning of the transportation infrastructure determines the geographic distribution of the traffic flows, and hence determines the time dependent location of the pollution sources. Dynamically, this system is not an isolated system – it interacts with its surroundings primarily with the troposphere and particularly chemically to produce and emit pollution gases mainly NOx (NOx = NO + $NO_2$), VOC and CO. These entities undergo chemical and photochemical transformations in the presence of the solar radiation and atmospheric free radicals to form ozone (Finlayson-Pitts and Pitts 1997, Seinfeld and Pandis 1997). Since the formation and accumulation of ozone and other secondary species is not instantaneous following the emission of their precursors, significant transport and mixing occurs simultaneously with the chemical reactions (Kley 1997, Seinfeld 1989). An illustration of transportation emission to ozone formation scenario is presented in Fig 1. These daily processes call for the need to factorize and elucidate the link between road traffic emissions, the dominant source of NOx and VOCs, and ozone production during the course of the day. Previous studies (Peleg et al. 1994) based on measurements performed during the early summer months of 1988-1991 combined with air mass back trajectories analysis pointed to the Tel Aviv metropolitan transportation system as the main source of the high levels of ozone precursors detected in central Israel. Fig 2a shows the map of the simulation area and depicts the major traffic roads, Tel-Aviv metropolitan region, Gaza-Strip and Jerusalem. Road traffic activities with peak emission rates take place between 06:00 to 09:00 LST and are represented by the red dots in the Tel-Aviv metropolis. Fig 2b displays ozone concentrations at about 350 m above ground level taken by an aircraft, during the afternoon hours of the 28/8/97-ozone episode. It is apparent that the broad geographic distribution of high ozone levels, which at first sight seems unrelated to its precursor source location, is an outcome of highly complex and dynamical processes. Previous works addressed ozone formation in different modes such as under the impact of NOx and VOCs on ozone formation (Derwent and Davies 1994; Dabdub et al., 1999), or in the context of photochemical pollution modeling where the transportation emissions, and photochemical transformations overlap spatially, such as in the case of Athens (e.g. Pilinis et al., 1993; Moussiopoulus and Papagrigoriou, 1997). This study addresses the impact of the transportation emissions in the context of rates, timing, and location on the spatial and temporal production of ozone under the influence of atmospheric dynamics and topography. Conducted in the framework of the Israeli-Palestinian peace talks, the presented work is aimed at understanding the dynamics of the regional transportation-to-ozone production. This linkage is coupled with the idea of devising a

Accepted for publication in *J of Geophysical Research*

predicting tool that potentially can assist in the present and future transportation infrastructure shaping, where air pollution in general - and ozone problems in particular - are to be considered.

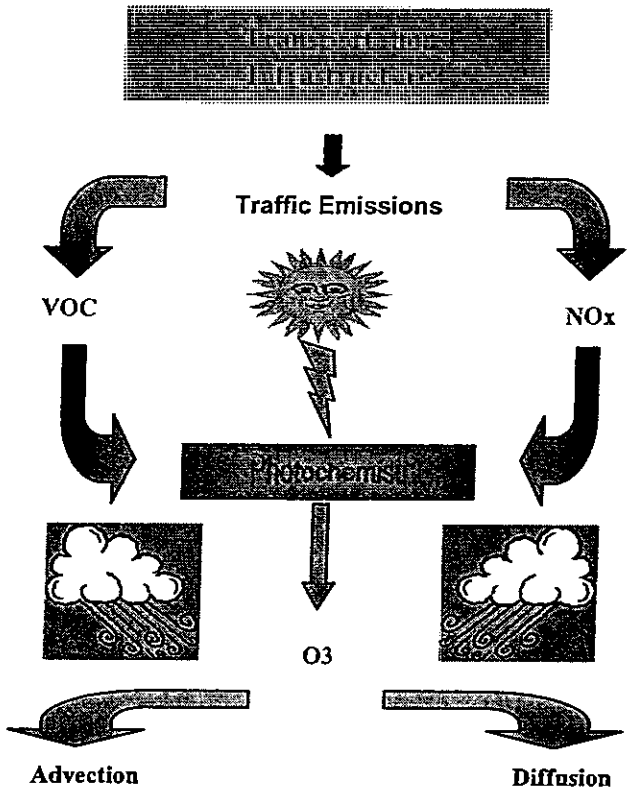


**Figure 1.** Schematic illustration of ozone formation from transportation sources.

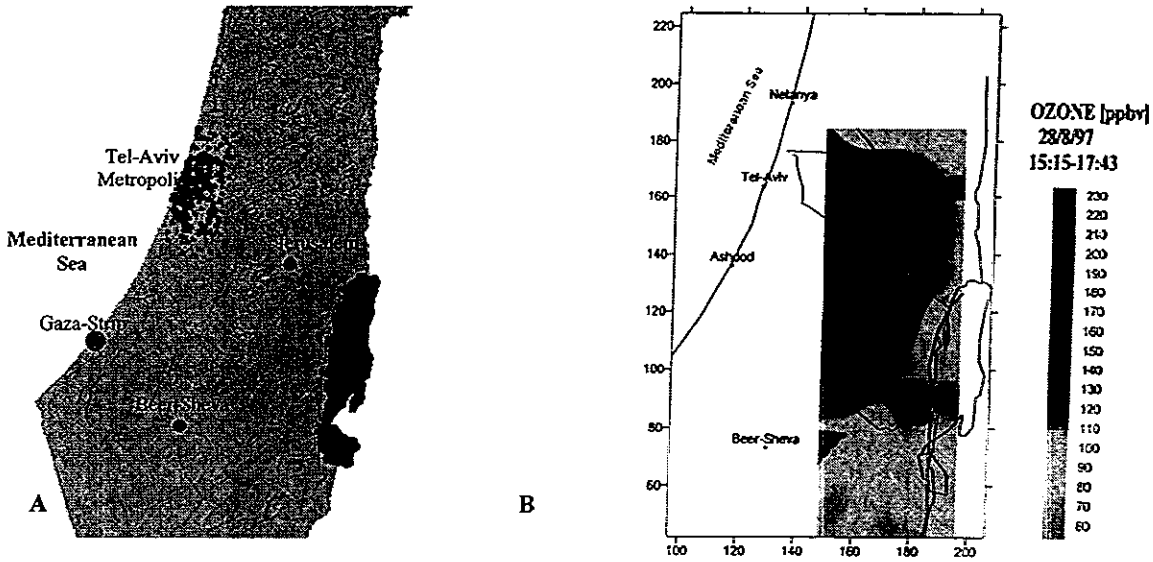


**Figure 2.** A – The simulation area, indicating the Tel Aviv metropolis and Gaza-Strip traffic sources (red) and traffic roads (red), B – ozone concentrations measured at 350 m above surface by aircraft.

141

## MODELING SYSTEMS

Understanding the spatial and temporal linkage between transportation emissions and ozone production called for the utilization and integration of interdisciplinary modeling systems covering the fields of: (i) transportation volumes, (ii) emission factors, (iii) atmospheric dynamics, (iv) pollutants transport and diffusion and (v) photochemistry. Fig 3 illustrates the modeling flow chart, which is based on an anthropogenic attribute – represented by the transportation and emission factors models (right branch) and the atmospheric dynamics attribute represented by the atmospheric model (left branch). The output from these two attributes intersects at the air pollution manifest through the transport and mixing of the transportation emissions. Finally, a photochemical model is interfaced to color the initially inert treated traffic pollutants with a photochemical dye, the final obligatory stage in ozone formation.

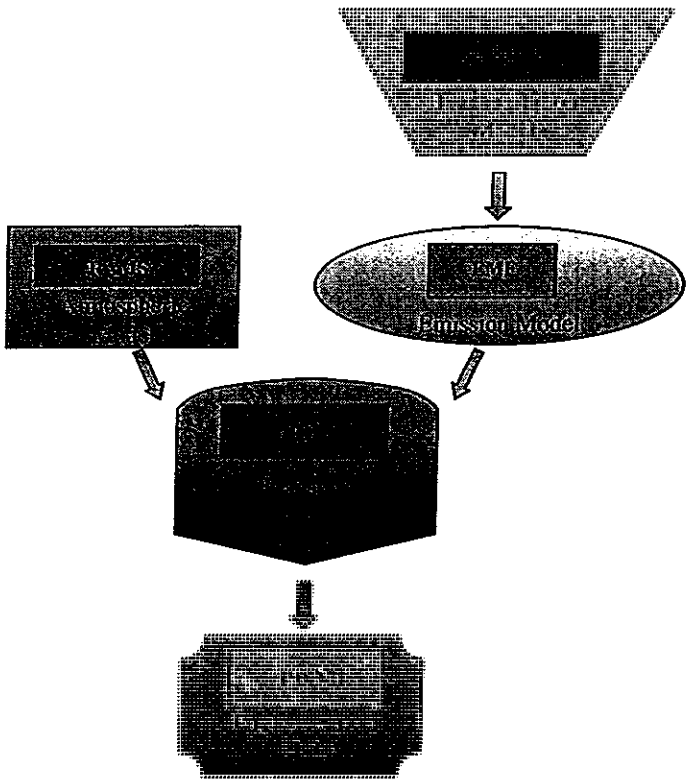


**Figure 3.** Schematic presentation of the modeling flow chart.

### Transportation model

The EMME/2 transportation system model (EMME/2 user Manuel and references therein) was used to analyze the combination of present transport flow dynamics and land use scenarios, and future conditions (year 2020) regarding transportation system performance. The results comprise the inputs for analyzing potential air quality levels, particularly ozone concentrations, under given scenarios. The modeling process assesses the balance between travel demand (based on land uses) and supply (based on transport facilities) under given scenarios. Land uses are aggregated to analysis zones (such as census tracts), which provide the basis for estimating a matrix of trips origin and destination. Networks to which the analysis zones are connected represent transport facilities, where each link of the network is characterized in terms of its capacity and speed components. The modeling process produced the desired origin-destination matrices of trips by the type of trip mode of travel and time of day as well as transport network data which depict the volumes of vehicles and passengers by road segment, travel speed, travel time, and delay of time. The traffic flow density per hour (TFD) for each road segment is obtained by multiplying the number of vehicles by the length (Km) of the road:

$$TFD = Vehicles \times Lengh/hr$$

**Emission Factor Model**

In a parallel study, fleet-wide motor-vehicle emission factors typical for Israel were estimated using road tunnel measurements.

The Vehicle EMission Factor (VEMF) of a specific pollutant is a parameter representing the pollutants' emission rate from the vehicle in units of g/km. The emission model is based on road tunnel measurements of NOx, NMOC, CO and $SO_2$. The emission model calculations were based on two complementary methods: Direct Method and Carbon Balance Method.

The direct method essentially produces the VEMF of specific pollutant in the tunnels' air based on its measured concentration, the tunnel length and number of vehicles present during the measurement:

$$\mathbf{EMFi = (\Delta Xi \times Vw \times S \times T)/(L \times N)}$$

EMFi – EMission Factor of pollutant i (g/(km x vehicle))
$\Delta$Xi – pollutant i concentration ($g/m^3$)
Vw – average wind speed in the tunnel (m/sec)
S – cross section area ($m^2$)
T– measurement time (sec)
L – tunnel length (m)
N – number of vehicles that passed during T

The Carbon Balance Method EMF is obtained from the following relation:

$$\mathbf{EMFi = Pi \times C}$$

where Pi is the mass of pollutant I divided by the total carbon in the tunnel air (units of g/kg C) and C is average carbon fuel consumption in the tunnel (units ofkg C/km).

Calculated concentrations of NMOC and NOx are given in Table 1. The results of both methods agree well with each other, which indicates on the accuracy of the calculated emission values.

| Method | NMOC | NOx |
|---|---|---|
| Direct | $1.9 \pm 0.6$ | $4.0 \pm 1.0$ |
| Carbon Balance | $1.7 \pm 0.5$ | $3.6 \pm 0.6$ |

**Table 1.** NMOC and NOx concentration (g/(km x vehicle)) obtained by the direct and carbon balance methods, and their ratio.

Thus, the coupling of the transportation and emission models yields the emission rate per traffic road for each relevant pollutant in the units of g/hr.

**Atmospheric Modeling**

The Regional Atmospheric Modeling System (RAMS) is the state of the art mesoscale atmospheric model accounting for the atmospheric attribute (Pielke et al., 1992). It is a multipurpose 3D versatile numerical prediction model designed to simulate weather systems by calculating multiple meteorological fields - primarily the wind, temperature, pressure, and humidity. It is constructed around the full set of equations in terrain following coordinates system, which govern atmospheric motions. The equations are supplemented with optional parameterizations for turbulence, radiation, thermodynamics, clouds, soil type and vegetation. The RAMS was initialized and updated every 6 hours with ECMWF data fields. The topography data was obtained from the GTOPO30 project which is global digital elevation model (DEM) with a horizontal grid spacing of 30 arc seconds (approximately 1 kilometer). The RAMS is equipped with a multiple grid-nesting scheme that allows a two-way interaction between computational grids of different 3D resolution. In the current simulation, the RAMS was executed in a hierarchical, three level nested grids (Fig. 4) to allow zooming in from synoptic scale phenomena (A: Grid 1) through the mesoscale dynamics (B: Grid 2) to the high-resolved local systems (C: Grid 3). The telescoping from large-scale environment with low resolution of 20-km mesh grid cells to small-scale atmospheric systems with fine-meshed high-resolution grid cells (1.25-km) enables us to account for small scale atmospheric features of the target area while simultaneously providing the impact of much larger meteorological systems.

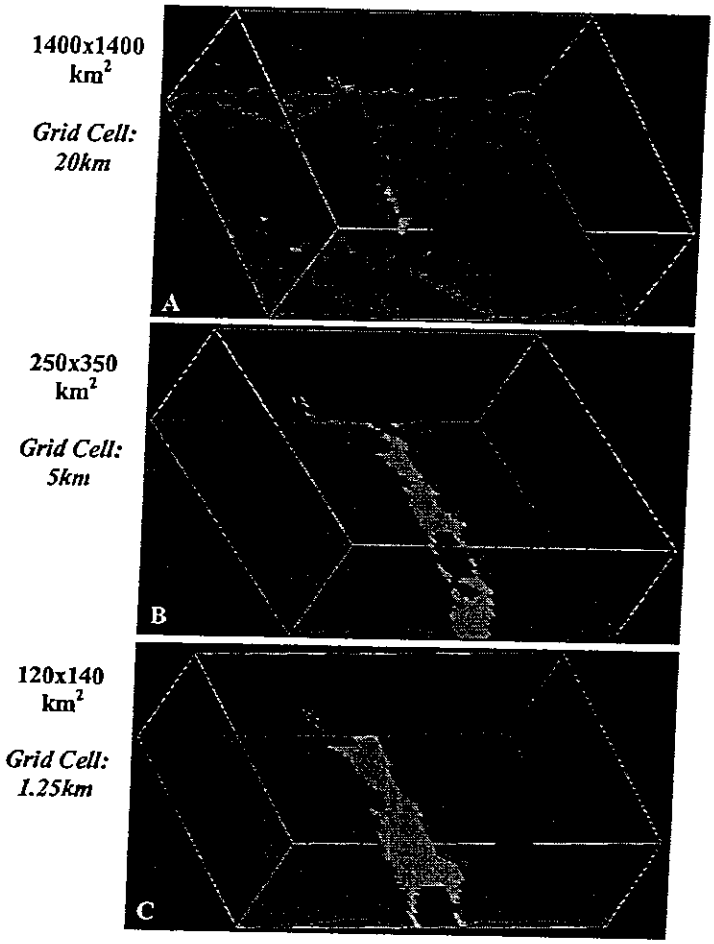


**Figure 4.** The hierarchical three level nested grids utilized in the RAMS.

### Transport Diffusion Simulation

The TDM is a Lagrangian 3D model that simulates the motion of atmospheric pollutants under the influence of atmospheric flow. The TDM was applied to the high resolution grid with a vertical grid resolution of 50m up to a height of 2km. The TDM was initiated and driven by the meteorological fields produced by the RAMS and interpolated them in time and space to the location of the pollutant elements. The coupled EMME/2-Emission model provided the TDM with the following transportation data (the anthropogenic driving force): (i) The number of traffic sources, (ii) Traffic sources location (iii) The emission rates of NOx and VOCs.

## SYNOPTIC CONDITIONS

The dominant synoptic condition prevailing in the east of the Mediterranean Sea from mid-June to mid-September is influenced by two major systems surrounding the region, overall resulting in monotonic weather conditions. From the east, mid and south Asia, land warming during the summer leads to the development of the Monsoon Low, resulting in predominant north winds in the Mediterranean. One of its centers is located in the Persian Gulf, forming the so called "Persian trough" which extends from the Persian-Golf towards the southern shores of Turkey, and dominates the Mediterranean in the summer. It forms northwest winds influencing the north and the central regions of Israel. Westerly to our region, we are influenced by the Azorean high, which is part of the subtropics

belts of highs. The Azorean high is centralized at the Atlantic Ocean, near the Azorean islands, and dictates northwest air motions. The combined synoptic winds will coincide with the see breeze reinforcing it during daytime and opposing it during the night, when land breeze takes over.

## MODEL APPLICATION

The non-hydrostatic mesoscale model RAMS utilized an intercalated three level nested grid scheme. The first grid was applied to an area of 1400x1400 km meso-$\alpha$ scaleato derive synoptic phenomena. The second grid was applied to an area of 250x350 km and the third to a 120x140 km zone (meso-$\beta$ scale, Orlanski 1975). These two higher resolved grids will also account for the sea/land breeze circulation along the west coast of Israel. The simulations were performed for 24-hour intervals starting at midnight. The dates selected for applying the integrated interdisciplinary modeling systems were based on high ozone levels episodes recorded from aircraft measurements taken at about 350 m above ground level. The ECMWF meteorological fields initialized the simulation at 00:00 GMT (03:00 LST) and updated the calculation at a 6-hour interval to produce the 24-hour atmospheric dynamics simulation.

The incorporation of the traffic emissions into the troposphere as the precursors for ozone production was based on a 3-hour release period, corresponding to the time interval of the highest traffic flow and emission rate during the morning rush hours, between 6 and 9 AM LST. Limiting the road traffic emissions interval to the rush hours will emphasize the impact of the Tel-Aviv metropolis traffic emissions during these hours on the evolution of ozone production in mid-Israel in general and over Jerusalem in particular.

In the presented simulation NOx was addressed as an inert, non-reactive entity throughout its spatial and temporal translocation. This assumption is based on the fundamental correlation found to exist between NOy (sum of all nitrogen oxides excluding $N_2O$) concentration and ozone mixing ratio (Trainer et. Al., 1993, Derwent R. G. & Davis T. J., 1994, Olszyna et al., 1994, Olszyna et al.,1997). This correlation prevails for a photochemically aged air mass, i.e. when most of NOx has been oxidized into NOz, (NOz defined as the oxidation products of NOx, i.e. NOz = NOy – NOx). This situation is also referred to as a NOx limited regime. Dynamically speaking, the link between NOx, NOz and NOy can be expressed as (Olszina et. al., 1994):

$$NOz = NOy(1-(NOx/NOy))$$

Prior to photooxidation, NOx levels prevailing in the early morning hours as a consequence of traffic emission equal NOy levels (NOz = 0). As time evolves, NOx is being oxidized, to give rise to the NOz oxidation products. Consequently, a NOx limited regime is established. $NO_x$-sensitive regimes are encountered in the rural area as a result of convection, dispersion and diffusion processes. At these rural areas high VOC/NOx ratios prevail in which ozone levels are essentially indifferent to elevation in the VOCs levels and correlate positively with increase in NOx concentrations.

## RESULTS and DISCUSSION

In the following section we present the early morning rush hours' impact (06:00 – 09:00 LST) of the NOx emission from the Tel-Aviv metropolis and Gaza-Strip transportation sources on its subsequent transport and mixing. Similar scenarios were executed for VOCs and CO emissions. Each dispersed particle represents a gram of pollutant as obtained by the coupled transportation-emission models. Fig 5a shows a top view of the state at 07:00 LST, one hour after the traffic emission release. It is apparent that the newly released particles were transported overseas due to easterly land breeze. Two hours later (Fig 5b) with the onset of the Mediterranean sea breeze the pollution cloud initially located oversea is recirulated towards the land, resulting in its mixing with the freshly released gases. Figures 5c – 5f displays the position of the particles at 10:00, 11:00, 13:00 and 15:00 LST. Two main driving forces manifest the NOx spatial and temporal evolution; an east-southeast-directed transport accompanied with a 3D expansion of the NOx cloud, emphasized visually by Fig 6. Figs 6a and 6a illustrate a 3D perspective view from the west at 08:00 and 13:00 LST. The vertical development of the particles clouds from Tel-Aviv metropolis and the Gaza-Strip is well depicted in these Figs. At 10:00 the particles cloud extends up to the height of 200 - 300 m. While at 13:00, with the inland penetration of the particles over the mountain range coupled with the increasing thermal instability, it elevates up to a height of 1500 m.

It is important to reemphasize the above mentioned photochemical aged air mass concept – as time progresses most of the NOx is being photochemically oxidized, so the NOx cloud essentially

represents NOy which correlates positively with ozone levels, the chemical transformations taking place in a NOx limited regime.

Comparing the final stages of the simulation i.e. Fig 5e and 5f to the real time ozone concentrations depicted in Fig 2b, reveals high degree of similarity in time and location between the modeling results of the photochemical aged air mass and the actual ozone levels. This time dependent overlapping fits nicely with the previous findings of the NOy/$O_3$ correlation (Trainer et. Al., 1993, Olszyna et al., 1994, Olszyna et al., 1997).

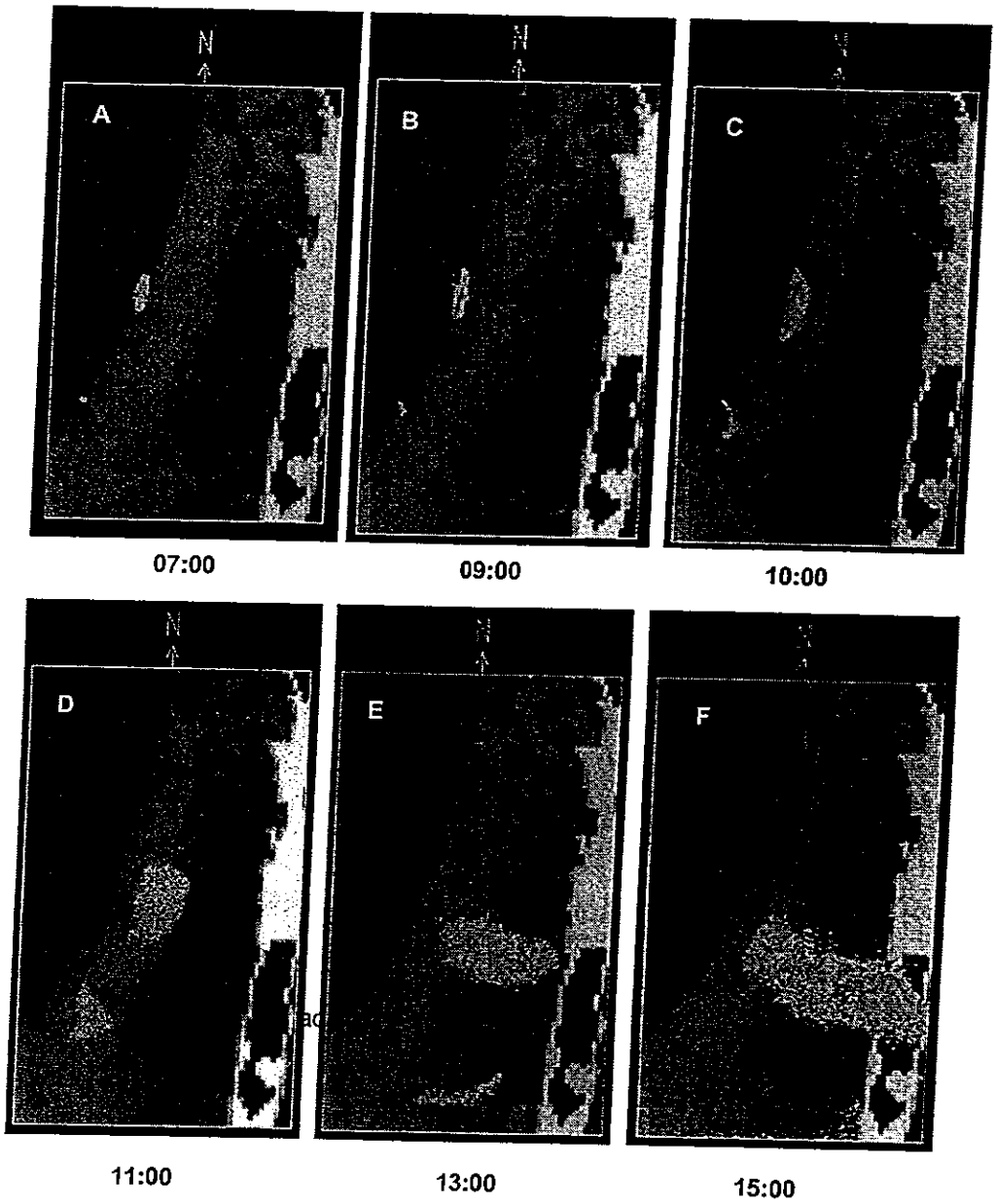


**Figure 5.** Top view of the particles location originating from the Tel-Aviv metropolis and the Gaza-Strip transportation sources for the 28.8.97 ozone epizode.

## CONCLUSION

Air pollution, with ozone generating processes, is among the most significant ecological impacts of the modern age network transportation. The presented work demonstrates the ability of an interdisciplinary modeling systems to collectively operate as a predicting tool/tracing device, capable of successfully simulating ozone formation when transportation emissions are addressed as their

precursor sources. This prediction and analysis tool hopefully will be able to assist in the present and future transportation infrastructure shaping, where air pollution in general - and ozone problems in particular - are to be considered.

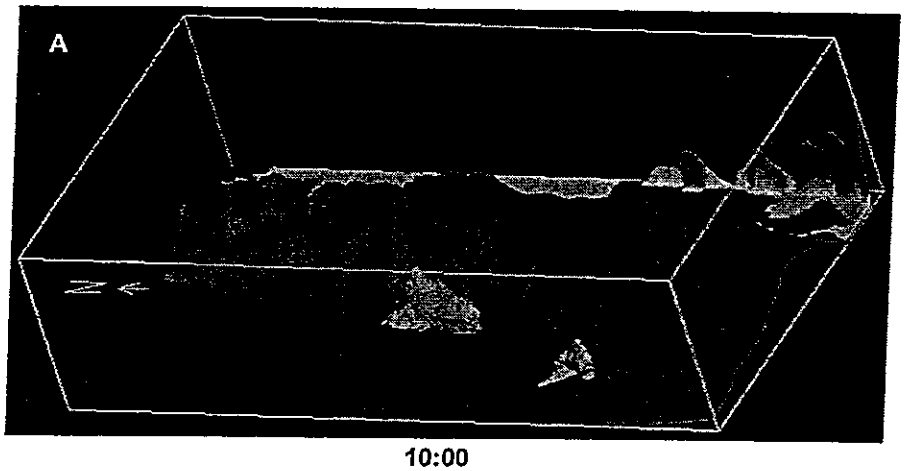


10:00

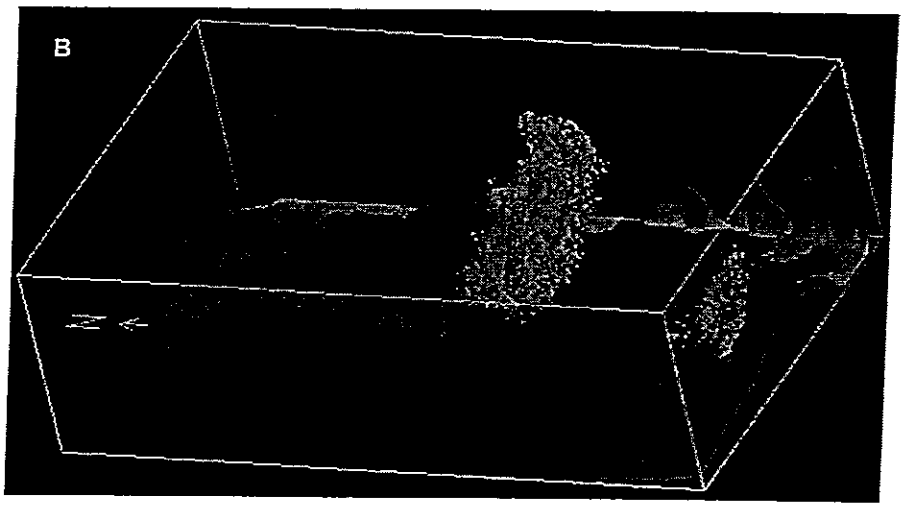


13:00

**Figure 6.** Side view displaying the vertical dimension of the particles locations, calculated for 10:00 and 13:00 LST.

The final stage currently under investigation aims to produce the actual mathematical link between ozone production NOx and VOC levels, solar radiation flux and temperature, to give the final, photochemical link in the transportation to ozone formation scenario.

## ACHNOWLEDGMENTS

This research was partially supported by the Israeli Ministry of Environment. We would like to thank the Rieger Foundation of Santa Barbara, California, for the Rieger-JNF Fellow scholarship in Environmental Studies, which provided additional financial support for the study.

REFERENCES

**Dabdub D., DeHaan L. L. & Seinfeld J. H.** ( 1999 ), *Analysis of ozone in the San Joaquin Valley of California,* Atmospheric Environment, Vol.33, p. 2501 – 2514, 1999.

**Derwent R. G. & Davies T. J.** ( 1994 ), *Modeling the impact of NOx or hydrocarbon control on photochemical ozone in Europe.,* Atmospheric Environment, Vol. 28, p 2039 – 2052, 1994.

**EMME/2 User's Manual, Software release** 9 ( 1998 ), INRO CONSULTANTS INC.

**Finlayson-Pitts B. J. & Pitts J. N.** ( 1997 ), *Tropospheric air pollution: Ozone, air born toxics, polycyclic aromatics, hydrocarbons, and particles.,* Science, Vol. 276, 1045 – 1052, 1997.

**Kley D.** ( 1997 ), *Tropospheric chemistry and transport,* Science, Vol. 276, 1043 – 1045, 1997.

**Moussiopoulos N. & Paragrigoriou S.** ( 1997 ), *Athens 2004 air quality.,* Proceedings of international scientific workshop "Athens 2004 air quality", pp. 183, 1997.

**Olszyna K. J., Bailey E. M., Simonaitis R., & Meagher J. F.** ( 1994 ), *$O_3$ and $NO_y$ relationships at a rural site.,* Journal of Geophysical Research, Vol. 99, p. 14,557 – 14,563, 1994.

**Olszyna K. J., Luria M., & Meagher J. F.** ( 1997 ), *The correlation of temperature and rural ozone levels in southeastern U.S.A.,* Atmospheric Environment, Vol. 29, 1997.

**Orlanski I.** ( 1975 ), *A rational subdivision of scales for atmospheric processes.,* Bulletin of American Meteorology Society, Vol. 56, p. 527 – 530, 1975.

**Peleg M., Luria M., Setter I., Perner D., & Russel P.** (1994 ), *Ozone levels in central Israel.,* Israel Journal of Chemistry, Vol. 34, p 375 – 386, 1994.

**Pielke R. A., Cotton W. R., Tremback C. J., Lyons W. A., Grasso L. D., Nicholls M. E., Moran M. D., Wesley D. A., Lee T. J. & Copeland J. H.** ( 1992 ), *A comprehensive meteorological modeling system,* Meteorology and Atmospheric Physics, Vol. 49, p. 69 – 91, 1992.

**Pinilis C., Kassomenos P. & Kallos G.** ( 1993 ), *Modeling of photochemical pollution in Athens, Greece. Application of the RAMS–CALGRID modeling system.,* Atmospheric Environment, Vol. 27B, p.353 – 370, 1993.

**Seinfeld J. H. & Pandis S.** ( 1997 ), *Atmospheric Chemistry and Physics : Air Pollution to Climate.,* John Wiley & Sons pub., pp. 1326, 1997.

**Seinfeld J. H.** ( 1989 ), *Urban air pollution: state of the art.,* Science, 745 – 752, 1989.

# PART IV

## *The impact of coastal transportation emissions on inland air pollution over Israel – utilizing numerical simulations, airborne measurements and synoptic analyses.*

**D.O. Ranmar[1], V. Matveev[2], U. Dayan[3], M. Peleg[2], J. Kaplan[3], A. W. Gertler[4], M. Luria[2], G. Kallos[5], P. Katsafados[5] and Y. Mahrer[1]**

**[1] The Department of Soil & Water Sciences, The Faculty of Agricultural, Food and Environmental Quality Sciences, The Hebrew University of Jerusalem, Rehovot 76100 Israel.**

**[2] Environmental Science Division, the School of Applied Sciences and Technology, The Hebrew University of Jerusalem, Jerusalem 91904, Israel.**

**[3] Department of Geography, The Hebrew University of Jerusalem, Jerusalem 91905, Israel.**

**[4] Desert Research Institute, P.O. Box 60220, Reno, NV 89506, U.S.A.**

**[5] University of Athens, Laboratory of Meteorology, Ippocratous 33, Athens 106 80, Greece.**

*Accepted for publication by the Journal of Geophysical Research*

*November, 2001*

---

# The impact of coastal transportation emissions on inland air pollution over Israel – utilizing numerical simulations, airborne measurements and synoptic analyses.

D.O. Ranmar, V. Matveev, U. Dayan, M. Peleg, J. Kaplan, A. W. Gertler, M. Luria, G. Kallos, P. Katsafados and Y. Mahrer

**Abstract**

The detection of high ozone levels over large inland areas in Israel during the early, mid and late summer triggered an analysis of air-mass back trajectories. This, in turn, pointed to the transportation system in the metropolitan coastal Tel Aviv region as the possible origin of the ozone's precursors. To link the daily dynamics of rush hour transportation emissions to inland air pollution in general and airborne ozone measurements in particular, an interdisciplinary modeling system was established. The simulations of transportation-to-inland air pollution integrated transportation, emission-factor, atmospheric, transport/diffusion and photochemical models. The modeling results elucidated a spatial and temporal overlap between the ozone precursors and ozone production. The model simulations indicated east to southeasterly dispersion of the pollution cloud. The results agreed well with both spatial and temporal ozone levels as recorded by aircraft over central Israel, as well as with ground-based monitoring station observations. The impact of the Tel Aviv metropolitan area as well as the Gaza Strip, as pivotal coastal transportation sources for inland air pollution in general and ozone formation in particular, is discussed. The synoptic analysis identified the conditions prevailing when elevated air pollution, and especially high ozone levels, exist over central Israel. The analysis showed that this season features a shallow mixed layer and weak zonal flow, which lead to poor ventilation rates and inhibit efficient dispersion of this secondary pollutant. These poor ventilation rates result in the slow transport of ozone precursors, enabling their photochemical transformation under intense solar radiation during their travel from the coast inland. Under these conditions, model results showed that traffic emissions during the morning rush hour from the Tel Aviv metropolitan area contribute about 60% to the observed ozone concentrations.

**Key word index:** Air pollution, numerical atmospheric modeling, transportation model, emission factors, photochemical model, ozone, photochemical aged air mass, $NO_x$, synoptic conditions.

150

## 1. INTRODUCTION

Elevated ozone levels, above the Israeli ambient standards, were observed at inland rural sites during the early summer months of 1988 to 1991 (Peleg et al., 1994). Air-mass back-trajectory analyses have shown that only air masses passing over the Tel Aviv metropolitan area caused the elevated ozone mixing ratios at rural sites over central Israel. Furthermore, the high ratio of $NO_x/SO_2$ patently indicates that ozone precursors such as nitrogen oxides ($NO_x$), carbon monoxide (CO), and volatile organic compounds (VOC) originate mainly from traffic fossil-fuel combustion ($NO_x$ represents the sum of NO and $NO_2$). These pollutants undergo chemical and photochemical transformations in the presence of solar radiation and atmospheric free radicals (Finlayson-Pitts and Pitts, 1997; Seinfeld and Pandis, 1998) to form ozone. The main source for the ozone precursors emitted along the Israeli coastline is transportation (Peleg et al., 1994). Since the formation of ozone and other secondary pollutants takes on the order of several hours, significant transport and mixing occurs simultaneously with the chemical reactions (Kley, 1997; Seinfeld, 1989). Thus, increasing urban and commercial activity along the highly populated Israeli coastal region, together with expanding transportation activity in the Gaza region, is expected to strongly affect inland air quality and specifically, to cause increasingly elevated ozone levels.

The effects of vehicular transport emissions have prompted studies in various disciplines, including: particulate composition of the atmosphere (Fraser et al., 1999; Staehelin et al., 1998), potential mutagenic activity (Kleindienst et al., 1992), the mode of city air pollution exposure from proximal highways (Roodra-Knape et al 1998) and as an integrated component in local-scale air pollution modeling (Pilinis et al., 1993; Moussiopoulos and Papagrigoriou, 1997; Silibello et al., 1998; Svensson, 1998), to name a few. In the latter studies, photochemical grid models were applied to the cities of Athens and Milan to address their regularly recurring air-quality problems. These simulations incorporated traffic emissions, together with other metropolitan emitters, as a source of the precursors feeding the simulated atmospheric photochemistry. In these cases, the emission area and the polluted atmosphere overlap spatially, forming what may be viewed as a "self-pollution" phenomenon, where the city is captured as the origin of primary pollutant emissions, and its overlaying

atmosphere as the "destination" for their subsequent photochemical transformation products. The involvement of major coastal metropolitan areas in inland ozone pollution was studied in regions such as the San Joaquin Valley in California (Dabdub et al., 1999) and the Los Angeles Basin (Lu and Turco, 1996). The former study addressed the differential impact of boundary conditions, winds, emissions, and $NO_x$/VOC sensitivity on the nature of ozone formation, with the San Francisco metropolitan area as one of the model-input pollution sources. It showed that significant inflow into the San Joaquin Valley imposes a strong dependency on the boundary concentration of pollutants and revealed the region as $NO_x$-sensitive, i.e. a dependency of ozone formation on incoming $NO_x$ and internally emitted $NO_x$ greater than that on VOC influx and emission. The latter work simulated ozone distribution over the Los Angeles Basin, revealing the association of the vertical circulation with sea breeze/mountain winds in the injection process of pollutants into the base of the inversion layer. The elevated reservoir of trapped photochemically aged pollutants may then mix downward to increase surface ozone concentration. Such a mechanism was speculated to take place in Israel, based on the similarities in geography and climate (Dayan and Kock, 1996]. These authors analyzed measurements of the Southern California Air Quality Study (SCAQS) and suggested a possible analogy between the build-up mechanism of inland surface ozone in Israel and the mechanism existing in southern California, due to the similarities between these regions (Mediterranean climate, sea breeze, and terrain features).

The present study addresses the dynamics of trans-boundary air pollution, where the transportation emissions (such as $NO_x$ and VOC) originating from major coastal sources impact the inland mixing layer. The research aimed to resolve the daily influence of rush-hour traffic emissions from these coastal locations on the neighboring inland areas. In this study, we focus on the transportation sources in the Tel Aviv metropolitan and Gaza Strip areas, the main coastal urbans areas in the conjugated Israel-Palestinian Authority region. This study includes numerical simulations, their spatial and temporal correlation with airborne-measured ozone from 1994 to 1997, and complementary ground-based measurements performed from June to September of 1999 and 2000.

Since almost no data is available in Israel regarding actual vehicle pollution emission rates, the present study includes measurements performed using the so-

called "tunnel technique". This method gives "real-world" emission rates for the composite vehicle fleet operating on Israeli roads that can be used as input for the transportation model. The data available from aircraft research measurement flights was employed in order to verify the model simulation studies.

## 2. MODELING SYSTEMS

Targeting the daily impact of the traffic infrastructure on subsequent spatial and temporal inland air pollution in general and ozone location in particular called for utilizing an integrated interdisciplinary modeling system covering the fields of transportation densities, emission factors, atmospheric dynamics, pollutant transport and diffusion, and photochemistry. For the purpose of this study, the following models were selected: a transportation model (Emme/2, pronounced *em-two*, named after the French letter "emme" for mobility model) coupled to the emission-factor model (EFM), the regional atmospheric modeling system (RAMS) and a transport and diffusion model (TDM). A photochemical module is addressed through a multiple-regression analysis, which found a correlation between ozone mixing ratios, $NO_y$ levels and air temperature (Olszyna et al., 1994, 1997) in photochemically aged air masses typical of the region under study (Peleg et al., 1994). The following subsections address the different modules of the modeling system (2.1 – 2.5) and provide a brief description of the ground-based measurements (2.6) used in present study.

### 2.1. Transportation Model

The Emme/2 urban/regional transportation system model (Emme/2 User's Manual and references therein; *http://www.inro.ca*) was used to analyze the combination of present transport flow dynamics and land-use scenarios, and future conditions regarding transportation system performance. The urban/regional transportation planning and modeling system assesses the balance between travel demand (based on land use) and supply (based on transport facilities) under given scenarios. Land uses are aggregated into analysis zones (such as census tracts), which provide the basis for estimating a matrix of trip origins and destinations. Networks to which the analysis zones are connected represent transport facilities, where each link of the

network is characterized in terms of its capacity and speed components. The modeling process produces the desired origin-destination matrices of trips by type of trip, mode of travel and time of day, as well as transport network data which depict the volumes of vehicles and passengers by road segment, travel speed, travel time, and delay time. The traffic flow density (TFD) per hour for each road segment is obtained by multiplying the number of vehicles by the length of the road.

### 2.2. Emission-Factor Model

Real world vehicular emission factors for Israel were required to feed the simulation model with the relevant pollution rates. Since almost no data are available for the Israeli scenario, it was necessary to obtain new experimental measurements. The "tunnel technique" (see experimental section) was employed to enable the calculation of vehicle pollutant emission rate. These rates will represent the accurate makeup (light and heavy duty mix, percent with catalytic converters, etc) of the vehicles traveling on the Israeli road system.

### 2.3. Atmospheric Modeling

The regional atmospheric modeling system (RAMS) adopted in this study is a state-of-the-art, well-documented mesoscale atmospheric model (Pielke et al., 1992; Walko et al., 1995). In brief, the RAMS is a multipurpose 3D versatile numerical prediction model designed to simulate weather systems by calculating multiple meteorological fields – primarily wind, temperature, pressure, and humidity, constructed around the full set of equations in a terrain-following coordinates system, which governs atmospheric motions. The equations are supplemented with optional parameterizations for turbulence, radiation, thermodynamics, clouds, soil type and vegetation. The RAMS is equipped with a multiple grid-nesting scheme that allows a two-way interaction between computational grids of different 3D resolution. In the current simulation, the RAMS was executed in hierarchical, three-level nested grids to allow zooming in from synoptic scale phenomena through the mesoscale dynamics to the highly-resolved local systems. The telescoping from large-scale environment, low-resolution grid cells to small-scale atmospheric systems with fine-meshed, high-resolution grid cells enables small-scale atmospheric features of the target area to be taken into account while simultaneously providing the impact of much larger meteorological systems.

## 2.4. Transport Diffusion Simulation

The transport and diffusion model (TDM) is based on the work of Hurley and Physick (1991), and Physick and Abbs (1991). It is a Lagrangian 3D model that simulates the motion of atmospheric pollutants under the influence of atmospheric flow. The TDM was applied to a high-resolution grid with a vertical grid resolution of 50 m and up to a height of 2 km. The TDM was initiated and driven by the meteorological fields produced by the RAMS and interpolated in time and space to the location of the pollutant elements. The coupled Emme/2-emission model provided the TDM with the following transportation data (the anthropogenic driving force): (i) the number of traffic sources, (ii) traffic source locations, (iii) the emission rates of NOx and VOC.

## 2.5. Photochemical Calculation

Quantitative estimation of inland ozone mixing ratios in photochemically aged air masses was established by incorporating a multivariate linear regression analysis (Olszyna et al., 1997) into the TDM model:

$$[O_3] = 9.33 \times [NO_y(ppbv)] + 2.42[Temperature(^0C)] - 28.18$$

Here, $NO_y$ is the sum of all nitrogen oxide species, excluding $N_2O$. Results from measurements performed at a rural inland site in Israel (Peleg et al., 1994) have shown that the above equation is also suitable for use in the present study. The application of this equation under the aforementioned conditions enabled the quantification of ozone formation in our cases. This assumption is based on the fundamental correlation found to exist between $NO_y$ concentration and the ozone mixing ratio in photochemically aged, $NO_x$-limited regimes (Trainer et. al., 1993; Olszyna et al., 1994, 1997).

The linear multiple regression model was sequentially operated after each dispersive time step to account for the newly formed ozone. The use of statistical modeling to estimate photochemical production of ozone via association of ozone concentration with meteorological and chemical variables has the advantages of simplicity and a negligible computation time compared to heavy-duty photochemical solvers. Furthermore, the method does not require the differential concentrations of the species participating in the chemical reactions used to initialize and propagate a photochemical model.

## 3. EXPERIMENTAL DESIGN

A detailed description of the research flight, tunnel measurements and ground level observations is provided in the following subsections.

### 3.1. Research Flights

Research flights were performed over Israel to determine the areas affected by elevated ozone and $NO_y$ levels and thus to calibrate and test the accuracy of the simulation model. The aircraft used in the investigation was a single-engine Cessna 192. The aircraft was equipped with a high-sensitivity $SO_2$ analyzer (TEII 43S, pulsed fluorescence method, ±0.1 ppbv sensitivity), a high-sensitivity NO-$NO_y$ analyzer (TEII 42S, chemiluminescence method, ±0.1 ppbv sensitivity), and an ozone monitor (Dasibi 1008 AH, UV photometric method, ±2 ppbv sensitivity). The zero levels of the monitors were verified both on the ground and in the air, using a PbO scrubber for $SO_2$, purafil-activated charcoal for $NO_y$, and activated charcoal for ozone. Span calibrations were performed daily on the ground before takeoff. A global positioning system (GPS) was used to continuously monitor the position of the aircraft during the research flight. The data were recorded every 10 seconds and stored on both a data logger and a personal computer.

All flights were performed during the summer at noon under westerly wind-flow conditions at an altitude of about 300 m (well within the boundary-mixing layer). The flights started at the coast in the Tel Aviv vicinity and attempted to follow the urban pollution plume as it drifted inland, under the westerly wind flows, towards the Judean mountains (up to 1000 m in height). Since photochemical activity is at a maximum at midday and sufficient time has elapsed from peak emission to allow maximum ozone production, the research flights were expected to identify the areas affected by the Tel Aviv pollution plume. Altogether, 32 flights were performed over three different years (1994, 1995 and 1997) in order to cover different periods and hence various meteorological conditions. In the present study, we report the results of three of the research flights, which were used for comparison with the model simulation studies.

### 3.2. Tunnel Experiment

The tunnel technique (De Fre et al., 1994; Pierson et al., 1996) was employed to measure real-world fleet-wide vehicle emission factors for the various pollutants. The tunnel, situated south of Jerusalem, is 902 m in length, with an average slope of 3.6% and a cross section of approximately 70 $m^2$. Traffic flows in both directions in single lanes. In the tunnel there are 17 sets of blowers to ensure that the CO level remains below 30 ppm at all times. The wind flow in the tunnel is normally in a north-south direction with speeds varying between 1 and 3 m/s. The air sampled for analyses was taken at the northern entrance to the tunnel (background pollution levels) and at a site two-thirds of the way into the tunnel towards the southern exit. Tunnel air was drawn into Tedlar inert sampling bags (30-liter capacity) at a rate of about 0.5 l/min. Thus the samples taken for analyses represented hourly averages. The sampled air was immediately analyzed using the following monitors: TEII (Thermo Environment Instruments Inc.) model 42S for $NO/NO_x$, TEII # 43C for $SO_2$, TEII # 48 for CO, TEII # 41C for $CO_2$, Dasibi hydrocarbon analyzer for NMHC (non-methane hydrocarbons) and a Verewa # F-101 for particulates. Vehicle counts, divided into light- and heavy-duty for each direction, and vehicle speed were taken concurrent to the air sampling. Additionally, wind speed (Met One # 010C), temperature and relative humidity (Campbell Scientific Inc. # 207) were monitored inside the tunnel. Altogether, 21 hourly samples were taken and analyzed during the research campaign.

### 3.3. Ground-Based Measurements and Data Analysis

Data available from the Israeli national air-quality monitoring network provided a variety of chemical and meteorological variables, such as $NO_x$, ozone (models 42C and 49C analyzers, respectively, Thermo Environmental Instruments Inc., USA), wind speed and direction, global sun radiation (GSR) and temperature. The Israeli monitoring network is based on USEPA approved instruments and measuring protocols. The statistical interpretation was based upon data collected between June 1 through September 30 for the years 1999 and 2000. Three locations, the metropolitan area of Tel-Aviv, Modiin and Jerusalem, were chosen, all of which are located within the experimental flight path and along the dominant summertime wind trajectory (see Fig. 1).

## 4. MODEL APPLICATION

### 4.1. Traffic Flow Simulation

For the purpose of this study, model implementation focused on detailing existing conditions (reflecting a total population of 6.3 million in the year 2000) to provide input data for a calibration run of the emissions model. The principal steps of the transportation modeling process were:

4.1.1. Trip Generation -- Travel demand (vehicle-trip productions and attractions) was calculated for each of the country's 370 traffic analysis zones based on socioeconomic data for year-2000 conditions (population, housing, vehicle availability, total employment and retail employment). The 1996-97 National Travel Survey for Israel (Central Bureau of Statistics) provides the basis for trip generation rates. Trip attractions were balanced model-wide to total trip productions.

4.1.2. Trip Distribution -- Matrices of the origin-destination travel patterns were estimated based on the marginal totals from the trip generation step, above, and using a two-way balancing gravity model as calibrated for Israeli conditions (the time-impedance curve can be expressed as the expression impedance = exp(-0.08*time).

4.1.3. Travel Assignment -- Matrix origin-destination pairs were assigned to the road network using an incremental capacity-constrained assignment calibrated to Israeli conditions (volume-delay functions adapted from the Department of Transport, Economic Assessment of Road Schemes, United Kingdom, September 1996).

Traffic speeds on road network segments were fed back into the trip distribution model in an iterative process to reflect the effects of traffic congestion on both origin-destination choice and travel-path choice.

### 4.2. Vehicle Emission Factors Calculation

The emission model calculations were based on two complementary methods: the direct and carbon balance method. The direct method essentially produces the EFM of a specific pollutant in the tunnel's air based on the measured pollution concentration, tunnel length, cross section and number of vehicles present during the measurement,

$$EMF_i = (X_i \times V_w \times S \times T)/(L \times N)$$

$EMF_i$ - emission factor of pollutant i (g/(km x vehicle))

$X_i$ - pollutant i concentration ($g/m^3$)

$V_w$ - average wind speed in the tunnel (m/s)

S - cross-sectional area ($m^2$)

T - measurement time (s)

L - tunnel length (m)

N - number of vehicles that passed during T

The carbon balance method EMF is obtained from the following relation:

$$EMF_i = P_i \times C$$

$P_i$ - mass of pollutant i divided by the total carbon in the tunnel air (g/kg C)

C - average carbon fuel consumption in the tunnel (units of kg C/km).

Calculated emission rates for $SO_2$, $NO_y$, NMHC and CO are given in Table 1 for average vehicle speeds of 60 to 80 km/h and an average deisel composition of 10%. The results of both methods agree well with one another, indicating the accuracy of the calculated emission values. These emission factors obtained in the present study are compatible with results obtained from similar studies performed both in the US (Pierson et al., 1966) and Europe (De Fre et al., 1994). Limited data available from measurements carried out on individual vehicles in Israel also shows good agreement with the present study. The results presented in Table 1 were used as input data for the modeling simulation studies since they represent similar conditions (such as speed and vehicle mix) to those expected in the region under examination.

Table 1. $SO_2$, $NO_x$, NMHC and CO concentration (g/(km per vehicle)) obtained by the direct and carbon balance methods

| Method | $SO_2$ | $NO_y$ | NMHC | CO |
|---|---|---|---|---|
| Direct | 0.38 ± 0.09 | 4.0 ± 1.0 | 1.9 ± 0.6 | 21.0 ± 3.4 |
| Carbon Balance | 0.34 ± 0.06 | 3.6 ± 0.6 | 1.7 ± 0.5 | 20.1 ± 4.1 |

The resulting integrated transportation and emission models provided the emission rate per traffic road segment for each relevant pollutant in units of g/h.

### 4.3 Atmospheric Modeling Aspects

The non-hydrostatic mesoscale-mode, three-way intercalated-nested grid scheme was utilized in the RAMS simulation. The first grid was applied to an area of 1400 x 1400 square km$^2$ (meso-$\alpha$ scale, Orlanski, 1975) at a 20-km resolution to derive synoptic phenomena. The latitude and longitude of the northwest and southeast corners of the modeling domain are (32.959, 27.146) and (25.618, 41.681), respectively. The second and third grids were applied to areas of 250 x 350 and 120 x 160 km$^2$ at 5-km and 1.25 km zooming-in resolutions, respectively. These two more highly resolved grids also account for the sea and land breezes and mountain and valley flows. All simulated zones were centered at the latitude/longitude coordinates of (32.0, 35.0), roughly representing the center of Israel. The simulations were performed for 24 h starting at midnight. The simulations were initialized and updated every 6 h with European Center for Medium-Range Weather Forecasts (ECMWF) data fields. The topographic data was obtained from the GTOPO30 project (*http://edcdaac.usgs.gov/gtopo30/ gtopo30.html*) which is a global topography digital elevation model (DEM) with a horizontal grid spacing of 30 arc seconds (approximately 1 km) derived from several raster and vector sources of topographic information. GTOPO30, completed in late 1996, was developed over a three-year period through a collaborative effort led by staff at the U.S. Geological Survey's EROS Data Center (EDC). The dates selected for applying the integrated interdisciplinary modeling system were based on days with high ozone level episodes as recorded by the flight measurements. The ECMWF meteorological fields initialized the simulation at 00:00 UTC (03:00 LST – local summer time) and provided the boundary conditions for the large-scale grid by updating the calculation at 6-h intervals to produce the 24-h atmospheric dynamics simulation. The fields produced by the RAMS were then used to initialize and drive the TDM, dispersing the traffic originated $NO_x$ and VOC from their emission origins in the Tel Aviv metropolitan area and the Gaza Strip. Applying the statistical multiple regression model following each dispersive time step gave the ozone mixing ratios. However, as mentioned previously, only ozone concentrations obtained in the time domain of photochemically aged air mass were used for inference and analysis, i.e. concentrations obtained about 4 h (or more) after release.

### 4.4. Rush Hour Determination

Analysis of $NO_y$ data collected from June 1 to September 30 for the years 1999 and 2000, at a monitoring station located in metropolitan Tel Aviv (see Fig. 2), as well as a traffic survey and Emme/2 simulations indicated that peak traffic emissions occurs between 06:00 and 09:00 (primarily as $NO_x$). This time period corresponds to "rush hour" peak transport loads. From 09:00 onwards, the $NO_y$ levels remain monotonically low. This daily time interval therefore reflects the main $NO_y$ pollution pulse and was used to initialize the simulation runs.

## 5. RESULTS and DISCUSSION

The following section addresses coastal transportation-to-inland trans-boundary air pollution processes as revealed by simulations and airborne/surface-measured ozone levels. Overall three scenarios are analyzed, corresponding to early, mid and late summer ozone episodes as detected by airborne measurements.

### 5.1. Model Simulation

Fig. 3 qualitatively illustrates a sequential top view of the $NO_y$ particles (released from transportation primarily as $NO_x$) over the simulation area at 300 m AGL (airborne measurement height for selected hours of the 25 July 1997 ozone episode). The particles were emitted from the Tel Aviv metropolitan and Gaza Strip transportation sources from 06:00 to 09:00 LST (rush hour). Each particle released represents one gram of pollutant emitted per minute. At 07:00 LST, one hour after emission had begun, particles were transported offshore by an easterly land breeze. During the next two hours, with the onset of the Mediterranean sea breeze, the pollution cloud initially located over the sea recirculated inland and mixed with freshly released pollution. Further inland, movement and dispersion of the particles is shown from 11:00 to 15:00 LST. Two main driving forces manifest the $NO_y$ spatial and temporal evolution: east-southeast transport accompanied by a 3D expansion of the $NO_y$ cloud. The particulate clouds from the Tel Aviv metropolis and the Gaza Strip extend to a height of 300 to 400 m (above sea level) by 11:00. At 13:00, with the inland penetration of the particles over the mountain range coupled with increasing thermal instability, the pollution clouds expand to a height of 1500 m. Almost identical patterns were obtained (not shown) for traffic-produced VOC and CO.

Fig. 4 shows a vertical east-west cross section of calculated ozone concentration over Jerusalem (Fig. 4a, August 28 1997) and Beer Sheva (Fig. 4b, May 25 1994) at

14:00, viewed from the south. On August 28, 1997, the maximal observed ozone values over Jerusalem ranged from 120 to more than 180 ppbv (Fig. 5f), compared to calculated values of about 110 ppbv (Fig. 4a). On May 25, 1994 (Fig. 4b), maximal observed ozone levels over Beer Sheva area ranged from 100 to 160 (Fig. 5b). The corresponding calculated maximal values were about 85 ppbv. The explicit inclusion of traffic pollution from metropolitan Tel Aviv during rush hour (06:00 - 09:00) suggests that it accounts for more than 60% of the observed inland ozone pollution. The rest may be attributed to (i) background concentrations (up to 60 ppbv in some of the airborne measurements) and (ii) alternative ozone sources, such as traffic emissions from other locations.

### 5.2. Flight and Model Comparison

Model results for three scenarios were compared with airborne measurements of ozone concentrations. The inland air pollution episodes represent early (25-26 May, 1994), middle (25 July, 1997) and late (28 August, 97) summer. Fig. 5 shows the measured ozone levels along the flight path at 13:00 – 15:00 LST (Fig. 5b, d, f) and their corresponding model-calculated photochemically aged $O_3$ particles (Fig. 5a, c, e) for 14:00. The actual ozone concentrations were presented in Fig. 4 while Fig 5 shows their spatial distribution in a qualitative manner.

Analysis of the research flight performed on May 25, 1994 reveals that the simulation study identified the main polluted area over Beer Sheva (Fig. 5a). This is in good qualitative agreement with the flight measurements (Fig. 5b). The wind-field pattern (Fig. 6a) traces back to the NNW, essentially originating from the Tel Aviv coastal area. The simulation results for July 25, 1997 (Fig. 5c) predict a widely dispersed pollution plume over the central-to-southern Judean Hills with Jerusalem at its northern peak. The research flights for this date (Fig. 5d), as well as the calculated wind field (Fig. 6b), which exhibits a general west-to-east flow, supports this general pattern. The high concentrations of $O_3$ measured north of Jerusalem were not captured by the model. This suggests that emission sources from alternative areas (not included in the Tel Aviv morning rush hour traffic emissions) may have contributed to the ozone formation: for example, transportation sources from Jerusalem and non-coastal cities, as well as continuous traffic emissions from the Tel Aviv metropolitan area, besides the rush hour emission (06:00 – 09:00). On this day (Fig. 6b), the wind-field pattern exhibited a northwesterly flow which transported inland pollutants from northern coastal sources (not overlapping the Tel Aviv sources as occurred under a NNW flow

– Fig. 5a, b). Consequently, an extended pollution area north of Jerusalem was measured. The simulation of a late summer episode (August 28, 1997) depicted ozone pollution over an extended region of central Israel and over Jerusalem extending to the Dead Sea, and a secondary polluted area to the south over Beer Sheva (Fig. 5e). The flight measurements similarly identified the highest ozone levels over central Israel extending to the Dead Sea. It appears that the Jerusalem region was affected by pollution sources originating from the central Israeli coastal plane while the area over Beer Sheva was affected by emissions from the Gaza Strip (Fig. 5f). The predicted wind field for the corresponding date (Fig. 6c) indicated west-to-southeast flow, resulting in an extended inland air pollution pattern. Its interesting to note that for days dominated by southwest winds, low levels of airborne measured ozone (60 ppbv) were detected over central Israel.

Surface wind speed and wind direction measured at a station in Tel Aviv (Fig. 7) agrees well with model results (Fig. 5a, b, c). Both model-predicted and measured data indicate that on May 25, 1994, the early morning NNW winds carried the newly emitted traffic pollution southward (Fig. 5a). For the mid-to-late summer episodes (July 25 and August 28, 1997), winds veering from west to NW, accompanied by intensified wind speed, dispersed the pollution towards the east and southeast (Figs. 5b, c).

**5.3. Relation of Air pollution Scenarios to Weather Conditions**

Spring and early summer are characterized by the overwhelming influence of the subtropical high-pressure system. This situation often leads to a shallow mixed layer accompanied by weak zonal winds. Both of these features result in poor ventilation conditions and consequently to rising air pollution concentrations within the stable profile formed (Dayan and Rodnizki, 1999).

All three episodes of elevated ozone concentration recorded by aircraft measurements and selected for simulation were found to fall into the "shallow Persian trough" synoptic category. This category occurs during warm summer days mainly at the start, but occasionally both in the middle and at the end of the summer season. This synoptic pressure pattern features stagnation conditions that evolve as a result of weak-pressure-gradient winds, a shallow mixed layer capped by subsiding warm and dry air and accordingly poor ventilation within the mixed layer. Several air pollution studies conducted in Israel, mainly over coastal environments, have already identified this synoptic category as being the main one affecting pollutants dispersion (Dayan et al., 1988; Hashmonay et al., 1991; Koch and Dayan, 1992; Dayan and Rodnizki, 1999). Table 2 describes the main elements

influencing the dispersion of pollutants and their measured values for three of the episodes analyzed. The calculated ventilation rates are based on mixing depths measured over the central coastal plain of Israel and are given in order to represent the worst regional transport conditions.

The first case analyzed (May 25 1994) typifies the dispersion conditions associated with the "Weak Persian Trough" mode (Fig. 8a). During the noon hour of this episode, a northerly wind blew along the coast up to a few hundred meters above ground within the shallow mixed layer. Both the simulation (Fig. 5a) and flight observation (Fig. 5b) results indicate transport of the emitted plume southward with very limited dilution. The second episode analyzed (July 25 1997) was characterized by a somewhat deeper "Persian trough" (Fig. 8b). The dispersion conditions during this event were much better since the mixed layer was deeper and the resultant onshore winds stronger, leading to three times the ventilation rate measured in the first case. Both the simulation and measurement results (Fig. 5c, 5d) show the elongated propagation of the plume during its transport southeast toward the inland elevated region. The "Persian trough" during the third case studied (August 28 1997) is in its weakest mode, leading to weak and variable winds onshore (Fig. 8c). Under such dispersion conditions, the polluted air mass drifts very slowly from the Tel Aviv metropolitan area towards Jerusalem, while keeping its initial rounded contours (as seen in Fig. 5e, 5f). These three cases indicate that in summer, when synoptic gradient winds are weak as manifested by low ventilation-rate values, central inland Israel is strongly affected by elevated ozone levels caused by urban pollution plumes originating along the Mediterranean coastline.

Data for the other research flights, not reported in the study, further indicate that observational and model simulations were generally in phase, the degree of overlap dependent on the aforementioned arguments. Furthermore, during the summer period, elevated ozone concentrations were recorded over central Israel on almost all days studied. Both observations and calculations point to the Tel Aviv metropolitan region as the origin for the inland air pollution.

Regarding the Gaza Strip transportation emission sources, the simulations suggested that the southern tail of the observed central Israel air pollution episodes are due to contributions from this region.

### 5.4. Data Analysis of Ground-Based Monitoring Stations

The available ground monitoring data was analyzed to discern any observable patterns for the pollution levels with increasing distance inland of the three monitoring sites. While data from the network was available only for two summer periods, (June to September of 1999 and 2000), these periods were representative of the general situation existing during the summer month of the research period, since no significant changes have occurred since then in the area under investigation. Furthermore, considering time-space scales in ambient ozone and meteorology data (Eskridge et al., 1997; Rao et al., 1997), the relevant long-term component (trend term) of the ozone time series, i.e. variations in climate, policy, and/or economics, is of no significance in our case. The monitoring data for the entire period under examination was averaged over 30-min time segments. Figures 9 and 2 show the data for ozone and $NO_y$, respectively. The ozone levels exhibited a distinct inland scale dependency. Ozone peaks at later hours (11:30, 13:00 and 14:00 in Tel Aviv, Modiin and Jerusalem, respectively) and on average reaches higher levels (50 ppbv, 56 ppbv, 70 ppbv for Tel Aviv, Modiin and Jerusalem, respectively) as progress is made inland. A comparison of the coastal $NO_y$ spectra (Tel Aviv) to the inland $NO_y$ profiles (Modiin and Jerusalem) discerns different dynamics for these locations. While the initial levels in the Tel Aviv metropolitan area are higher during the morning rush hour emissions, they experience a pronounced bleaching by the late morning sea breeze in comparison to inland locations, which level out at relatively higher midday concentrations. This may indicate, in the absence of any alternative $NO_y$ source, that the early morning $NO_x$ produced by transportation sources in Tel Aviv is transported inland, providing additional $NO_y$ to the regions in its path. These results correspond well with the dynamics of the inland-penetrating plume. The observed increase in ozone concentrations is attributed to ongoing photochemical transformations while traversing inland. Thus, the superposition of the transported ozone cloud, originating from the coastal metropolitan traffic sources, with the native formed ozone results in the higher observed ozone levels.

## 6. CONCLUSIONS

Airborne measurements showed that central inland Israel is strongly affected by pollution originating along the Mediterranean coastline, where urban transportation sources play a pivotal role. The flight measurements, model simulations and ground-level monitoring all showed that under northwesterly winds, elevated ozone values can be found over central Israel. These findings establish a scenario in which

the physical process of inland movement of pollutants in general, and ozone precursors in particular, is established. The Tel Aviv metropolitan area and possibly the Gaza Strip region emit transportation pollutants into the troposphere on a daily basis, initiating their subsequent photochemical transformation as they are transported downwind. Model simulations showed that about 60% of the detected inland ozone concentration is nourished by traffic emissions during the morning rush hours from the Tel Aviv metropolitan area.

The assumption of a photochemically aged air mass regime may enable the application of multivariate linear regression analysis to quantitatively appraise ozone production over central Israel. Thus, under these conditions, the application of a relatively simple statistical analysis method for evaluating ozone concentrations may replace the need for comprehensive photochemical solvers.

Air pollution, with ozone-generating processes, is among the most significant ecological impacts of modern age network transportation. The problem is especially acute in regions with poor dispersion conditions such as those existing in Israel during the highly photochemically active summer period. The work presented here demonstrates the ability of interdisciplinary modeling systems to operate collectively as a prediction tool/tracing device, capable of successfully predicting air pollution hotspots. The model is now being expanded to include photochemical transformations that will enable simulating ozone formation under additional conditions. This prediction and analysis tool is expected to assist in the shaping of present and future transportation infrastructure, where air pollution in general – and ozone problems in particular – are to be considered.

**Acknowledgements:**

This study was funded under the US Middle East Regional Cooperation (MERC) Program (USAID Award Number PCE-G-00-99-00037-00), project title "Transboundary Air-Quality Effects from the Urbanization of Israel-Gaza Mediterranean Coast".

We would like to acknowledge the assistance provided by the Israeli Ministry of the Environment (air quality monitoring national network) and the Israeli Meteorological Service for providing the relevant air quality and meteorological data. We would also like to thank Prof. Robert Bornstein for helpful discussions, and encouragement during the performance of the above research.

## 8. REFERENCES

Dabdub D., L. L. DeHaan and J. H., Seinfeld, Analysis of ozone in the San Joaquin Valley of California. *Atmospheric Environment*, 33, 2501- 2514, 1999.

Dayan U. and L. Koch, Ozone concentration profiles in the Los Angeles Basin – A possible similarity in the build-up mechanism of inland surface ozone in Israel. *J. Appl. Meteor.*, 35, 1085-1090, 1996.

Dayan U. and J. Rodnizki, The temporal behavior of the atmospheric boundary layer in Israel. *J. Appl. Meteorol.*, 38, 830-836, 1999.

Dayan U., R. Shenhav and M. Graber, The spatial and temporal behavior of the mixed layer in Israel. *J. Appl. Meterol.*, 27, 1382-1394, 1988.

De Fre R., P. Bruynserade and J.G. Kretzschmar, Air pollution measurements in traffic tunnels. *Environ. Health Perspec.* 102, 31-37, 1994.

Department of Transport, Economic Assessment of Road Schemes: Cost Benefit Analysis (COBA) Manual. *Design Manual for Roads and Bridges (v.13)*, HMSO, United Kingdom, ISBN 0115516697, September 1996.

Emme/2 User's Manual, Software release 9. INRO CONSULTANTS INC., 1998.

Eskridge R. E., J. Y. Ku, S.T. Rao, S. P. Porter and I. Zurbenko, Separating different scales of motion in time Series of Meteorological variables. *Bull. Amer. Meteor. Soc.*, 78, 1473-1483, 1997.

Finlayson-Pitts B. J. and J. N. Pitts, Tropospheric air pollution: Ozone, air born toxics, polycyclic aromatics, hydrocarbons, and particles. *Science*, 276, 1045-1052, 1997.

Fraser M. P., G. R. Cass and Brend R. T. Simoneit, Particulate organic compounds emitted from vehicle exhaust and in the urban atmosphere. *Atmos. Environ.*, 33, 2715-2724, 1999.

Hashmonay R., A. Cohen and U. Dayan, Lidar observation of the atmospheric boundary layer in Jerusalem. *J. Appl. Meteorol.*, 30, 1228-1236, 1991.

Hurley P. and W. Physick, A Lagrangian particle model of fumigation by breakdown of the nocturnal inversion. *Atmospheric Environment*, 25A, 1313-1325, 1991.

Kleindienst, T. E., D. F. Smith, E. E. Hudgens and R. F. Snow, The photooxidation of automobile emission: measurements of the transformation products and their mutagenic activity. *Atmos. Enviro.*, 26A, 3039-3053, 1992.

Kley D., Tropospheric chemistry and transport. *Science*, 276, 1043-1045, 1997.

Koch J. and U. Dayan, A synoptic analysis of the meteorological conditions affecting dispersion of pollutants emitted from tall stacks in the coastal plain of Israel. *Atmos. Environ.* 26A, 2537-2543, 1992.

Lu R. and R.P. Turco, Ozone distribution over the Los Angeles Basin: Three-dimensional simulations with the SMOG model. *Atmospheric Environment*, 30, 4155-4176, 1996.

Moussiopoulos N. and S. Papagrigoriou (Eds.), Athens 2004 air quality. Proceedings of International Scientific Workshop "Athens 2004 Air Quality", 183pp, 1997.

Olszyna K. J., Bailey E. M., Simonaitis R., & J. F. Meagher, $O_3$ and $NO_y$ relationships at a rural site. *J. of Geophys. Res.* 99, 14,557-14,563, 1994.

Olszyna K. J., Luria M., and J. F. Meagher, The correlation of temperature and rural ozone levels in southeastern U.S.A. *Atmos. Environ.*, 31, 3011-3022, 1997.

Orlanski I., A rational subdivision of scales for atmospheric processes. *Bulletin of American Meteorology Society*, 56, 527-530, 1975.

Peleg M., M. Luria, I. Setter, D. Perner and P. Russel, Ozone levels in central Israel. *Israel Journal of Chemistry*, 34, 375-386, 1994.

Physick W. L. and D. J Abbs, Modeling of summertime flow and dispersion in the coastal terrain of Southeastern Australia. *Monthly Weather Review*, 119, 1014-1030, 1991.

Pielke R. A., W. R. Cotton, C. J. Tremback, W. A. Lyons, L. D. Grasso, M. E. Nicholls, M. D. Moran, D. A. Wesley, T. J. Lee and J. H. Copeland, A comprehensive meteorological modeling system. *Meteorology and Atmospheric Physics* 49, 69-91, 1992.

Pierson, W. R., A. W. Gertler, N. F. Robinson, J. C. Sagebiel, B. Zielinska, G. A. Bishop, D. H. Stedman, R. B. Zweidinger and W. D. Ray, Real-World Automotive Emissions. Summary of Studies in the Fort McHenry and Tuscarora Mountain Tunnels. *Atmos. Environ.*, 30, 2233-2256, 1996.

Pilinis C., P. Kassomenos and G. Kallos, Modeling of photochemical pollution in Athens, Greece. Application of the RAMS-CALGRID modelling system. *Atmospheric Environment* 27B, 353-370, 1993.

Rao S. T., I. G. Zurbenko, R. Neagu, P. S. Porter, J. Y. Ku and R. Henry, Space and time scales in ambient ozone data. *Bull. Amer. Meteor. Soc.*, 78, 2153-2166, 1997.

Roorda-Knape M. C., N. A. H. Janssen, J. J. De Hartog, P. H. N. Van Vliet, H. Harssema and B. Brunekreef, Air pollution from traffic city districts near major motorways. *Atmos. Enviro.*, 32, 1921-1930, 1998.

Seinfeld J. H.,Urban air pollution: state of the science. *Science*, 243, 745-752, 1989.

Seinfeld J. H. and S. N. Pandis (Eds.), *Atmospheric Chemistry and Physics : Air Pollution to Climate*, 1326 pp., John Wiley & Sons Pub., Canada, 1998.

Silibello C., G. Calori, G. Brusasca, G. Catenacci and G. Finzi, Application of photochemical grid model to Milan metropolitan area. *Atmos. Enviro.*, 25, 2025-2038, 1998.

Staehelin J., C.Keller, W. Stahel, K. Schlapfer and S. Wunderli, Emission factors from road traffic from a tunnel measurements (Gubrist Tunnel,Switzerland). Part III: Results of organic compounds, $SO_2$ and speciation of organic exhaust emission. *Atmos. Enviro.*, 32, 999-1009, 1998.

Svensson G., Model simulation of the quality in Athens, Greece, during the Medcaphot-trace campaign. *Atmos. Enviro.*, 32, 2239-2268, 1998.

Trainer M. et al., Correlation of ozone with $NO_y$ in photochemically aged air, *J. Geophys. Res.*, 98, 2917-2925, 1993.

Walko R. L., C. J. Tremback, and R. F. A Hertenstein, RAMS – Regional Atmospheric Modeling System version 3b, *User's Guide*, ASTER Division, Mission Research Cooperation, Fort Collins, CO, 1995.

**LIST OF FIGURES:**

Fig. 1: Map of central Israel and the Gaza region.

Fig. 2: Averaged diurnal cycles of measured $NO_y$ concentrations in Tel Aviv, Modiin and Jerusalem for the periods of June-September in 1999 and 2000.

Fig. 3: Qualitative top view of simulated $NO_y$ particles location over Israel at 300 m AGL at selected hours (LST). Particles originated from Tel Aviv metropolitan and the Gaza Strip transportation sources at rush hour, between 06:00 and 09:00 LST. T – Tel Aviv metropolitan, J – Jerusalem, G – Gaza strip, B – Beer Sheva.

Fig. 4: Vertical east-west cross section (Y-Z plane) of model-calculated ozone concentrations for: a) Aug 28 1997 over Jerusalem area and b) May 25 1994 over Beer Sheva area at 14:00 LST. Zero distance represents the coast of Tel Aviv. The values of outer contours are indicated. Dark area represents the topography in the studied regions.

Fig. 5: Qualitative Comparison of model simulation with aircraft measurements of ozone for the three days studied.
May 25 1994, 14:00-16:00 LST (a) model simulation (b) flight measurements
Jul 25 1997, 14:00-16:00 LST (c) model simulation (d) flight measurements
Aug 28 1997, 14:00-16:00 LST (e) model simulation (f) flight measurements.

Fig. 6: Simulated wind fields at Z = 600 m for:
a) May 25 1994, b) Jul 25 1997, and c) Aug 28 1997 at 12:00 LST.
Wind arrows below topography height are truncated. T – Tel Aviv metropolitan, J – Jerusalem, G – Gaza strip, B – Beer Sheva.

Fig. 7: Measured wind direction (WD) and wind speed (WS) in Tel Aviv for May 25 1994, Jul 25 1997 and Aug 28 1997 (LST).

Fig. 8: Synoptic maps of the three examined days (heavy lines indicate isobars in milibars):
(A) May 25 1994, 15:00 LST
(B) July 25 1997, 15:00 LST
(C) August 28 1997, 16:00 LST

Fig. 9: Averaged diurnal cycles of measured ozone concentrations in Tel Aviv, Modiin and Jerusalem for the periods of June-September in 1999 and 2000.

**Figure 1**

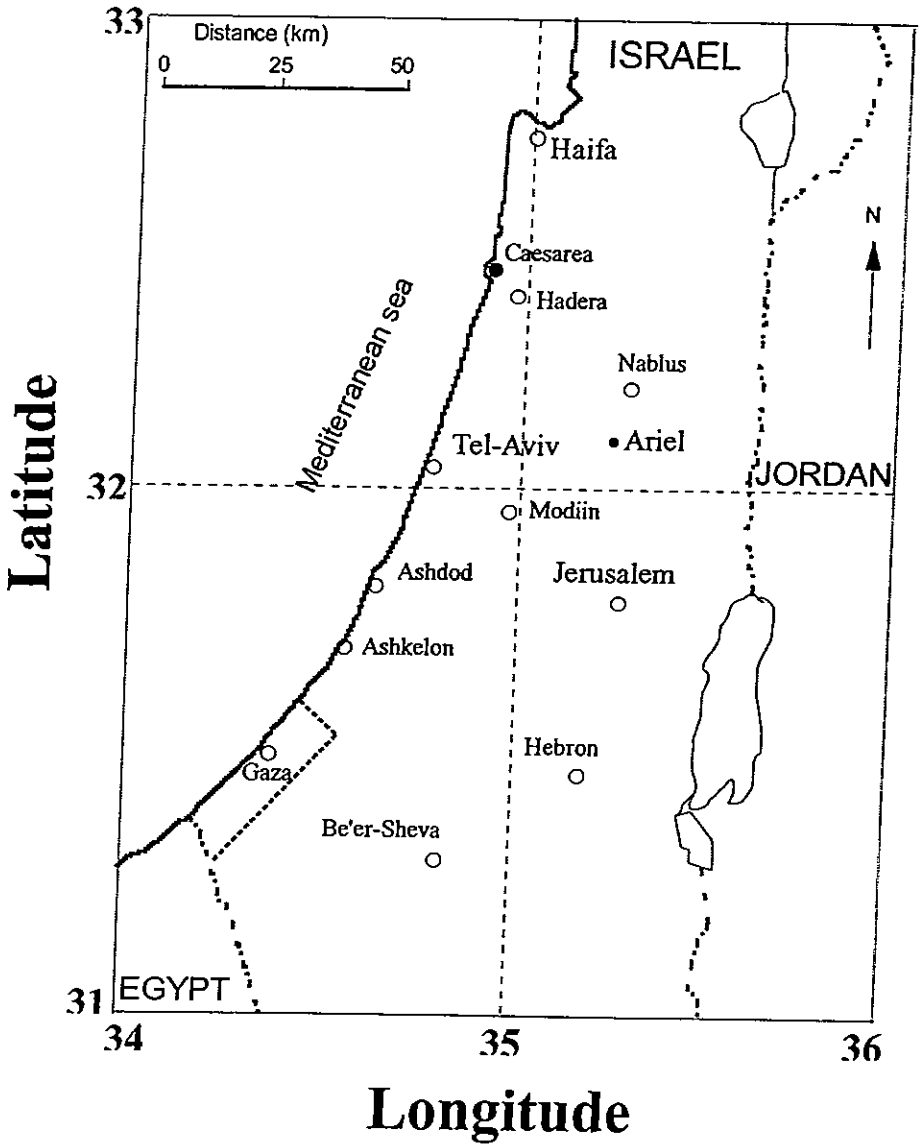
Distance (km)
0
25
50
ISRAEL
Haifa
Caesarea
Hadera
Mediterranean sea
Nablus
Tel-Aviv
Ariel
JORDAN
Modiin
Ashdod
Jerusalem
Ashkelon
Hebron
Gaza
Be'er-Sheva
EGYPT
N
33
32
31
34
35
36
Latitude
Longitude

**Figure 2**

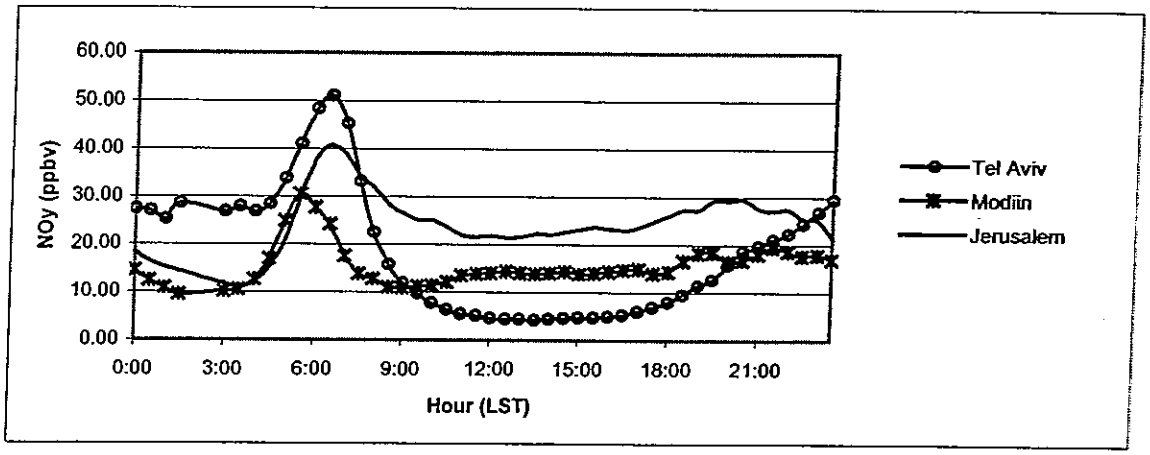
60.00
50.00
40.00
30.00
20.00
10.00
0.00
NOy (ppbv)
0:00
3:00
6:00
9:00
12:00
15:00
18:00
21:00
Hour (LST)
Tel Aviv
Modiin
Jerusalem

**Figure 3**

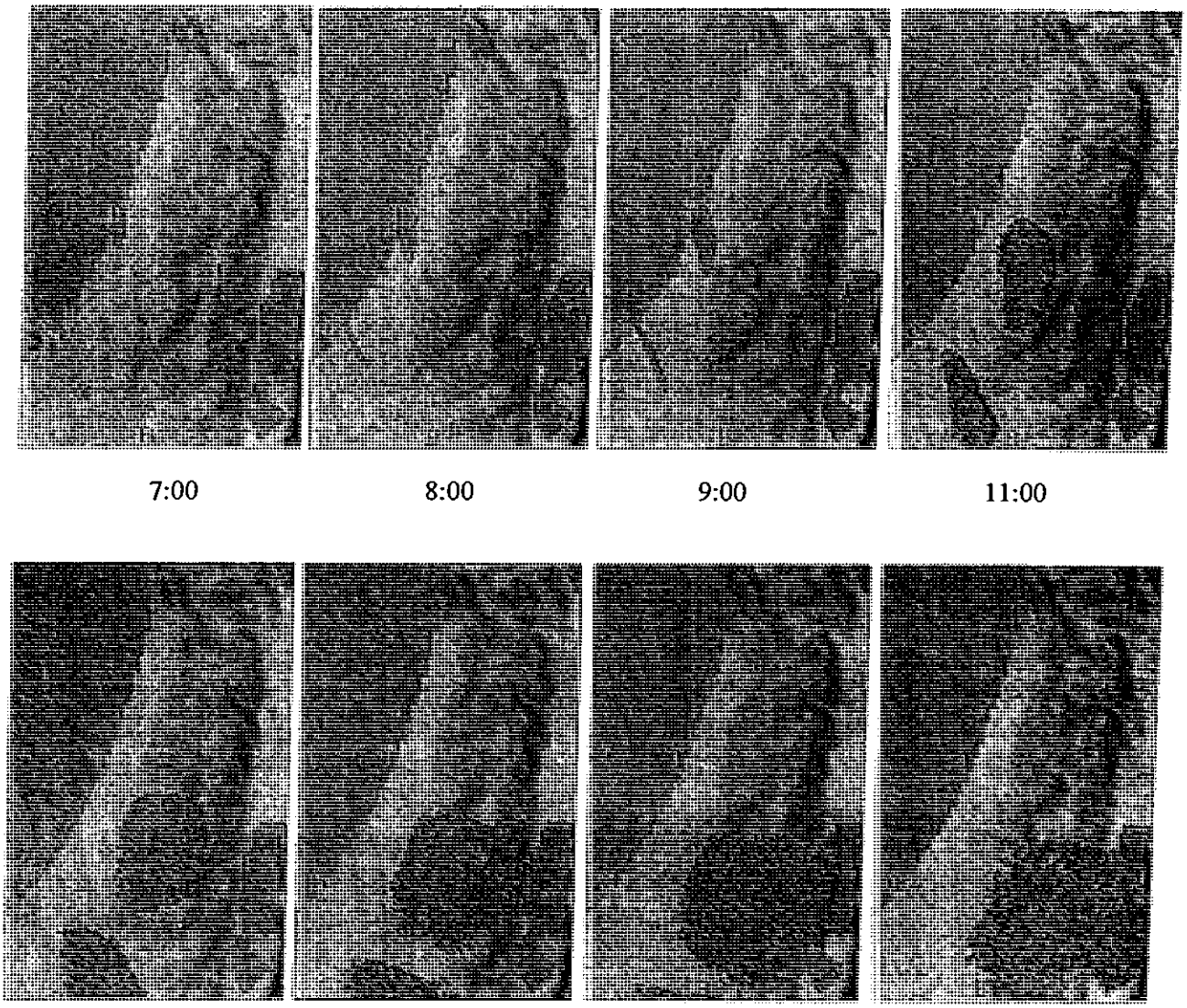


173

**Figure 4**

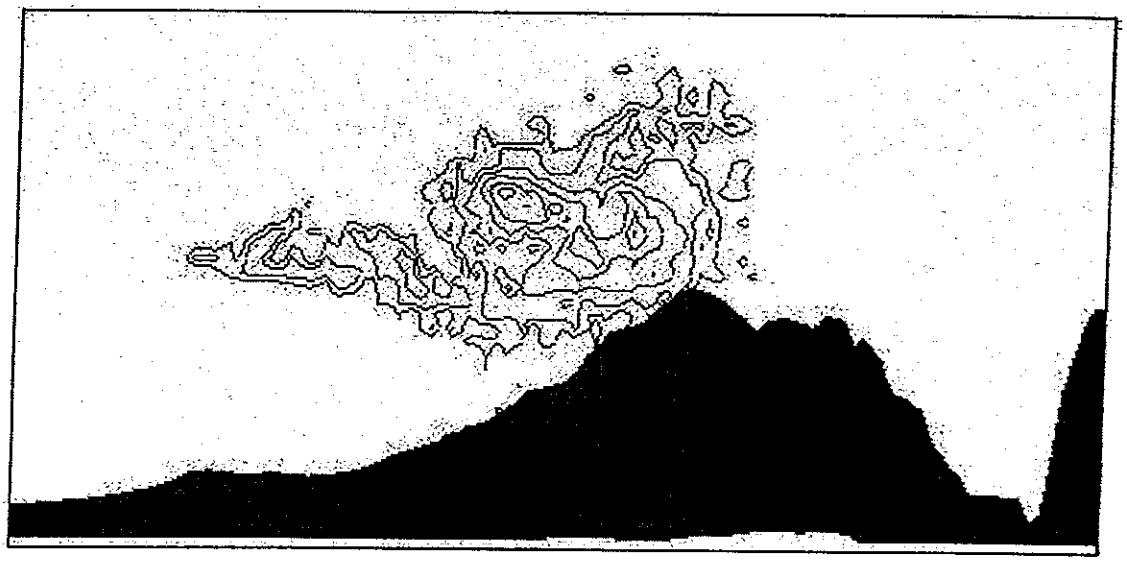

**Figure 6**

175

**Figure 7**

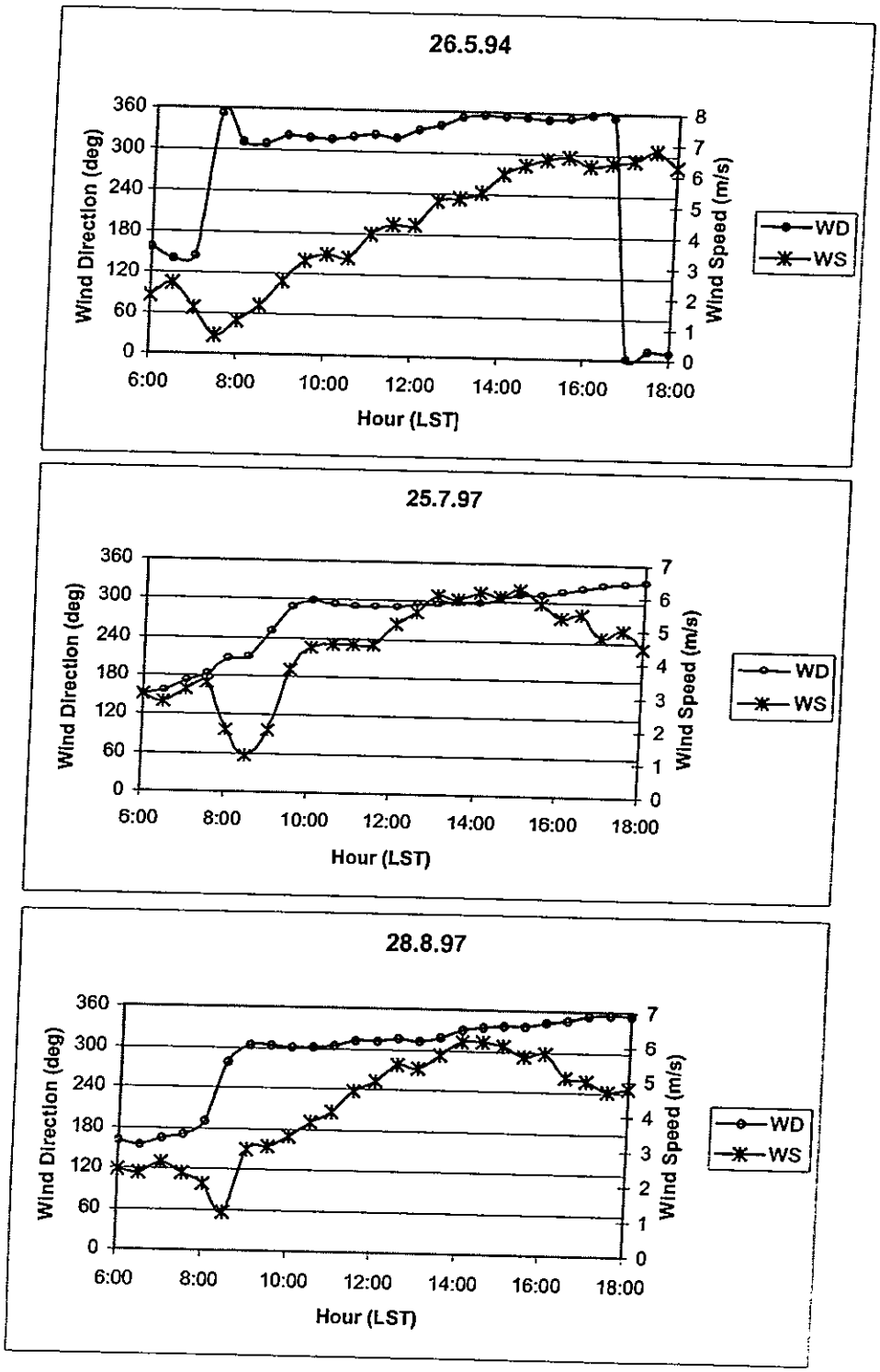
26.5.94
Wind Direction (deg)
Wind Speed (m/s)
Hour (LST)
WD
WS
25.7.97
Wind Direction (deg)
Wind Speed (m/s)
Hour (LST)
WD
WS
28.8.97
Wind Direction (deg)
Wind Speed (m/s)
Hour (LST)
WD
WS

176

# Figure 8

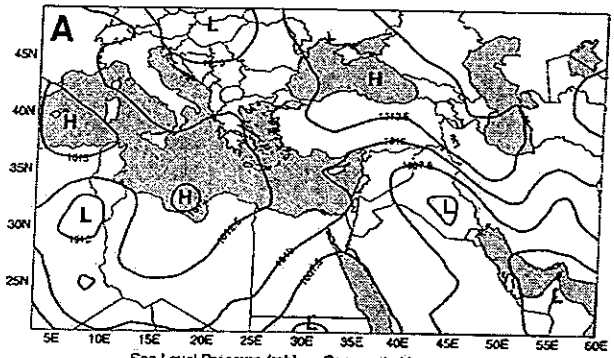


Sea Level Pressure (mb) Composite Mean
5/25/1994
NCEP/NCAR Reanalysis

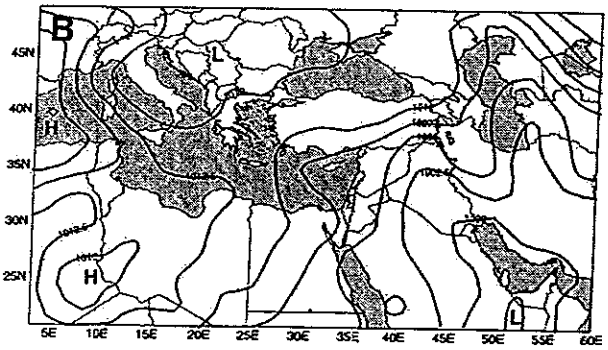


Sea Level Pressure (mb) Composite Mean
7/25/1997
NCEP/NCAR Reanalysis

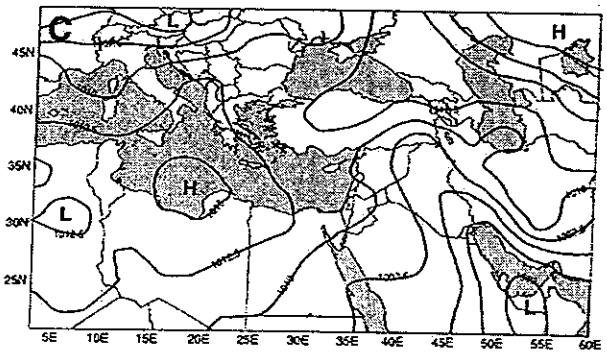


Sea Level Pressure (mb) Composite Mean
8/25/1997
NCEP/NCAR Reanalysis

**Figure 9**

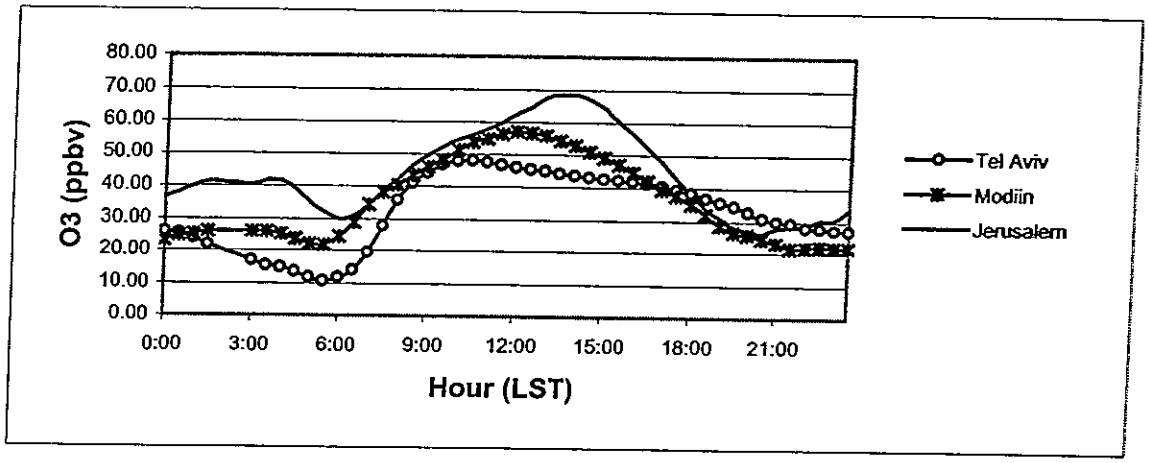
80.00
70.00
60.00
50.00
40.00
30.00
20.00
10.00
0.00
O3 (ppbv)
0:00
3:00
6:00
9:00
12:00
15:00
18:00
21:00
Hour (LST)
Tel Aviv
Modiin
Jerusalem

178

PART V

## *Analyses of urban and rural surface ozone levels in Israel*

### I. Introduction

Sustaining an optimal balance between human activity and economic development on one hand, and environmental air quality on the other, requires a comprehensive understanding of the mixing layer, as well as of ground-level urban and rural air pollution dynamics. Ground level ozone has become a problem of major concern in many metropolitan areas in Israel that experience recurring high concentrations during the summertime "photochemical smog season" [Israel Environment Bulletin, 1999]. The need to account for its adverse effects on humans, crops, and materials, calls for the implementation of management and public warning strategies for ozone levels, particularly near densely populated areas.

Previous studies have addressed the upper-level (about 300 m AGL) inland air pollution over Israel in the framework of photochemically aged-$NO_x$ limited air masses [Peleg et al., 1994; Luria et al., 1998 (in Hebrew); Ranmar et al., 2001]. These studies showed that pollutants originating from the Tel Aviv metropolitan area traverse inland while undergoing extensive dispersion accompanied by chemical and photochemical processes. They also pointed to the possible impact of additional coastal sources on air pollution formation in central Israel, depending on the specifics of the prevailing wind field.

In this study, urban ground-level ozone data were analyzed from five stations of the national air-pollution-monitoring network. Selected locations were shown as influenced aloft by the migrating coast-to-inland pollution cloud under different meteorological conditions. The five sites included the densely populated Tel Aviv metropolitan and Jerusalem areas (over $5x10^5$ people), the moderately populated Be'er Sheva ($2x10^5$ people) and Modiin ($6x10^4$ people), and the rural town Ariel (less than $2x10^4$ people) (Fig. 1). The last two locations lack industrial facilities and employment opportunities and usually experience daily early-morning, transportation-dependent population migration to Tel Aviv and Jerusalem. Time periods

studied were 1 May to Sep 30 for 1999 and 2000 (306 days), excluding the Be'er Sheva monitoring site (established in late 1999), which only provided data for the year 2000 (153 days).

The transition from pollution composition aloft to urban ground-level air chemistry is generally coupled to the transformation from $NO_x$-limited photochemically aged air masses to a VOC-limited regime. Conversion results from urban traffic emissions of high concentrations of $NO_x$ at the surface (primarily in early morning urban regions), resulting in the titration of ozone through the reaction

(1) $NO + O_3 \rightarrow NO_2 + O_2$,

as well as by way of removing hydroxyl radical ($OH^{\cdot}$) from the system through the reaction

(2) $OH\cdot + NO_2 \rightarrow HNO_3$.

The objective of the presented statistical data analysis is to provide preliminary characteristics of the ground-level ozone profiles of densely populated and industrial areas, as well as of remote less populated regions in Israel. Specifically:

> We address monthly and site-specific profiles of ozone concentrations in terms of 1-h maxima and 8-h (10:00h – 17:00h) averages.

> We address the variation in daily ozone profiles as a function of weekday and week-end differences in the targeted areas.

> We examine surface and upper-air meteorological variables associated with daily 1-h maximum and 8-h average concentrations of surface ozone.

These factors are then used to develop mathematical models aimed at predicting 1-h maximum, 8-h average concentrations, and daily 1-h averages of ozone at four locations in Israel. Meteorological and chemical data with invalid or missing values were eliminated from the statistical analysis.

## II. Month and Site Dependency

Figure 2 shows hourly averaged ozone profiles (0000–2300LST) for May through September at the five sites. Self-calibration is executed each day between 0100-0300 LST, producing the somewhat discontinuous graphical pattern at these hours. In general, nocturnal ozone concentrations result from a balance between destructive mechanisms (such as titration by NO molecules, precipitation, and land breeze) and constructive pathways (such as the ascending of the inversion base that caps ozone in a smaller volumes as well the transport of ozone from other locations). Each site may experience a different mixture of these processes depending on their respective geography and demography.

Site-specific, and to a lesser extent month-specific ozone average concentration spectra are revealed. For example, Tel Aviv exhibits slightly higher ozone levels in May, Modiin, Ariel and Be'er Sheva in July, while Jerusalem experiences a more variable pattern, with no dominant month in terms of peak ozone pollution. Figure 3 presents daily 1-h mean $O_3$ and $NO_x$ concentrations per site for the entire period. Figures 2 and 3a indicate that the Tel Aviv metropolitan station has the lowest concentration of daily ozone, which is reached early in the morning (before 1100 LST, Fig. 3b). These dynamics result primarily from interaction with the high concentration of traffic-originated $NO_x$ and the early onset of the sea breeze, which disperses the photochemically formed ozone inland. Ariel on the other hand, experiences a low-level $NO_x$ environment (Fig. 3b) favoring ozone production (Figs. 2 and 3a).

Two distinct regimes may be deduced from these observations: one concerns the time-space dependency of the trans-boundary Tel Aviv-to-Modiin-to-Jerusalem inland air pollution trajectory [Ranmar et al., 2001] and the other the isolated, "self-sustained" ozone producers represented by Be'er Sheva and Ariel. The latter locations are less influenced on a daily basis by fluctuations in incoming ozone precursors from neighboring sources, exhibiting similar daily average ozone formation and peaking at about the same time (1300 LST). The main

difference between these sites, manifested by the rate of ozone production and peak concentration reached, may stem from the more favorable $NO_x$/VOC ratios prevailing in the Ariel environment. Another point that can be culled from Fig. 3 is the early morning titration of ozone, whose rate of decreasing concentration is mirrored by the increase in $NO_x$ levels emitted by early morning traffic sources. Such ozone bleaching is absent from Ariel, which lacks significant internal and apparently externally transported traffic sources, resulting in the absence of daily fluctuations in the levels of $NO_x$ species.

In 1997 the U.S. EPA promulgated an alternative frame for referencing ozone pollution (replacing the 120 ppbv standard) by defining a new standard of daily maximum 8-h ozone concentration to more appropriately reflect human health effects of ozone [U.S. EPA, 1996]. Such a time window reflects the center of gravity of photochemical activity in the atmosphere and averaging upon it reflects its chemical formation potential. John and Chameides [1997] studied the 1-h vs. 8-h ozone exceedence standards (120 ppbv and 80 ppbv, respectively) over the Atlanta metropolitan area to reevaluate the new standard in terms of the perception of polluted regions and the need for redesigning ozone pollution management strategies.

They found a regionally high correlation between the daily 1-h maxima and the 8-h average ($R^2 = 0.92$), with a daily 1-h maximum of 120 ppbv climatologically equivalent to an 8-h average of 98 ppbv. The correlation between the 1-h daily maxima and the 8-h means was somewhat lower in our study, ranging from $R^2 = 0.69$ in Ariel to $R^2 = 0.76$ at the Tel Aviv metropolitan station, with the climatology equivalence of 120 to 84 ppbv and 120 to 91 ppbv, respectively. Furthermore, these authors found that the transition from 1-h average to 8-h average concentration to gauge the severity of ozone pollution transforms the Atlanta metropolitan area into one with three times the tendency to exceed the 80 ppbv threshold.



152

In our study region (for the time frame defined above), seven 8-h standard exceedences (≥ 80 ppbv) were encountered, five of them in Jerusalem. No 1-h (≥ 120 ppbv) exceedences were recorded during this time period. These preliminary findings suggest that the 8-h standard increases the number of non-attainment episodes experienced in different locations and sets a higher barrier for air-quality attainment.

Tables 1 and 2 present cross-correlations between the five sites in terms of the daily 8-h average and 1-h maximum ozone concentrations. Results indicate that the 8-h average standard generally exhibits a higher spatial correlation than its 1-hr daily maxima concentration counterpart. While all correlation coefficients were positive, values ranged from essentially no correlation (1-h maxima between Ariel and Tel Aviv of about $R = 0.055$) to relatively high linear correlation (1-h maxima between Be'er Sheva and Modiin of about $R = 0.745$).

Overall under both standards, Modiin best associates regionally with proximal and distant neighbors (average correlation coefficients of 0.57 and 0.59 for 1-h daily max and 8-h average, respectively). On the opposite end of the correlation scale, Ariel exhibits the lowest regional association with the rest of the sites (average correlation coefficients of 0.25 and 0.35 for 1-h daily maximum and 8-h average, respectively). This asynchronous relationship suggests that Ariel experiences a somewhat isolated and/or independent environment of ozone formation, partially reflected by its time-independent daily $NO_x$ concentrations (Fig. 3b). Such an autonomic pathway may stem from the lack of internal as well as nearby sources of pollutants, as mentioned earlier. Alternatively, the low correlation between the Tel Aviv metropolitan and Jerusalem areas is essentially "bridged" by their respective higher correlation with Modiin, positioned as the "mediator" in the inland air pollution transport [Ranmar et al., 2001].

A 1-day-lagged autocorrelation for the five locations in terms of the 8-h and 1-h daily averages is presented in Table 3. The 1-day-lagged autocorrelations were based on at least 260 observations for the 2-year derived data sets and 140 observations for the 1-year derived data set (Be'er Sheva). Aside from Modiin, all sites showed higher 8-h 1-day lagged autocorrelation values than the corresponding 1-h variable. Additionally, Ariel and Jerusalem retained the highest autocorrelation values for both variables.

To better understand current to 1-day lagged ozone level dependency, a "quasi-autocorrelation" was examined, associating daily 0600-0900 LST ozone averages with the corresponding previous day 1-h ozone maxima (Table 4). Comparing Tables 3 (for the 1-h maximum results) and 4 indicates a stronger linkage between sequential daily peak ozone levels (1-h max averages) compared to the related quasi-autocorrelation relationship.

The fact that the correlation between the two pairs of variables [$(\text{1-h max})_{k-1}$:$(\text{1-h max})_k$] and [$(\text{1-h max})_{k-1}$:$(\text{06:00-09:00h average})_k$] is reciprocal to the time difference spanning their corresponding diurnal time of formation suggests different mechanisms linking successive daily ozone concentrations. In the first case, the persistence driving force reflects on the dynamical day to day time series of peak ozone levels [Robeson and Steyn, 1990; Comrie, 1997]. A potential mechanism may convolute from the vertical circulation associated with sea breeze and mountain slope winds injecting mixing-layer-produced ozone (as well as various other pollutants) into the base of the thermal inversion to form a reservoir of high pollutant concentration aloft. These chemicals can then mix downward on subsequent days to enhance surface concentrations.

Such a structure-function mechanism was predicted in simulations of ozone distributions over the Los Angeles Basin [Lu and Turco, 1996] and were postulated to accrue locally based on similarities in geography and climate [Dayan and Coch, 1996]. In the second case,

early morning (0600h–0900 LST) surface ozone concentrations arise from ozone formed the previous day and retained at the surface. This ground level ozone than undergoes enhanced evening and nighttime titration by NO emissions, eventually giving rise to following day low levels of early morning ozone.

In contrast to the highly dynamic nature of the vertical influx and convergence of chemicals into the inversion base, which can then project on the overall ozone concentrations of the following day, the titration of ozone by anthropogenic sources of NO during the night is essentially independent of end-of-day ozone levels. This difference may explain the lower correlation existing in the second case. Following their tendency for successive dependencies on previously formed ozone (as in the case of 1- and 8-h averages), Jerusalem and Arial exhibit the highest quasi-autocorrelation characteristics, while Tel Aviv and Modiin showed essentially none. These different dependency profiles may indicate that each of these locations is "embedded" in a distinct environment in terms of the mechanisms forming the pollutant reservoir aloft, as well as the sensitivity of nighttime titration pathways of ozone on ozone levels reached by sunset.

## III. Day of Week Profiles

The weekend-to-weekday air pollution-ozone formation relationship provides insight into the impact of differential transportation emissions per day of the week and the dependency on meteorological conditions on ozone formation potential. Addressing such a time window dependency may help in devising better emission control standards/strategies by assessing the impact of the "natural" day-of-week variation in traffic flow demand and on resulting emission levels on ozone formation.

Studies addressing emission-control strategies have suggested that reduced $NO_x$ and VOC emissions leads to increased ozone formation. Such examples include case studies of Montreal [McKendry, 1993], the large urban areas in the northeast U.S. [Possiel and Cox,

1993], and Switzerland under unfavorable conditions for ozone formation [Brönnimann and Neu, 1997]. Reduced traffic emissions are characteristic of weekends with drops of 35 to 50% in $NO_x$ and 17 to 35% in VOC/CO levels [Brönnimann and Neu, 1997; Pont and Fontan, 2001]. In Europe and the U.S., statistical studies have indicated that the average ozone concentrations are higher at almost all sites on weekends than on weekdays for mean and maxima values [Elkus and Wilson, 1977; Bower et al., 1989; Altshuler et al., 1995; Vecchi and Valli, 1999]. Little difference in peak ozone levels was found between weekend and weekdays in both the New York metropolitan area [Rao et al., 1991] and in large cities in France (Fridays vs. Sundays) [Pont and Fontan, 2001], despite substantial reductions in traffic emissions during these time periods.

Day-of-week dependency of the ozone profile for the five sites is displayed in Fig. 4 along with corresponding daily 1-h-averaged peak ozone concentration. $NO_x$ and CO concentrations, both prominent indicators of traffic-flow activity, exhibit a weekend decline in monitored levels (not shown). The interplay between traffic activity (represented by $NO_x$ levels) and ozone production is presented in Fig. 5, which shows their corresponding 8-h averages per day-of-week at each site. These findings reveal two transportation emission-ozone formation regimes.

The first corresponds to the more highly populated urbanized areas (Tel Aviv, Jerusalem, and Be'er Sheva), where the decrease in weekend (Friday and Saturday) traffic emissions results in a slight increase in ozone levels. Such a weekday-to-weekend dependency reflects the transition from a VOC-limited regime to a $NO_x$-limited regime found in populated industrial urban areas. On weekdays, high $NO_x$ levels confine ozone concentrations through reactions (1) and (2). On weekends, reduced traffic flow results in reduced $NO_x$ levels, lifting the barrier to ozone production by creation of a chemical environment that favors ozone formation.



156

The opposite results are encountered in Ariel, lacking "internally produced" high-density traffic flows. Switching to a "weekend chemical environment" transforms the surrounding air into a $NO_x$-starved regime, inhibiting the ozone formation. In Modiin, the relatively high weekend concentrations may be attributed to transport mechanisms (e.g. originating from the Tel Aviv metropolitan area) over-riding the environmental constraints found in Ariel. Sunday, the first working day in Israel, is found to exhibit average higher ozone concentrations than mid-week days, even though traffic activities are on a par.

A possible pathway for the increase is downward mixing of the aforementioned ozone reservoir at the inversion base, replenished by the relative high weekend concentrations. In all cases, the variation in day-of-week ozone levels is smaller than associated variations (weekend decrease) in traffic emissions (Fig. 5). A similar nonlinear correspondence was shown by Pont and Fontan [2001] in large cities in France.

Such transitions in the day-of-week cycles of ozone forming potential are dependent on meteorology, as shown by Brönnimann and Neu [1997], who addressed weekend-weekday differences in Switzerland. They indicated several distinct patterns of ozone formation, including situations in which favorable meteorology (high GSR, high temperature, and low wind speed) produced an inverse pattern, with mean ozone peaks 10 to 15% lower on Sundays than on Thursday or Friday. The frequency of occurrence of such pattern-breaking meteorology is important when considering emission-control strategies.

In Switzerland, these "favorable" conditions were found on about 30 to 50 days per year, corresponding well with "summer smog days". Such a classification has yet to be examined in our region, since basing primary pollutant emission reduction strategies only on weekday differences may miss the target if the "favorable" pattern-breaking conditions take place above a certain yet-to-be-determined threshold. In the 2-year database used in this study, hardly any exceedences were recorded upon which such a pattern might be defined.

This preliminary study would seem to suggest that control strategies involving local reductions in traffic emission levels are insufficient in reducing ozone levels on the scale of cities, especially when considering the potential role of advection on the origin of ozone. Additional work needs to be done for a better quantitative understanding of the correspondence between ozone levels and the dynamics of daily traffic levels.

## IV. Prediction of Daily 1-h Maxima, 8-h Averages, and Hourly Ozone Levels

### a. *Background*

A variety of statistical methods for ground-level ozone adjustments have been proposed in the literature identifying meteorological variables and atmospheric chemicals most strongly associated with high ozone concentrations and aiming to accurately forecasting atmospheric ozone concentrations [Thompson et al., 2001]. Multivariate statistical techniques are the most widely used approach in operational ozone forecasting and research-oriented statistical modeling [e.g., Wolff and Lioy, 1978; Clark and Karl, 1982; Ryan, 1995; Davis et al., 1998; Hubbard and Cobourn, 1998; Davis and Speckman, 1999; Thompson et al., 2001]. Multiple (multivariate) linear regression models are the most popular of these techniques, having the general form:

$$Y_i = \beta_0 + \sum_{j=1}^{n} \beta_j X_{ij} + \varepsilon_i \qquad \text{with } i = 1, \ldots, p,$$

where for a set of $p$ successive observations, the predicted variable $Y$ (response variable) is a linear combination of offset $\beta_0$, a set of $n$ predictor variables $X$ with $n$ matching $\beta_j$ coefficients and residual error $\varepsilon$. The $\beta$ coefficients are model parameters to be estimated.

These models typically incorporate from one or two explanatory variables [Robeson and Steyn, 1990; Olszyna et al., 1997; Chaloulakou et al., 1999] up to as many as 313 (accounting for a range of meteorological characteristics derived from several atmospheric levels that potentially associate with daily average surface ozone levels) [Feister and Balzer, 1991].



188

Of all the meteorological variables, surface air temperature has the strongest correlation with ozone concentration [Robeson and Steyn, 1990; Hubbard and Cobourn, 1998]. This may result from two main reasons: (i) high air temperature and intense solar radiation are excellent indicators of environmental conditions conducive to ozone formation and accumulation, such as the stagnating anticyclones associated with clear skies that increase photolytic activity, light winds which keep local emissions from being dispersed, and subsidence at higher levels confining the depth of the turbulent layer into which ozone precursors are released [Vukovich et al., 1977; Clark, 1980; Vukovich and Fishman, 1986; Eder et al., 1994] and (ii) photochemical rate constants are highly temperature-dependent [OECD, 1979].

However, Feister and Balzer [1991] found solar radiation as the most important meteorological predictor among the 313 atmospheric variables addressed, whereas Davis and Speckman [1999] found the combination of wind speed, opaque cloud cover, and morning mixing height to best relate to observed surface ozone levels. Cox and Chu [1993, 1996], considering some 100 meteorological variables, found maximum surface temperature, wind speed, relative humidity, mixing height, opaque cloud cover and wind speed-by-temperature interactions to be significant meteorological predictors over most major metropolitan areas in the U.S. These differences suggest that regional variations in emission, meteorology, and geography more precisely define the dominant variables related to ground-level ozone formation.

In this section, three multiple linear regression prediction models are developed: (i) two designed to capture the daily 1-h peak and 8-h average ozone concentrations, based on the same set of predictor variables and (ii) a third, aimed at simulating the 1-h-averaged daily profile of ozone levels, based on a different set of predictor variables.

(ii) *1-h peak and 8-h average ozone concentration*

The present effort focused on developing a comprehensive statistical prediction model to evaluate ozone levels at four locations in Israel. Currently, there is no operational 24-h forecasting model to estimate high ozone levels in Israel. The developed model is based on various aspects of surface-weather variables, as well as on chemical pollutants intimately related to traffic sources, even though industrial and power plants contribution are possible. Since daily maximum ozone levels are partially dependent on the previous day levels, ozone concentrations exhibit a strong serial correlation, also referred to as persistence. The importance of the persistence was accounted for by some investigators by incorporation of lagged ozone concentrations from the previous day as an additional predictor variable in the model [Robeson and Steyn, 1990; Feister and Blazer, 1991].

Data used for model development was not subject to any smoothing procedures, such as the moving average or "lowess" and "loess" local regression smoothing [Cleveland and Devlin, 1988] used by some investigators [Davis and Speckman, 1999; Hubbard and Cobourn, 1998], thus retaining original variances. Overall 19 predictors were considered in the models construction. Variables depicting upper-level atmospheric dynamics represented in the statistical analysis are mixing depth AGL (m) at 1100 GMT and a corresponding factor depicting mixing layer ventilation rate (product of mixing depth and wind speed at its median location) [Ranmar et al. 2001]. This latter predictor represents the capacity of the mixing layer to disperse pollutants in the atmosphere.

The following explanatory statistical analyses were carried out in order to identify prominent predictor variables and develop multiple linear regression models addressing the daily 1-h peak ozone level as the response variable. A parallel mathematical pathway followed for model development of the 8-h daily average (omitted for space). Table 5 presents the meteorological and chemical variables considered in the model development for 1-h max



199

ozone concentration prediction and their corresponding explanatory variance ($R^2$) (bivariate regression analysis). The predictors show striking site-specific explained variance. For example, daily peak temperatures have the most prominent explanatory variance of ozone concentration in Ariel, with essentially none in Tel Aviv and Jerusalem. All $R^2$-values for the temperature predictor are considerably lower then that obtained by Hubbard and Cobourn [1998] ($R^2 = 0.487$). These authors used a fourth-order polynomial regression function, which had a negligible effect on our data, as did exponential, logarithmic and power functional transformations. The 8-h average of $NO_x$ variable on the other hand, carries some explained variance for the Tel Aviv ozone concentrations, none in the other locations. It's interesting to note that the early morning averaged ozone concentrations (06:00–09:00h) was not found to be a deterministic indicator for maximal ozone levels obtained later for the same day, the highest explained variance (positive correlation coefficient) being found for Jerusalem ozone ($R^2 = 0.18$). Furthermore, surface ozone concentrations at all 4 sites show no association with upper-level atmospheric parameters represented by the mixing layer, considered in the model development. Early morning and mid-day averaged wind speeds correlated negatively ($R<0$) with ozone levels for all the sites on par with elementary pollutant dispersion models [e.g. De Nevers, 1995]. However, their corresponding explained variance is low compared to values obtained by Davis and Speckman [1999] ($R^2 = 0.32$ and $R^2 = 0.31$, for 06:00-09:00h and 10:00-17:00h averaged wind speeds, respectively) and Hubbard and Cobourn [1998] ($R^2 = 0.165$), the latter using an exponential decaying regression function. In both those studies, the wind speed variables were among the best two single predictors in their mathematical prediction model. Applying inverse wind speed as an explanatory variable did not improve ozone calculation. In general, the corresponding bivariate regression analyses for 8-h ozone averages as the response variable produced $R^2$ values on par with 1-h peak values.

A stepwise regression procedure was executed (SAS, 1991) to profile the minimal variables accounting for maximal coefficient of multiple determination ($R^2$), and is presented in Table 6. The explained variance of bivariate regressions predictors (Table 5) differ in their absolute value and relative significance when used in the step-up addition procedure of the predictors, pointing to possible cross-correlation and dependencies between some of the variables. Furthermore, site-specific dependency of the maximal explained variance on the composition of prediction variables is observed. Thus, to maximize explained variance (particularly for the Tel Aviv site $R^2 = 0.48$, Table 6), and to be able to coherently compare prediction performance per monitoring site, the entire set of explanatory variables defined in Table 5 were incorporated into the final models. The construction of "deterministic" 24-h in advance forecasting models requires a more parsimonious approach, where special care should be taken regarding the chemical variables estimation. The present study addressed the overall capacity of atmospheric and chemical explanatory variables to capture statistical characteristics of ozone levels, rather than the ability to develop a "real-time" prediction tool. For practical purposes one would choose to incorporate the minimal representative set of regressor variables per site, based on the bivariate and stepwise regression analyses, in order to construct a prediction-orientd model for the 1-h and 8-h ozone concentration response variables.

Residual analyses of the models indicated reasonable homoscedasticity (constant variance), an approximate zero mean and a Gaussian probability distribution of the model error terms, satisfying the necessary conditions for the general form of multiple linear regression applicability.

For each monitoring site, the mathematical models were established by fitting data from the May to September 1999 and 2000 database. Seventy days per site, representing approximately one week per month, were kept out of the database and used to test forecasted

daily 1-h peak and 8-h average ozone concentrations. Forecasts were compared with actual observed ozone levels for the excluded days. Statistical regression coefficients of the explanatory variables for the five sites are presented in Table 7 and validation results for each of the four ozone monitoring sites are summarized in Table 8. Statistics include root-mean square error of the residuals (RMSE model error), coefficient of determination ($R^2$) for the built-in data, and root-mean square prediction error (RMSE pred. error) for the forecast data.

For peak ozone levels at the four sites, RMSE model errors ranged from 5.7 to 10.8 ppbv, while $R^2$ values were site independent. For the 8-h average, the RMSE model error ranged from 4.8 to 6.7 ppbv, $R^2$ values from 0.58 to 0.69. As expected, errors were greater for the daily 1-h peaks than for the 8-h values. Figure 5 displays the daily 1-h maximum ozone predictions (dashed line) for 70 days per monitoring site for the years 1999–2000 and the corresponding observed values (solid line).

In general, predicted daily 1-h peaks and 8-h averages (not shown) tracked observed values at the four stations and the daily variation was generally captured reasonably well by the models. However, the models did not fare well with extreme values, and showed some tendency toward underestimating high concentrations of observed ozone, particularly when following days of low observed values. These results stem from the general drawback with regression analyses, i.e., the inherent averaging. With the use of lagged ozone as a predictor in the model [Milionis and Davies, 1994], swinging day-to-day (low-to-high) ozone levels may inhibiting the modeling of high-value predictions.

An attempt to fine-tune the models to identify high 1-h and 8-h ozone levels by filtering lower values produced slight improvement in capturing such maxima (highest for screening ozone less than 60 ppbv) at the expense of lower explained variance and higher standard errors. However, no underestimations were eliminated and the number of overestimations somewhat increased (not shown).

(iii) *Daily 1-h average ozone concentration spectrum*

To capture the dynamics of daily ozone evolution, a multiple linear regression model was established for each of the four sites in a manner similar to the aforementioned stepwise procedures. The time domain targeted for simulation was 0400 to 2300 LST, and was based on hourly averaged $NO_x$ (ppbv), CO (ppmv), wind speed (m/s), west-east ($u$, positive from west, m/s) wind component, south-north ($v$, positive from south, m/s) wind component, temperature ($^0$C), and GSR (w/m$^2$). Additionally, a forth order polynomial in time ($t$) was introduced into the model to capture the observed time-dependent shape of the daily ozone profile (Fig. 3a), introducing four additional predictor variables ($t^n$ = 1 at 0400 LST, n = 1,...,4).

Model development was based on the same database used for establishing the 1-h and 8-h mathematical prediction models, and were applied to data recorded during May–Aug 2001. Generated predictions were then compared with the actual observed ozone concentrations. The model statistical attributes ($R^2$ and model RMSE, respectively) were: Tel Aviv (0.78, 7.4 ppbv), Ariel (0.66, 8.8 ppbv), Modiin (0.76, 8.4 ppbv), and Jerusalem (0.64, 10.9 ppbv). Table 9 provides predictors and corresponding regression coefficients used in the forecasting model (daily 0400-2300 LST) for the Tel Aviv station.

Figure 7 displays predicted vs. observed daily time series of hourly averaged ozone concentrations for the last week of June for the Tel Aviv station. The predicted daily evolution of hourly averaged ozone concentrations overlaps closely with measured concentrations on most days. Generally similar agreement was seen at the other locations (not shown). As in the case of daily 1-h maxima and 8-h averages, the "continuous" time series models under predicted days encountered with high values of ozone. This phenomenon was especially conspicuous when a secondary late afternoon to late evening peak was established, probably resulting from the combined mechanisms of transport and descending mixing layer height due



194

to land cooling processes. To improve model performance in terms of capturing daily peak values, models fine-tuned to resolve day-of-week and month-of-year daily ozone concentrations were developed. While these time-domain telescoping-in models on average improved $R^2$ and standard error (Tables 10 and 11 for day-of-week and month-of-year model statistics, respectively), underestimations still remained.

In all cases, scatter plots of forecast vs. observed ozone were best fitted by a least-squares quadratic curve. This relationship suggested a small systematic underprediction of ozone concentration that increased with increasing ozone values (a model bias). To account for the biased higher value predictions, Hubbard and Cobourn [1998] suggested application of a revision step to the models in which biased predictions are used as variables in the quadratic polynomial just described. The final output is then used as the corrected unbiased prediction of ozone concentration. They obtained a slight improvement in $R^2$ and standard error upon first-stage forecast transformation (increase of about 0.015 explained variance and decrease of about 0.4 ppbv in standard error). In our case, the least-squared quadratic equation for each model per site had a low $R^2$ (about 0.3) and improvements over the original prediction were not significant (not shown).

(iv) *Model improvement*

A number of points and issues need to be addressed to improve overall ozone predictions:

> The effects of vertical mixing and ground-level transport of ozone were not taken into account. As mentioned earlier, ozone trapped above the nocturnal inversion may be mixed downward on subsequent days as the convective boundary layer is established, or transported and relocated to other sites, introducing additional ozone at these locations by the same downward mixing mechanism. Additionally, ozone produced upwind (e.g. Tel Aviv) is transported inland by the sea breeze, reinforcing locally formed

ozone, or recirculated over the sea at the onset of the evening land breeze to be returned in the next day sea breeze circulation. Profiling vertical ozone data as well as quantifying the complex surface transport of ozone could be introduced into the database upon which the model is developed. With this additional information, higher resolution, accuracy and flexibility in predicting ozone concentrations might be achieved.

> Wind direction, while introduced implicitly through wind components *u* and *v*, may need to be addressed explicitly as a categorical variable, specifically set to identify cross-effects, such as the effects of wind direction from one location on downwind locations' ozone levels.

> Improved spatial resolution of meteorological data is also essential. Models based on "domain" data, i.e., data derived from a cluster of monitoring stations may better represent meteorological fields and chemical concentrations at specific locations, reducing variability and increasing the reliability of variables used as predictors for ozone formation.

> Introduction of additional meteorological variables (e.g., opaque cloud cover [Davis and Speckman, 1999) as well as functionally transforming (polynomial, exponenttial, etc.) the ones used may improve explained variance, reduce standard errors and improve predictions. The effect of day-of-week on model performance (regarding the 1-h and 8-h forecasts) may be studied by either setting the days as categorical variables [Hubbard and Cobourn, 1998] or explicitly devising models suited for specific days as described here for the continuous daily 1-h ozone spectrum.

> Since successful implementation of episodic ozone forecasting is judged by its ability to alert the general public of harmful air quality levels, "classification" or "categoryical" models may be considered. In such models, ozone air-quality measures, released to the public may be divided into a number of categories, such as Hubabard and

Cobourn's [1998]: "good" ([$O_3$] < 60 ppbv), "moderate" (60 < [$O_3$] ≤ 95 ppbv), "approaching unhealthful" (95 < [$O_3$] ≤ 120 ppbv) and "unhealthful" ([$O_3$] < 120ppbv). This procedure simplifies air-quality information for the general public. Furthermore, they showed that predicting "domain" concentrations, i.e., where predicted and observed concentrations fall into the same category, yielded higher prediction accuracy than the "conventional" discrete approach.

> Extreme-value models were not developed in this work, since no such values were encountered during the studied period. While a database of such values is prerequisite for model development, capturing extreme values is difficult with the inherent averageing regression-oriented models utilized in this study. Alternative approaches should be considered, such as those reviewed by Thompson et al. [2001].

(7) Finally as mentioned earlier, to develop a prediction model aimed at forecasting high ozone levels (at least 24-h in advance), a different approach should be implimented that results in a parsimonious model that maximizes explained variance. Such a model should be based on explanatory variables by themselves reasonably easily and accurately estimated (e.g., max temperature, RH, and radiation). Inclusion of chemical explanatory variables, may turn out to be difficult in view of the high variance associated with their complex interactions with the surroundings.

## IV. Conclusion

This study addressed the characteristics of ground level ozone at five locations in Israel. The following points were derived:

> The five sites experienced different combinations of atmospheric, environmental and anthropogenic impacts imprinted by their respective monthly, diurnally, 1-h and 8-h ozone profiles. Two distinct ozone-formation regimes were resolved, one involving

time-space dependency (Tel-Aviv, Modiin and Jerusalem) and the other isolated, self-sustained ozone production activity (Ariel and Beer-Sheva).

> Comparison between the 1-h and 8-h standards showed that the latter increased the number of threshold exceedance episodes, but however retained a higher spatial correlation between sites. The 1-h maximum standard showed a stronger association with the previous day, when compared with the same day's early morning (0600–0900 LST) averaged value. Such a phenomenon was attributed to persistence and to a possible elevated secondary pollutant reservoir in the inversion layer that may entrain down into the mixed layer on subsequent day(s), impacting on resulting late morning ozone levels.

> The variations of daily hourly-averaged ozone concentrations reveal different weekday-to-weekend characteristics associated with population density and industrial activity. High anthropogenic-activity cities (Tel Aviv, Jerusalem and Beer Sheva) exhibit increased weekend ozone levels linked to decreased traffic emissions, which reflects a decline in $NO_x$ titration capacity. Alternatively, low transportation-dependent cities (Modiin and Ariel) showed reduced ozone levels on weekends corresponding to sub-optimal levels of primary ozone precursors. Such a decline may be partially offset by transport from other urbanized sources.

> Statistical ozone prediction models addressing the 1-h maximum, 8-h average and daily 1-h averaged profile were developed and verified for four locations in Israel. These models, rooted in multiple linear regression techniques, and based on meteorological and chemical variables, examined the capacity of these regressor variables to account for ozone level fluctuations. While the models did not reach the predictive realization we would like to see (particularly considering calculative errors would be expected to be somewhat larger when meteorological and chemical variables used in the models are to be forecast), they did

provide the first statistical procedures addressing decision-grade ozone forecast levels in Israel.

## References

לוריא מ., פלג מ., מטבייב ו., תגר א., לפידות ע., צחי י., רזון ד., וד. סימנטוב, התפתחות אוזון בתימרה העירונית של גוש דן, דו"ח מדעי סופי לקרן בלפר, דאות. העבריית בירושלים, הבי"ס למדע ישומי, המעבדה לחקר איכות האויר, 1998.

Altshuler S. L., Arcado T. D. and D. R. Lawson, Weekday vs weekend ambient ozone concentrations: discussion and hypotheses with focus on Northern California. *J. Air Waste Man. Assoc.*, 45, 967-972, 1995.

Bower J. S. et al., Surface ozone concentration in the U.K. in 1987-1988. *Atmos. Environ.*, 23, 2003-2016, 1989.

Brönnimann S. and U. Neu, Weekend-weekday differences of near-surface ozone concentrations in Switzerland for different meteorological conditions. *Atmos. Environ.*, 31, 1127-1135, 1997.

Chaloulakou A., Assimacopoulos A. and T. Lekkas, Forcasting daily maximum ozone concentration in the Athens basin. *Environ. Monitor. Assess.*, 56, 97-112, 1999.

Clark T. L., Annual anthropogenic pollutant emissions in the United States and southern Canada east of the rocky mountains. *Atmos. Environ.*, 14, 961-970, 1980.

Clark T. L. and T. R. Karl, Application of prognostic meteorological variables to forecasts of daily maximum one-hour ozone concentrations in northeastern United States. *J. Appl. Meteor.*, 21, 1662-1671, 1982.

Cleveland C. S. and S. J. Devlin, Locally weighted regression: an approach to regression analysis by local fitting. *J. Am. Stat. Assoc.*, 83, 596-610, 1988.

Cox W. and S. Chu, Meteorological adjusted ozone trends in urban areas: a probabilistic approach. *Atmos. Environ.*, 27B, 425-434, 1993.

Cox W. and S. Chu, Assesment of interannual ozone variation in urban areas from a climatological perspective. *Atmos. Environ.*, 30, 2615-2625, 1996.



202

Davis J. M. and P. Speckman, A model for predicting maximun and 8 h average ozone in Houston. *Atmos. Environ.,* 33, 2487-2500, 1999.

Dayan U. and L. Koch, Ozone concentration profiles in the Los Angeles Basin – A possible similarity in the build-up mechanism of inland surface ozone in Israel, *J. Appl. Meteor.*, 35, 1085-1090, 1996.

De Nevers N., Air pollution control Engineering. McGraw-Hill, New York, pp. 108, 1995.

Eder B. K., Davis J. M. and P. Bloomfield, An automated classification scheme designed to better elucidate the dependence of ozone on meteorology. *J. Appl. Meteor.,* 23, 2739-2750, 1994.

Elkus B. and K. R. Wilson, Photochemical air pollution: weekend-weekday differences. *Atmos. Environ.,* 11, 509-515, 1977.

Feister U. and K. Balzer, Surface ozone and meteorological predictors on a subregional scale. *Atmos. Environ.,* 25A, 1781-1790, 1991.

Hubbard M. C. and W. G. Cobourn, Development of a regression model to forecast ground-level ozone concentration in Louisville, KY. *Atmos. Environ.,* 32, 2637-2647, 1998.

Israel Environment Bulletin, Spring 1999-5759, 22, 1999.

John J. C. ST. and W. L. Chameides, Climatology of ozone exceedences in the Atlanta metropolitan area: 1-hour vs 8-hour standard and the role of plume recirculation air pollution episodes. *Environ. Sci. Technol.,* 31, 2797-2804, 1997.

Lu R. and R. P. Turco, Ozone distribution over the Los Angeles Basin: Three-dimensional simulations with the SMOG model. *Atmos. Environ.,* 30, 4155-4176, 1996.

McKendry I. G., Ground-level ozone in Montreal, Canada. *Atmos. Environ.,* 27(B1), 93-103, 1993.

Milionis A. E. and T. D. Davies, Regression and stochastic models for air pollution – I. Review, comments and suggestions. *Atmos. Environ.*, 28, 2801-2810, 1994.

OECD (Organization of Economic Co-operation and Development), Photochemical Oxidants and their Precursors in the Atmosphere. OECD, Paris, 1979.

Olszyna K. J., Luria M. and J. F. Meagher, The correlation of temperature and rural ozone levels in southeastern U.S.A. *Atmospheric Environment*, 31, 3011-3022, 1997.

Peleg M., Luria M., Setter I., Perner D. and P. Russel, Ozone levels in Central Israel, *Israel J. of Israel*, 34, 375, 1994.

Pont V. and J. Fontan, Comparison between weekend and weekday ozone concentration in large cities in France. *Atmos. Environ.*, 35, 1527-1535, 2001.

Possiel N. C. and W. M. Cox, The relative effectiveness of $NO_x$ and VOC strategies in reducing northeast US ozone concentrations. *Water, Air and Soil Pollution*, 67, 161-179, 1993.

Ranmar, D.O., Matveev V., Dayan U., Peleg M., Kaplan J., Gertler A. W., Luria M., Kallos G., Katsafados P. and Y. Mahrer, The impact of coastal transportation emissions on inland air pollution over Israel – utilizing numerical simulations, airborne measurements and synoptic analyses. Submitted to *J. Geophys. Res.* (revised), 2001.

Rao S. T., Sistla G., Schere K. and J. Godowitch, Analysis of ozone quality over New York metropolitan area. In: *Air Pollution Modeling and its Application* VIII. Plenum Press, NY, pp. 111-121, 1991.

Robeson S. M. and D. G. Steyn, Evaluation and comparison of statistical forecast models for daily maximum ozone concentrations. *Atmos. Environ.*, 24B, 303-312, 1990.

Ryan W. F., Forcasting severe ozone epizodes in the Baltimore metropolitan area. *Atmos. Environ.*, 29, 2387-2398, 1995.

SAS Procedure Guide, SAS release 6.03. SAS Institute Inc., Cary, NC, 1991.

Thompson M. L., Renolds J., Cox L. H., Guttorp P. and P. D. Sampson, A review of statistical methods for the meteorological adjustment of tropospheric ozone. *Atmos. Environ.*, 35, 617-630, 2001.

U.S.-EPA, National ambient air quality standards for ozone: Proposed decision, *40 CFR Part*, 50, 1996.

Vecchi R. and G. Valli, Ozone assessment in the southern part of the Alps. *Atmos. Environ.*, 33, 97-109, 1999.

Vukovich F. M. and J. Fishman, The climatology of summertime $O_3$ and $SO_2$ (1977-1981). *Atmos. Environ.*, 20, 2423-2433, 1986.

Vukovich F. M., Bach Jr. W. D., Crissman B. W. and W. J. King, On the relationship between high ozone in the rural surface layer and high pressure systems. *Atmos. Environ.*, 11, 967-983, 1977.

Wolff G. T. and P. J. Lioy, An empirical model for forecasting maximum daily ozone levels in the north-eastern US. *J. Air Poll. Contr. Assoc.*, 28, 1035-1038, 1978.

Table 1. Pearson correlation coefficients† for daily peak 1-h ozone levels.

| | Tel Aviv | Modiin | Jerusalem | Ariel | Be'er Sheva |
|---|---|---|---|---|---|
| Tel Aviv | 1 | 0.41142 | 0.2488 | 0.05489 | 0.44604 |
| Observations* | 149 | 149 | 142 | 149 | 147 |
| Modiin | 0.41142 | 1 | 0.74642 | 0.37848 | 0.74499 |
| Observations | 149 | 153 | 146 | 153 | 151 |
| Jerusalem | 0.2488 | 0.74642 | 1 | 0.27202 | 0.57889 |
| Observations | 142 | 146 | 146 | 146 | 144 |
| Ariel | 0.05489 | 0.37848 | 0.27202 | 1 | 0.31622 |
| Observations | 149 | 153 | 146 | 153 | 151 |
| Be'er Sheva | 0.44604 | 0.74499 | 0.57889 | 0.31622 | 1 |
| Observations | 147 | 151 | 144 | 151 | 151 |

* Observations – number of observations used to derive the correlation coefficients.

† Pearson correlation coefficient (r) – $r = \frac{\sum z_x z_y}{N}$, where $z_x$ and $z_y$ are the variables $X$ and $Y$ converted into their corresponding $Z$ scores.

Table 2. Pearson correlation coefficients for daily 8-h average ozone levels.

| | Tel Aviv | Modiin | Jerusalem | Ariel | Be'er Sheva |
|---|---|---|---|---|---|
| Tel Aviv | 1 | 0.55189 | 0.31754 | 0.26193 | 0.54639 |
| Observations* | 149 | 149 | 142 | 149 | 147 |
| Modiin | 0.55189 | 1 | 0.64488 | 0.43143 | 0.73801 |
| Observations | 149 | 153 | 146 | 153 | 151 |
| Jerusalem | 0.31754 | 0.64488 | 1 | 0.24972 | 0.52434 |
| Observations | 142 | 146 | 146 | 146 | 144 |
| Ariel | 0.26193 | 0.43143 | 0.24972 | 1 | 0.48744 |
| Observations | 149 | 153 | 146 | 153 | 151 |
| Be'er Sheva | 0.54639 | 0.73801 | 0.52434 | 0.48744 | 1 |
| Observations | 147 | 151 | 144 | 151 | 15 |

*Observations – number of observations used to derive the correlation coefficients.

Table 3. One-day lagged autocorrelation of 1-h peak and 8-h averages.

| | Tel Aviv | Modiin | Jerusalem | Ariel | Be'er Sheva |
|---|---|---|---|---|---|
| 1-h peak | 0.34142 | 0.41962 | 0.45024 | 0.47962 | 0.43354 |
| 8-h average | 0.43019 | 0.37610 | 0.57159 | 0.53618 | 0.45345 |

Table 4. "Quasi-autocorrelation" between 06:00 – 09:00h ozone average and 1-day lagged peak 1-h ozone.

| | Tel Aviv | Modiin | Jerusalem | Ariel | Be'er Sheva |
|---|---|---|---|---|---|
| Correlation ($R$) | 0.03579 | -0.04174 | 0.32421 | 0.23267 | 0.10077 |

Table 5. Predictor variables considered in the peak 1-h ozone model and their corresponding bivariate coefficients of determination ($R^2$).

| **Predictor** | **Timing** | **$R^2$ for bivariate regression** | | | |
|---|---|---|---|---|---|
| | | **Tel Aviv** | **Ariel** | **Modiin** | **Jerusalem** |
| $O_3$ Persistence | 1-day lag 1-h max | 0.12 | 0.23 | 0.18 | 0.2 |
| Mixing height (m) | 11Z (GMT) | 0.01 | 0.08 | 0.07 | 0.04 |
| Ventilation rate ($m^2/s$) | 11Z (GMT) | 0.02 | 0.06 | 0.04 | 0.03 |
| Peak temperature (°C) | 1-h daily max | 0 | 0.29 | 0.11 | 0.05 |
| Peak GSR* ($W/m^2$) | 1-h daily max | 0.01 | 0.11 | 0.02 | 0.01 |
| Average $NO_x$ (ppbv) | 10:00-17:00 | 0.13 | 0 | 0 | 0 |
| Average CO (ppmv) | 10:00-17:00 | 0 | 0.12 | 0.07 | 0.01 |
| Average Wind Speed (m/s) | 10:00-17:00 | 0 | 0.03 | 0 | 0.06 |
| Avg u wind component (m/s) | 10:00-17:00 | 0.05 | 0.01 | 0.1 | 0.05 |
| Avg v wind component (m/s) | 10:00-17:00 | 0.07 | 0 | 0.12 | 0.1 |
| Average temperature (°C) | 10:00-17:00 | 0.2 | 0.29 | 0.1 | 0.03 |
| Average relative humidity (%) | 10:00-17:00 | 0.2 | 0.02 | 0.06 | 0.07 |
| Average GSR ($W/m^2$) | 10:00-17:00 | 0.01 | 0.15 | 0.02 | 0 |
| Avg early morning $O_3$ (ppbv) | 06:00-09:00 | 0.03 | 0.05 | 0.01 | 0.18 |
| Avg early morning $NO_x$ (ppbv) | 06:00-09:00 | 0.03 | 0.01 | 0.08 | 0 |
| Avg early morning CO (ppbv) | 06:00-09:00 | 0 | 0.15 | 0.06 | 0 |
| Avg early morning WS* (m/s) | 06:00-09:00 | 0.08 | 0.04 | 0.03 | 0.05 |
| Avg early morning u (m/s) | 06:00-09:00 | 0.03 | 0.01 | 0.04 | 0.09 |
| Avg early morning v (m/s) | 06:00-09:00 | 0.09 | 0 | 0.15 | 0.07 |

* GSR – global sun radiation, WS – wind speed.

Table 6. Stepwise regression analysis for 1-h peak ozone concentration at four stations.

| Tel Aviv | Variable entered | Timing | Number in | Partial $R^2$ | Model $R^2$ | F | Prob>F |
|---|---|---|---|---|---|---|---|
| | RH (%) | 10:00-17:00 avg. | 1 | 0.2031 | 0.2031 | 73.6497 | 0.0001 |
| | $O_3$ (ppbv) | 1-day lag 1-h max | 2 | 0.0741 | 0.2772 | 29.5382 | 0.0001 |
| | $NO_x$ (pphv) | 10:00-17:00 avg. | 3 | 0.0295 | 0.3068 | 12.2337 | 0.0005 |
| | $O_3$ (ppbv) | 06:00-09:00 avg. | 4 | 0.0353 | 0.342 | 15.3354 | 0.0001 |
| | WS* (m/s) | 06:00-09:00 avg. | 5 | 0.0512 | 0.3932 | 24.0466 | 0.0001 |
| | U (m/s) | 06:00-09:00 avg. | 6 | 0.0523 | 0.4455 | 26.7659 | 0.0001 |
| | $NO_X$ (ppbv) | 06:00-09:00 avg. | 7 | 0.0288 | 0.4743 | 15.5208 | 0.0001 |
| | WS (m/s) | 10:00-17:00 avg. | 8 | 0.0079 | 0.4822 | 4.2885 | 0.0393 |
| **Ariel** | **Variable entered** | | **Number in** | **Partial $R^2$** | **Model $R^2$** | **F** | **Prob>F** |
| | T (°C) | 10:00-17:00 avg. | 1 | 0.2965 | 0.2965 | 107.4907 | 0.0001 |
| | GSR (w/m²) | 10:00-17:00 avg. | 2 | 0.0613 | 0.3578 | 24.2399 | 0.0001 |
| | CO (ppmv) | 06:00-09:00 avg. | 3 | 0.03 | 0.3878 | 12.3843 | 0.0005 |
| | CO (ppmv) | 10:00-17:00 avg. | 4 | 0.0325 | 0.4203 | 14.1356 | 0.0002 |
| | $O_3$ (ppbv) | 1-day lag 1-h max | 5 | 0.0218 | 0.4421 | 9.8112 | 0.0019 |
| | RH (%) | 10:00-17:00 avg. | 6 | 0.0153 | 0.4574 | 7.0415 | 0.0085 |
| | WS (m/s) | 10:00-17:00 avg. | 7 | 0.0171 | 0.4745 | 8.0975 | 0.0048 |
| | $O_3$ (ppbv) | 06:00-09:00 avg. | 8 | 0.0117 | 0.4862 | 5.6628 | 0.0181 |
| | $NO_X$ (ppbv) | 06:00-09:00 avg. | 9 | 0.0329 | 0.5191 | 16.8713 | 0.0001 |
| | $NO_X$ (ppbv) | 10:00-17:00 avg. | 10 | 0.0161 | 0.5352 | 8.5304 | 0.0038 |
| **Modiin** | **Variable entered** | | **Number in** | **Partial $R^2$** | **Model $R^2$** | **F** | **Prob>F** |
| | $O_3$ (ppbv) | 1-day lag 1-h max | 1 | 0.1761 | 0.1761 | 55.1379 | 0.0001 |
| | V (m/s) | 06:00-09:00 avg. | 2 | 0.0796 | 0.2557 | 27.4873 | 0.0001 |
| | T (°C) | 1-h daily max | 3 | 0.0512 | 0.3069 | 18.9232 | 0.0001 |
| | $O_3$ (ppbv) | 06:00-09:00 avg. | 4 | 0.0711 | 0.3781 | 29.1663 | 0.0001 |
| | $NO_X$ (ppbv) | 06:00-09:00 avg. | 5 | 0.0865 | 0.4645 | 41.0177 | 0.0001 |
| | CO (ppmv) | 10:00-17:00 avg. | 6 | 0.0313 | 0.4959 | 15.7248 | 0.0001 |
| | CO (ppmv) | 06:00-09:00 avg. | 7 | 0.0311 | 0.527 | 16.5946 | 0.0001 |
| | WS (m/s) | 06:00-09:00 avg. | 8 | 0.0241 | 0.5511 | 13.4597 | 0.0003 |
| | $NO_X$ (ppbv) | 10:00-17:00 avg. | 9 | 0.0252 | 0.5763 | 14.8622 | 0.0001 |
| | U (m/s) | 10:00-17:00 avg. | 10 | 0.0096 | 0.5859 | 5.7762 | 0.017 |
| | RH (%) | 10:00-17:00 avg. | 11 | 0.0092 | 0.5951 | 5.6609 | 0.0181 |
| | MIXHT* | 11Z (GMT) | 12 | 0.0065 | 0.6016 | 4.0268 | 0.0459 |
| **Jerusalem** | **Variable entered** | | **Number in** | **Partial $R^2$** | **Model $R^2$** | **F** | **Prob>F** |
| | $O_3$ (ppbv) | 1-day lag 1-h max | 1 | 0.2027 | 0.2027 | 68.9052 | 0.0001 |
| | $O_3$ (ppbv) | 06:00-09:00 avg. | 2 | 0.0835 | 0.2862 | 31.5914 | 0.0001 |
| | WS (m/s) | 10:00-17:00 avg. | 3 | 0.1027 | 0.3889 | 45.1845 | 0.0001 |
| | V (m/s) | 10:00-17:00 avg. | 4 | 0.0523 | 0.4412 | 25.0912 | 0.0001 |
| | CO (ppmv) | 06:00-09:00 avg. | 5 | 0.051 | 0.4922 | 26.8253 | 0.0001 |
| | $NO_X$ (ppbv) | 06:00-09:00 avg. | 6 | 0.0178 | 0.5101 | 9.691 | 0.0021 |
| | VENTRT* | 11Z (GMT) | 7 | 0.0171 | 0.5271 | 9.5622 | 0.0022 |
| | CO (ppmv) | 10:00-17:00 avg. | 8 | 0.0094 | 0.5366 | 5.3688 | 0.0213 |
| | CO (ppmv) | 06:00-09:00 avg. | 7 | 0.0021 | 0.5345 | 1.1975 | 0.2748 |

* WS – wind speed, MIXHT – Mixing height (m), VENTRT – Ventilation rate (m²/s), GSR – global sun radiation.

Table 9. Predictors and coefficients in the daily (04:00-23:00h) multiple regression model for Tel Aviv station.

| *Predictor* | Intercept | t* (h) | $t^2$ | $t^3$ | $t^4$ | $NO_x$ ppbv |
|---|---|---|---|---|---|---|
| *Coefficient* | 48.3801 | 9.51739 | -1.4263 | 0.08152 | -0.0016 | -0.368 |
| *Predictor* | CO ppbv | U $ms^{-1}$ | V $ms^{-1}$ | RH % | Temp $^0$C | UVB $wm^{-2}$ |
| *Coefficient* | 0.58338 | 2.94391 | 0.21519 | -0.3329 | -0.1961 | -2.977 |

* t – time in h (t = 1 for 04:00h; $t^n$ = time to the power of *n*)

Table 10. Summary of day-of-week-dependent model statistics for each monitoring site.

| | *Statistic* | Sun | Mon | Tue | Wed | Thu | Fri | Sat |
|---|---|---|---|---|---|---|---|---|
| Tel Aviv | $R^2$ | 0.8 | 0.84 | 0.78 | 0.73 | 0.84 | 0.83 | 0.78 |
| | RMSE | 7.5 | 6.3 | 7.2 | 8.7 | 6.2 | 6.6 | 7 |
| Ariel | $R^2$ | 0.69 | 0.66 | 0.72 | 0.68 | 0.68 | 0.67 | 0.64 |
| | RMSE | 8.3 | 8.8 | 7.9 | 8.8 | 8.9 | 8.9 | 8.01 |
| Modiin | $R^2$ | 0.78 | 0.75 | 0.72 | 0.74 | 0.79 | 0.81 | 0.81 |
| | RMSE | 8.3 | 8.7 | 9.1 | 8.7 | 7.7 | 7.3 | 7.3 |
| Jerusalem | $R^2$ | 0.69 | 0.69 | 0.63 | 0.64 | 0.65 | 0.58 | 0.71 |
| | RMSE | 10.1 | 10.6 | 11.5 | 11.6 | 11.7 | 10.5 | 9.5 |

Table 11. Summery of month-of-year-dependent model statistics for each monitoring site.

| | *Statistic* | May | June | July | August | September |
|---|---|---|---|---|---|---|
| Tel Aviv | $R^2$ | 0.77 | 0.86 | 0.83 | 0.85 | 0.79 |
| | RMSE | 8.7 | 5.5 | 5.9 | 6 | 7.8 |
| Ariel | $R^2$ | 0.64 | 0.7 | 0.73 | 0.7 | 0.7 |
| | RMSE | 7.9 | 7.6 | 9 | 8.6 | 7.2 |
| Modiin | $R^2$ | 0.76 | 0.77 | 0.78 | 0.82 | 0.79 |
| | RMSE | 8.7 | 8 | 8.3 | 7.3 | 7.9 |
| Jerusalem | $R^2$ | 0.54 | 0.74 | 0.69 | 0.76 | 0.7331 |
| | RMSE | 11.9 | 9 | 10.3 | 9 | 8.9 |

# PART VI

## *Summary*

The objective of the presented research was to develop a reliable, operational and functional prediction tool for determining the impact of the transportation system on the spatial evolution and distribution of ozone. The study addresses the interaction between traffic flow, atmospheric dynamics of pollution emissions and ozone formation. For this purpose a "5D interdisciplinary modeling system" was established from the separate modules linked to the transportation-to-inland air pollution dynamics, by integrated transportation, emission-factor, atmospheric, transport/diffusion and photochemical models. The systematically integrated prediction tool was then applied to simulate ozone episodes as detected over central Israel by air borne measurements. These measurements showed that central inland Israel is strongly affected by pollution originating along the Mediterranean coastline, where urban transportation sources play a pivotal role. The flight measurements, model simulations and ground-level monitoring all showed that under northwesterly winds, elevated ozone values can be found over central Israel. These findings establish a scenario in which the physical process of inland movement of pollutants in general, and ozone precursors in particular, is established. The Tel Aviv metropolitan area and possibly the Gaza Strip region emit transportation pollutants into the troposphere on a daily basis, initiating their subsequent photochemical transformation as they are transported downwind. Model simulations showed that about 60% of the detected inland ozone concentration is nourished by traffic emissions during the morning rush hours from the Tel Aviv metropolitan area.

The assumption of a photochemically aged air mass regime has enabled the application of multivariate linear regression analysis to quantitatively appraise ozone production over central Israel. Thus, under these conditions, the application of a relatively simple statistical analysis method for evaluating ozone concentrations may replace the need for comprehensive photochemical solvers.

The work presented here demonstrates the ability of interdisciplinary modeling systems to operate collectively as a prediction tool/tracing device, capable of successfully predicting air pollution hotspots. The model is now being expanded to include photochemical transformations that will enable simulating ozone formation under additional conditions. This prediction and analysis tool is expected to assist in the shaping of present and future transportation infrastructure, where air pollution in general – and ozone problems in particular – are to be considered.

In order to complement the ozone pollution modeling aloft, statistical multiple-regression models were developed to estimate ground-level ozone concentration. The models designed to capture 1-h peak, 8-h average and hourly ozone levels were developed for and applied to four stations in the Israeli air pollution-monitoring network. In general, the predicted ozone-derived variables agreed quite closely with the observed values at the four stations. However, while the models captured the general feature of the temporal variation fairly well, they underestimated high values. These observations were particularly evident on days that followed days with low observed values, or in the case of daily 1-h averages, when a secondary late afternoon-to-late evening peak was established. While the prediction models did not reach the anticipated predictive levels, they provide the first statistical procedures addressing decision-grade forecast levels in Israel.

Appendix E: Erez Weinroth (HUJI) Ph.D. thesis work to date

# EFFECTS OF MAJOR EMISSION SOURCES ON AIR QUALITY:

# A NUMERICAL STUDY

(Preliminary Draft of Certain Sections)

A Thesis Presented to

The Faculty of Environmental Sciences

Hebrew University of Jerusalem (HUJI)

Israel

In Partial Fulfillment

Of the Requirements for the Degree

Doctor of Science

by

Erez Weinroth

August 2002

211

January 2002


# EREZ WEINROTH

*Faculty of Agriculture, Food and Environmental Quality Sciences*
*The Freddy and Nadine Herrmann Graduate School of Applied Science*
*Hebrew University of Jerusalem, Israel*
*weinroth@agri.huji.ac.il*


## EDUCATION

**Institute of Earth Sciences, Faculty of Science, Hebrew University of Jerusalem (HUJI)**
B.Sc. Atmospheric Sciences and Geology, with Honors. June 1994, Grade: 88/100.
Three summer scholarships for scholastic excellence.

**Freddy and Nadine Herrmann Graduate School of Applied Science, HUJI**
M. Sc. Environmental Sciences, December 1997, Grade: 90/100.
Thesis: Estimation of the Movements of Emitted Plumes from Motor Vehicles and Comparison to Measurements.

**Faculty of Agriculture, Food and Environmental Quality Sciences, and Freddy and Nadine Herrmann Graduate School of Applied Science, HUJI**
PhD. Environmental Sciences, in progress, expected completion: end 2002 beginning 2003.
Eli Ravitz award for scholastic and teaching excellence
Thesis: Effects of Major Emission Sources on Air Quality in Israel: A Numerical Study.

## EXPERIENCE

**Department of Soil and Water, Faculty of Agriculture, Food and Environmental Quality Sciences, HUJI (1998-Present)**
> **Research Assistant, Ozone Project:** Maintain RAMS, CAMx, and data conversion software; modify FORTRAN codes; prepare emission inventory for Israel; GIS
> **Research Assistant, Aerosol project:** Propagation of dust particles due to desiccation of Aral Sea with ETA model. Instructed foreign exchange students in Arcview software and ETA model
> **Teaching Assistant** (lecturer; grade papers/exams)
Physics (1998-present), Atmospheric Dynamics (1994-1995), Environmental Measurements and Instruments (1994-1995)
> **GIS computer lab assistant:** graded papers/exams (1999-2000)

**Freddy and Nadine Herrmann Graduate School of Applied Science, HUJI (1995 – 97)**
**Graduate Assistant:** Maintained meso-meteorological model, programmed advection models in ARC/INFO GRID environment (AML).

**CITIZENSHIPS:** USA and Israel
**LANGUAGES:**
**Hebrew:** native language
**English:** excellent written and oral skills.
**Arabic:** proficient.
**COMPUTER SKILLS:**
**Operative systems:** DOS, Windows 95/98NT/2000, Unix, Linux
**Programming languages:** Pascal, Fortran 77/90, AML, Mat lab
**Scientific visualization:** VIS5D, IDT, ARCVIEW 3.2,
**Internet programs:** FTP, Telnet, Netscape, Explorer

## PRESENTATIONS:

Mahrer, Y., Weinroth, E., and Poberezsky, L. 1999: Dust propagation following desiccation of the Aral Sea. Poster presentation, Boulder, Colorado.
Weinroth, E., 1997: GIS-Based Models and GIS Tools for Sustainable Transport Planning in Israel and Palestine. Presentation, Bonn, Germany.

**Table of contents (anticipated)**

Abstract

1. PART I. Introduction
    a. background
    b. general
    c. air pollutant emissions: anthropogenic and biogenic
    d. NOx
    e. VOC
    f. photochemical relationship between O3, NOx, and VOC
    g. air pollution models
    h. photochemical models

2. Research Objectives

3. Research Significance

4. Literature cited

5 PART II. Methodology

6. PART III. Paper "EMISSION INVENTORY FOR ISRAEL"
    a. abstract
    b. introduction
    c. emission sources
    d. geographical location of sources
    e. results and discussion
    f. conclusion
    g. acknowledgment
    h. reference

7. PART IV. Paper "MODEL SIMULATIONS OF OZONE FORMATION OVER ISRAEL, WEST BANK, AND JORDAN"

8. PART V. Paper "ANALYSIS THE EFFECTS OF DIFFERENT EMISSION SOURCES ON OZONE FORMATION IN ISRAEL"

9. Conclusion

# PART III: EMISSION INVENTORY FOR ISRAEL

(Updated for Report 2)

**Erez Weinroth**

Environmental Sciences
The Hebrew University
Jerusalem, ISRAEL

August 2002

## INTRODUCTION

A study of the quantitative influence of the different air pollution sources (stationary, mobile) on ozone creation is being conducted in the Hebrew University in Jerusalem. The study includes a simulation of the effects of various air pollution sources (including industrial, biogenic and transportation pollutants) through the use of a system of computer models including a photochemical model. The preparation of an extensive database for emissions from the different pollution sources, which also includes geographical information, is a cornerstone of the study as it is a prerequisite for running the photochemical model.

The pollution sources for which emission data was required were:

1. Large Stationary (point) sources;
2. Medium Stationary (point) sources;
3. Small Stationary (area) sources;
4. Biogenic Stationary (area) sources;
5. Mobile (area) sources, both ground based and aerial.

This paper summarizes the process of collecting data with respect to emissions from the pollution sources listed above. Where data regarding the emission amounts themselves was available, it could be readily used within the model. However, often only raw data was available, and certain calculations and assumptions were required to make it suitable for use within the model. This document will outline such calculations and assumptions used in the preparation of the database.

Data regarding the exact geographical location of each emission source was also collected and integrated into the database for use within the model. This data is critical for obtaining optimal results from the photochemical model, as it is a three dimensional model. The collection and processing of the geographical data with respect to all pollution sources will be explained in a separate section of this paper.

Finally, we will focus on proposed improvements to the database.



215

## LARGE STATIONARY (POINT) SOURCES

The principal large stationary sources in Israel are the five electrical company power plants, the Haifa and Ashdod refineries and the three "Nesher" cement processing plants. These sources together account for over 71% of the fuel consumption by stationary sources and 58% from overall fuel consumption[1]. Each of these facilities has installed monitors that record, on a per-hour per-stack basis, the amounts of the various pollutants emitted and/or the plant capacity. All the locations of large stationary point sources can be seen in map 1.

### Electrical Company Facilities

We collected data regarding the hourly output of electricity manufacture (*P*), the average hourly fuel consumption to output (watt) ratio (*D*), and the fuel amount (Kg) to emission amount (gm) ratio (*F*) (F was calculated for $SO_2$ and NOx). By multiplying these three parameters, we received the hourly $SO_2$ and NOx emissions. To calculate CO, VOC (Volatile Organic Compounds) emissions, we multiplied the amounts of fuel used by the electrical company (P*D) by the EPA stationary sources emission factors (henceforth, the "EPA Factors") (EPA, 1995), which required us to collect data regarding the fuel type, as the EPA Factors are fuel type sensitive[2].

### Haifa and Ashdod Oil Refineries

From the Haifa and Ashdod oil refineries we collected data with respect to $SO_2$ emissions, as well as the hourly fuel consumption. To calculate the hourly emissions of the, CO, NOx and VOC pollutants, we used the calculations described in the electrical company section above, as well as the following calculations:

It is noteworthy that the data received from the electrical company and the Haifa and Ashdod refineries was the most accurate available to us, as it enabled us to calculate the emissions on an exact hourly basis, whereas with all other emission sources the

[1] There is a direct and linear link between fuel consumption and emission amounts.
[2] Unless otherwise stipulated herein, fuel type, consumption, CO, $SO_2$ and NOx emissions data was collected with respect to stationary sources, where applicable, and EPA Factors were then used to calculate VOC (species) and missing data on CO, $SO_2$ and NOx emissions..



216

only way to calculate the hourly emissions was to calculate an average out of annual data.

**Nesher Cement Factories emissions**

Average hourly CO, $SO_2$ and NOx emissions were available from measurements taken at the source by an independent company. The accuracy of this data is reasonable rather than excellent, as the exact hourly variations are not accounted for. When calculating such an average for Nesher, we did not take into account the difference between day and night and between workdays and weekends/holidays , because the Nesher plants work on a continuous basis. When calculating the average for the medium stationary sources (see below) we took into account that when the plants were monitored they were probably not monitored at 100% capacity, so we decided arbitrarily that the plants were monitored at 70% output. This allowed us to disregard the difference between day and night and workdays or week days/holidays with respect to such plants.

## MEDIUM STATIONARY (POINT) SOURCES

These sources together account for over 8.1 % of the fuel consumption by stationary sources and 6.6% from overall fuel consumption.

**Plants which Monitor Emissions**

There are over 100 plants in this category. These plants are required by law to have their emissions monitored by an independent company once a year. The data is then reported to the Ministry of the Environment or the Municipal Associations, who were gracious enough to provide us with access to it.

The data in the emission reports usually included hourly particles, CO, $SO_2$, and NOx emissions. We then assume that the plant emits these hourly pollution levels on a continuing basis. Where only one or several of these pollutants' emissions was reported, we used hourly fuel consumption and fuel type data, which collected to calculate the other pollutant emissions, according to the calculations above.

**Plants which report Fuel Consumption**

There are numerous medium plants that do not monitor their emissions. We therefore approached the Fuel Authority, which collects annual information as to fuel consumption in Israel, and received data regarding such plants' fuel consumption. By using the fuel consumption data were able to calculate the annual amounts of pollutants emitted ($SO_2$, CO, NOx and VOC species), and then calculated average hourly emissions (dividing the annual amounts by 365*24).

The hourly calculation is only an approximation, as it is known to us that these plants do not work at the same capacity on a 24 hours 365 day basis. For example, some plants work at maximum capacity for 12-14 hours a day, and some work at full capacity 24 hours a day but only 5.5 days a week.

Map 2. (Medium sources spatial distribution).

## SMALL STATIONARY (AREA) SOURCES

These sources together account for over 15% of the fuel consumption by stationary sources and 12.2% from overall fuel consumption.

After taking into account the large and medium stationary sources, we are left with the myriad small plants that we did not treat as separate stationary sources, as information about individual fuel consumption and exact geographic location was unavailable. Rather, by using aggregate fuel consumption[3] (taking for account the fuel type) data regarding such small stationary sources, we calculated the aggregate emissions from such sources using the EPA Factors, and divided such emissions uniformly over the geographical locations of industrial areas in Israel.

Industrial zones (Orange color polygons) can be seen in Map 1. are

[3] The aggregate fuel consumption for the small stationary sources was calculated by taking the data regarding aggregate stationary source fuel consumption and subtracting the fuel consumption by the large and medium stationary sources.

## BIOGENIC STATIONARY (AREA) SOURCES

Biogenic sources which may effect the results of the photochemical model are trees and vegetation which emit the pollutants Isoprene and Monoterpene (VOC species). Each plant type has a different VOC emission factor (see above), but to avoid having to cope with huge amounts of data, we created nine categories of plant types (Coniferous (Pines), Acer, Acacia, Quercus, etc). As no extensive and reliable study on vegetation VOC emissions was done in Israel we used studies published on such emission factors in California (Winer et al 1992; Benjamin et al 1996,1997,1998), the reason being that California has a climate similar to the Mediterranean climate. The taxonomy and genome of some of the vegetation in California is similar to that of Israel's. We created an additional category of plant types (giving ten categories in all) to include all plant types that grow in Israel but are not found in California, and as no emission factor was available for this category, we arbitrarily assigned it an emission factor which is an average of the emission factors of the other nine categories.

The emissions from each category of plant type in each grid block were calculated as follows:

| | | | |
|---|---|---|---|
| Biomass Amount per hectare | * Vegetation Coverage percentage | * VOC emissions per Biomass Amount | = VOC emissions per hectare |

To calculate the Biomass amount of each plant type we used Biomass tables (Benjamin et al 1997). The vegetation coverage percentage was found using data on annual rainfall in each particular geographic area and the assumption that there is a linear connection between the annual rainfall and vegetation coverage. Map 3. annual rainfall and Map 4. vegetation coverage.

Data regarding plant types was collected from several sources. With respect to some geographical areas data was available from the Reservation and National Parks Authority. Such data was relatively detailed, and from it we were able to single out the dominant plant type in each defined area, and assign that plant type's emission category to that area. Where the Authority's data was not available, we received more general data regarding the vegetation types in other areas was received from several

government ministries after being processed by the Hebrew University's GIS laboratory.

## MOBILE (AREA) SOURCES

### Ground Based Transportation

The emissions from mobile sources were received as point sources from the Mobile5 (MOBILE5, 1994) and EMFAC7 (ARB, 1993) transportation models run by Mr. Jay Kaplan (1997), and were converted into area sources (grid cells applicable for the photochemical model input). These models provided data on emissions at three points on each transportation route – the entry point and exit point of such route, and the point halfway in between.

The transportation models are built on numerous assumptions with respect to travel time, type of travel (to work, pleasure, from work etc.), geo-economic structure of the country studied and other variables. The models also utilize an emission-vehicle speed curve (Fig. 1.), which was derived from measurements taken in Fort Mc-Henry tunnel (Pierson, 1996), Haifa (Tratakovsky, 1997) and Jerusalem (Yavin, 1998).

The results obtained from running the transportation models were CO, NOx and TOC (Total Organic Compounds) emission amounts emitted by ground (road) based transportation. (Map 5-6). The various compounds comprising the TOC amounts were calculated by using the percentages of VOC vehicle emission out of total TOC from a study conducted by Kleindienst (1992). Although Kleindienst only found emission percentages for 82% of the organic compounds emitted in combustion, we assumed that such organic compounds in their respective ratios also constituted the remaining 18% of the emitted pollutants.

It is noteworthy that the results obtained from running the transportation model all related to emissions during the morning rush hours. In order to calculate the emissions with respect to the remaining hours of the day, we used the vehicle-time of day curve for a medium sized city (Netanya 1995, Fig 2.), under the assumption that a

medium sized city would represent the average between rural areas and large urban areas.

**Aerial Transportation**

To calculate the NOx, VOC and CO emissions from civilian aerial transportation sources we first requested from the Aviation Administration the number of daily incoming and outgoing flights from Ben Gurion Airport,The daily flights were divided into heavy (Boeing 757, 767 and 747 or equivalents) and medium plane categories by assuming an average fleet distribution (EL-AL fleet: 65% medium sized planes 35% heavy planes). We multiplied the number of flights in each category by the appropriate fuel consumption factor, which were received from El-Al. The fuel consumption factors relate to the fuel consumed between Israel's Ben-Gurion airport and Israel's Mediterranean coastline. We then multiplied the result by the EPA Factors in order to obtain the emission amounts.

Table 1. demonstrates the emission inventory.

## GEOGRAPHICAL LOCATION OF SOURCES

In conjunction with collecting data regarding the amount of emissions we attempted to ascertain the exact geographical location of the emission source in three dimensional space.

For stationary sources, we used each plant's address, if available, together with the Central Bureau of Statistics' G.I.S. address database, to determine the precise two dimensional coordinates of such plant. Where the address was not available, we used a 1:50,000 Map to identify the plant's location. We then calculated the emission sources location plum-in grid) in the third dimension by gathering data regarding output, emission speed, emission temperature, stack circumference and stack height, and calculating effective stack height.

The data required to calculate effective stack height was available for all the large stationary sources and part of the medium stationary sources.

When considering the geographic point of emission from aerial sources we took the flight corridor from Ben Gurion Airport to the Mediterranean coastline as a diagonal line, and calculated the emissions as being released at the airport itself and from three points along this line, in such ratios as were provided to us by El-Al.

To make the data available for the photochemical model we had to calculate the emissions as being emitted from cells and not form points, this procedure was made to the small and medium sources, (that had no information for calculating stack height), mobile sources, and Biogenic sources. Cell size is 1250x1250 $m^2$.

## RESULTS

Various emission sources contribute differently to the creation of pollutants. after completion of the emission inventory we can present conclusions regarding spatial distribution of the sources and their contribution to the emission of primary pollutants.

In table two we see the total emissions from the different sources divided into groups of pollutants species. The table clearly shows that most of the primary pollution is emitted by vehicles although they account for only a fifth of fuel consumption. Figures 3 through 6 show in graph format the contribution of the different sources to the creation of CO ,$SO_2$ ,NOx and Alkane .

Spatial situation of the different groups (pollutant species) can be seen in the in figures 8-18 (fig. 7 displays the study area). We may make additional interesting deductions from figures 8–18. In some cases we see that certain groups of pollution sources do not contribute to the creation of certain pollutants, as in the case of Formaldehyde which is only emitted by stationary sources (certain industry plants). Also noteworthy is figure 14, which shows that both stationary sources and mobile sources contribute to the creation of NOx, and that despite the fact that the total emission of NOx from mobile sources is greater than its emission from stationary sources, the emission output flux at the point of emission (the electric company plants) are much higher (at least 20 times higher) than the highest output flux emitted from any point along the transport routes.

In order to aid the viewer with interpreting figures 8 through 18 we note that the legend in each figure was divided into groups as follows:

| Stationary Sources |
|---|
| 0 |
| 0 to median |
| median to two standard deviations |
| > two standard deviations |

| Mobile Sources |
|---|
| 0 |
| 0 to median |
| median to one standard deviation |
| one standard deviation to two standard deviations |
| two standard deviations to three standard deviations |
| > three standard deviations |

In figures 19 through 27 one may observe the hourly distribution of emissions of pollutants from vehicles (on road) in graph format. Three columns of each graph are highlighted in red – these are selected hours which are shown on separate maps in each figure – morning rush hour, afternoon and night. The legend for all three maps in each figure is uniform – it was created in accordance with the division into groups for mobile sources as described above, in accordance with morning rush hour data in that figure.

## SUGGESTED IMPROVEMENTS

The following actions would improve the database we made:

1. Collecting data regarding all small stationary (point) emission sources, rather than treating some of these sources as a general area emission source.
2. Collecting data regarding the various plants' actual operation hours.
3. Discerning between trucks and smaller vehicles while running the transportation models with respect to the following variables: differences in use between week days and weekends, differences in use during the various hours of the day, and usage of different transportation routes.

4. Measurement of VOC emissions from vegetation in Israel, rather than reliance upon California measurements.
5. Calculation of vegetation cover through use of satellite photography and area measurements rather than reliance upon the connection between rainfall and vegetation cover.
6. Addition of emission data from flights out of military airports.

**Acknowledgments**

Hagar Leshner, Prof. Avinoam Danin , Dr. Ronen Kadmon, Yonat Magal Yisrael Taober,Igodie Arim Ashdod, Ashkelon, Haifa, Hadera, Yavne, Jerusalem. Adi Benon, Shahar Kats, Jay Kaplan, Orit Stone, Prof.Isaac Mahrer, Prof. Menachem Luria, Eran Tas, Dr Mordechai Peleg.

## References:

ARB (California Air Resources Board).(1993). EMFAC7 Computer Model, Technical Support Division.

Benjamin Mt.,Sudol M., Vorsatz D. and Winer MW. (1997). A spatially and temporally resolved biogenic hydrocarbon emissions inventory for the California South coast air basin. *Atmos. Environ.*,31, 18, 3078-3100

Benjamin Mt.,Sudol M., Bloch L. and Winer MW. (1996).Low emitting urban forests: A taxonomic methodology for assigning Isoprene and Monoterpene emission rates. *Atmos. Environ.*,30, 9, 1437-1452

Benjamin Mt. and Winer MW.(1998) Estimating the Ozone-forming potential of urban trees and shrubs. *Atmos. Environ.*,32, 1, 53-68

Kaplan J., (1997). Model Structure and Data Requirements. Working Paper for the Trilateral Research Project on GIS Tools for Sustainable Transport in Palestine and Israel.(Personal communication).

Kleindienst TE., Smith DF., Hudgens EE., Snow RF., Perry E., Claxton LD., Bufalini JJ., Black F. and Cupitt LT.(1992). The Photooxidation of automobile emissions - measurements of the transformation products and their mutagenic activity., *Atmos. Environ.*,26, 16, 3039-3053

Pierson w., et al.,(1996).Real world automobile emissions – Summery of studies in Fort Mc-Henry tunnel. , *Atmos. Environ.*, 30, 2233-2256.

Tratakovsky L., Gotman M., Zvirin Y., Golgotio I. and Alinikov Y.,(1997). Estimation of vehicles emission factors in Israel, *Research report –Technion Israel Institute of Technology, Transportation research Institute,* 87 pp.

US-EPA (ed.) (1995), Compilation of the Pollutant Emission Factors; Volume 1: Stationary Point and Area Sources fifth edition. *Office of Air Quality Planning and Standards Research Triangle Park NC.*

225

User's guide to MOBILE5(mobile source emission factor model)(1994) U.S.EPA Office of air and radiation office of mobile sources emission planning and strategies division air quality analysis branch 2565 Plymouth road Ann Arbor, Michigan 48105

Winer MW., Arey J., Atkinson R., Aschmann SM., Long WD., Morrison L. and Olszyk DM.(1992) Emission rates of organics from vegetation in California's central valley., *Atmos. Environ.*, 26A, 14, 2647-2659

| PLANT | SO2 | NOx | CO | OLE | PAR | TOL | XYL | FORM | ALD2 | ETH | ISOP |
|---|---|---|---|---|---|---|---|---|---|---|---|
| Stationary Total | 8.64E+05 | 8.56E+05 | 2.83E+04 | 3.27E+00 | 4.31E+01 | 1.04E+01 | 3.37E-01 | 1.09E+02 | 6.33E+00 | 0.00E+00 | 0.00E+00 |
| Refineries | 1.88E+04 | 1.54E+04 | 2.04E+03 | 1.00E-04 | 1.06E-01 | 3.23E-01 | 6.72E-03 | 5.50E+00 | 0.00E+00 | 0.00E+00 | 0.00E+00 |
| ECI | 5.70E+05 | 6.38E+05 | 1.51E+04 | 2.81E+00 | 3.60E+01 | 6.08E+00 | 2.30E-01 | 4.55E+01 | 5.43E+00 | 0.00E+00 | 0.00E+00 |
| Cement factories | 2.81E+04 | 2.66E+04 | 9.52E+02 | 9.21E-02 | 1.24E+00 | 3.64E-01 | 1.10E-02 | 4.29E+00 | 1.78E-01 | 0.00E+00 | 0.00E+00 |
| Industry (R) | 2.47E+05 | 1.76E+05 | 1.02E+04 | 3.68E-01 | 5.75E+00 | 3.63E+00 | 8.93E-02 | 5.37E+01 | 7.22E-01 | 0.00E+00 | 0.00E+00 |
| Vehicles | 8.45E+03 | 1.25E+06 | 1.87E+06 | 4.26E+03 | 1.68E+05 | 8.12E+03 | 7.96E+03 | 0.00E+00 | 3.79E+03 | 6.87E+04 | 0.00E+00 |
| Vegetation | 0.00E+00 | 0.00E+00 | 0.00E+00 | 0.00E+00 | 1.24E+03 | 0.00E+00 | 0.00E+00 | 0.00E+00 | 1.27E+02 | 0.00E+00 | 9.55E+02 |
| Airplanes | 2.33E+02 | 5.28E+03 | 8.97E+03 | 2.95E+01 | 5.50E+02 | 0.00E+00 | 0.00E+00 | 8.34E+02 | 9.24E+01 | 5.40E+02 | 0.00E+00 |
| Total | 8.73E+05 | 2.11E+06 | 1.90E+06 | 4.30E+03 | 1.69E+05 | 8.13E+03 | 7.96E+03 | 9.43E+02 | 4.01E+03 | 6.93E+04 | 9.55E+02 |

Table 2. (Contribution of Emission Sources to Creation of Pollutants (mol/hour))

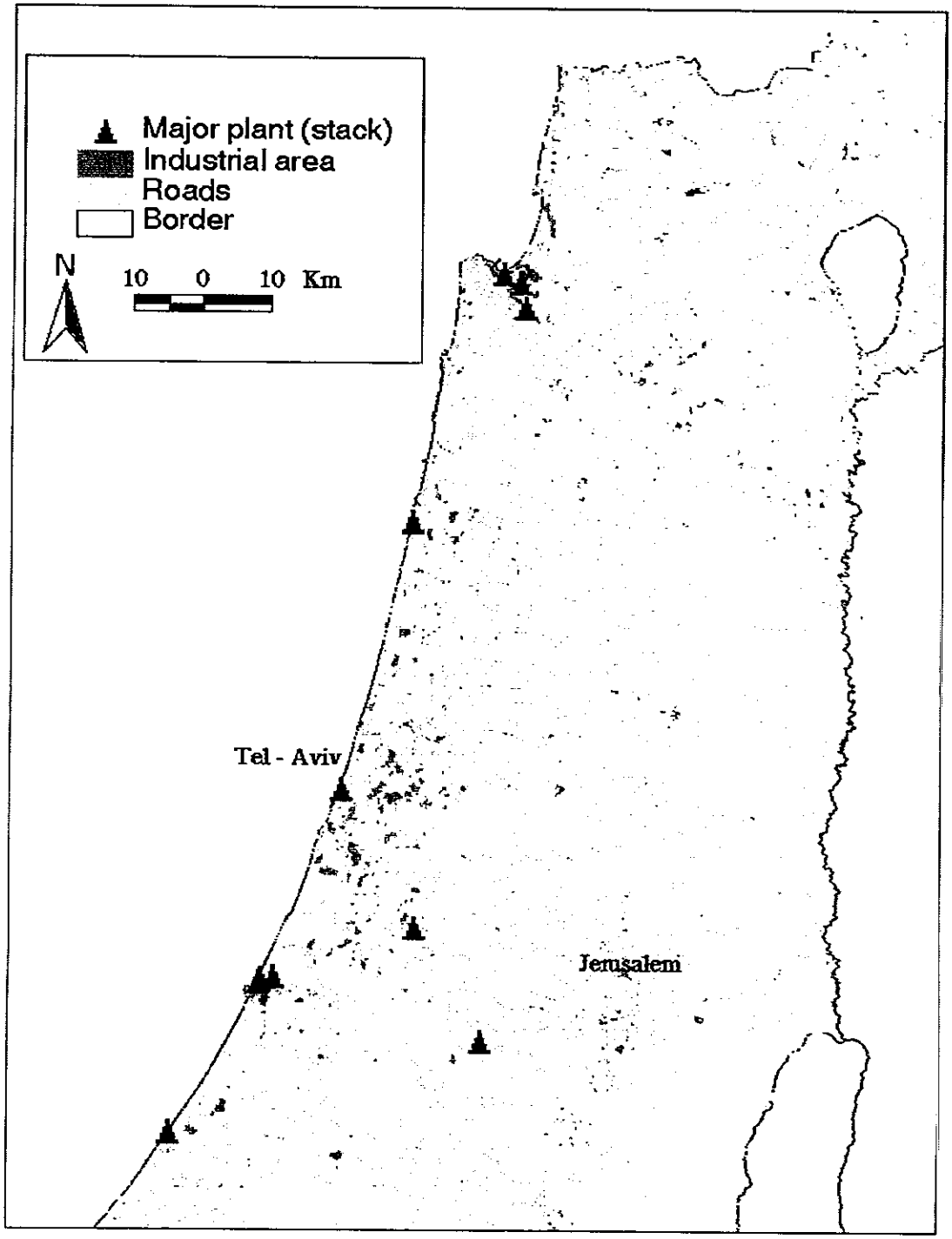


Map 1. Large stationary point sources and industrial areas

# Nox emissions from Point Sources g/hour

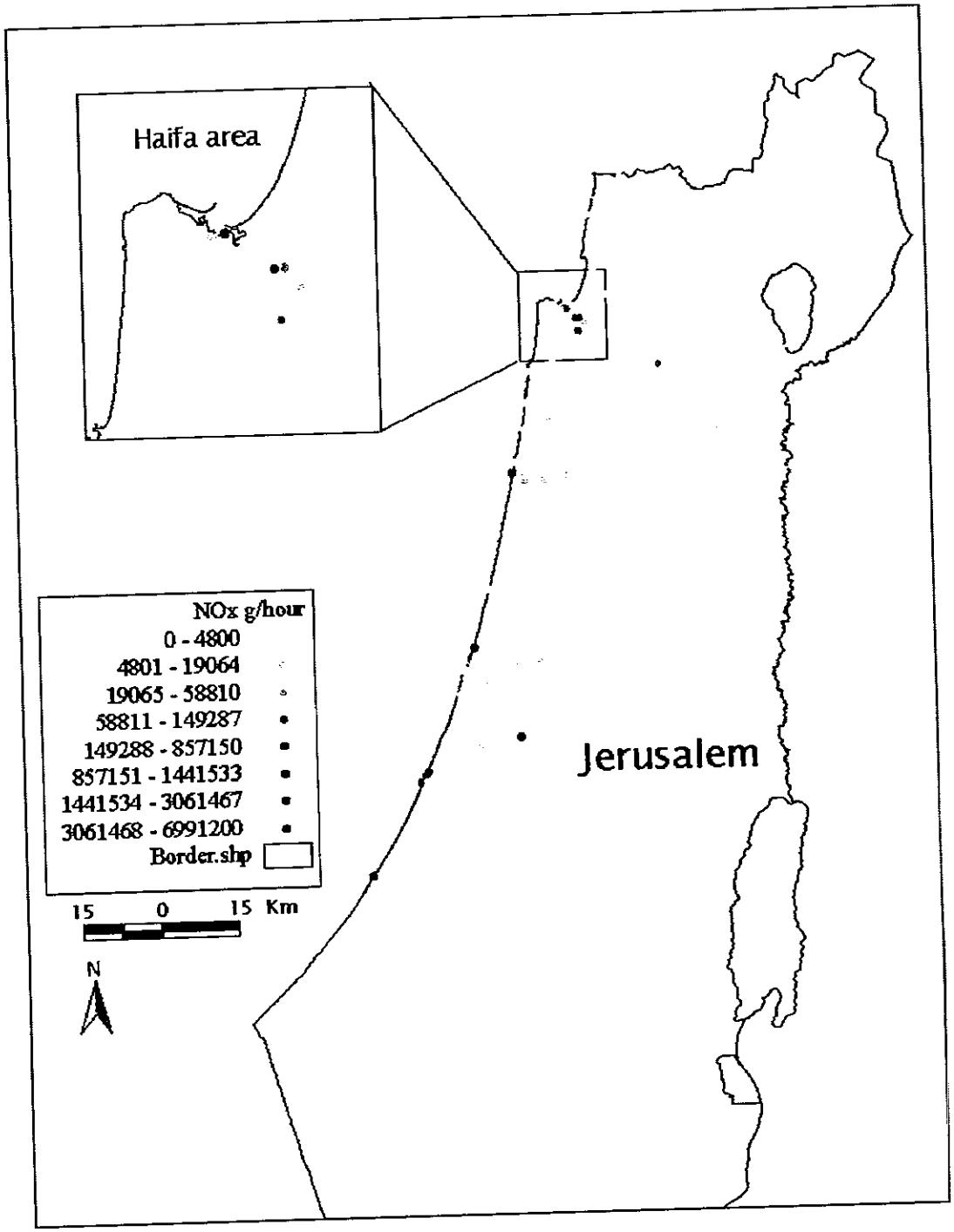


Map 2. Medium stationary (point) sources

# Rainfall mm ( Yearly Average)

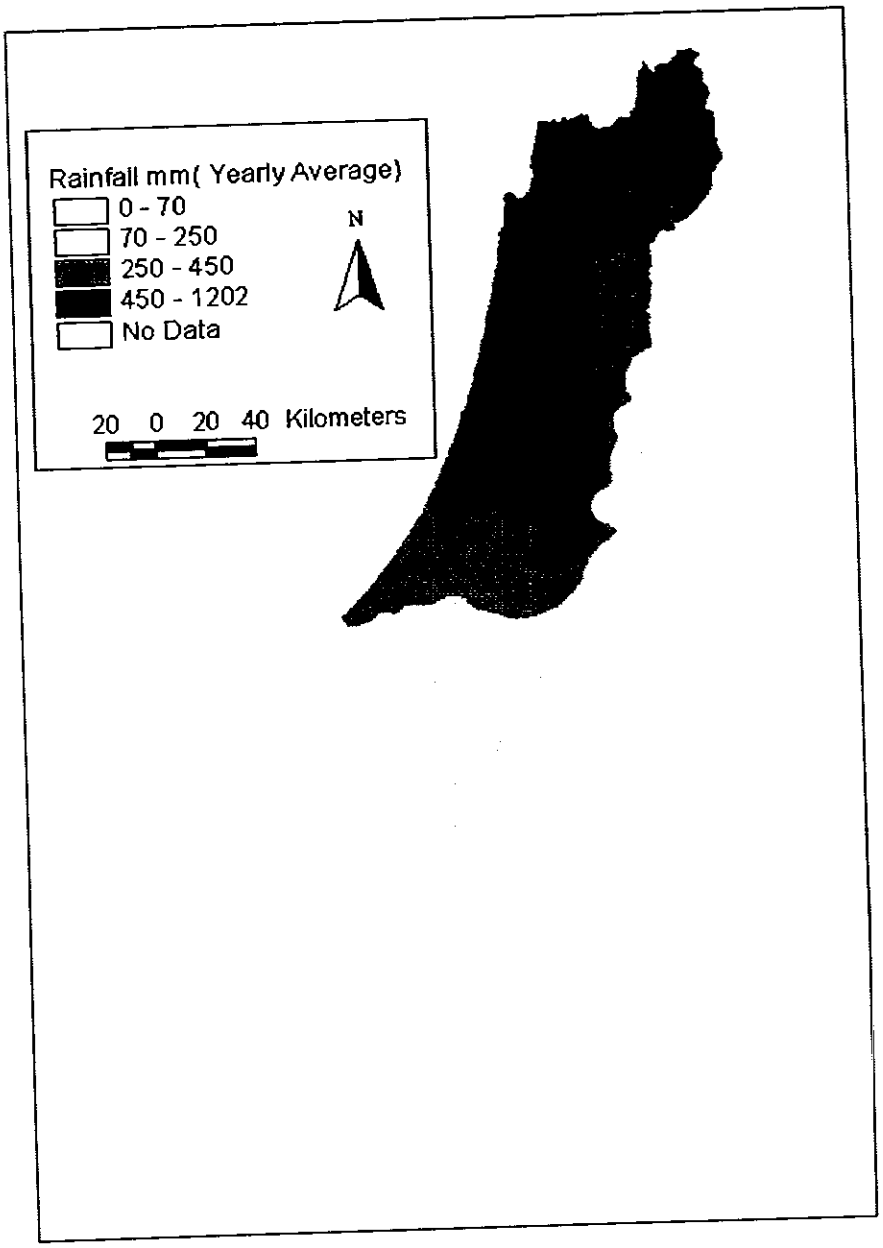


Map 3. Annual rainfall

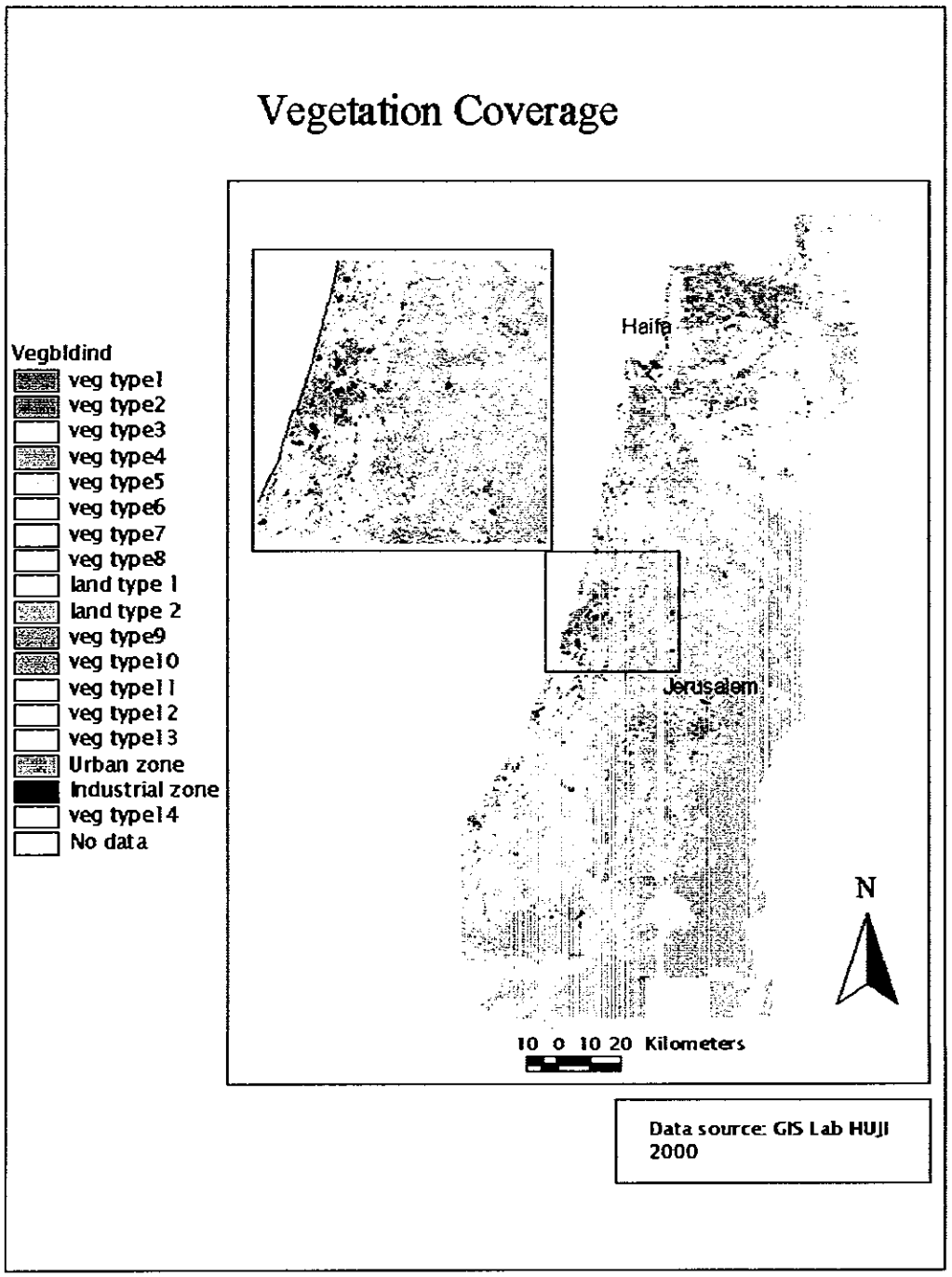


Map 4. Vegetation coverage

## NOx emissions gr/hour

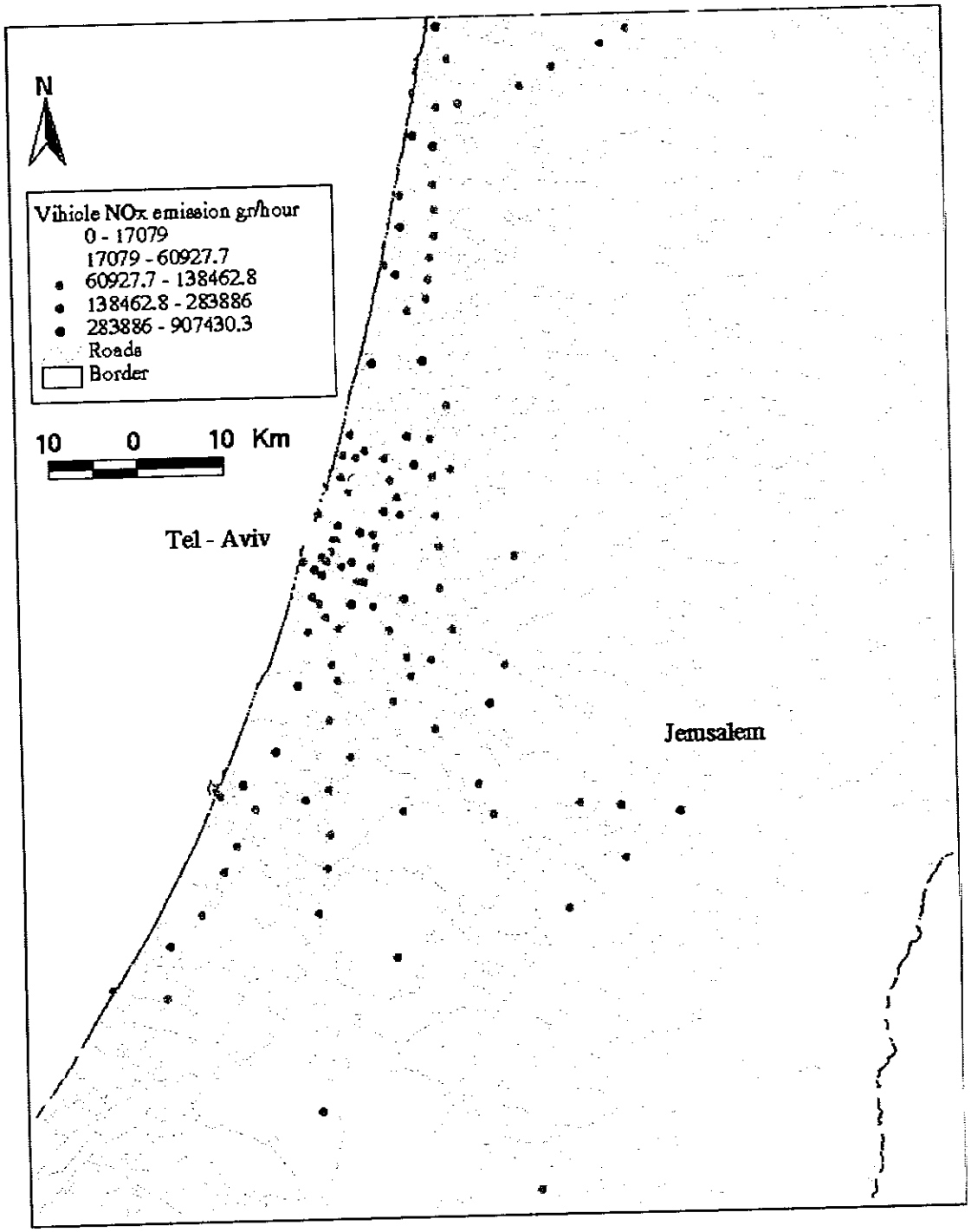


Map 5. NOx emissions emitted by ground (road) based transportation

## TOG( Total Organic Compounds) emissions gr/hour

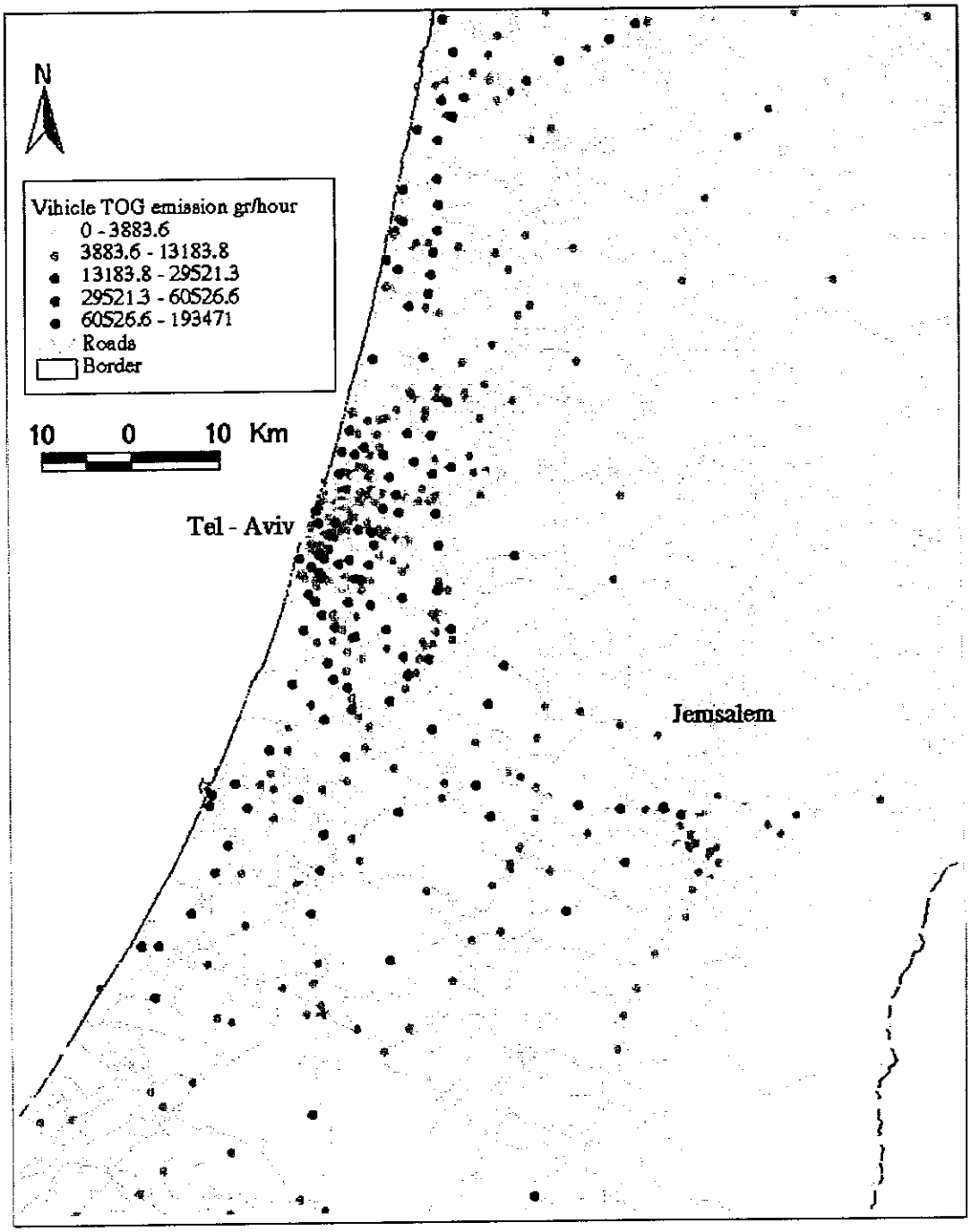


Map 6. VOC emissions emitted by ground (road) based transportation

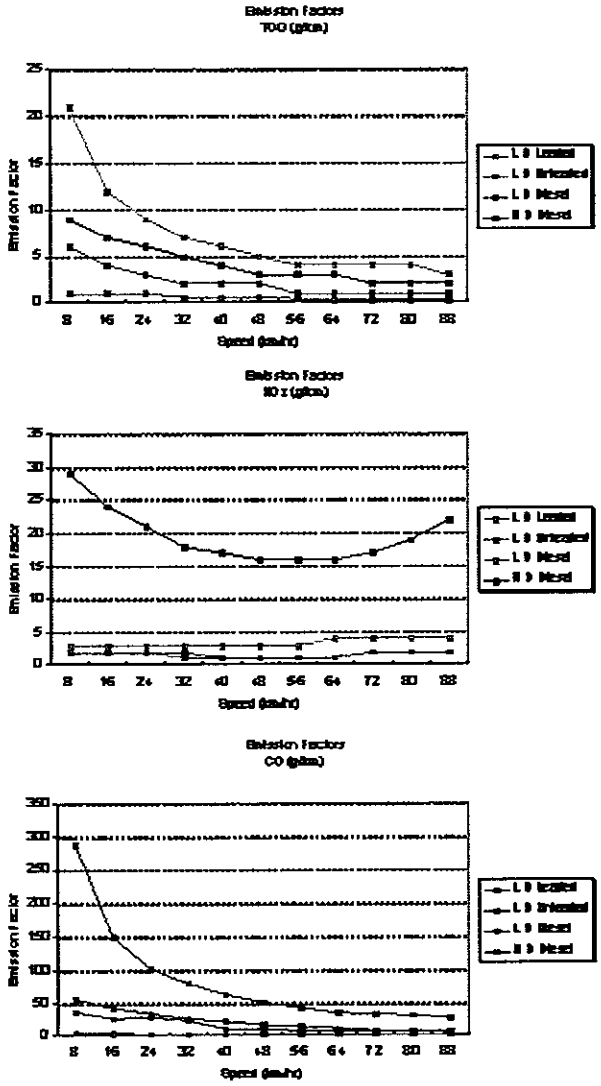


Fig. 1. (Emission-vehicle speed curves)

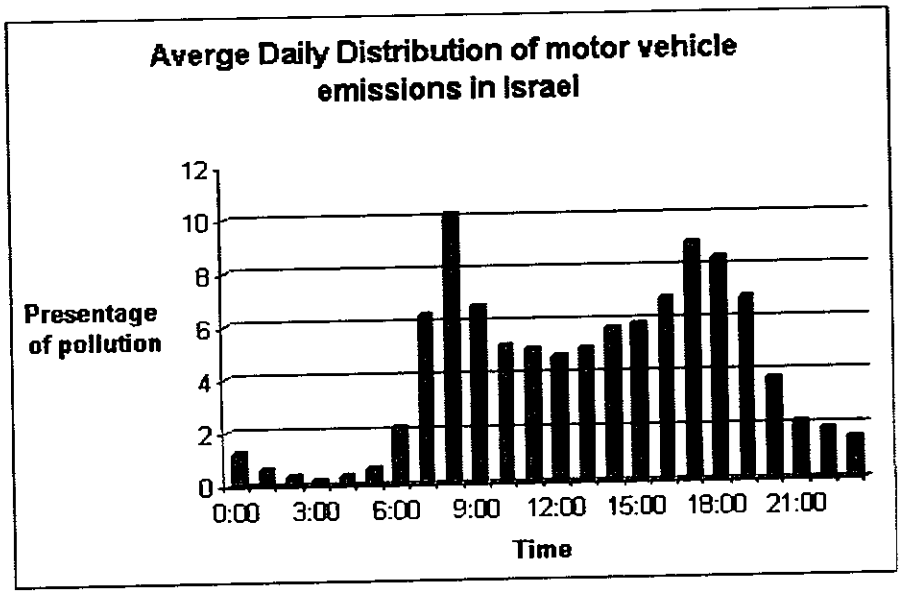


Fig. 2 Average daily distribution of motor vehicle emissions (Natanya, Israel 1995)

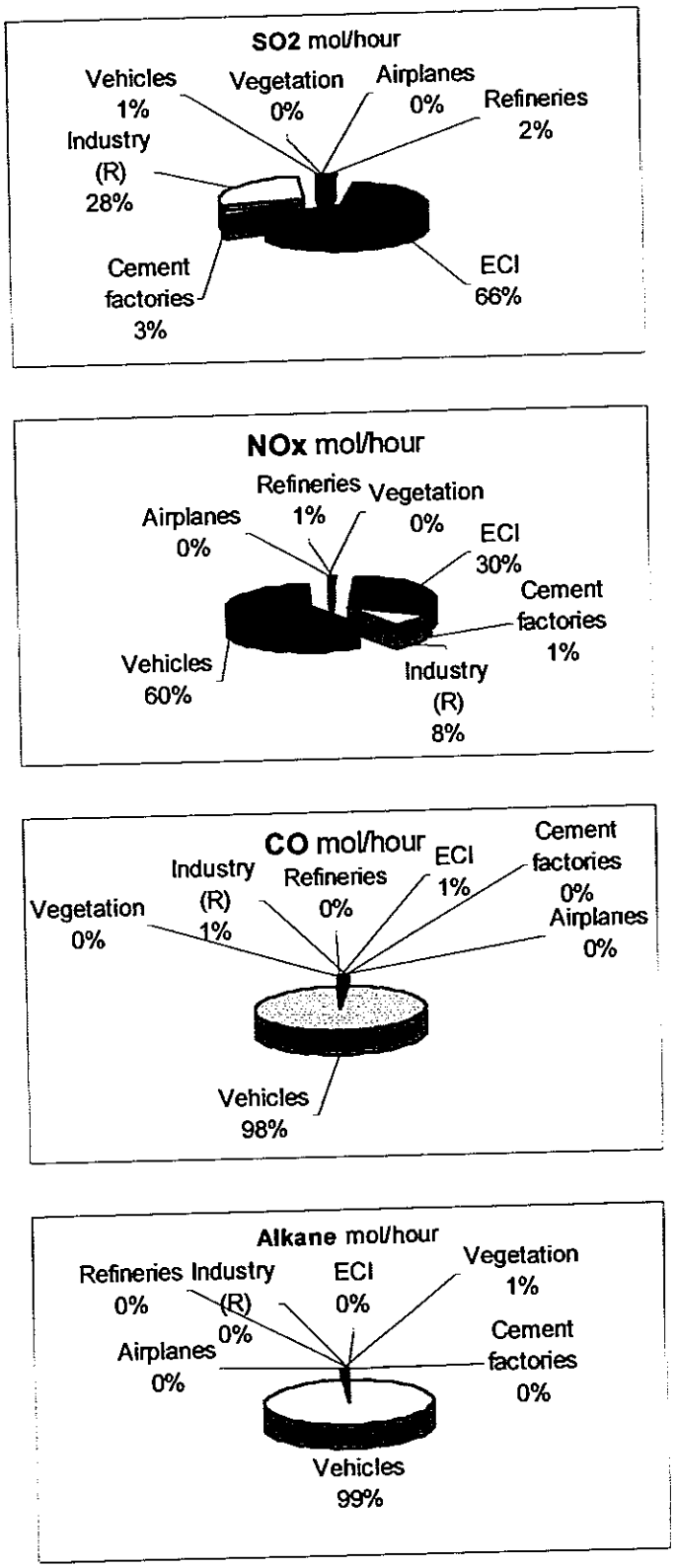


Fig. 3 - 6 (Contribution of Emission Sources to Creation of Pollutants)

# Study Area

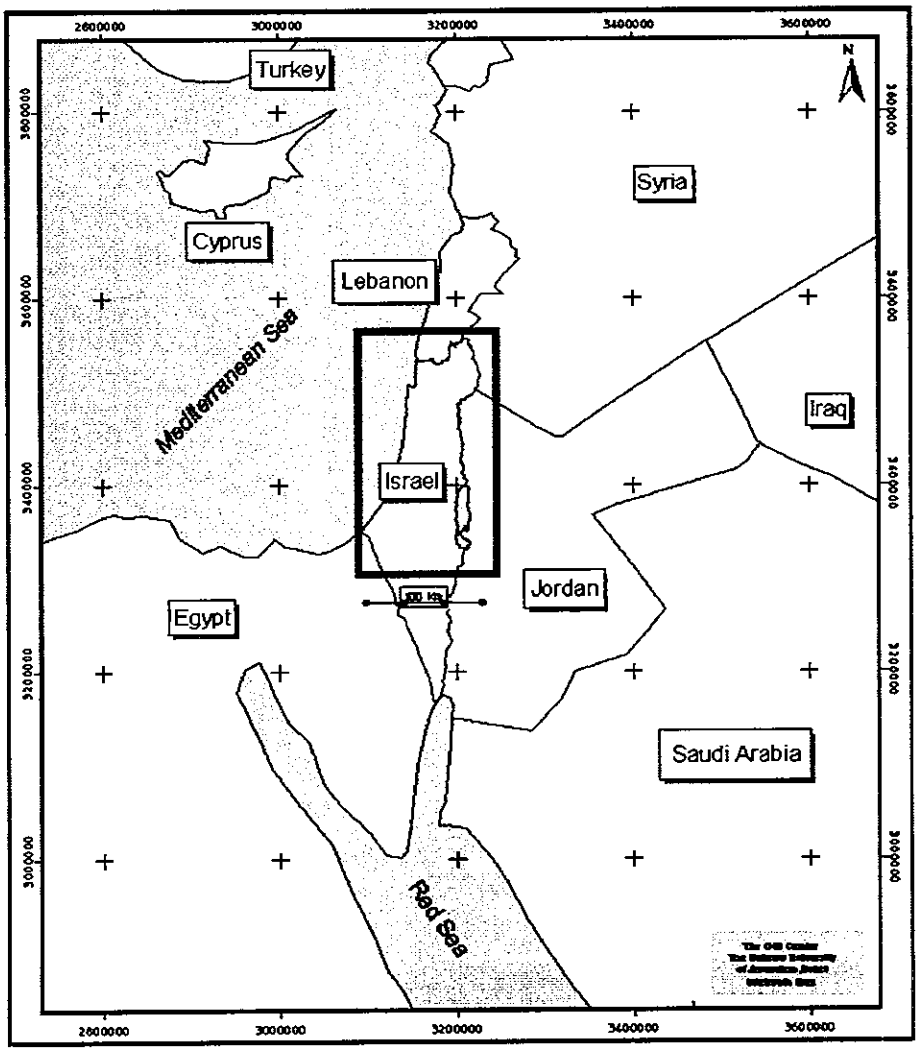


Fig. 7 (Study Area)

# Aldehydes Emission Sources Mol/hour

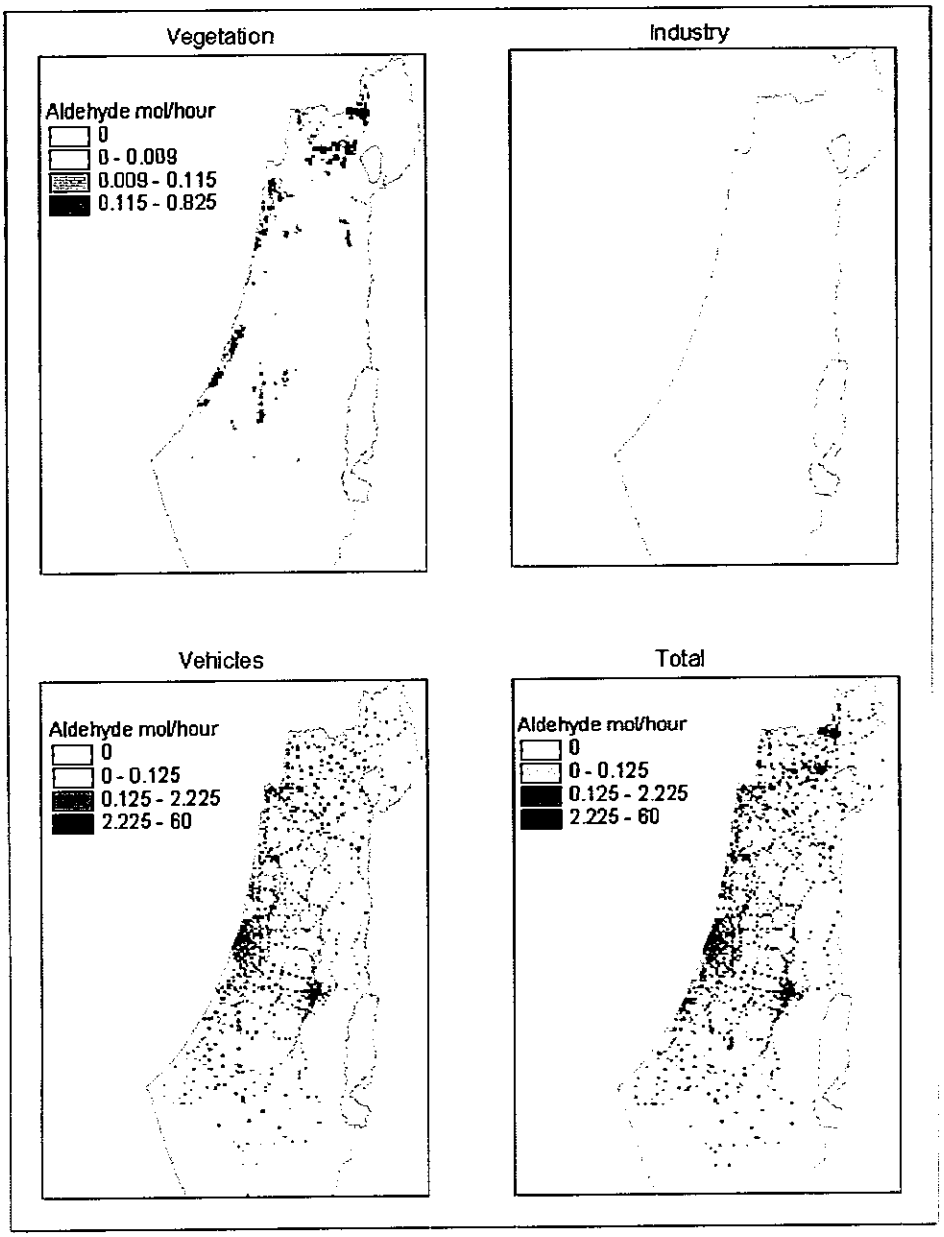


Fig. 8

# Alkanes Emission Sources Mol/hour

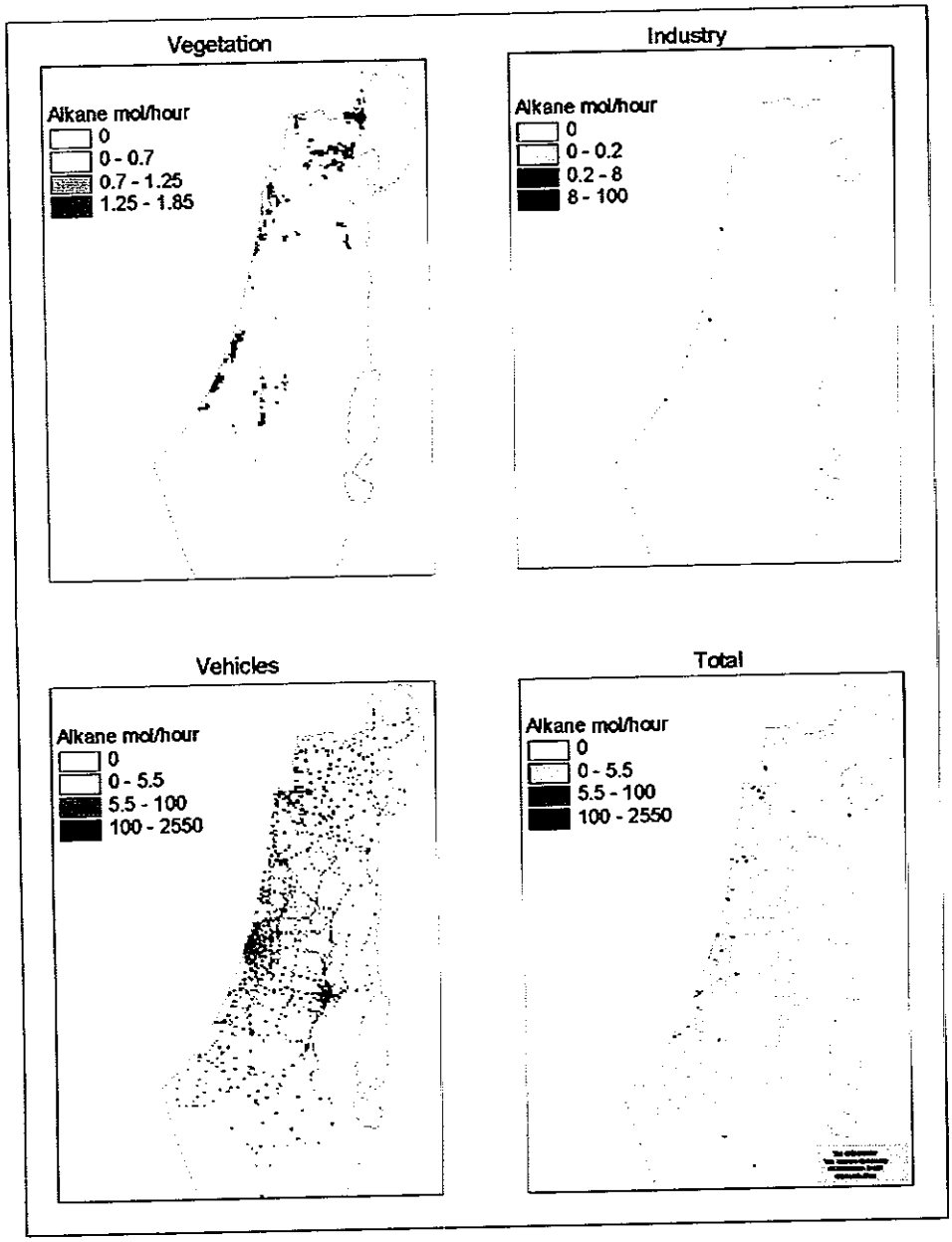


Fig. 9

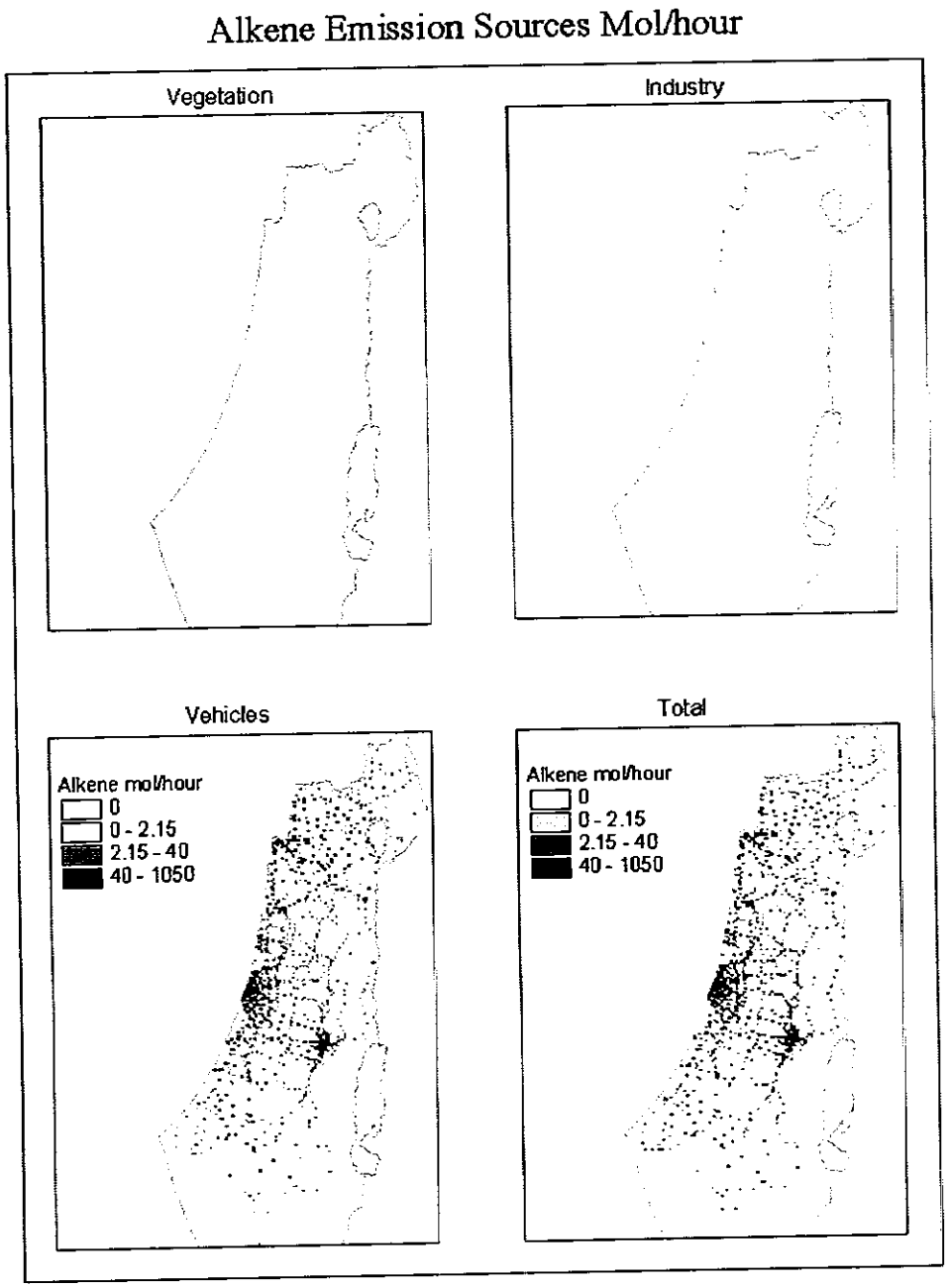
Alkene Emission Sources Mol/hour
Vegetation
Industry
Vehicles
Alkene mol/hour
0
0 - 2.15
2.15 - 40
40 - 1050
Total
Alkene mol/hour
0
0 - 2.15
2.15 - 40
40 - 1050

Fig. 10

# CO Emission Sources Mol/hour

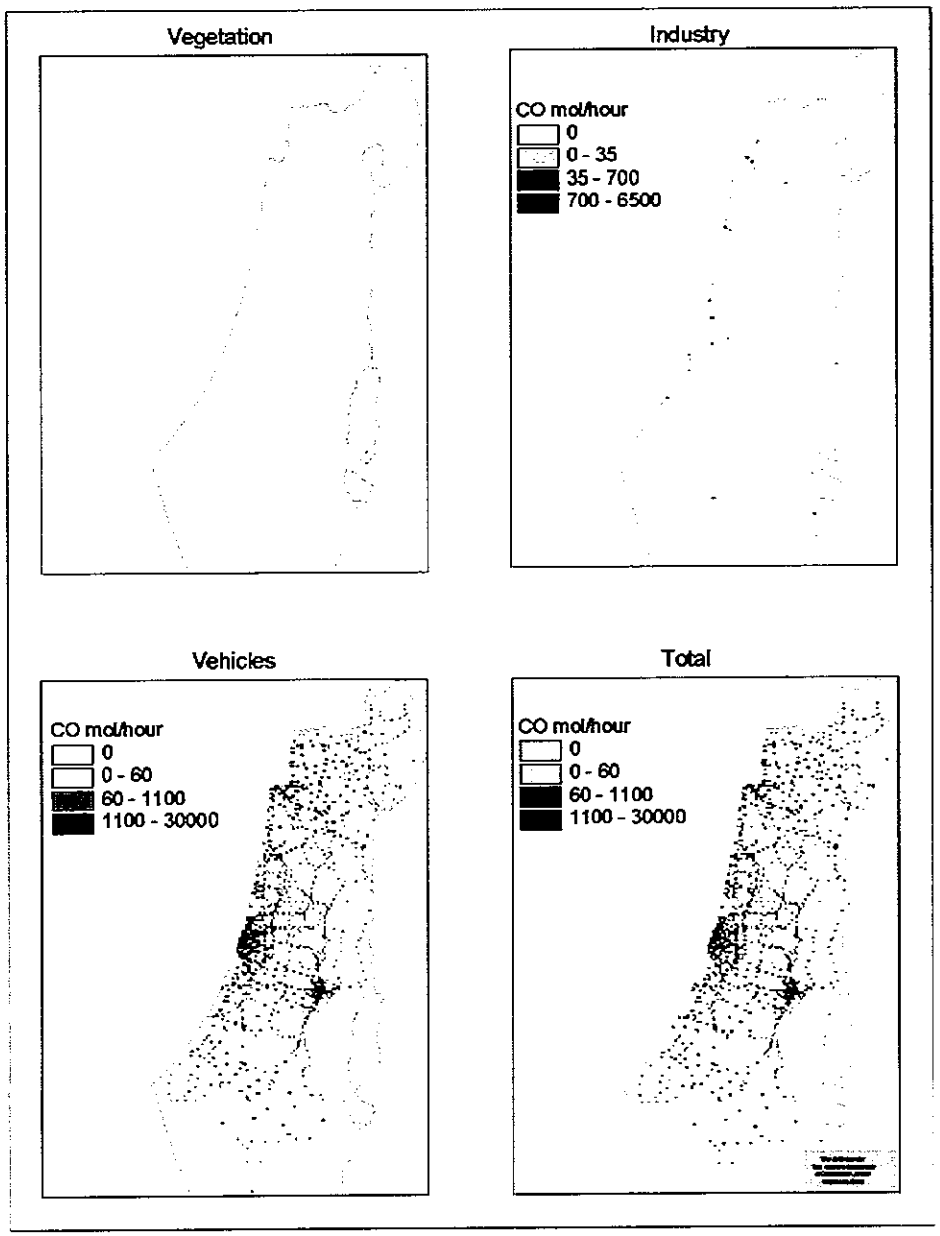


Fig. 11

# Formaldehyde Emission Sources Mol/hour

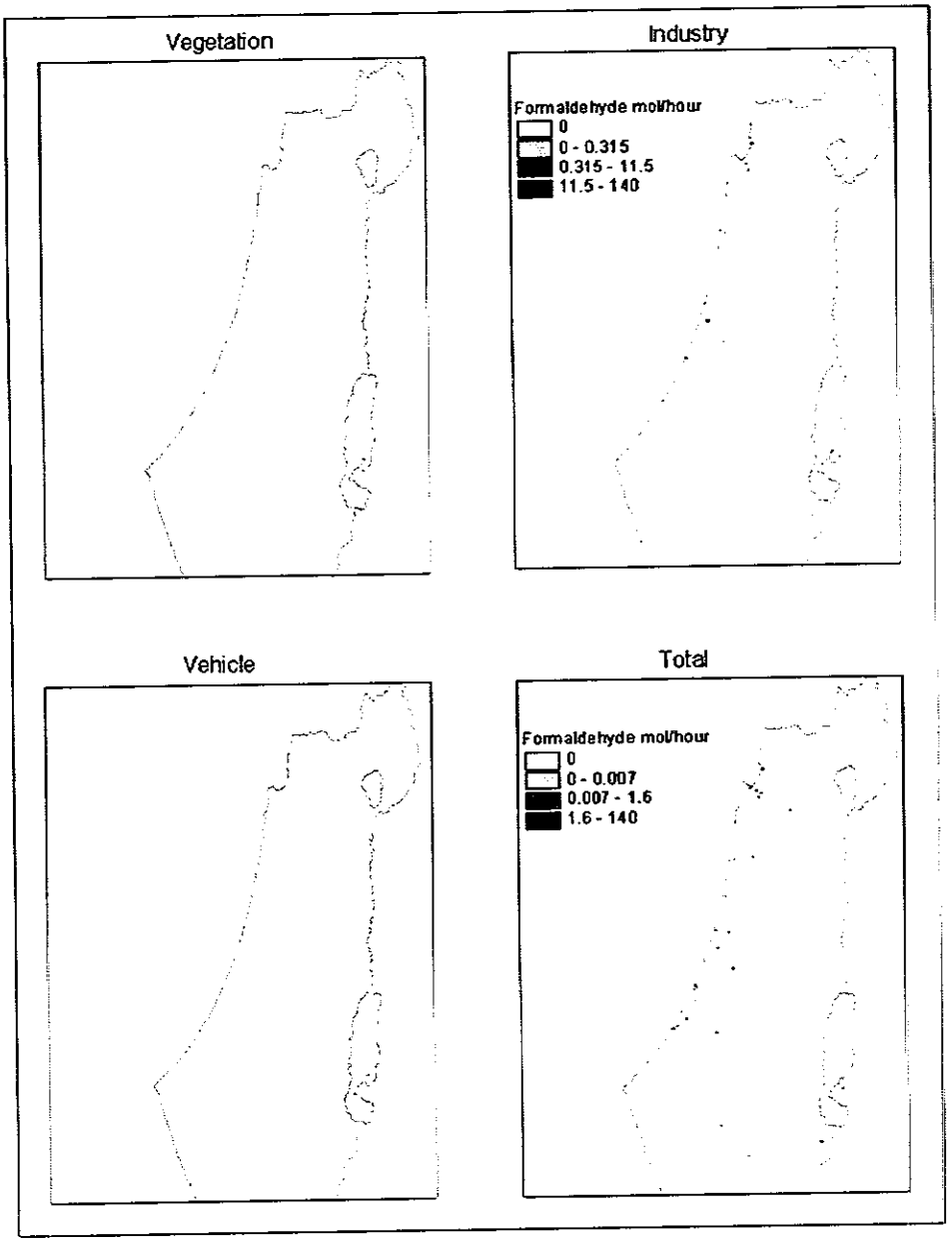


Fig. 12

# Isoprene Emission Sources Mol/hour

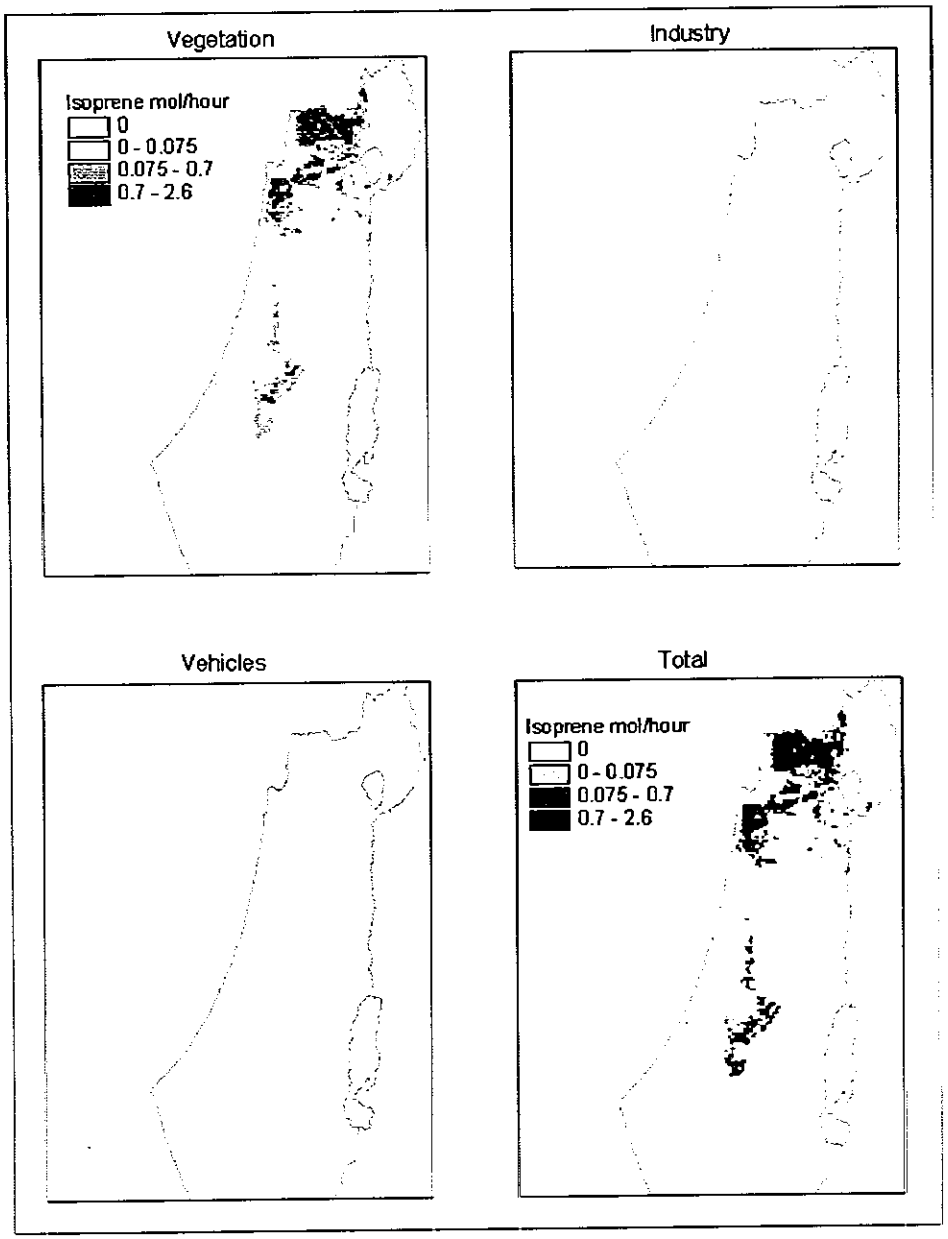


Fig. 13

# NOx Emission Sources Mol/hour

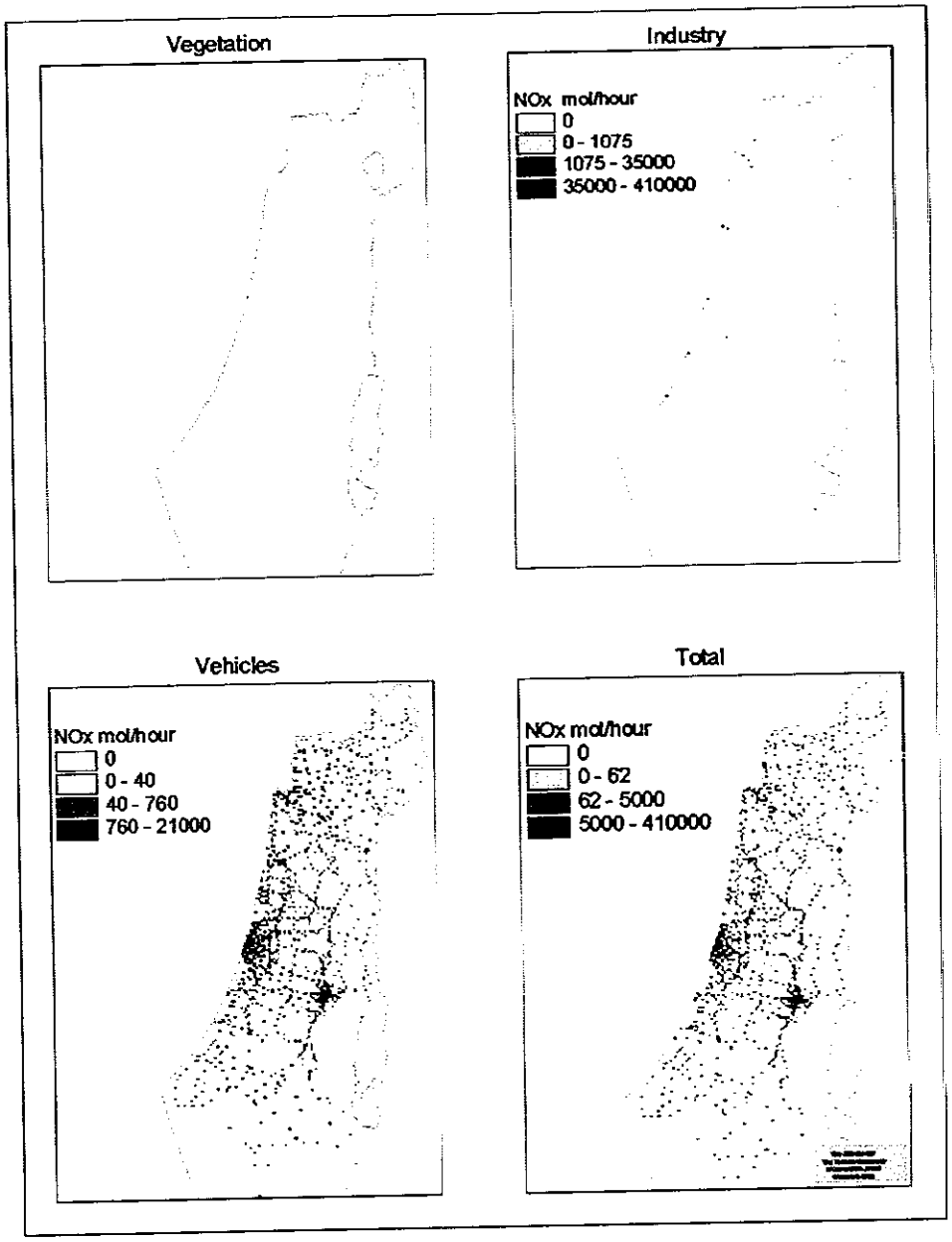


Fig. 14

Olefines Emissions Mol/hour

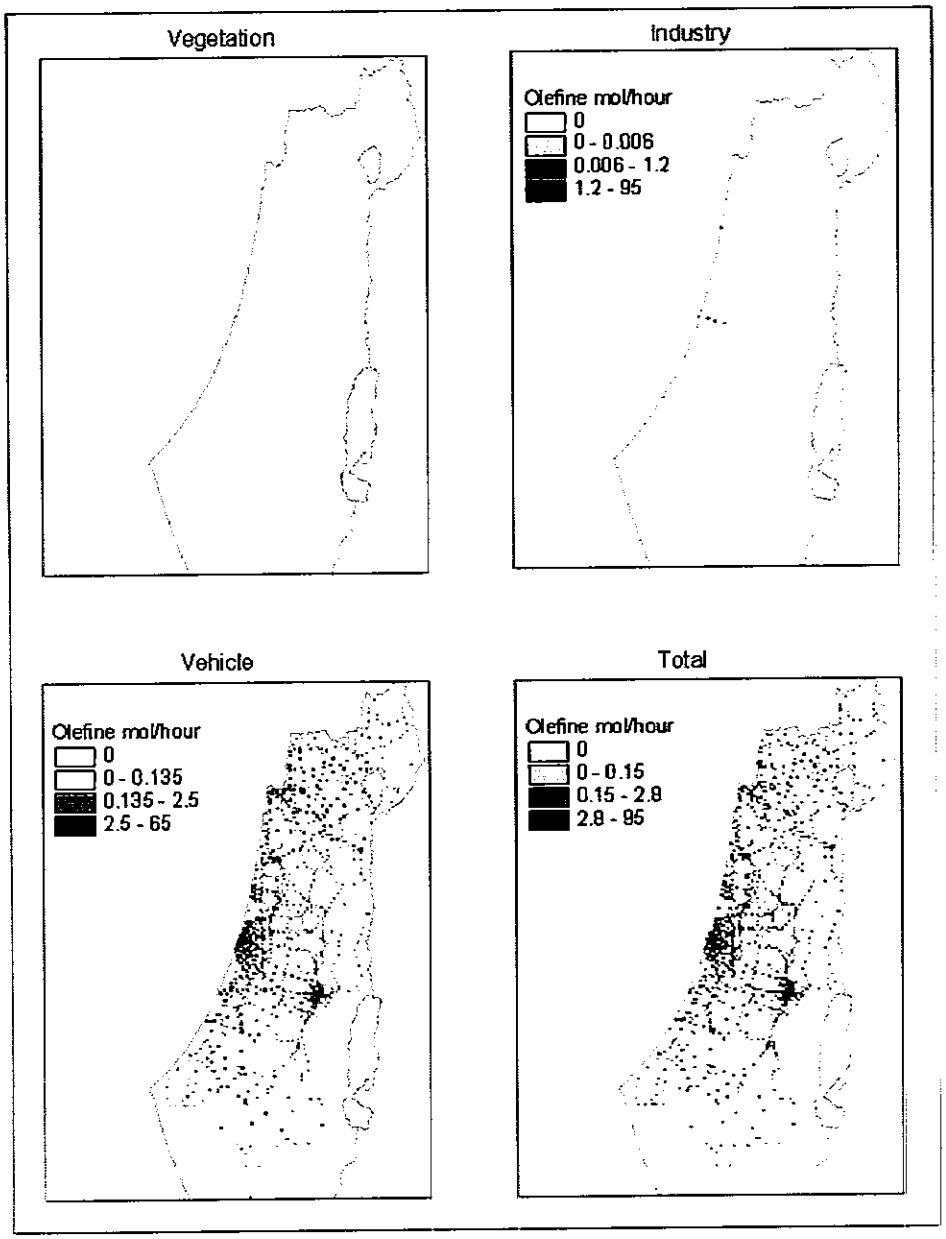


Fig. 15

SO2 Emission Sources Mol/hour

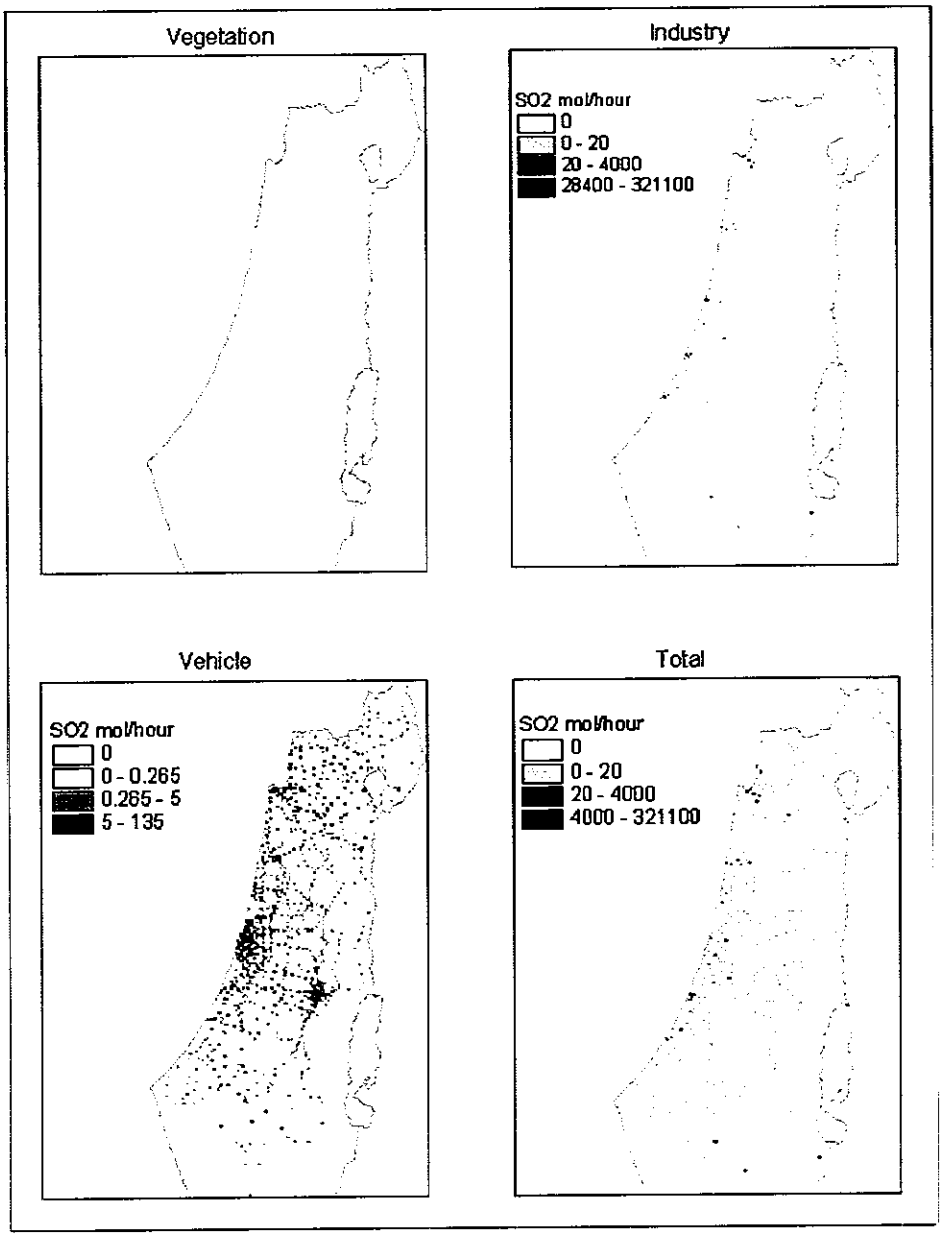


Fig. 16

# Toluenes Emission Sources Mol/hour

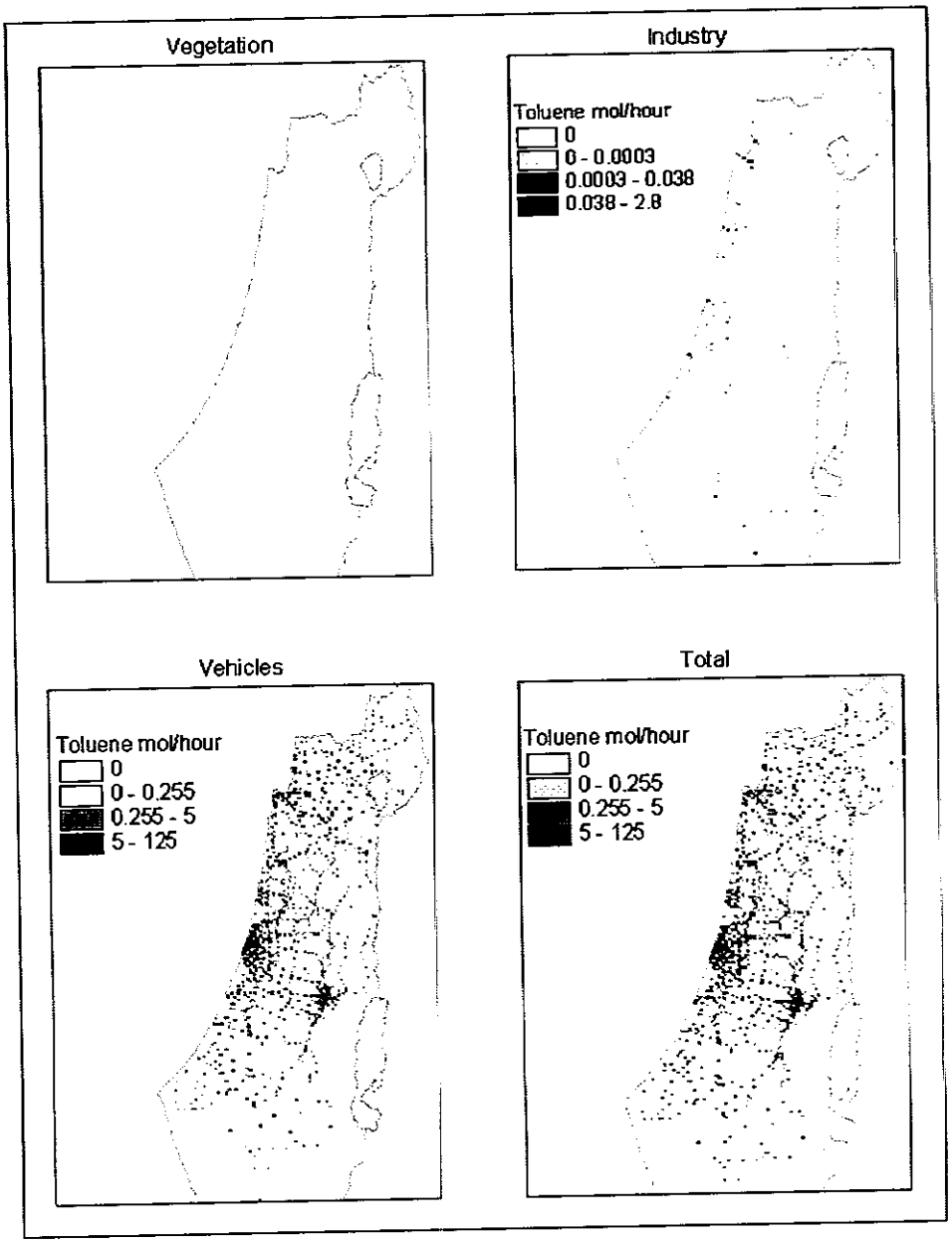


Fig. 17

# Xylenes Emission Sources Mol/hour

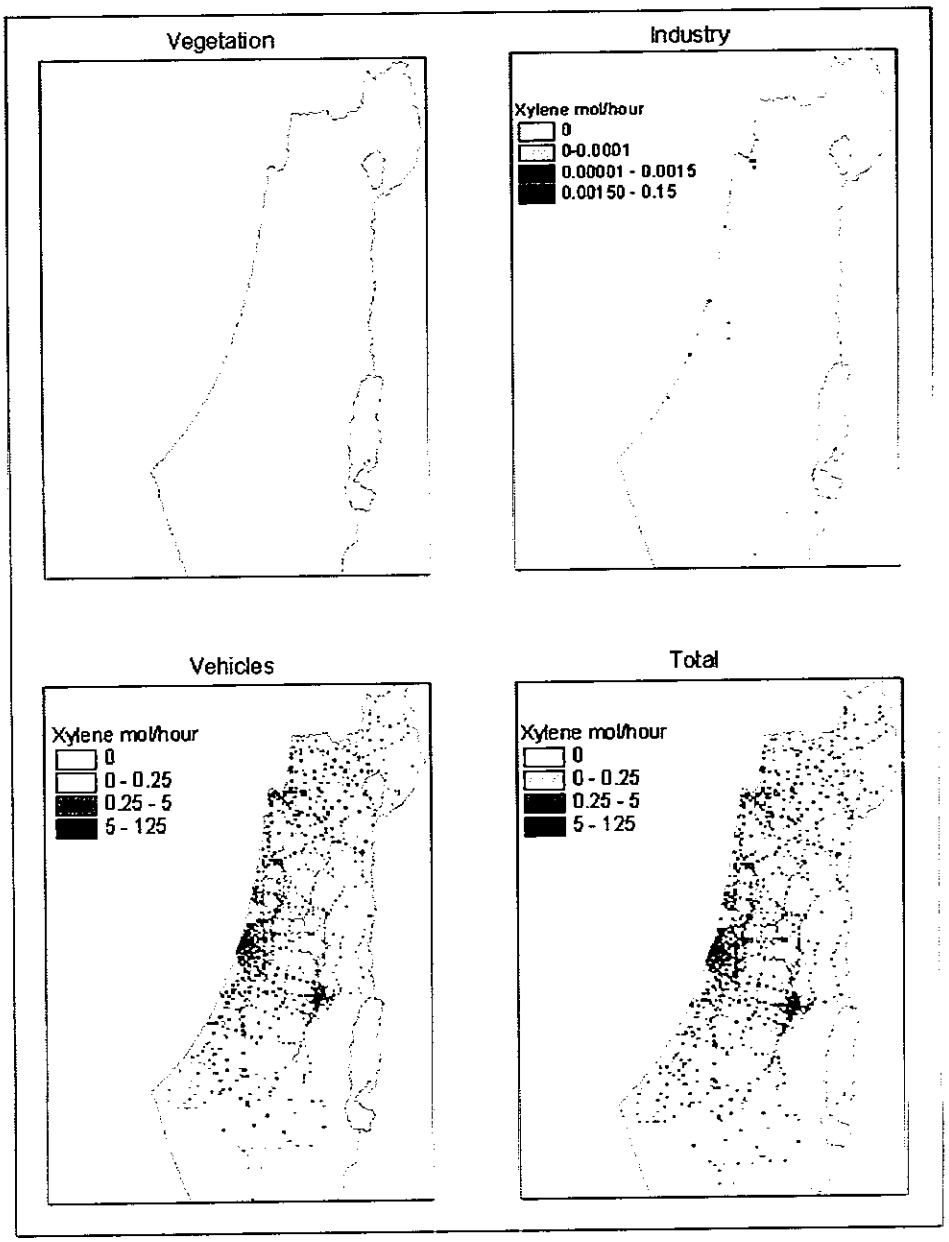


Fig. 18

# Aldehyde Emission Vehicle Sources Mol/hour

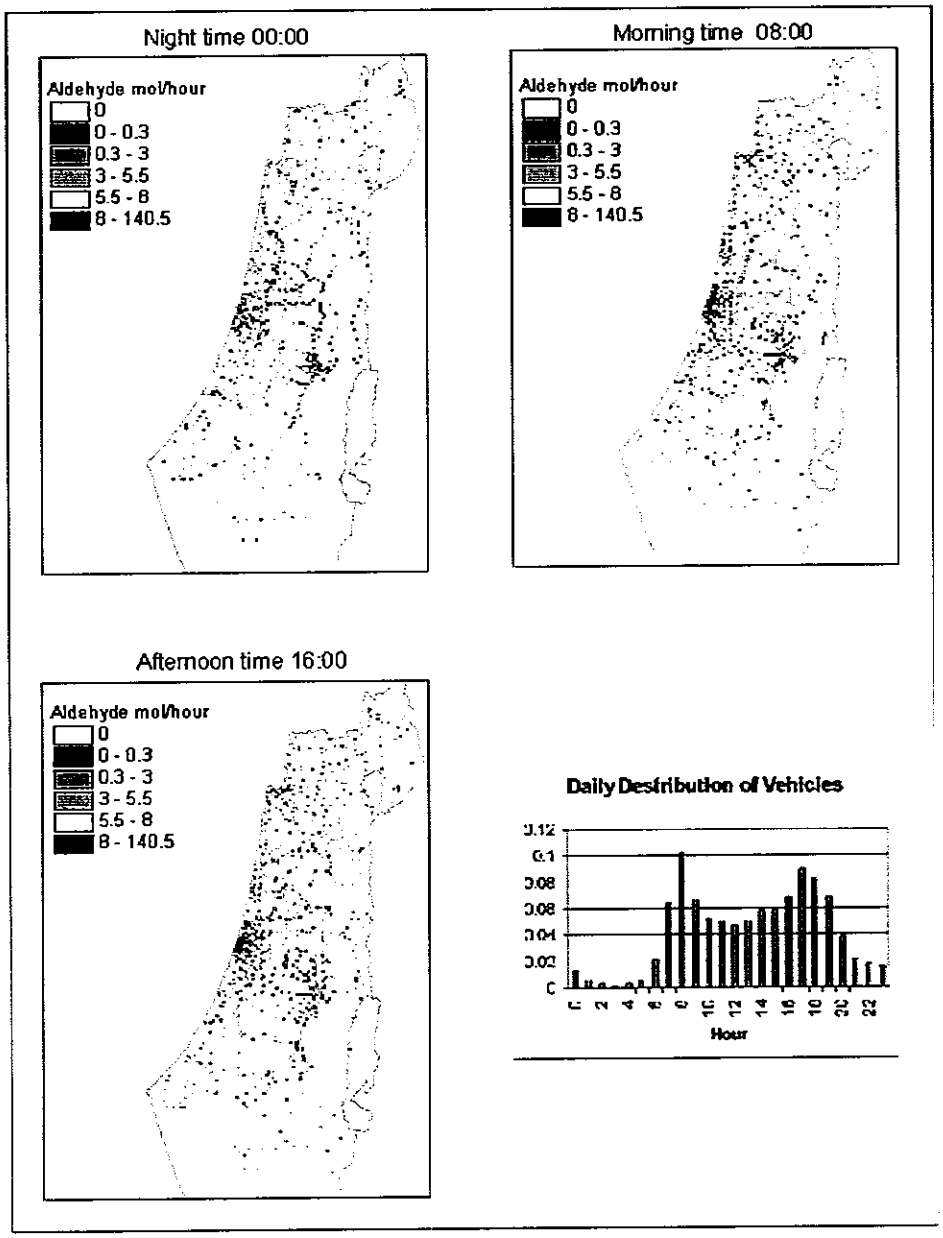


Fig. 19

# Alkane Emission Vehicle Sources Mol/hour

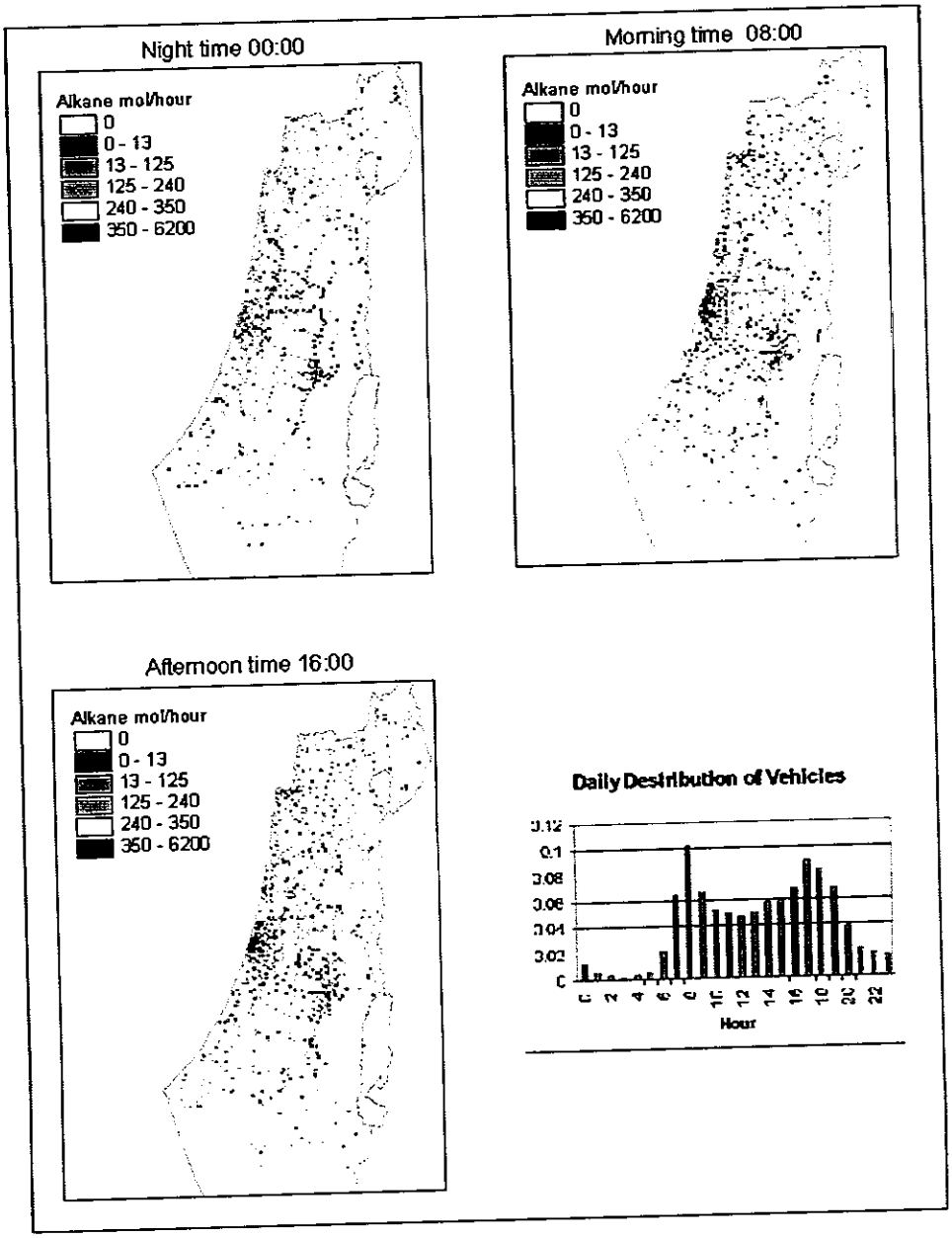


Fig. 20

# Alkene Emission Vehicle Sources Mol/hour

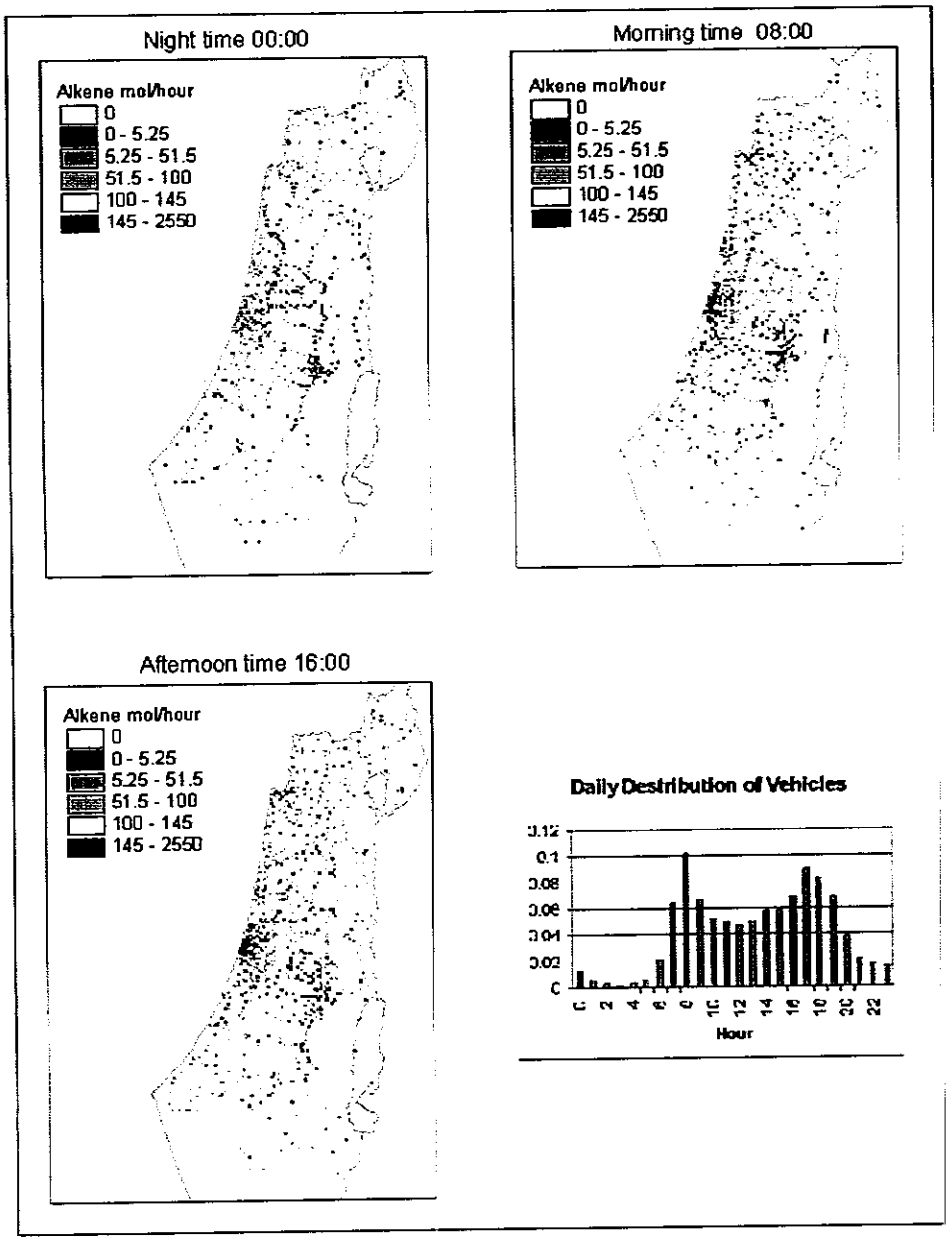


Fig. 21

# CO Emission Vehicle Sources Mol/hour

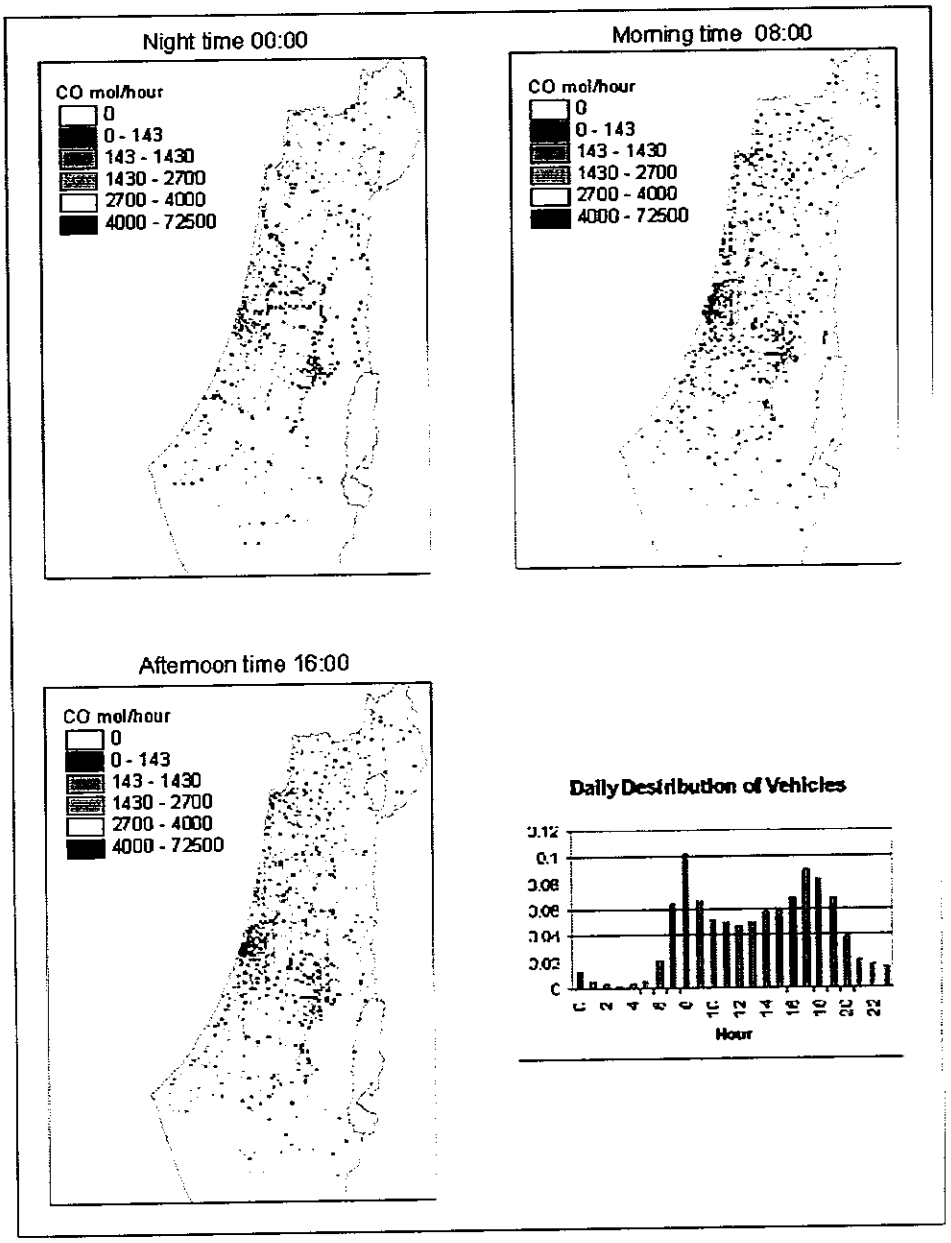


Fig. 22

# NOx Emission Vehicle Sources Mol/hour

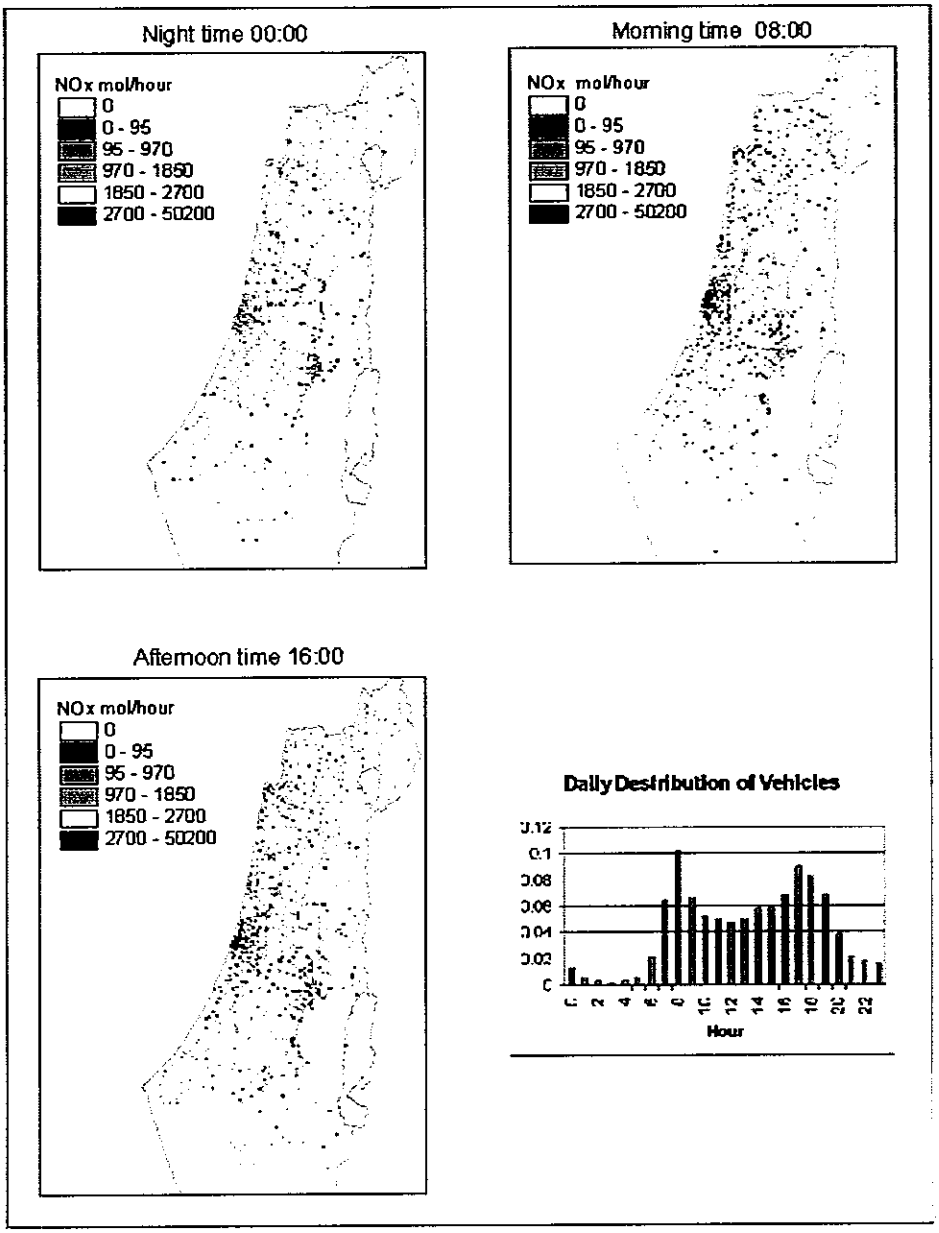


Fig. 23

# Olefine Emission Vehicle Sources Mol/hour

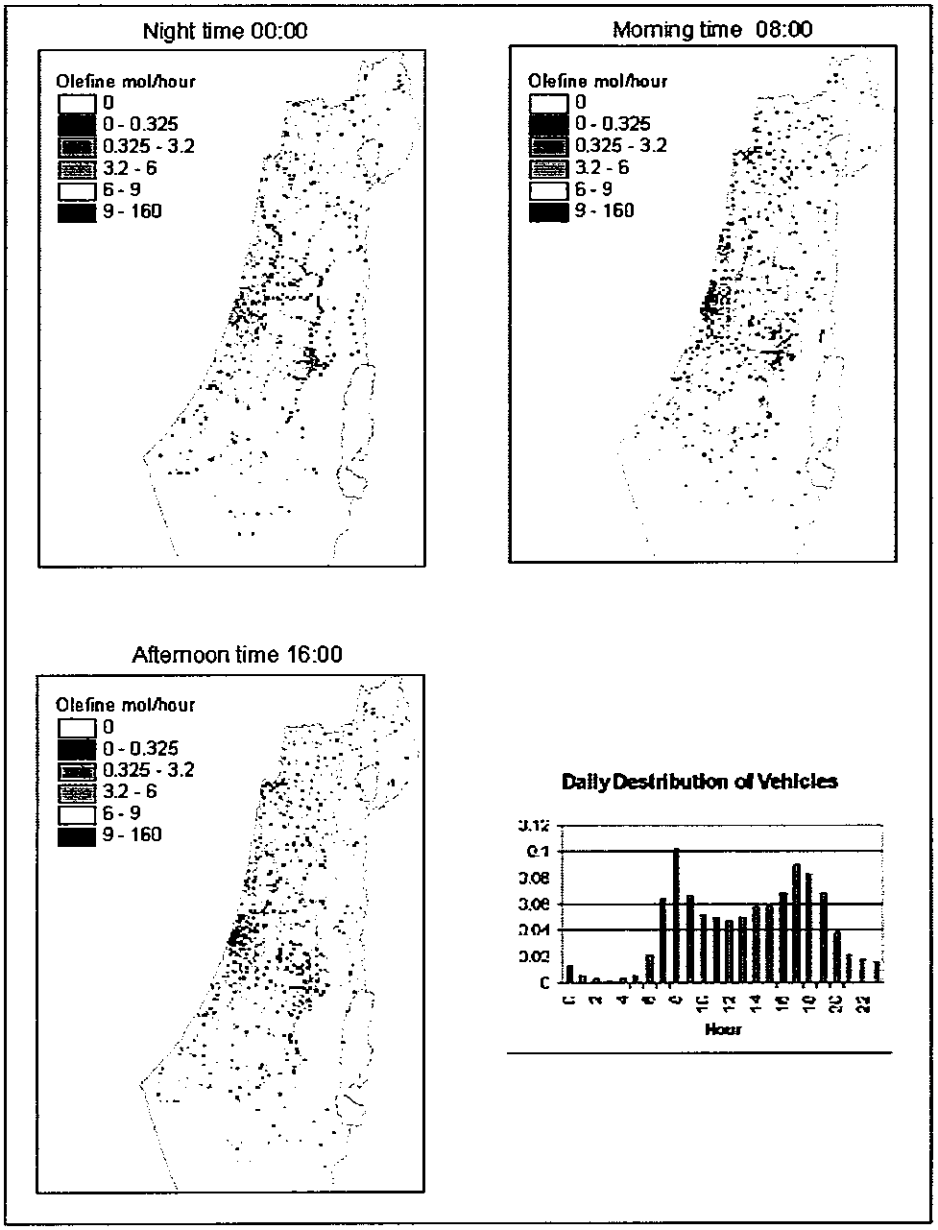


Fig. 24

# SO2 Emission Vehicle Sources Mol/hour

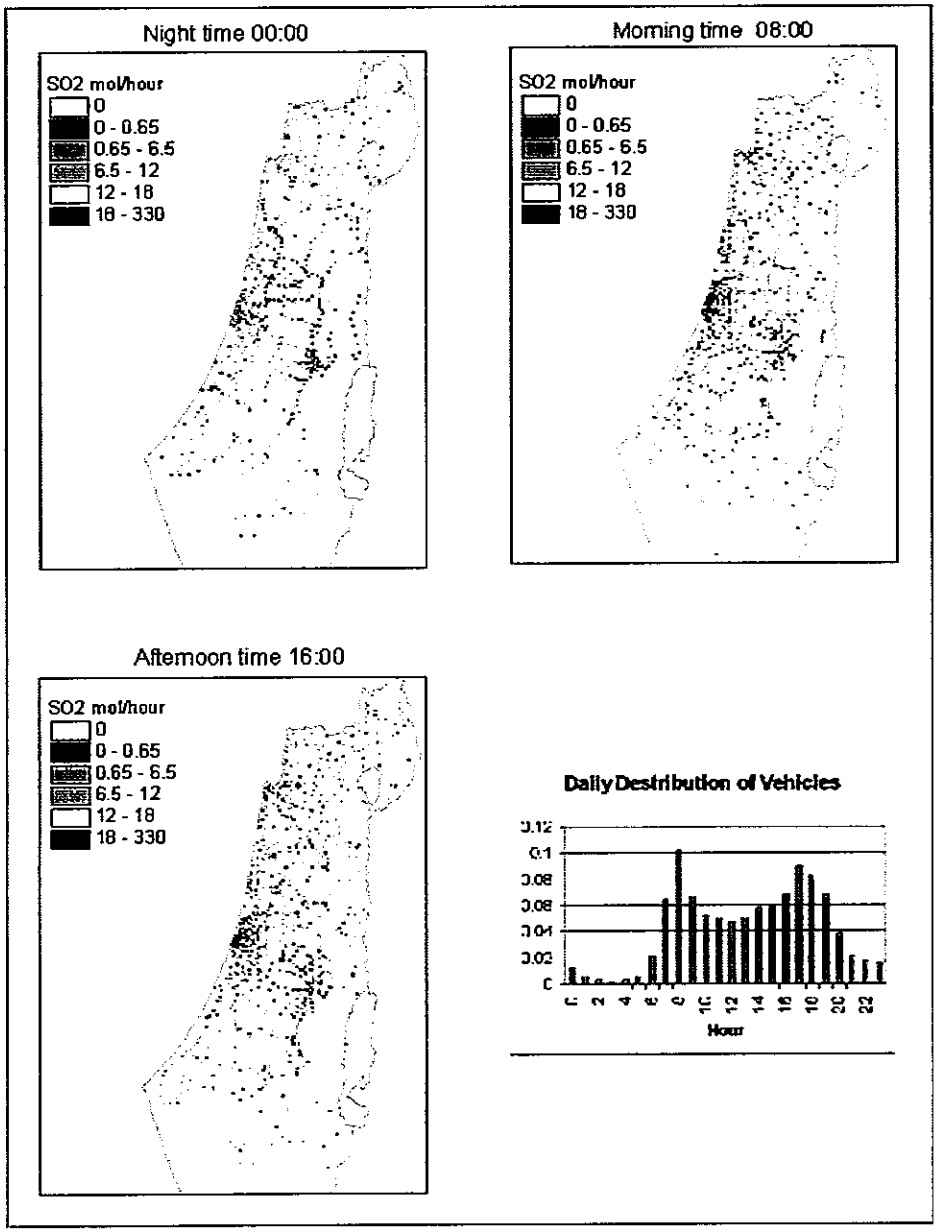


Fig. 25

# Toluene Emission Vehicle Sources Mol/hour

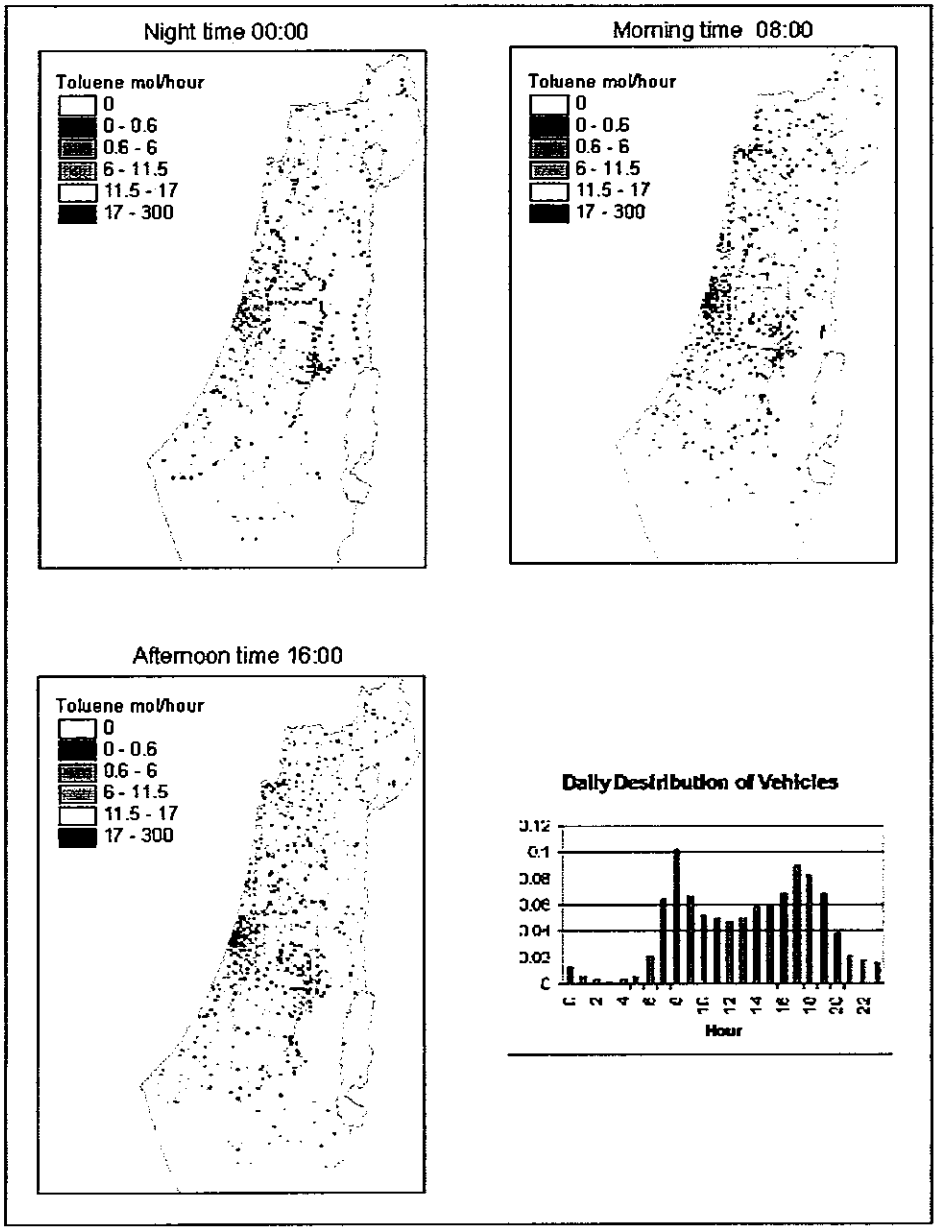


Fig. 26

# Xylene Emission Vehicle Sources Mol/hour

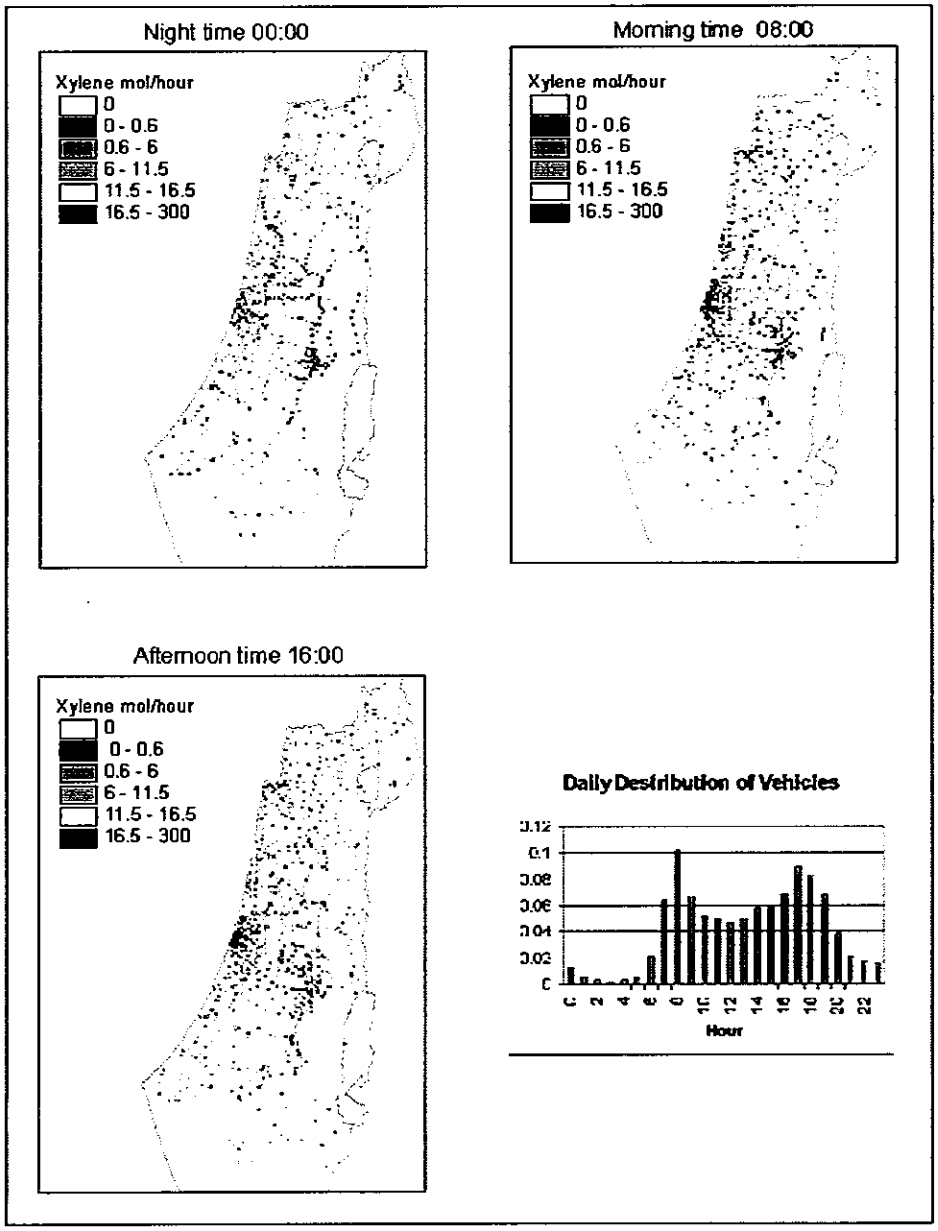


Fig. 27

## Part IV: Very preliminary RAMS and CAMx results

The current research began with the gathering of accurate emission data from various stationary and mobile sources (spatial emission inventory for Israel). These data will be input, together with the results from the execution of the RAMS dynamic atmospheric model, into a photochemical diffusion transport model (CAMx).

The Comprehensive Air quality Model with extensions (CAMx) is an Eulerian photochemical grid model that allows for integrated assessment of gaseous and particulate air-pollution over many scales, from individual point source impacts to urban-regional effects. It is designed to unify all of the technical features required of "state-of-the-science" air quality models into a single system that is computationally efficient, easy to use, and publicly available.

CAMx can directly utilize many existing photochemical modeling databases such as those developed for the Lake Michigan Ozone Study (LMOS), the Coastal Oxidant Assessment for Southeast Texas (COAST), and the Ozone Transport Assessment Group (OTAG). The model code has a highly modular and well-documented structure, which eases the insertion of new or alternate algorithms and features. CAMx simulates the emission, dispersion, and removal of inert and chemically reactive pollutants in the lower troposphere by solving the pollutant continuity equation for each chemical species on a system of nested three-dimensional grids. Once the entire model system has been run, it will be calibrated according to measurements. The final stage will be to run simulations: (1) with the various sources of air-pollution disabled so as to find their quantitative effect on Ozone and (2) to run a simulation for the year 2020.

What has been accomplished until now is to conclude the emission inventory and to run the RAMS model as pre-processor of meteorological data for the CAMx

model. Results from RAMS show the wind flow that governs the area at the time there were high ozone levels. (Figs. 1-2) When we compare potential temperature field from RAMS with real data from NCEP, good agreement was found (Figs. 3 and 4).

After preparing the output from RAMS, the CAMx model was run. The CAMX ozone results, however, did not fully comply with measurements made by an airplane at the same date (Fig. 5). The peak ozone concentration was almost at the correct strength, but it was predicted to be at different spatial location and time. The measurements showed a 122 ppb ozone concentration in the vicinity of Jerusalem and Rammhala. The modeled peak ozone of 118 ppb occurred three hours before the measured one and 30 km north of it (Figs. 5a,b versus 6).

Another problem was that predicted surface ozone concentrations were less than they should have been. It was then found that current VOC emissions were too low by a factor of four. Similar problems have been found in US emission inventory emission factors. This problem has been solved, and thus simulations of the required scenarios can proceed.

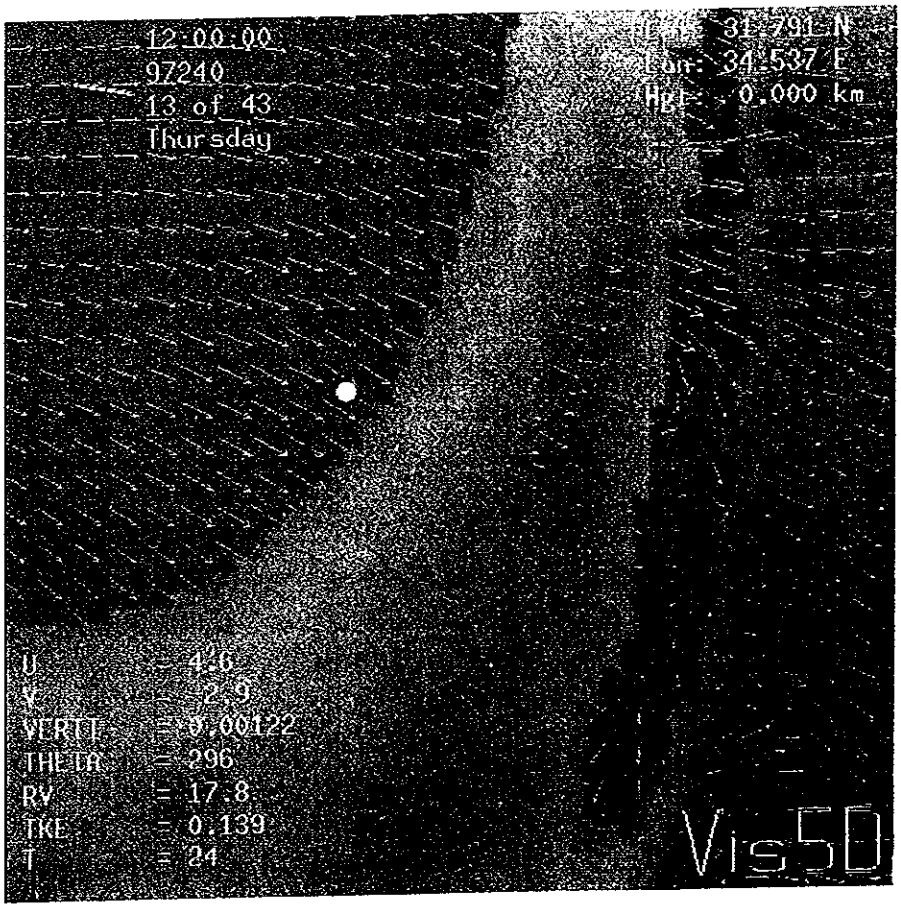


Fig. 1. RAMS surface winds at 1200 UTC on 28 August 1997. Colors represent ground level heights, while white dot represents location of data in left lower corner of figure

Fig 2. Same as Fig. 1, but for 1800 UTC.

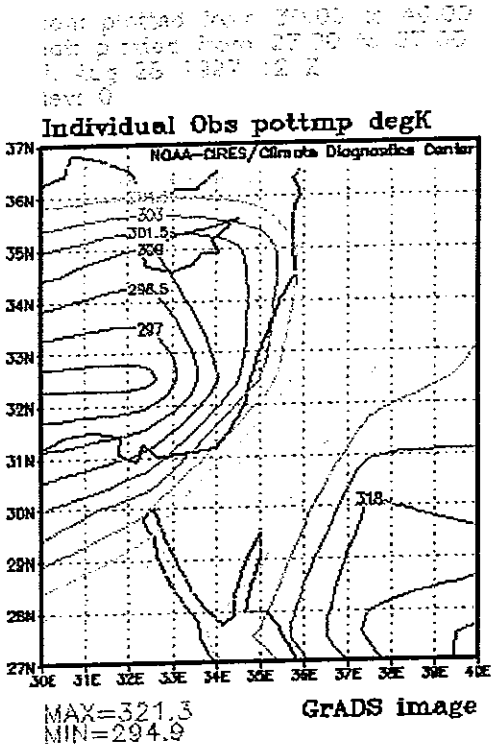


Figure 4. NCEP surface potential temperatures (K) and pressure (Pa) at 1200 UTC on 28 August 1997.

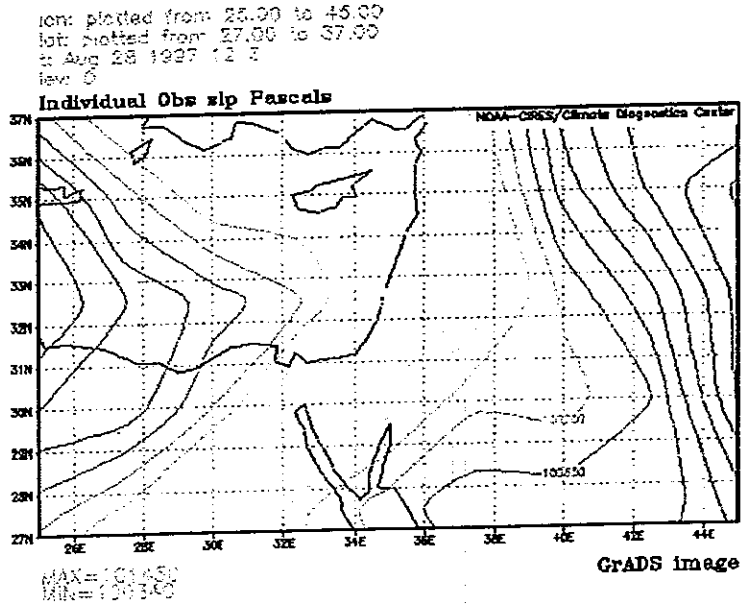

10:00
25.7.97

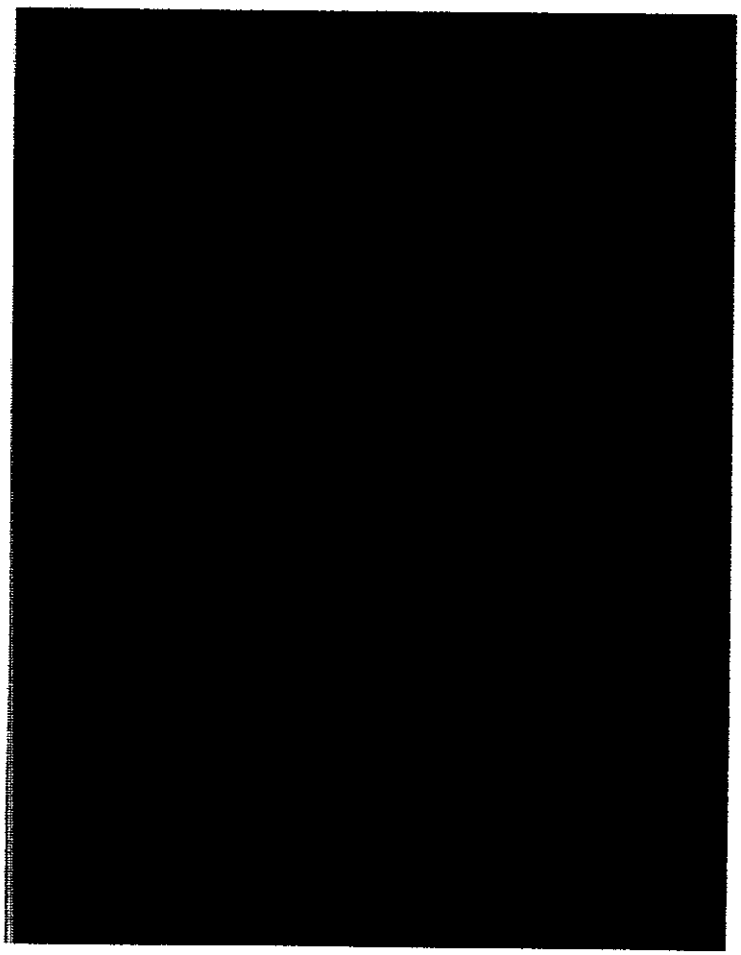

Figure 5a. CAMX ozone predictions on July 25 1997 at 1000UTC.

11:00
25/7/97

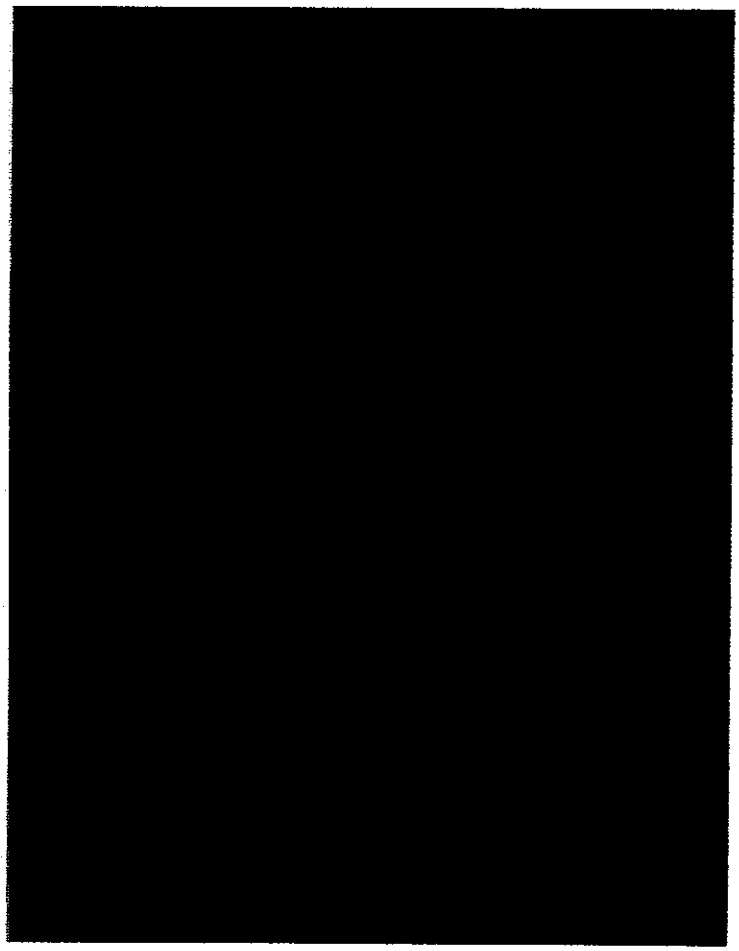

Figure 5b. CAMX ozone predictions on July 25 1997 at 1100UTC.

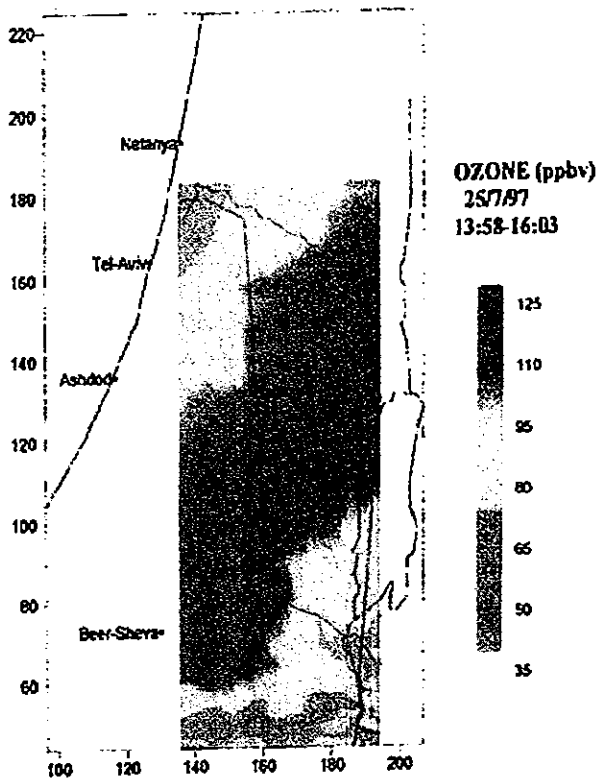


Figure 6. Observed aircraft 300 m MSL ozone (ppbV), where line is aircraft route during 1358-1603 UTC on 25 July 1997.

Appendix F: Ramar et al. (2002a,b) journal article page proofs

JOURNAL OF GEOPHYSICAL RESEARCH, VOL. 107, NO. 0, 10.1029/2001JD000808, 2002

# Impact of coastal transportation emissions on inland air pollution over Israel: Utilizing numerical simulations, airborne measurements, and synoptic analyses

D. O. Ranmar,[1] V. Matveev,[2] U. Dayan,[3] M. Peleg,[2] J. Kaplan,[3] A. W. Gertler,[4] M. Luria,[2] G. Kallos,[5] P. Katsafados,[5] and Y. Mahrer[1]

Received 3 May 2001; revised 30 October 2001; accepted 19 November 2001; published XX Month 2002.

[1] The detection of high ozone levels over large inland areas in Israel during the early, mid and late summer triggered an analysis of air mass back-trajectories. This, in turn, pointed to the transportation system in the metropolitan coastal Tel Aviv region as the possible origin of the ozone's precursors. To link the daily dynamics of rush hour transportation emissions to inland air pollution, in general, and airborne ozone measurements, in particular, an interdisciplinary modeling system was established. The simulations of transportation-to-inland air pollution integrated transportation, emission factor, atmospheric, transport/diffusion, and photochemical models. The modeling results elucidated a spatial and temporal overlap between the ozone precursors and ozone production. The model simulations indicated east to southeasterly dispersion of the pollution cloud. The results agreed well with both spatial and temporal ozone levels as recorded by aircraft over central Israel, as well as with ground-based monitoring station observations. The impact of the Tel Aviv metropolitan area as well as the Gaza Strip, as pivotal coastal transportation sources for inland air pollution in general and ozone formation in particular, is discussed. The synoptic analysis identified the conditions prevailing when elevated air pollution, and especially high ozone levels, exists over central Israel. The analysis showed that this season features a shallow mixed layer and weak zonal flow, which leads to poor ventilation rates and inhibit efficient dispersion of this secondary pollutant. These poor ventilation rates result in the slow transport of ozone precursors, enabling their photochemical transformation under intense solar radiation during their travel from the coast inland. Under these conditions, model results showed that traffic emissions during the morning rush hour from the Tel Aviv metropolitan area contribute about 60% to the observed ozone concentrations. *INDEX TERMS:* 0345 Atmospheric Composition and Structure: Pollution—urban and regional (0305); *KEYWORDS:* air pollution, numerical atmospheric modeling, transportation model, emission factors, photochemical model, ozone, photochemical aged air mass

## 1. Introduction

[2] Elevated ozone levels, above the Israeli ambient standards, were observed at inland rural sites during the early summer months of 1988 to 1991 [*Peleg et al.*, 1994]. Air mass back-trajectory analyses have shown that only air masses passing over the Tel Aviv metropolitan area caused the elevated ozone mixing ratios at rural sites over central Israel. Furthermore, the high ratio of $NO_x/SO_2$ patently indicates that ozone precursors such as nitrogen oxides ($NO_x$), carbon monoxide (CO), and volatile organic compounds (VOC) originate mainly from traffic fossil-fuel combustion ($NO_x$ represents the sum of NO and $NO_2$). These pollutants undergo chemical and photochemical transformations in the presence of solar radiation and atmospheric free radicals [*Finlayson-Pitts and Pitts*, 1997; *Seinfeld and Pandis*, 1998] to form ozone. The main source for the ozone precursors emitted along the Israeli coastline is transportation [*Peleg et al.*, 1994]. Since the formation of ozone and other secondary pollutants takes on the order of several hours, significant transport and mixing occurs simultaneously with the chemical reactions [*Kley*, 1997; *Seinfeld*, 1989]. Thus increasing urban and commercial activity along the highly populated Israeli coastal region, together with expanding transportation activity in the Gaza region, is expected to strongly affect inland air quality and specifically, to cause increasingly elevated ozone levels.

[1]Department of Soil and Water Sciences, Faculty of Agricultural, Food and Environmental Quality Sciences, Hebrew University of Jerusalem, Rehovot, Israel.
[2]Environmental Science Division, School of Applied Sciences and Technology, Hebrew University of Jerusalem, Jerusalem, Israel.
[3]Department of Geography, Hebrew University of Jerusalem, Jerusalem, Israel.
[4]Desert Research Institute, Reno, Nevada, USA.
[5]Laboratory of Meteorology, University of Athens, Athens, Greece.

Copyright 2002 by the American Geophysical Union.
0148-0227/02/2001JD000808$09.00



267

[3] The effects of vehicular transport emissions have prompted studies in various disciplines, including the following: particulate composition of the atmosphere [*Fraser et al.*, 1999; *Staehelin et al.*, 1998], potential mutagenic activity [*Kleindienst et al.*, 1992], the mode of city air pollution exposure from proximal highways [*Roorda-Knape et al.*, 1998] and as an integrated component in local-scale air pollution modeling [*Pilinis et al.*, 1993; *Moussiopoulos and Papagrigoriou*, 1997; *Silibello et al.*, 1998; *Svensson*, 1998], to name a few. In the latter studies, photochemical grid models were applied to the cities of Athens and Milan to address their regularly recurring air quality problems. These simulations incorporated traffic emissions, together with other metropolitan emitters, as a source of the precursors feeding the simulated atmospheric photochemistry. In these cases, the emission area and the polluted atmosphere overlap spatially, forming what may be viewed as a "self-pollution" phenomenon, where the city is captured as the origin of primary pollutant emissions, and its overlaying atmosphere as the "destination" for their subsequent photochemical transformation products. The involvement of major coastal metropolitan areas in inland ozone pollution was studied in regions such as the San Joaquin Valley in California [*Dabdub et al.*, 1999] and the Los Angeles Basin [*Lu and Turco*, 1996]. The former study addressed the differential impact of boundary conditions, winds, emissions, and $NO_x$/VOC sensitivity on the nature of ozone formation, with the San Francisco metropolitan area as one of the model-input pollution sources. It showed that significant inflow into the San Joaquin Valley imposes a strong dependency on the boundary concentration of pollutants and revealed the region as $NO_x$-sensitive, i.e., a dependency of ozone formation on incoming $NO_x$ and internally emitted $NO_x$ greater than that on VOC influx and emission. The latter work simulated ozone distribution over the Los Angeles Basin, revealing the association of the vertical circulation with sea breeze/mountain winds in the injection process of pollutants into the base of the inversion layer. The elevated reservoir of trapped photochemically aged pollutants may then mix downward to increase surface ozone concentration. Such a mechanism was speculated to take place in Israel, based on the similarities in geography and climate [*Dayan and Koch*, 1996]. These authors analyzed measurements of the Southern California Air Quality Study (SCAQS) and suggested a possible analogy between the build-up mechanism of inland surface ozone in Israel and the mechanism existing in southern California, due to the similarities between these regions (Mediterranean climate, sea breeze, and terrain features).

[4] The present study addresses the dynamics of transboundary air pollution, where the transportation emissions (such as $NO_x$ and VOC) originating from major coastal sources impact the inland mixing layer. The research aimed to resolve the daily influence of rush-hour traffic emissions from these coastal locations on the neighboring inland areas. In this study, we focus on the transportation sources in the Tel Aviv metropolitan and Gaza Strip areas, the main coastal urban areas in the conjugated Israel-Palestinian Authority region. This study includes numerical simulations, their spatial and temporal correlation with airborne-measured ozone from 1994 to 1997, and complementary ground-based measurements performed from June to September of 1999 and 2000.

[5] Since almost no data are available in Israel regarding actual vehicle pollution emission rates, the present study includes measurements performed using the so-called "tunnel technique". This method gives "real-world" emission rates for the composite vehicle fleet operating on Israeli roads that can be used as input for the transportation model. The data available from aircraft research measurement flights were employed in order to verify the model simulation studies.

## 2. Modeling Systems

[6] Targeting the daily impact of the traffic infrastructure on subsequent spatial and temporal inland air pollution in general and ozone location in particular called for utilizing an integrated interdisciplinary modeling system covering the fields of transportation densities, emission factors, atmospheric dynamics, pollutant transport and diffusion, and photochemistry. For the purpose of this study, the following models were selected: a transportation model (Emme/2, pronounced em-two, named after the French letter "emme" for mobility model) coupled to the emission factor model (EFM), the regional atmospheric modeling system (RAMS) and a transport and diffusion model (TDM). A photochemical module is addressed through a multiple-regression analysis, which found a correlation between ozone mixing ratios, $NO_y$ levels and air temperature [*Olszyna et al.*, 1994, 1997] in photochemically aged air masses typical of the region under study [*Peleg et al.*, 1994]. The following subsections address the different modules of the modeling system (2.1–2.5) and provide a brief description of the ground-based measurements (2.6) used in present study.

### 2.1. Transportation Model

[7] The Emme/2 urban/regional transportation system model [*INRO Consultants Inc.*, 1998, and references therein, available at http://www.inro.ca] was used to analyze the combination of present transport flow dynamics and land use scenarios, and future conditions regarding transportation system performance. The urban/regional transportation planning and modeling system assesses the balance between travel demand (based on land use) and supply (based on transport facilities) under given scenarios. Land uses are aggregated into analysis zones (such as census tracts), which provide the basis for estimating a matrix of trip origins and destinations. Networks to which the analysis zones are connected represent transport facilities, where each link of the network is characterized in terms of its capacity and speed components. The modeling process produces the desired origin-destination matrices of trips by type of trip, mode of travel and time of day, as well as transport network data which depict the volumes of vehicles and passengers by road segment, travel speed, travel time, and delay time. The traffic flow density (TFD) per hour for each road segment is obtained by multiplying the number of vehicles by the length of the road.

### 2.2. Emission Factor Model

[8] Real world vehicular emission factors for Israel were required to feed the simulation model with the relevant pollution rates. Since almost no data are available for the Israeli scenario, it was necessary to obtain new experimental

measurements. The "tunnel technique" (see experimental section) was employed to enable the calculation of vehicle pollutant emission rate. These rates will represent the accurate makeup (light and heavy-duty mix, percent with catalytic converters, etc) of the vehicles traveling on the Israeli road system.

### 2.3. Atmospheric Modeling

[9] The regional atmospheric modeling system (RAMS) adopted in this study is a state-of-the-art, well-documented mesoscale atmospheric model [*Pielke et al.*, 1992; *Walko et al.*, 1995]. In brief, the RAMS is a multipurpose 3-D versatile numerical prediction model designed to simulate weather systems by calculating multiple meteorological fields (primarily wind, temperature, pressure, and humidity, constructed around the full set of equations in a terrain-following coordinates system, which governs atmospheric motions). The equations are supplemented with optional parameterizations for turbulence, radiation, thermodynamics, clouds, soil type and vegetation. The RAMS is equipped with a multiple grid-nesting scheme that allows a two-way interaction between computational grids of different 3-D resolution. In the current simulation, the RAMS was executed in hierarchical, three-level nested grids to allow zooming in from synoptic scale phenomena through the mesoscale dynamics to the highly resolved local systems. The telescoping from large-scale environment, low-resolution grid cells to small-scale atmospheric systems with fine-meshed, high-resolution grid cells enables small-scale atmospheric features of the target area to be taken into account while simultaneously providing the impact of much larger meteorological systems.

### 2.4. Transport Diffusion Simulation

[10] The transport and diffusion model (TDM) is based on the work of *Hurley and Physick* [1991], and *Physick and Abbs* [1991]. It is a Lagrangian 3-D model that simulates the motion of atmospheric pollutants under the influence of atmospheric flow. The TDM was applied to a high-resolution grid with a vertical grid resolution of 50 m and up to a height of 2 km. The TDM was initiated and driven by the meteorological fields produced by the RAMS and interpolated in time and space to the location of the pollutant elements. The coupled Emme/2-emission model provided the TDM with the following transportation data (the anthropogenic driving force): (1) the number of traffic sources, (2) traffic source locations, (3) the emission rates of $NO_x$ and VOC.

### 2.5. Photochemical Calculation

[11] Quantitative estimation of inland ozone mixing ratios in photochemically aged air masses was established by incorporating a multivariate linear regression analysis [*Olszyna et al.*, 1997] into the TDM model:

$$[O_3] = 9.33 \times [NO_y(\text{ppbv})] + 2.42[\text{Temperature}(^\circ\text{C})] - 28.18$$

Here, $NO_y$ is the sum of all nitrogen oxide species, excluding $N_2O$. Results from measurements performed at a rural inland site in Israel [*Peleg et al.*, 1994] have shown that the above equation is also suitable for use in the present study. The application of this equation under the aforementioned conditions enabled the quantification of ozone formation in our cases. This assumption is based on the fundamental correlation found to exist between $NO_y$ concentration and the ozone mixing ratio in photochemically aged, $NO_x$-limited regimes [*Trainer et al.*, 1993; *Olszyna et al.*, 1994, 1997].

[12] The linear multiple regression model was sequentially operated after each dispersive time step to account for the newly formed ozone. The use of statistical modeling to estimate photochemical production of ozone via association of ozone concentration with meteorological and chemical variables has the advantages of simplicity and a negligible computation time compared to heavy-duty photochemical solvers. Furthermore, the method does not require the differential concentrations of the species participating in the chemical reactions used to initialize and propagate a photochemical model.

## 3. Experimental Design

[13] A detailed description of the research flight, tunnel measurements, and ground level observations is provided in the following subsections.

### 3.1. Research Flights

[14] Research flights were performed over Israel to determine the areas affected hy elevated ozone and $NO_y$ levels and thus to calibrate and test the accuracy of the simulation model. The aircraft used in the investigation was a single-engine Cessna 192. The aircraft was equipped with a high-sensitivity $SO_2$ analyzer (TEII 43S, pulsed fluorescence method, ±0.1 ppbv sensitivity), a high-sensitivity NO-$NO_y$ analyzer (TEII 42S, chemiluminescence method, ±0.1 ppbv sensitivity), and an ozone monitor (Dasibi 1008 AH, UV photometric method, ±2 ppbv sensitivity). The zero levels of the monitors were verified both on the ground and in the air, using a PbO scrubber for $SO_2$, purafil-activated charcoal for $NO_y$, and activated charcoal for ozone. Span calibrations were performed daily on the ground before takeoff. A global positioning system (GPS) was used to continuously monitor the position of the aircraft during the research flight. The data were recorded every 10 s and stored on both a data logger and a personal computer.

[15] All flights were performed during the summer at noon under westerly wind-flow conditions at an altitude of about 300 m (well within the boundary-mixing layer). The flights started at the coast in the Tel Aviv vicinity and attempted to follow the urban pollution plume as it drifted inland, under the westerly wind flows, toward the Judean mountains (up to 1000 m in height). Since photochemical activity is at a maximum at midday and sufficient time has elapsed from peak emission to allow maximum ozone production, the research flights were expected to identify the areas affected by the Tel Aviv pollution plume. Altogether, 32 flights were performed over three different years (1994, 1995, and 1997) in order to cover different periods and hence various meteorological conditions. In the present study, we report the results of three of the research flights, which were used for comparison with the model simulation studies.

### 3.2. Tunnel Experiment

[16] The tunnel technique [*De Fre et al.*, 1994; *Pierson et al.*, 1996] was employed to measure real-world fleet-wide vehicle emission factors for the various pollutants. The

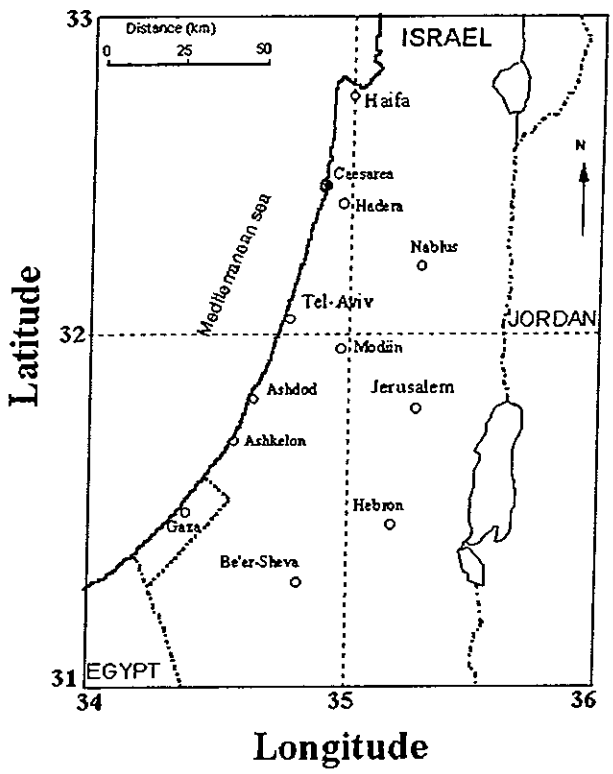


**Figure 1.** Map of central Israel and the Gaza region.

tunnel, situated south of Jerusalem, is 902 m in length, with an average slope of 3.6% and a cross section of approximately 70 $m^2$. Traffic flows in both directions in single lanes. In the tunnel there are 17 sets of blowers to ensure that the CO level remains below 30 ppm at all times. The wind flow in the tunnel is normally in a north-south direction with speeds varying between 1 and 3 m/s. The air sampled for analyses was taken at the northern entrance to the tunnel (background pollution levels) and at a site two-thirds of the way into the tunnel toward the southern exit. Tunnel air was drawn into Tedlar inert sampling bags (30-L capacity) at a rate of about 0.5 L/min. Thus the samples taken for analyses represented hourly averages. The sampled air was immediately analyzed using the following monitors: TEII (Thermo Environment Instruments Inc.) model 42S for $NO/NO_x$, TEII 43C for $SO_2$, TEII 48 for CO, TEII 41C for $CO_2$, Dasibi hydrocarbon analyzer for NMHC (nonmethane hydrocarbons) and a Verewa # F-101 for particulates. Vehicle counts, divided into light- and heavy-duty for each direction, and vehicle speed were taken concurrent to the air sampling. Additionally, wind speed (Met One 010C), temperature and relative humidity (Campbell Scientific Inc. 207) were monitored inside the tunnel. Altogether, 21 hourly samples were taken and analyzed during the research campaign.

### 3.3. Ground-Based Measurements and Data Analysis

[17] Data available from the Israeli national air quality monitoring network provided a variety of chemical and meteorological variables, such as $NO_x$, ozone (models 42C and 49C analyzers, respectively, Thermo Environmental Instruments Inc., USA), wind speed and direction, global sun radiation (GSR) and temperature. The Israeli monitoring network is based on USEPA approved instruments and measuring protocols. The statistical interpretation was based upon data collected between 1 June through 30 September for the years 1999 and 2000. Three locations, the metropolitan area of Tel Aviv, Modiin, and Jerusalem, were chosen, all of which are located within the experimental flight path and along the dominant summertime wind trajectory (see Figure 1).

## 4. Model Application

### 4.1. Traffic Flow Simulation

[18] For the purpose of this study, model implementation focused on detailing existing conditions (reflecting a total population of 6.3 million in the year 2000) to provide input data for a calibration run of the emissions model. The principal steps of the transportation modeling process were the following.

#### 4.1.1. Trip Generation

[19] Travel demand (vehicle-trip productions and attractions) was calculated for each of the country's 370 traffic analysis zones based on socioeconomic data for year-2000 conditions (population, housing, vehicle availability, total employment and retail employment). The 1996–97 National Travel Survey for Israel (Central Bureau of Statistics) provides the basis for trip generation rates. Trip attractions were balanced model-wide to total trip productions.

#### 4.1.2. Trip Distribution

[20] Matrices of the origin-destination travel patterns were estimated based on the marginal totals from the trip generation step, above, and using a two-way balancing gravity model as calibrated for Israeli conditions (the time-impedance curve can be expressed as the expression impedance = exp(−0.08*time).

#### 4.1.3. Travel Assignment

[21] Matrix origin-destination pairs were assigned to the road network using an incremental capacity-constrained assignment calibrated to Israeli conditions (volume-delay functions adapted from the Department of Transport, Economic Assessment of Road Schemes, United Kingdom, September 1996).

[22] Traffic speeds on road network segments were fed back into the trip distribution model in an iterative process to reflect the effects of traffic congestion on both origin-destination choice and travel-path choice.

### 4.2. Vehicle Emission Factors Calculation

[23] The emission model calculations were based on two complementary methods: the direct and carbon balance method. The direct method essentially produces the EFM of a specific pollutant in the tunnel's air based on the measured pollution concentration, tunnel length, cross section and number of vehicles present during the measurement,

$$EMF_i = (X_i \times V_w \times S \times T)/(L \times N)$$

$EMF_i$ emission factor of pollutant i (g/(km × vehicle));
$X_i$ pollutant i concentration (g/$m^3$);
$V_w$ average wind speed in the tunnel (m/s);

Table 1. $SO_2$, $NO_x$, NMHC, and CO Concentration Obtained by the Direct and Carbon Balance Methods[a]

| Method | $SO_2$ | $NO_y$ | NMHC | CO |
|---|---|---|---|---|
| Direct | 0.38 ± 0.09 | 4.0 ± 1.0 | 1.9 ± 0.6 | 21.0 ± 3.4 |
| Carbon balance | 0.34 ± 0.06 | 3.6 ± 0.6 | 1.7 ± 0.5 | 20.1 ± 4.1 |

[a]Concentration in g/(km per vehicle).

S cross-sectional area ($m^2$);
T measurement time (s);
L tunnel length (m);
N number of vehicles that passed during T.

[24] The carbon balance method EMF is obtained from the following relation:

$$EMF_i = P_i \times C$$

where $P_i$ is the mass of pollutant i divided by the total carbon in the tunnel air (g/kg C) and C is the average carbon fuel consumption in the tunnel (units of kg C/km).

[25] Calculated emission rates for $SO_2$, $NO_y$, NMHC and CO are given in Table 1 for average vehicle speeds of 60 to 80 km/h and an average deisel composition of 10%. The results of both methods agree well with one another, indicating the accuracy of the calculated emission values. These emission factors obtained in the present study are compatible with results obtained from similar studies performed both in the United States [*Pierson et al.*, 1966] and Europe [*De Fre et al.*, 1994]. Limited data available from measurements carried out on individual vehicles in Israel also show good agreement with the present study. The results presented in Table 1 were used as input data for the modeling simulation studies since they represent similar conditions (such as speed and vehicle mix) to those expected in the region under examination.

[26] The resulting integrated transportation and emission models provided the emission rate per traffic road segment for each relevant pollutant in units of g/h.

### 4.3. Atmospheric Modeling Aspects

[27] The nonhydrostatic mesoscale-mode, three-way intercalated-nested grid scheme was utilized in the RAMS simulation. The first grid was applied to an area of 1400 × 1400 square $km^2$ (meso-α scale) [*Orlanski*, 1975] at a 20-km resolution to derive synoptic phenomena. The latitude and longitude of the northwest and southeast corners of the modeling domain are (32.959, 27.146) and (25.618, 41.681), respectively. The second and third grids were applied to areas of 250 × 350 and 120 × 160 $km^2$ at 5-km and 1.25 km zooming-in resolutions, respectively. These two more highly resolved grids also account for the sea and land breezes and mountain and valley flows. All simulated zones were centered at the latitude/longitude coordinates of (32.0, 35.0), roughly representing the center of Israel. The simulations were performed for 24 hours starting at midnight. The simulations were initialized and updated every 6 hours with European Center for Medium-Range Weather Forecasts (ECMWF) data fields. The topographic data were obtained from the GTOPO30 project (http://edcdaac.usgs.gov/gtopo30/ gtopo30.html), which is a global topography digital elevation model (DEM) with a horizontal grid spacing of 30 arc seconds (approximately 1 km) derived from several raster and vector sources of topographic information. GTOPO30, completed in late 1996, was developed over a three-year period through a collaborative effort led by staff at the U.S. Geological Survey's EROS Data Center (EDC). The dates selected for applying the integrated interdisciplinary modeling system were based on days with high ozone level episodes as recorded by the flight measurements. The ECMWF meteorological fields initialized the simulation at 0000 UTC (0300 LST – local summer time) and provided the boundary conditions for the large-scale grid by updating the calculation at 6-hour intervals to produce the 24-hour atmospheric dynamics simulation. The fields produced by the RAMS were then used to initialize and drive the TDM, dispersing the traffic originated $NO_x$ and VOC from their emission origins in the Tel Aviv metropolitan area and the Gaza Strip. Applying the statistical multiple regression model following each dispersive time step gave the ozone mixing ratios. However, as mentioned previously, only ozone concentrations obtained in the time domain of photochemically aged air mass were used for inference and analysis, i.e., concentrations obtained about 4 hours (or more) after release.

### 4.4. Rush Hour Determination

[28] Analysis of $NO_y$ data collected from 1 June to 30 September for the years 1999 and 2000, at a monitoring station located in metropolitan Tel Aviv (see Figure 2), as well as a traffic survey and Emme/2 simulations, indicated that peak traffic emissions occurs between 0600 and 0900 (primarily as $NO_x$). This time period corresponds to "rush hour" peak transport loads. From 0900 onward, the $NO_y$ levels remain monotonically low. This daily time interval therefore reflects the main $NO_y$ pollution pulse and was used to initialize the simulation runs.

## 5. Results and Discussion

[29] The following section addresses coastal transportation-to-inland trans-boundary air pollution processes as revealed by simulations and airborne/surface-measured ozone levels. Overall three scenarios are analyzed, corresponding to early, mid and late summer ozone episodes as detected by airborne measurements.

### 5.1. Model Simulation

[30] Figure 3 qualitatively illustrates a sequential top view of the $NO_y$ particles (released from transportation primarily as $NO_x$) over the simulation area at 300 m AGL (airborne measurement height for selected hours of the 25 July 1997 ozone episode). The particles were emitted from the Tel Aviv metropolitan and Gaza Strip transportation sources from 0600 to 0900 LST (rush hour). Each particle released represents one gram of pollutant emitted per minute. At 0700 LST, one hour after emission had begun,

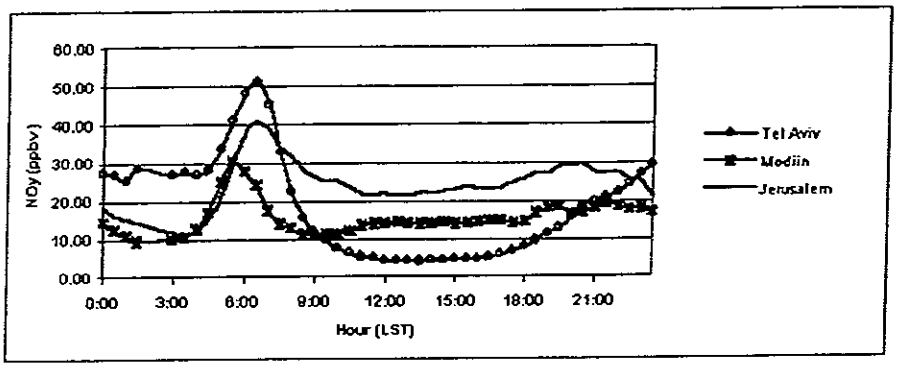


**Figure 2.** Averaged diurnal cycles of measured $NO_y$ concentrations in Tel Aviv, Modiin and Jerusalem for the periods of June-September in 1999 and 2000.

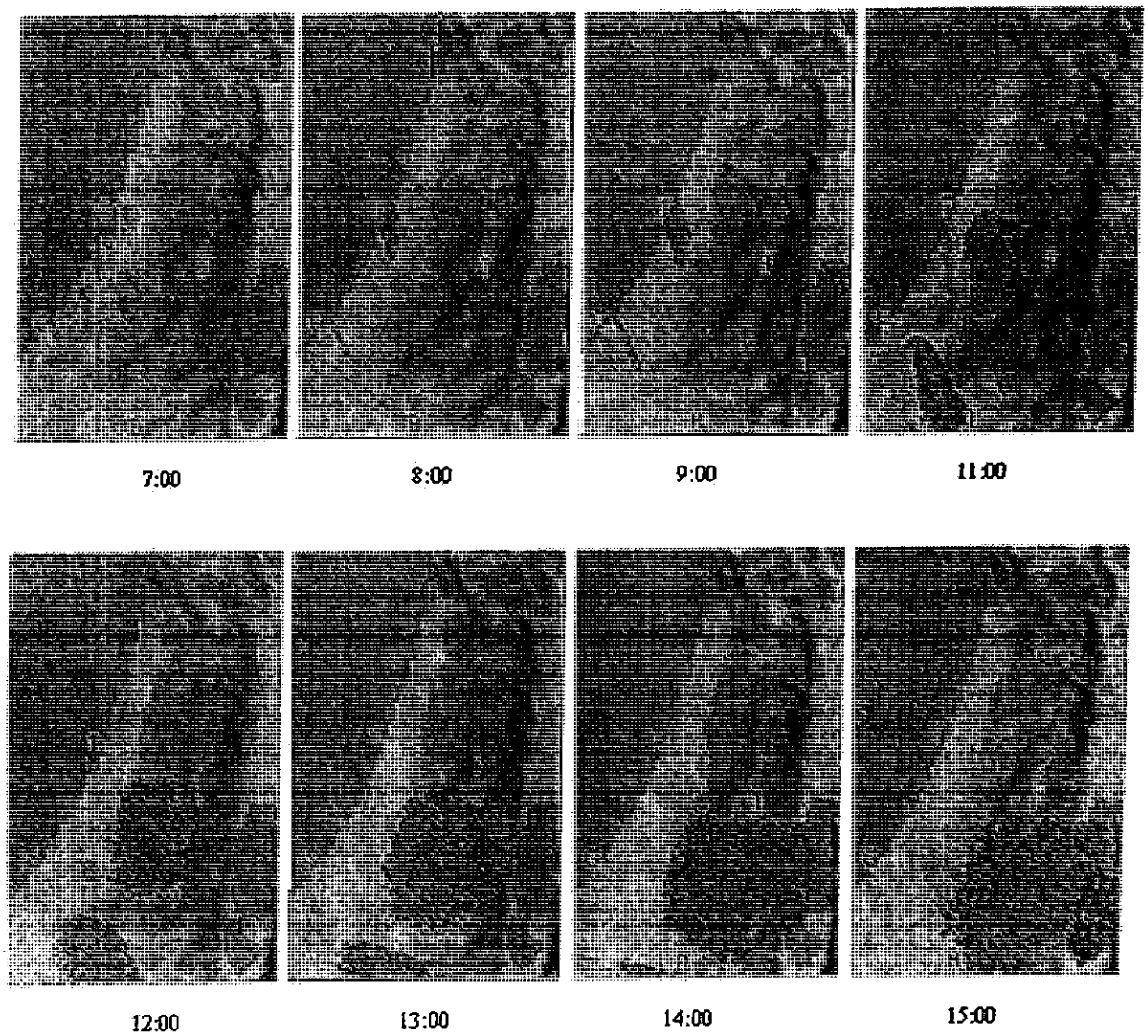


**Figure 3.** Qualitative top view of simulated $NO_y$ particles location over Israel at 300 m AGL at selected hours (LST). Particles originated from Tel Aviv metropolitan and the Gaza Strip transportation sources at rush hour, between 0600 and 0900 LST. T, Tel Aviv metropolitan; J, Jerusalem; G, Gaza strip; B, Beer Sheva.

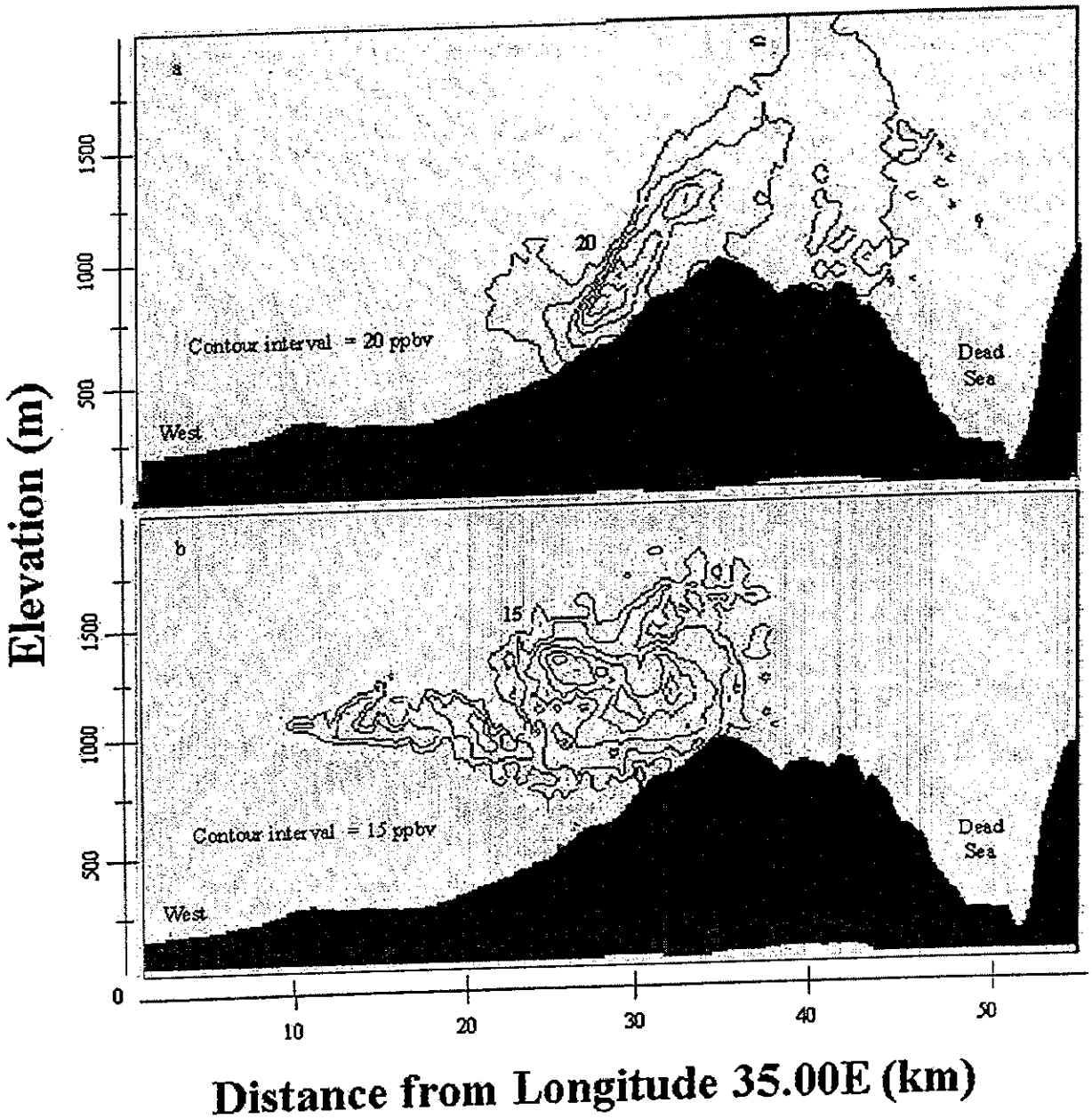


**Figure 4.** Vertical east-west cross section (Y-Z plane) of model-calculated ozone concentrations for (a) 28 August 1997 over Jerusalem area and (b) 25 May 1994 over Beer Sheva area at 1400 LST. Zero distance represents the coast of Tel Aviv. The values of outer contours are indicated. Dark area represents the topography in the studied regions.

particles were transported offshore by an easterly land breeze. During the next 2 hours, with the onset of the Mediterranean sea breeze, the pollution cloud initially located over the sea recirculated inland and mixed with freshly released pollution. Further inland, movement and dispersion of the particles is shown from 1100 to 1500 LST. Two main driving forces manifest the $NO_y$ spatial and temporal evolution: east-southeast transport accompanied by a 3-D expansion of the $NO_y$ cloud. The particulate clouds from the Tel Aviv metropolis and the Gaza Strip extend to a height of 300 to 400 m (above sea level) by 1100. At 1300, with the inland penetration of the particles over the mountain range coupled with increasing thermal instability, the pollution clouds expand to a height of 1500 m. Almost identical patterns were obtained (not shown) for traffic-produced VOC and CO.

[31] Figure 4 shows a vertical east-west cross section of calculated ozone concentration over Jerusalem (Figure 4a, 28 August 1997) and Beer Sheva (Figure 4b, 25 May 1994) at 1400, viewed from the south. On 28 August 1997, the maximal observed ozone values over Jerusalem ranged from 120 to more than 180 ppbv (Figure 5f), compared to

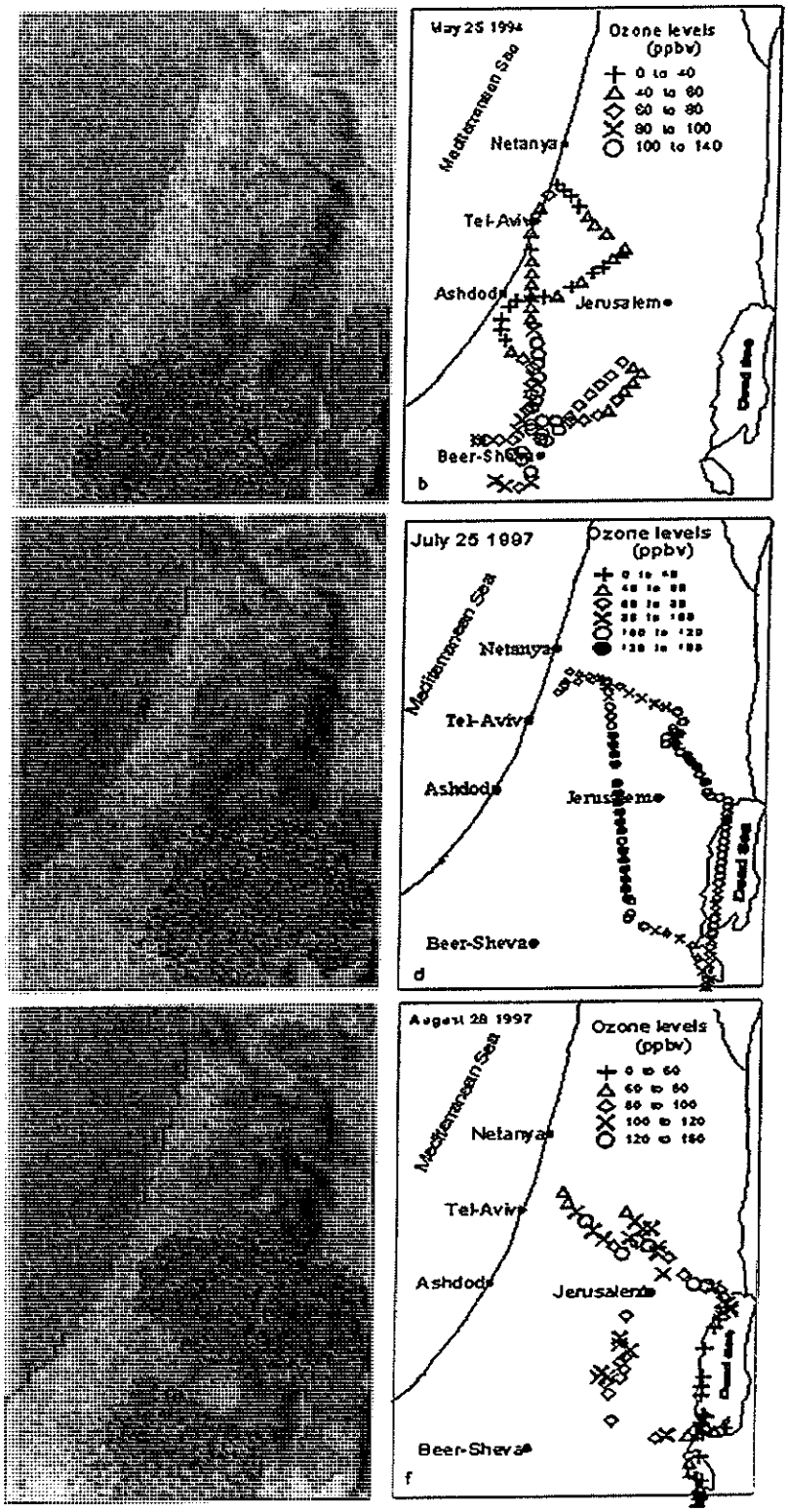


**Figure 5.** Qualitative comparison of model simulation with aircraft measurements of ozone for the three days studied: 25 May 1994, 1400–1600 LST, (a) model simulation and (b) flight measurements; 25 July 1997, 1400–1600 LST, (c) model simulation and (d) flight measurements; 28 August 1997, 1400–1600 LST, (e) model simulation and (f) flight measurements.

calculated values of about 110 ppbv (Figure 4a). On 25 May 1994 (Figure 4b), maximal observed ozone levels over Beer Sheva area ranged from 100 to 160 (Figure 5b). The corresponding calculated maximal values were about 85 ppbv. The explicit inclusion of traffic pollution from metropolitan Tel Aviv during rush hour (0600-0900) suggests that it accounts for more than 60% of the observed inland ozone pollution. The rest may be attributed to (1) background concentrations (up to 60 ppbv in some of the airborne measurements) and (2) alternative ozone sources, such as traffic emissions from other locations.

### 5.2. Flight and Model Comparison

[32] Model results for three scenarios were compared with airborne measurements of ozone concentrations. The inland air pollution episodes represent early (25–26 May, 1994), middle (25 July 1997) and late (28 August 1997) summer. Figure 5 shows the measured ozone levels along the flight path at 1300–1500 LST (Figures 5b, 5d, and 5f) and their corresponding model-calculated photochemically aged $O_3$ particles (Figures 5a, 5c, and 5e) for 1400. The actual ozone concentrations were presented in Figure 4, while Figure 5 shows their spatial distribution in a qualitative manner.

[33] Analysis of the research flight performed on 25 May 1994 reveals that the simulation study identified the main polluted area over Beer Sheva (Figure 5a). This is in good qualitative agreement with the flight measurements (Figure 5b). The wind field pattern (Figure 6a) traces back to the NNW, essentially originating from the Tel Aviv coastal area. The simulation results for 25 July 1997 (Figure 5c) predict a widely dispersed pollution plume over the central-to-southern Judean Hills with Jerusalem at its northern peak. The research flights for this date (Figure 5d), as well as the calculated wind field (Figure 6b), which exhibits a general west-to-east flow, supports this general pattern. The high concentrations of $O_3$ measured north of Jerusalem were not captured by the model. This suggests that emission sources from alternative areas (not included in the Tel Aviv morning rush hour traffic emissions) may have contributed to the ozone formation: for example, transportation sources from Jerusalem and noncoastal cities, as well as continuous traffic emissions from the Tel Aviv metropolitan area, besides the rush hour emission (0600–0900). On this day (Figure 6b), the wind field pattern exhibited a northwesterly flow that transported inland pollutants from northern coastal sources (not overlapping the Tel Aviv sources as occurred under a NNW flow, Figures 5a and 5b). Consequently, an extended pollution area north of Jerusalem was measured. The simulation of a late summer episode (28 August 1997) depicted ozone pollution over an extended region of central Israel and over Jerusalem extending to the Dead Sea, and a secondary polluted area to the south over Beer Sheva (Figure 5e). The flight measurements similarly identified the highest ozone levels over central Israel extending to the Dead Sea. It appears that the Jerusalem region was affected by pollution sources originating from the central Israeli coastal plane while the area over Beer Sheva was affected by emissions from the Gaza Strip (Figure 5f). The predicted wind field for the corresponding date (Figure 6c) indicated west-to-southeast flow, resulting in an extended inland air pollution pattern. It's interesting to note that for days dominated by

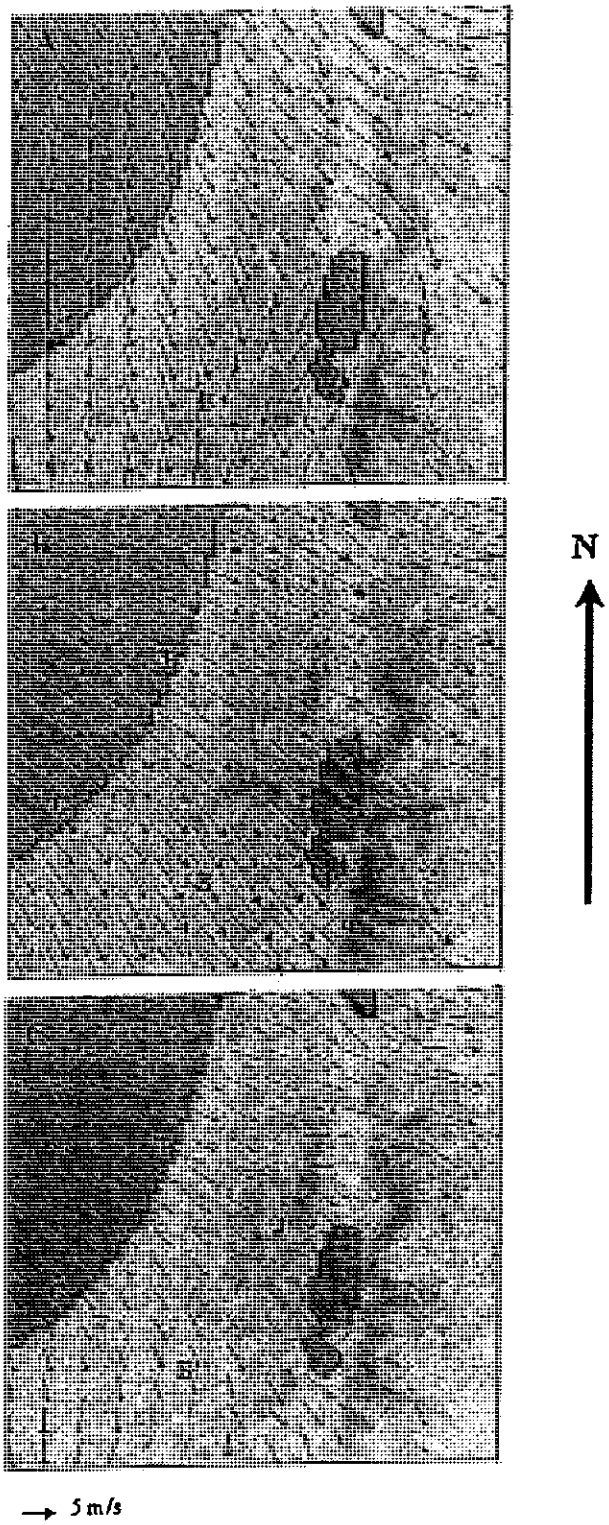


**Figure 6.** Simulated wind fields at Z = 600 m for (a) 25 May 1994, (b) 25 July 1997, and (c) 28 August 1997 at 1200 LST. Wind arrows below topography height are truncated. T, Tel Aviv metropolitan; J, Jerusalem; G, Gaza strip; B, Beer Sheva.

275

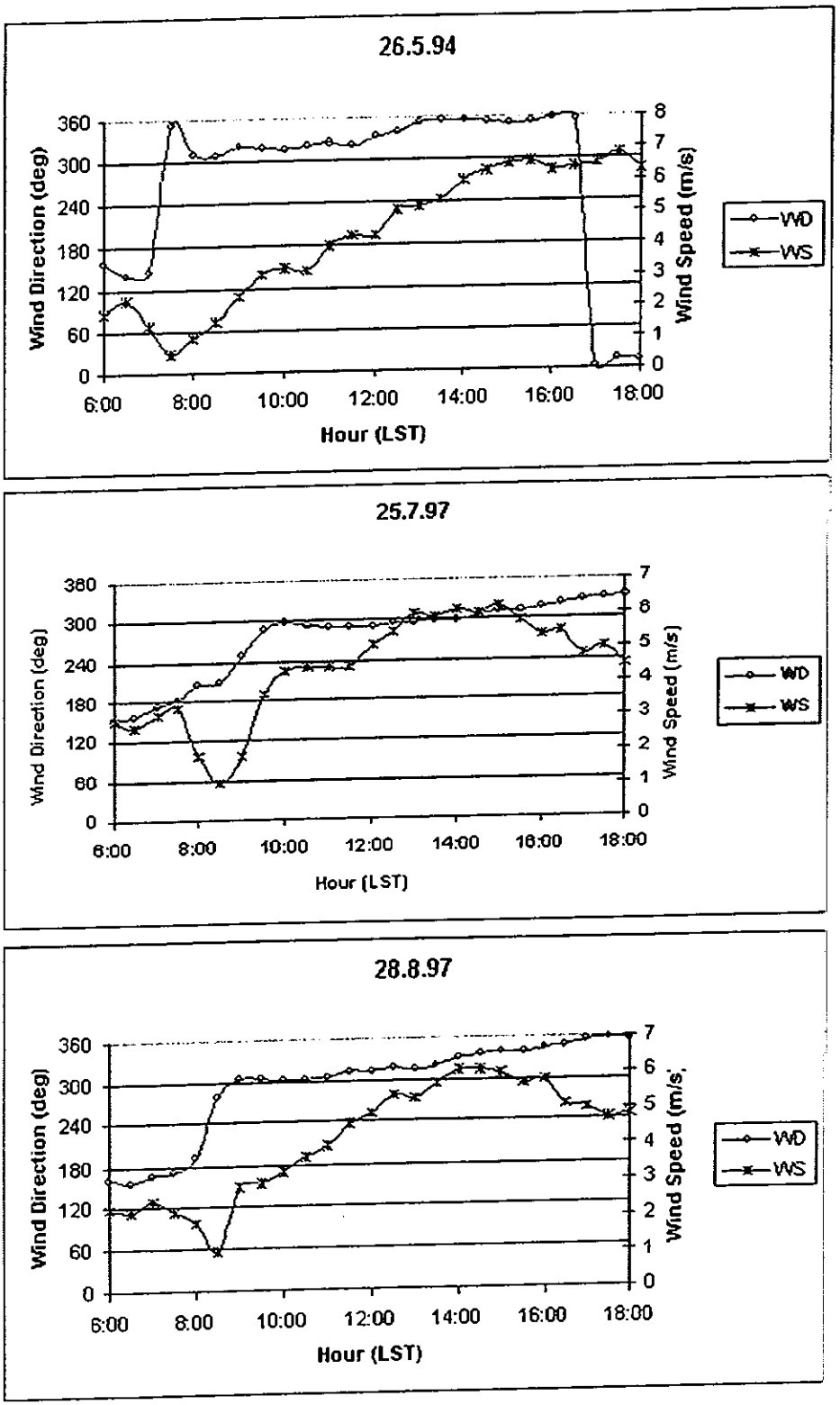


Figure 7. Measured wind direction (WD) and wind speed (WS) in Tel Aviv for 25 May 1994, 25 July 1997, and 28 August 1997 (LST).

Table 2. Synoptic and Meteorological Conditions During the Three Elevated Ozone Concentration Episodes Analyzed (Noontime)

| Season | Dates | Synoptic Conditions (Surface and Upper Atmospheric Layers) | Resultant Surface Flow | Mixed Layer (ML) Depth | Mean Wind Speed in ML, m $s^{-1}$ | Ventilation,[a] $m^2$ $s^{-1}$ | $T_{max\ Jer}$ − $T_{max\ TA}$[b] | $GSR_J - GSR_{TA}$[c], $Wm^{-2}$ |
|---|---|---|---|---|---|---|---|---|
| Spring–early summer | 25–26 May 1994 | Weak warm trough at the surface accompanied by weak zonal flow at 500 hPa atmospheric level | NE inland and NW breeze resulting in a northerly wind along the coast veering to NW inland | 350 m capped by a sharp inversion layer | 2.5 | 875 | 0.7°C | 50 |
| Mid-summer | 25 July 1997 | Weakening of the "Persian Trough" accompanied by a subtropical anticyclone inducing subsidence at mid- and high atmospheric layers | NW sea breeze as the prominent meso-scale system | 700 m capped by a subsiding inversion | 4 | 2800 | −0.6°C | 75 |
| End of summer | 28 August 1997 | Weakening of the "Persian trough" accompanied by a subtropical anti cyclone – inducing subsidence in mid and high atmospheric layers | NW winds caused mainly by the sea breeze veering to W winds farther inland | 800 m capped by a subsiding inversion aloft | 2.5 | 2000 | 0.5°C | 110 |

[a] Ventilation rate: Mixed-layer depth times the mean wind speed in the mixed layer representing the ability of the atmosphere to transport contaminants away from a source region. The average ventilation rate over the Israeli coastal plain for the entire summer ranges from less than 1000 $m^2s^{-1}$ to over 10000 $m^2s^{-1}$.

[b] $T_{max}$ Jer. - $T_{max}$ TA: A measure of the intensity of subsidence caused by prominence of the subtropical anticyclone (the upper-air synoptic system that governs the eastern Mediterranean during summer months). A more positive difference indicates more strongly subsiding conditions.

[c] $GSR_J$ - $GSR_{TA}$: The difference in maximum global solar radiation between Jerusalem and Tel Aviv. A more positive difference indicates that the inversion behaves like a perfect lid on the atmosphere below it, preventing upward motions and augmenting turbidity aboveground.

southwest winds, low levels of airborne measured ozone (60 ppbv) were detected over central Israel.

[34] Surface wind speed and wind direction measured at a station in Tel Aviv (Figure 7) agrees well with model results (Figures 5a, 5b, and 5c). Both model-predicted and measured data indicate that on 25 May 1994, the early morning NNW winds carried the newly emitted traffic pollution southward (Figure 5a). For the mid-to-late summer episodes (25 July and 28 August 1997), winds veering from west to NW, accompanied by intensified wind speed, dispersed the pollution toward the east and southeast (Figures 5b and 5c).

### 5.3. Relation of Air Pollution Scenarios to Weather Conditions

[35] Spring and early summer are characterized by the overwhelming influence of the subtropical high-pressure system. This situation often leads to a shallow mixed layer accompanied by weak zonal winds. Both of these features result in poor ventilation conditions and consequently to rising air pollution concentrations within the stable profile formed [*Dayan and Rodnizki*, 1999].

[36] All three episodes of elevated ozone concentration recorded by aircraft measurements and selected for simulation were found to fall into the "shallow Persian trough" synoptic category. This category occurs during warm summer days mainly at the start, but occasionally both in the middle and at the end of the summer season. This synoptic pressure pattern features stagnation conditions that evolve as a result of weak-pressure-gradient winds, a shallow mixed layer capped by subsiding warm and dry air and accordingly poor ventilation within the mixed layer. Several air pollution studies conducted in Israel, mainly over coastal environments, have already identified this synoptic category as being the main one affecting pollutants dispersion [*Dayan et al.*, 1988; *Hashmonay et al.*, 1991; *Koch and Dayan*, 1992; *Dayan and Rodnizki*, 1999]. Table 2 describes the main elements influencing the dispersion of pollutants and their measured values for three of the episodes analyzed. The calculated ventilation rates are based on mixing depths measured over the central coastal plain of Israel and are given in order to represent the worst regional transport conditions.

[37] The first case analyzed (25 May 1994) typifies the dispersion conditions associated with the "Weak Persian Trough" mode (Figure 8a). During the noon hour of this episode, a northerly wind blew along the coast up to a few hundred meters above ground within the shallow mixed layer. Both the simulation (Figure 5a) and flight observation (Figure 5b) results indicate transport of the emitted plume southward with very limited dilution. The second episode analyzed (25 July 1997) was characterized by a somewhat deeper "Persian trough" (Figure 8b). The dispersion conditions during this event were much better since the mixed layer was deeper and the resultant onshore winds stronger, leading to three times the ventilation rate measured in the first case. Both the simulation and measurement results (Figures 5c and 5d) show the elongated propagation of the plume during its transport southeast toward the inland elevated region. The "Persian trough" during the third case studied (28 August 1997) is in its weakest mode, leading to weak and variable winds onshore (Figure 8c). Under such dispersion conditions, the polluted air mass drifts very slowly from the Tel Aviv metropolitan area toward Jerusalem, while keeping its initial rounded contours (as seen in Figures 5e and 5f). These three cases indicate that in summer, when synoptic gradient winds are weak as manifested by low ventilation-rate values, central inland Israel is strongly affected by elevated ozone levels caused by urban pollution plumes originating along the Mediterranean coastline.

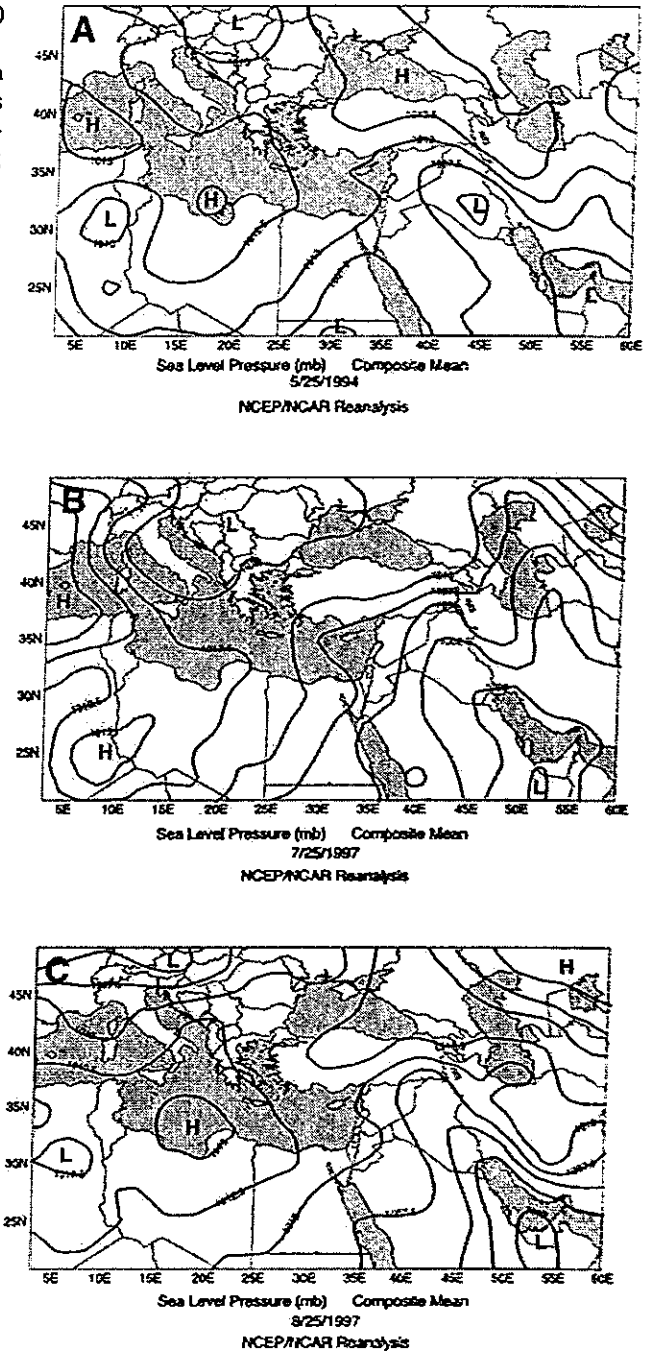


**Figure 8.** Synoptic maps of the three examined days (a) 25 May 1994, 1500 LST; (b) 25 July 1997, 1500 LST; (c) 28 August 1997, 1600 LST.

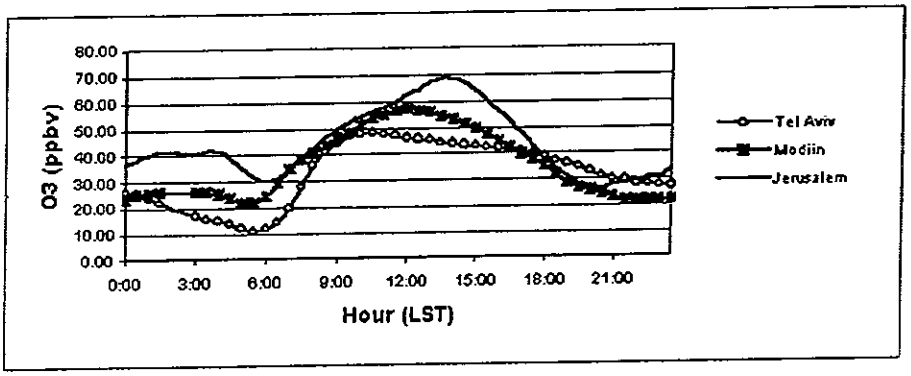


**Figure 9.** Averaged diurnal cycles of measured ozone concentrations in Tel Aviv, Modiin and Jerusalem for the periods of June–September in 1999 and 2000.

[38] Data for the other research flights, not reported in the study, further indicate that observational and model simulations were generally in phase, the degree of overlap dependent on the aforementioned arguments. Furthermore, during the summer period, elevated ozone concentrations were recorded over central Israel on almost all days studied. Both observations and calculations point to the Tel Aviv metropolitan region as the origin for the inland air pollution.

[39] Regarding the Gaza Strip transportation emission sources, the simulations suggested that the southern tail of the observed central Israel air pollution episodes are due to contributions from this region.

### 5.4. Data Analysis of Ground-Based Monitoring Stations

[40] The available ground monitoring data were analyzed to discern any observable patterns for the pollution levels with increasing distance inland of the three monitoring sites. While data from the network were available only for two summer periods (June to September of 1999 and 2000), these periods were representative of the general situation existing during the summer month of the research period, since no significant changes have occurred since then in the area under investigation. Furthermore, considering time-space scales in ambient ozone and meteorology data [*Eskridge et al.*, 1997; *Rao et al.*, 1997], the relevant long-term component (trend term) of the ozone time series, i.e., variations in climate, policy, and/or economics, is of no significance in our case. The monitoring data for the entire period under examination were averaged over 30-min time segments. Figures 9 and 2 show the data for ozone and $NO_y$, respectively. The ozone levels exhibited a distinct inland scale dependency. Ozone peaks at later hours (1130, 1300, and 1400 in Tel Aviv, Modiin and Jerusalem, respectively) and on average reaches higher levels (50 ppbv, 56 ppbv, 70 ppbv for Tel Aviv, Modiin, and Jerusalem, respectively) as progress is made inland. A comparison of the coastal $NO_y$ spectra (Tel Aviv) to the inland $NO_y$ profiles (Modiin and Jerusalem) discerns different dynamics for these locations. While the initial levels in the Tel Aviv metropolitan area are higher during the morning rush hour emissions, they experience a pronounced bleaching by the late morning sea breeze in comparison to inland locations, which level out at relatively higher midday concentrations. This may indicate, in the absence of any alternative $NO_y$ source, that the early morning $NO_x$ produced by transportation sources in Tel Aviv is transported inland, providing additional $NO_y$ to the regions in its path. These results correspond well with the dynamics of the inland-penetrating plume. The observed increase in ozone concentrations is attributed to ongoing photochemical transformations while traversing inland. Thus the superposition of the transported ozone cloud, originating from the coastal metropolitan traffic sources, with the native formed ozone results in the higher observed ozone levels.

## 6. Conclusions

[41] Airborne measurements showed that central inland Israel is strongly affected by pollution originating along the Mediterranean coastline, where urban transportation sources play a pivotal role. The flight measurements, model simulations and ground-level monitoring all showed that under northwesterly winds, elevated ozone values can be found over central Israel. These findings establish a scenario in which the physical process of inland movement of pollutants in general, and ozone precursors in particular, is established. The Tel Aviv metropolitan area and possibly the Gaza Strip region emit transportation pollutants into the troposphere on a daily basis, initiating their subsequent photochemical transformation as they are transported downwind. Model simulations showed that about 60% of the detected inland ozone concentration is nourished by traffic emissions during the morning rush hours from the Tel Aviv metropolitan area.

[42] The assumption of a photochemically aged air mass regime may enable the application of multivariate linear regression analysis to quantitatively appraise ozone production over central Israel. Thus, under these conditions, the application of a relatively simple statistical analysis method for evaluating ozone concentrations may replace the need for comprehensive photochemical solvers.

[43] Air pollution, with ozone-generating processes, is among the most significant ecological impacts of modern age network transportation. The problem is especially acute in regions with poor dispersion conditions such as those existing in Israel during the highly photochemically active summer period. The work presented here demonstrates the

ability of interdisciplinary modeling systems to operate collectively as a prediction tool/tracing device, capable of successfully predicting air pollution hot spots. The model is now being expanded to include photochemical transformations that will enable simulating ozone formation under additional conditions. This prediction and analysis tool is expected to assist in the shaping of present and future transportation infrastructure, where air pollution in general, and ozone problems in particular, are to be considered.

[44] **Acknowledgments.** This study was funded under the U.S. Middle East Regional Cooperation (MERC) Program (USAID Award PCE-G-00-99-00037-00), project title "Transboundary Air-Quality Effects from the Urbanization of Israel-Gaza Mediterranean Coast". We would like to acknowledge the assistance provided by the Israeli Ministry of the Environment (air quality monitoring national network) and the Israeli Meteorological Service for providing the relevant air quality and meteorological data. We would also like to thank Robert Bornstein for helpful discussions and encouragement during the performance of the above research.

## References

Dabdub, D., L. L. DeHaan, and J. H. Seinfeld, Analysis of ozone in the San Joaquin Valley of California, *Atmos. Environ.*, *33*, 2501–2514, 1999.

Dayan, U., and L. Koch, Ozone concentration profiles in the Los Angeles Basin—A possible similarity in the buildup mechanism of inland surface ozone in Israel, *J. Appl. Meteorol.*, *35*, 1085–1090, 1996.

Dayan, U., and J. Rodnizki, The temporal behavior of the atmospheric boundary layer in Israel, *J. Appl. Meteorol.*, *38*, 830–836, 1999.

Dayan, U., R. Shenhav, and M. Graber, The spatial and temporal behavior of the mixed layer in Israel, *J. Appl. Meterol.*, *27*, 1382–1394, 1988.

De Fre, R., P. Bruynserade, and J. G. Kretzschmar, Air pollution measurements in traffic tunnels, *Environ. Health Perspect.*, *102*, 31–37, 1994.

Eskridge, R. E., J. Y. Ku, S. T. Rao, S. P. Porter, and I. Zurbenko, Separating different scales of motion in time series of meteorological variables, *Bull. Am. Meteorol. Soc.*, *78*, 1473–1483, 1997.

Finlayson-Pitts, B. J., and J. N. Pitts, Tropospheric air pollution: Ozone, airborne toxics, polycyclic aromatics, hydrocarbons, and particles, *Science*, *276*, 1045–1052, 1997.

Fraser, M. P., G. R. Cass, and R. T. Brend, Particulate organic compounds emitted from vehicle exhaust and in the urban atmosphere, *Atmos. Environ.*, *33*, 2715–2724, 1999.

Hashmonay, R., A. Cohen, and U. Dayan, Lidar observation of the atmospheric boundary layer in Jerusalem, *J. Appl. Meteorol.*, *30*, 1228–1236, 1991.

Her Majesty's Stationery Office (HMSO), Economic assessment of road schemes: Cost benefit analysis (COBA) manual, in *Design Manual for Roads and Bridges*, vol. 13, Dep. of Transp., ISBN 0115516697, Norwich, England, UK, 1996.

Hurley, P., and W. Physick, A Lagrangian particle model of fumigation by breakdown of the nocturnal inversion, *Atmos. Environ.*, *25A*, 1313–1325, 1991.

INRO Consultants Inc., *Emme/2 User's Manual*, Software release 9, Montreal, Canada, 1998.

Kleindienst, T. E., D. F. Smith, E. E. Hudgens, and R. F. Snow, The photooxidation of automobile emission: Measurements of the transformation products and their mutagenic activity, *Atmos. Environ.*, *26A*, 3039–3053, 1992.

Kley, D., Tropospheric chemistry and transport, *Science*, *276*, 1043–1045, 1997.

Koch, J., and U. Dayan, A synoptic analysis of the meteorological conditions affecting dispersion of pollutants emitted from tall stacks in the coastal plain of Israel, *Atmos. Environ.*, *26A*, 2537–2543, 1992.

Lu, R., and R. P. Turco, Ozone distribution over the Los Angeles Basin: Three-dimensional simulations with the SMOG model, *Atmos. Environ.*, *30*, 4155–4176, 1996.

Moussiopoulos, N., and S. Papagrigoriou (Eds.), Athens 2004 air quality, in *Proceedings of the International Scientific Workshop on "Athens 2004 Air Quality,"* 183 pp., FiatLux Publ., Fremont, Calif., 1997.

Olszyna, K. J., E. M. Bailey, R. Simonaitis, and J. F. Meagher, $O_3$ and $NO_y$ relationships at a rural site, *J. Geophys. Res.*, *99*, 14,557–14,563, 1994.

Olszyna, K. J., M. Luria, and J. F. Meagher, The correlation of temperature and rural ozone levels in southeastern U.S.A., *Atmos. Environ.*, *31*, 3011–3022, 1997.

Orlanski, I., A rational subdivision of scales for atmospheric processes, *Bull. Am. Meteorol. Soc.*, *56*, 527–530, 1975.

Peleg, M., M. Luria, I. Setter, D. Perner, and P. Russel, Ozone levels in central Israel, *Isr. J. Chem.*, *34*, 375–386, 1994.

Physick, W. L., and D. J. Abbs, Modeling of summertime flow and dispersion in the coastal terrain of Southeastern Australia, *Mon. Weather Rev.*, *119*, 1014–1030, 1991.

Pielke, R. A., W. R. Cotton, C. J. Tremback, W. A. Lyons, L. D. Grasso, M. E. Nicholls, M. D. Moran, D. A. Wesley, T. J. Lee, and J. H. Copeland, A comprehensive meteorological modeling system, *Meteorol. Atmos. Phys.*, *49*, 69–91, 1992.

Pierson, W. R., A. W. Gertler, N. F. Robinson, J. C. Sagebiel, B. Zielinska, G. A. Bishop, D. H. Stedman, R. B. Zweidinger, and W. D. Ray, Real-world automotive emissions, Summary of Studies in the Fort McHenry and Tuscarora Mountain Tunnels, *Atmos. Environ.*, *30*, 2233–2256, 1996.

Pilinis, C., P. Kassomenos, and G. Kallos, Modeling of photochemical pollution in Athens, Greece, Application of the RAMS-CALGRID modelling system, *Atmos. Environ.*, *27B*, 353–370, 1993.

Rao, S. T., I. G. Zurbenko, R. Neagu, P. S. Porter, J. Y. Ku, and R. Henry, Space and time scales in ambient ozone data, *Bull. Am. Meteorol. Soc.*, *78*, 2153–2166, 1997.

Roorda-Knape, M. C., N. A. H. Janssen, J. J. De Hartog, P. H. N. Van Vliet, H. Harssema, and B. Brunekreef, Air pollution from traffic city districts near major motorways, *Atmos. Environ.*, *32*, 1921–1930, 1998.

Seinfeld, J. H., Urban air pollution: State of the science, *Science*, *243*, 745–752, 1989.

Seinfeld, J. H., and S. N. Pandis (Eds.), *Atmospheric Chemistry and Physics: Air Pollution to Climate*, 1326 pp., John Wiley, New York, 1998.

Silibello, C., G. Calori, G. Brusasca, G. Catenacci, and G. Finzi, Application of photochemical grid model to Milan metropolitan area, *Atmos. Environ.*, *25*, 2025–2038, 1998.

Staehelin, J., C. Keller, W. Stahel, K. Schlapfer, and S. Wunderli, Emission factors from road traffic from tunnel measurements (Gubrist Tunnel, Switzerland), part III, Results of organic compounds, $SO_2$ and speciation of organic exhaust emission, *Atmos. Environ.*, *32*, 999–1009, 1998.

Svensson, G., Model simulation of the quality in Athens, Greece, during the Medcaphot-trace campaign, *Atmos. Environ.*, *32*, 2239–2268, 1998.

Trainer, M., et al., Correlation of ozone with $NO_y$ in photochemically aged air, *J. Geophys. Res.*, *98*, 2917–2925, 1993.

Walko, R. L., C. J. Tremback, and R. F. A. Hertenstein, RAMS—Regional Atmospheric Modeling System version 3b, in *User's Guide*, ASTER Div., Mission Res, Coop., Fort Collins, Colo., 1995.

U. Dayan and J. Kaplan, Department of Geography, Hebrew University of Jerusalem, Jerusalem 91905, Israel.

A. W. Gertler, Desert Research Institute, P.O. Box 60220, Reno, NV 89506, USA.

G. Kallos and P. Katsafados, University of Athens, Laboratory of Meteorology, Ippocratous 33, Athens 106 80, Greece.

M. Luria, V. Matveev, and M. Peleg, Environmental Science Division, School of Applied Sciences and Technology, Hebrew University of Jerusalem, Jerusalem 91904, Israel.

Y. Mahrer and D. O. Ranmar, Department of Soil and Water Sciences, Faculty of Agricultural, Food and Environmental Quality Sciences, Hebrew University of Jerusalem, Rehovot 76100, Israel.

# Utilization and Integration of Interdisciplinary Computer Models as a Tool for analyzing Ozone Production from Transportation Sources

D. O. Ranmar[1], M. Luria[2], J. Kaplan[3], and Y. Mahrer[1]

**ABSTRACT**
High ozone levels detected over large inland areas in Israel triggered analysis of air mass back trajectory, which pointed to the coastal Tel-Aviv metropolitan transportation system as the origin of the ozone's precursors. In order to link the transportation emissions to ozone formation interdisciplinary modeling systems were utilized and integrated. The transportation-to-ozone formation simulation, coupled transportation, emission factors, atmospheric and transport/diffusion models. The modeling results elucidated the spatial and temporal overlap between the ozone precursors and ozone production. The model simulations indicated an eastward transport accompanied with a 3D expansion of the pollution cloud. The results agreed well with observed spatial and temporal ozone levels.

**KEYWORDS**
Air pollution, numerical atmospheric modeling, transportation model, emission factors, ozone, advection/diffusion model.

## INTRODUCTION

The transportation network and the traffic flow constitute a system, which is the most elementary part of a country's infrastructure and a prerequisite for its economic growth. The spatial positioning of the transportation infrastructure determines the geographic distribution of the traffic flows, and hence determines the time dependent location of the pollution sources. Dynamically, this system is not an isolated system – it interacts with its surroundings primarily with the troposphere and particularly chemically to produce and emit pollution gases mainly NOx ($NOx = NO + NO_2$), VOC and CO. These entities undergo chemical and photochemical transformations in the presence of the solar radiation and atmospheric free radicals to form ozone (Finlayson-Pitts and Pitts 1997, Seinfeld and Pandis 1997). Since the formation and accumulation of ozone and other secondary species is not instantaneous following the emission of their precursors, significant transport and mixing occurs simultaneously with the chemical reactions (Kley 1997, Seinfeld 1989). An illustration of transportation emission to ozone formation scenario is presented in Fig 1. These daily processes call for the need to factorize and elucidate the link between road traffic emissions, the dominant source of NOx and VOCs, and ozone production during the course of the day. Previous studies (Peleg et al. 1994) based on measurements performed during the early summer months of 1988-1991 combined with air mass back trajectories analysis pointed to the Tel Aviv metropolitan transportation system as the main source of the high levels of ozone precursors detected in central Israel. Fig 2a shows the map of the simulation area and depicts the major traffic roads, Tel-Aviv metropolitan region, Gaza-Strip and Jerusalem. Road traffic activities with peak emission rates take place between 06:00 to 09:00 LST and are represented by the red dots in the Tel-Aviv metropolis. Fig 2b displays ozone concentrations at about 350 m above ground level taken by an aircraft, during the afternoon hours of the 28/8/97-ozone episode. It is apparent that the broad geographic distribution of high ozone levels, which at first sight seems unrelated to its precursor source location, is an outcome of highly complex and dynamical processes. Previous works addressed ozone formation in different modes such as under the impact of NOx and VOCs on ozone formation (Derwent and Davies 1994; Dabdub et al., 1999), or in the context of photochemical pollution modeling where the transportation emissions, and photochemical transformations overlap spatially, such as in the case of Athens (e.g. Pilinis et al., 1993; Moussiopoulus and Papagrigoriou, 1997). This study addresses the impact of the transportation emissions in the context of rates, timing, and location on the spatial and temporal production of ozone under the influence of atmospheric dynamics and topography. Conducted in the framework of the Israeli-Palestinian peace talks, the presented work is aimed at understanding the dynamics of the regional transportation-to-ozone production. This linkage is coupled with the idea of devising a

predicting tool that potentially can assist in the present and future transportation infrastructure shaping, where air pollution in general - and ozone problems in particular - are to be considered.

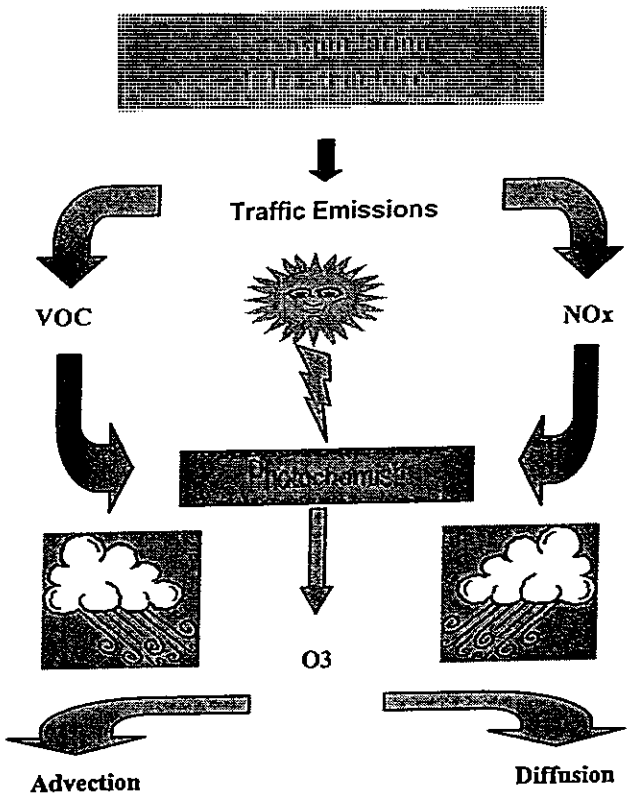


**Figure 1.** Schematic illustration of ozone formation from transportation sources.

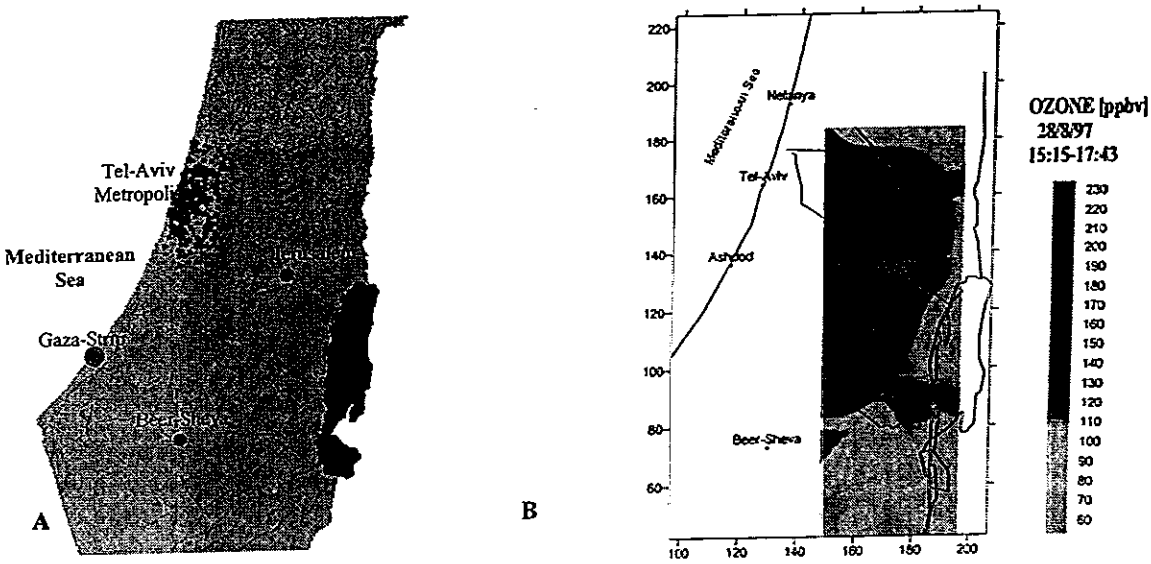


**Figure 2.** A – The simulation area, indicating the Tel Aviv metropolis and Gaza-Strip traffic sources (red) and traffic roads (red), B – ozone concentrations measured at 350 m above surface by aircraft.

## MODELING SYSTEMS

Understanding the spatial and temporal linkage between transportation emissions and ozone production called for the utilization and integration of interdisciplinary modeling systems covering the fields of: (i) transportation volumes, (ii) emission factors, (iii) atmospheric dynamics, (iv) pollutants transport and diffusion and (v) photochemistry. Fig 3 illustrates the modeling flow chart, which is based on an anthropogenic attribute – represented by the transportation and emission factors models (right branch) and the atmospheric dynamics attribute represented by the atmospheric model (left branch). The output from these two attributes intersects at the air pollution manifest through the transport and mixing of the transportation emissions. Finally, a photochemical model is interfaced to color the initially inert treated traffic pollutants with a photochemical dye, the final obligatory stage in ozone formation.

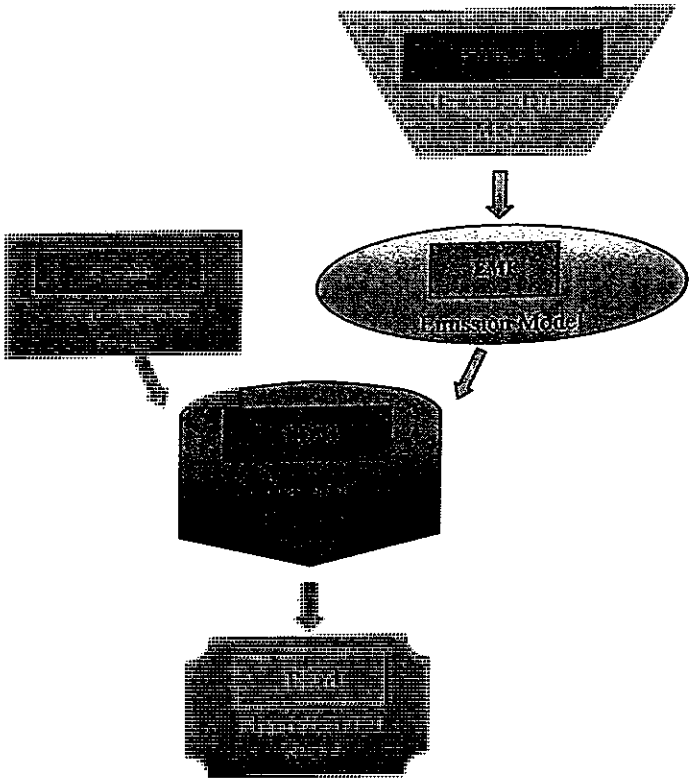


**Figure 3.** Schematic presentation of the modeling flow chart.

### Transportation model

The EMME/2 transportation system model (EMME/2 user Manuel and references therein) was used to analyze the combination of present transport flow dynamics and land use scenarios, and future conditions (year 2020) regarding transportation system performance. The results comprise the inputs for analyzing potential air quality levels, particularly ozone concentrations, under given scenarios. The modeling process assesses the balance between travel demand (based on land uses) and supply (based on transport facilities) under given scenarios. Land uses are aggregated to analysis zones (such as census tracts), which provide the basis for estimating a matrix of trips origin and destination. Networks to which the analysis zones are connected represent transport facilities, where each link of the network is characterized in terms of its capacity and speed components. The modeling process produced the desired origin-destination matrices of trips by the type of trip mode of travel and time of day as well as transport network data which depict the volumes of vehicles and passengers by road segment, travel speed, travel time, and delay of time. The traffic flow density per hour (TFD) for each road segment is obtained by multiplying the number of vehicles by the length (Km) of the road:

$$TFD = Vehicles \times Lengh/hr$$

**Emission Factor Model**

In a parallel study, fleet-wide motor-vehicle emission factors typical for Israel were estimated using road tunnel measurements.

The Vehicle EMission Factor (VEMF) of a specific pollutant is a parameter representing the pollutants' emission rate from the vehicle in units of g/km. The emission model is based on road tunnel measurements of NOx, NMOC, CO and $SO_2$. The emission model calculations were based on two complementary methods: Direct Method and Carbon Balance Method.

The direct method essentially produces the VEMF of specific pollutant in the tunnels' air based on its measured concentration, the tunnel length and number of vehicles present during the measurement:

$$\mathbf{EMFi} = (\Delta \mathbf{Xi} \times \mathbf{Vw} \times \mathbf{S} \times \mathbf{T})/(\mathbf{L} \times \mathbf{N})$$

EMFi – EMission Factor of pollutant i (g/(km x vehicle))
$\Delta$Xi – pollutant i concentration ($g/m^3$)
Vw – average wind speed in the tunnel (m/sec)
S – cross section area ($m^2$)
T– measurement time (sec)
L – tunnel length (m)
N – number of vehicles that passed during T

The Carbon Balance Method EMF is obtained from the following relation:

$$\mathbf{EMFi} = \mathbf{Pi} \times \mathbf{C}$$

where Pi is the mass of pollutant I divided by the total carbon in the tunnel air (units of g/kg C) and C is average carbon fuel consumption in the tunnel (units ofkg C/km).

Calculated concentrations of NMOC and NOx are given in Table 1. The results of both methods agree well with each other, which indicates on the accuracy of the calculated emission values.

| Method | NMOC | NOx |
|---|---|---|
| Direct | 1.9 ± 0.6 | 4.0 ± 1.0 |
| Carbon Balance | 1.7 ± 0.5 | 3.6 ± 0.6 |

**Table 1.** NMOC and NOx concentration (g/(km x vehicle)) obtained by the direct and carbon balance methods, and their ratio.

Thus, the coupling of the transportation and emission models yields the emission rate per traffic road for each relevant pollutant in the units of g/hr.

**Atmospheric Modeling**

The Regional Atmospheric Modeling System (RAMS) is the state of the art mesoscale atmospheric model accounting for the atmospheric attribute (Pielke et al., 1992). It is a multipurpose 3D versatile numerical prediction model designed to simulate weather systems by calculating multiple meteorological fields - primarily the wind, temperature, pressure, and humidity. It is constructed around the full set of equations in terrain following coordinates system, which govern atmospheric motions. The equations are supplemented with optional parameterizations for turbulence, radiation, thermodynamics, clouds, soil type and vegetation. The RAMS was initialized and updated every 6 hours with ECMWF data fields. The topography data was obtained from the GTOPO30 project which is global digital elevation model (DEM) with a horizontal grid spacing of 30 arc seconds (approximately 1 kilometer). The RAMS is equipped with a multiple grid-nesting scheme that allows a two-way interaction between computational grids of different 3D resolution. In the current simulation, the RAMS was executed in a hierarchical, three level nested grids (Fig. 4) to allow zooming in from synoptic scale phenomena (A: Grid 1) through the mesoscale dynamics (B: Grid 2) to the high-resolved local systems (C: Grid 3). The telescoping from large-scale environment with low resolution of 20-km mesh grid cells to small-scale atmospheric systems with fine-meshed high-resolution grid cells (1.25-km) enables us to account for small scale atmospheric features of the target area while simultaneously providing the impact of much larger meteorological systems.

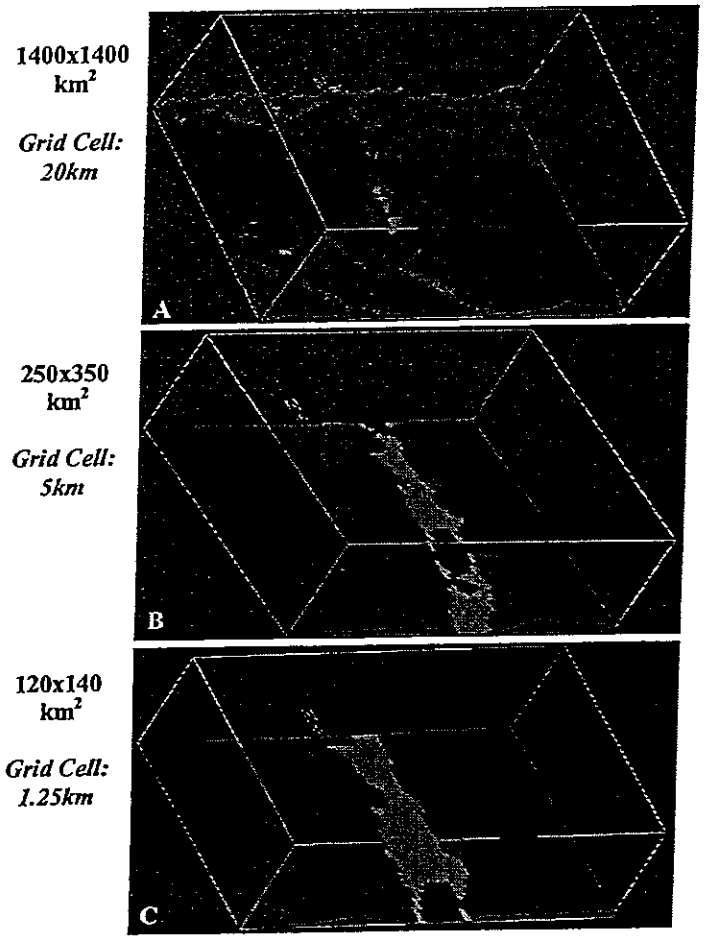


**Figure 4.** The hierarchical three level nested grids utilized in the RAMS.

**Transport Diffusion Simulation**

The TDM is a Lagrangian 3D model that simulates the motion of atmospheric pollutants under the influence of atmospheric flow. The TDM was applied to the high resolution grid with a vertical grid resolution of 50m up to a height of 2km. The TDM was initiated and driven by the meteorological fields produced by the RAMS and interpolated them in time and space to the location of the pollutant elements. The coupled EMME/2-Emission model provided the TDM with the following transportation data (the anthropogenic driving force): (i) The number of traffic sources, (ii) Traffic sources location (iii) The emission rates of NOx and VOCs.

## SYNOPTIC CONDITIONS

The dominant synoptic condition prevailing in the east of the Mediterranean Sea from mid-June to mid-September is influenced by two major systems surrounding the region, overall resulting in monotonic weather conditions. From the east, mid and south Asia, land warming during the summer leads to the development of the Monsoon Low, resulting in predominant north winds in the Mediterranean. One of its centers is located in the Persian Gulf, forming the so called "Persian trough" which extends from the Persian-Golf towards the southern shores of Turkey, and dominates the Mediterranean in the summer. It forms northwest winds influencing the north and the central regions of Israel. Westerly to our region, we are influenced by the Azorean high, which is part of the subtropics

belts of highs. The Azorean high is centralized at the Atlantic Ocean, near the Azorean islands, and dictates northwest air motions. The combined synoptic winds will coincide with the see breeze reinforcing it during daytime and opposing it during the night, when land breeze takes over.

## MODEL APPLICATION

The non-hydrostatic mesoscale model RAMS utilized an intercalated three level nested grid scheme. The first grid was applied to an area of 1400x1400 km meso-$\alpha$ scaleato derive synoptic phenomena. The second grid was applied to an area of 250x350 km and the third to a 120x140 km zone (meso-$\beta$ scale, Orlanski 1975). These two higher resolved grids will also account for the sea/land breeze circulation along the west coast of Israel. The simulations were performed for 24-hour intervals starting at midnight. The dates selected for applying the integrated interdisciplinary modeling systems were based on high ozone levels episodes recorded from aircraft measurements taken at about 350 m above ground level. The ECMWF meteorological fields initialized the simulation at 00:00 GMT (03:00 LST) and updated the calculation at a 6-hour interval to produce the 24-hour atmospheric dynamics simulation.

The incorporation of the traffic emissions into the troposphere as the precursors for ozone production was based on a 3-hour release period, corresponding to the time interval of the highest traffic flow and emission rate during the morning rush hours, between 6 and 9 AM LST. Limiting the road traffic emissions interval to the rush hours will emphasize the impact of the Tel-Aviv metropolis traffic emissions during these hours on the evolution of ozone production in mid-Israel in general and over Jerusalem in particular.

In the presented simulation NOx was addressed as an inert, non-reactive entity throughout its spatial and temporal translocation. This assumption is based on the fundamental correlation found to exist between NOy (sum of all nitrogen oxides excluding $N_2O$) concentration and ozone mixing ratio (Trainer et. Al., 1993, Derwent R. G. & Davis T. J., 1994, Olszyna et al., 1994, Olszyna et al.,1997). This correlation prevails for a photochemically aged air mass, i.e. when most of NOx has been oxidized into NOz, (NOz defined as the oxidation products of NOx, i.e. NOz = NOy – NOx). This situation is also referred to as a NOx limited regime. Dynamically speaking, the link between NOx, NOz and NOy can be expressed as (Olszina et. al., 1994):

$$NOz = NOy(1-(NOx/NOy))$$

Prior to photooxidation, NOx levels prevailing in the early morning hours as a consequence of traffic emission equal NOy levels (NOz = 0). As time evolves, NOx is being oxidized, to give rise to the NOz oxidation products. Consequently, a NOx limited regime is established. $NO_x$-sensitive regimes are encountered in the rural area as a result of convection, dispersion and diffusion processes. At these rural areas high VOC/NOx ratios prevail in which ozone levels are essentially indifferent to elevation in the VOCs levels and correlate positively with increase in NOx concentrations.

## RESULTS and DISCUSSION

In the following section we present the early morning rush hours' impact (06:00 – 09:00 LST) of the NOx emission from the Tel-Aviv metropolis and Gaza-Strip transportation sources on its subsequent transport and mixing. Similar scenarios were executed for VOCs and CO emissions. Each dispersed particle represents a gram of pollutant as obtained by the coupled transportation-emission models. Fig 5a shows a top view of the state at 07:00 LST, one hour after the traffic emission release. It is apparent that the newly released particles were transported overseas due to easterly land breeze. Two hours later (Fig 5b) with the onset of the Mediterranean sea breeze the pollution cloud initially located oversea is recirulated towards the land, resulting in its mixing with the freshly released gases. Figures 5c – 5f displays the position of the particles at 10:00, 11:00, 13:00 and 15:00 LST. Two main driving forces manifest the NOx spatial and temporal evolution; an east-southeast-directed transport accompanied with a 3D expansion of the NOx cloud, emphasized visually by Fig 6. Figs 6a and 6a illustrate a 3D perspective view from the west at 08:00 and 13:00 LST. The vertical development of the particles clouds from Tel-Aviv metropolis and the Gaza-Strip is well depicted in these Figs. At 10:00 the particles cloud extends up to the height of 200 - 300 m. While at 13:00, with the inland penetration of the particles over the mountain range coupled with the increasing thermal instability, it elevates up to a height of 1500 m.

It is important to reemphasize the above mentioned photochemical aged air mass concept – as time progresses most of the NOx is being photochemically oxidized, so the NOx cloud essentially

represents NOy which correlates positively with ozone levels, the chemical transformations taking place in a NOx limited regime.

Comparing the final stages of the simulation i.e. Fig 5e and 5f to the real time ozone concentrations depicted in Fig 2b, reveals high degree of similarity in time and location between the modeling results of the photochemical aged air mass and the actual ozone levels. This time dependent overlapping fits nicely with the previous findings of the $NOy/O_3$ correlation (Trainer et. Al., 1993, Olszyna et al., 1994, Olszyna et al., 1997).

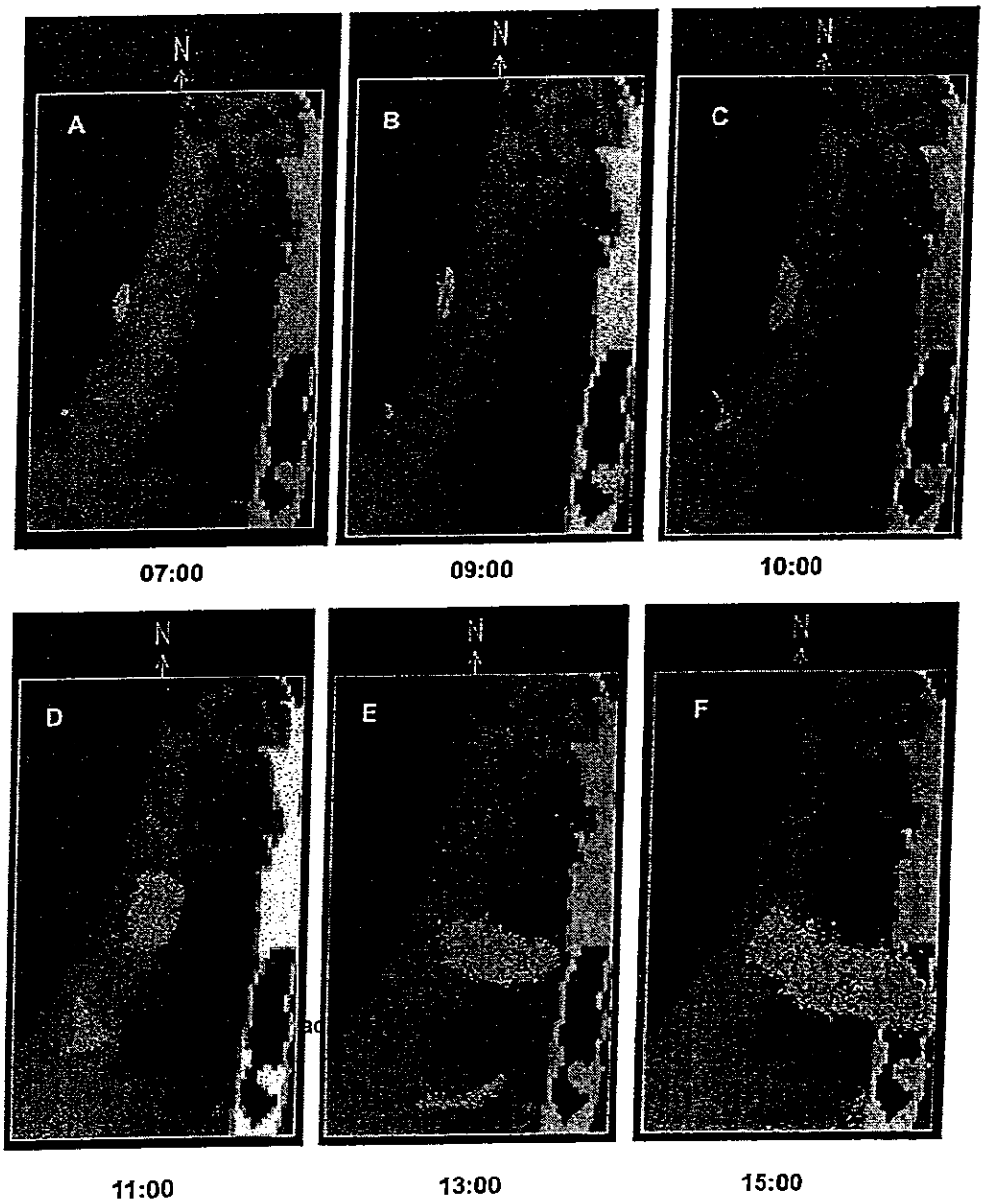


**Figure 5.** Top view of the particles location originating from the Tel-Aviv metropolis and the Gaza-Strip transportation sources for the 28.8.97 ozone epizode.

## CONCLUSION

Air pollution, with ozone generating processes, is among the most significant ecological impacts of the modern age network transportation. The presented work demonstrates the ability of an interdisciplinary modeling systems to collectively operate as a predicting tool/tracing device, capable of successfully simulating ozone formation when transportation emissions are addressed as their

precursor sources. This prediction and analysis tool hopefully will be able to assist in the present and future transportation infrastructure shaping, where air pollution in general - and ozone problems in particular - are to be considered.

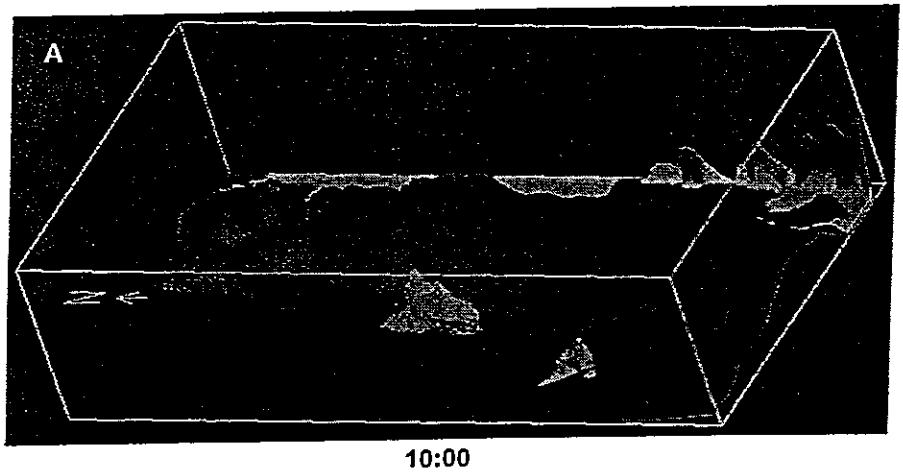


10:00

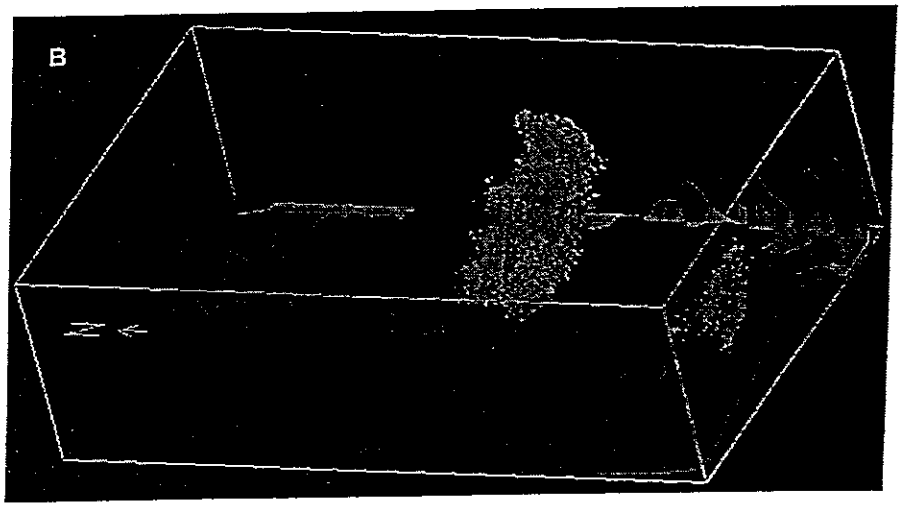


13:00

**Figure 6.** Side view displaying the vertical dimension of the particles locations, calculated for 10:00 and 13:00 LST.

The final stage currently under investigation aims to produce the actual mathematical link between ozone production NOx and VOC levels, solar radiation flux and temperature, to give the final, photochemical link in the transportation to ozone formation scenario.

## ACHNOWLEDGMENTS

This research was partially supported by the Israeli Ministry of Environment. We would like to thank the Rieger Foundation of Santa Barbara, California, for the Rieger-JNF Fellow scholarship in Environmental Studies, which provided additional financial support for the study.

REFERENCES

**Dabdub D., DeHaan L. L. & Seinfeld J. H.** ( 1999 ), *Analysis of ozone in the San Joaquin Valley of California,* Atmospheric Environment, Vol.33, p. 2501 – 2514, 1999.

**Derwent R. G. & Davies T. J.** ( 1994 ), *Modeling the impact of NOx or hydrocarbon control on photochemical ozone in Europe.,* Atmospheric Environment, Vol. 28, p 2039 – 2052, 1994.

**EMME/2 User's Manual, Software release 9** ( 1998 ), INRO CONSULTANTS INC.

**Finlayson-Pitts B. J. & Pitts J. N.** ( 1997 ), *Tropospheric air pollution: Ozone, air born toxics, polycyclic aromatics, hydrocarbons, and particles.,* Science, Vol. 276, 1045 – 1052, 1997.

**Kley D.** ( 1997 ), *Tropospheric chemistry and transport,* Science, Vol. 276, 1043 – 1045, 1997.

**Moussiopoulos N. & Paragrigoriou S.** ( 1997 ), *Athens 2004 air quality.,* Proceedings of international scientific workshop "Athens 2004 air quality", pp. 183, 1997.

**Olszyna K. J., Bailey E. M., Simonaitis R., & Meagher J. F.** ( 1994 ), *$O_3$ and $NO_y$ relationships at a rural site.,* Journal of Geophysical Research, Vol. 99, p. 14,557 – 14,563, 1994.

**Olszyna K. J., Luria M., & Meagher J. F.** ( 1997 ), *The correlation of temperature and rural ozone levels in southeastern U.S.A.,* Atmospheric Environment, Vol. 29, 1997.

**Orlanski I.** ( 1975 ), *A rational subdivision of scales for atmospheric processes.,* Bulletin of American Meteorology Society, Vol. 56, p. 527 – 530, 1975.

**Peleg M., Luria M., Setter I., Perner D., & Russel P.** (1994 ), *Ozone levels in central Israel.,* Israel Journal of Chemistry, Vol. 34, p 375 – 386, 1994.

**Pielke R. A., Cotton W. R., Tremback C. J., Lyons W. A., Grasso L. D., Nicholls M. E., Moran M. D., Wesley D. A., Lee T. J. & Copeland J. H.** ( 1992 ), *A comprehensive meteorological modeling system,* Meteorology and Atmospheric Physics, Vol. 49, p. 69 – 91, 1992.

**Pinilis C., Kassomenos P. & Kallos G.** ( 1993 ), *Modeling of photochemical pollution in Athens, Greece. Application of the RAMS–CALGRID modeling system.,* Atmospheric Environment, Vol. 27B, p.353 – 370, 1993.

**Seinfeld J. H. & Pandis S.** ( 1997 ), *Atmospheric Chemistry and Physics : Air Pollution to Climate.,* John Wiley & Sons pub., pp. 1326, 1997.

**Seinfeld J. H.** ( 1989 ), *Urban air pollution: state of the art.,* Science, 745 – 752, 1989.

Appendix G: Bornstein et al. (2003a,b) and Weinroth (2002) submitted conference abstracts

# MODEL SIMULATIONS OF OZONE FORMATION OVER ISRAEL, THE WEST BANK AND JORDAN

E. Weinroth, A. Ben-Nun[+], C. Emery*, M. Luria[++] and Y. Mahrer

Seagram Center for Soil and Water Sciences Faculty of Agriculture

The Hebrew University Rehovot 76100 Israel

Prepared for Presentation at the 2002 RAMS Modelers Users Workshop

**Abstract** -High ozone levels are regularly reached in the east Mediterranean area during summer periods when air parcels transport the pollution from the populated shore line of Israel inland. A study of the quantitative influence of the different air pollution sources (stationary, mobile) on ozone creation is being conducted in the Hebrew University in Jerusalem. The study includes numerical simulations of the effects of various air pollution sources (industrial, biogenic and transportation) by applying a Regional Atmospheric Modeling System (RAMS) and a Comprehensive Air quality Model with extensions (CAMx).

A detailed emission inventory which includes most important and influencing emission sources in Israel was performed. The simulations were carried out for several periods in the summer of 1997 when airborne measurements of episodes of high ozone levels are available. We compared model with the measurements and found good agreement. We performed several numerical simulations which include only part of the pollution sources in order to determine the individual and synergetic influence of the different sources. Results during several meteorological episodes will be presented and discussed.

[+] G.I.S Laboratory Hebrew University Berman Bldg. Givat-Ram, Jerusalem 91904 Israel

*ENVIRON International Corporation 101 Rowland Way, Suite 220

Novato, CA 94945-5010

++School for Applied Science, Environmental Sciences Division, The Hebrew University, Jerusalem 91904, Israel

# Observations and RAMS/CAMEX Results from the Middle-East Transboundary Pollutant Transport Study

R. Bornstein
San Jose State University
San Jose, CA, USA

M. Luria, Y. Mahrer, M. Peleg, D. Rammar, E. Weinroth
E. Tas, V. Matziev, E. Feitelson, J. Kaplan, U. Dayan
The Hebrew University
Jerusalem, Israel

J. Issac, K. Rishmawi
Applied Research Institute-Jerusalem
Bethlehem, West Bank

J. Safi, Y. El-Nahhal
Environmental Protection & Research Institute
Gaza City, Gaza Strip

The overall aim of this USAID sponsored project is to generate information required by government air quality planning agencies in Israel and West Bank/Gaza to develop strategies for the socially and environmentally sustainable urbanization of their coastal areas. The project research team is composed of experts (from Israel, West Bank/Gaza, and U. S.) in meteorology, atmospheric chemistry, pollutant emissions, land use/GIS, (urban and regional) planning, and socio-economic impacts. Specific results to date include: (1) typical diurnal and monthly variations of environmental data from sites in Gaza, West Bank, and Israel, (2) analysis of field observational campaigns during periods conducive to poor regional air quality that involved measurement of both surface and PBL meteorological and air quality parameters during periods with west to east transboundary effects, and (3) results from the RAMS regional meteorological model, HYPACT Lagrangian particle model, emission models, and CAMX photochemical air quality model.

Results show: (1) typical diurnal and monthly variations of observed atmospheric surface pollutant concentrations with interesting spatial patterns, (2) aircraft observations of elevated high-concentrtion ozone plumes, (3) regional anthropogenic and natural emission patterns, (4) RAMS mesometeorological modeling results of sea breeze flow cases, (5) particle dispersion patterns showing the influence of the inland hills around Jerusalem, and (6) CAMX produced precursor and secondary pollutant plumes at the surface and aloft that agree well with observations.

**Submitted for presentation at the:**
**8th International ASAAQ Conference, 11-13 March 2003, Tsukuba, Japan**



292

# Middle-East Transboundary Pollutant Transport Study: Observations and RAMS/CAMEX Results

R. Bornstein
San Jose State University
San Jose, CA, USA

M. Luria, Y. Mahrer, M. Peleg, D. Rammar, E. Weinroth
E. Tas, V. Matziev, E. Feitelson, J. Kaplan, U. Dayan
The Hebrew University
Jerusalem, Israel

J. Issac, K. Rishmawi
Applied Research Institute-Jerusalem
Bethlehem, West Bank

J. Safi, Y. El-Nahhal
Environmental Protection & Research Institute
Gaza City, Gaza Strip

The overall aim of this USAID sponsored project is to generate information required by government air quality planning agencies in Israel and West Bank/Gaza to develop strategies for the socially and environmentally sustainable urbanization of their coastal areas. The project research team is composed of experts (from Israel, West Bank/Gaza, and U. S.) in meteorology, atmospheric chemistry, pollutant emissions, land use/GIS, (urban and regional) planning, and socio-economic impacts. Specific results to date include: (1) typical diurnal and monthly variations of environmental data from sites in Gaza, West Bank, and Israel, (2) analysis of field observational campaigns during periods conducive to poor regional air quality that involved measurement of both surface and PBL meteorological and air quality parameters during periods with west to east transboundary effects, and (3) results from the RAMS regional meteorological model, HYPACT Lagrangian particle model, emission models, and CAMX photochemical air quality model.

Results show: (1) typical diurnal and monthly variations of observed atmospheric surface pollutant concentrations with interesting spatial patterns, (2) aircraft observations of elevated high-concentration ozone plumes, (3) regional anthropogenic and natural emission patterns, (4) RAMS mesometeorological modeling results of sea breeze flow cases, (5) particle dispersion patterns showing the influence of the inland hills around Jerusalem, and (6) CAMX produced precursor and secondary pollutant plumes at the surface and aloft that agree well with observations.

**Submitted for presentation at the:**
**26th NATO/CCMS/ITM, 26-30 May 2003, Istanbul. Turkey**



293

Appendix H: Bornstein et al. (2001a,b, 2002) preprint volume papers

# Middle-East Transboundary Pollutant Transport Study

**R. Bornstein*, M. Luria+, Y. Mahrer+, M. Peleg+, D. Rammar+, E. Weinroth+, E. Tas+, V. Matziev+, E. Feitelson+, J. Kaplan+, U. Dayan+, J. Issac#, H. Maoh#, M. Ghanayem#, J. Safi0, Y. Einahhal0, A. Bitan^, E. Ben-Dor^, L Benenson^, Setter%, & Y. Levi%**

*San Jose State University, San Jose, CA, USA
+The Hebrew University, Jerusalem, Israel
#Applied Research Institute-Jerusalem, Bethlehem, West Bank
0Environmental Protection & Research Institute, Gaza City, Gaza
^Tel Aviv University, Tel Aviv, Israel
%Israel Meteorological Service, Bet Dagan, Israel*

## 1. Introduction

The overall aim of this USAID sponsored project is to generate information required by government air quality planning agencies in Israel and West Bank/Gaza to develop strategies for the socially and environmentally sustainable urbanization of their coastal areas. The project research team is composed of experts (from Israel, West Bank/Gaza, and U. S.) in meteorology, atmospheric chemistry, pollutant emissions, land use/GIS, (urban and regional) planning, and socio-economic impacts.

Specific research objectives include: (1) Installation of environmental monitoring sites and preparation of a comprehensive environmental database and a regional climatology, (2) Intensive field observational campaigns during periods conducive to poor regional air quality during July 2002, (3) Adaptation and application of the RAMS meteorological model and the CAMx photochemical air quality model to increase understanding of air quality problems.

## 2. Objectives

The overall aim of the proposed effort is to generate the information required by government planning agencies in Israel and West Bank/Gaza to develop strategies for the socially and environmentally sustainable development of their coastal areas. The four main research objectives instrumental to achievement of the above overall aim are (Bornstein et al. 2001)[1]:

### Objective 1: Data Bases

The main objectives of this task are: (1) installation of three new environmental monitoring sites in the Gaza and West Bank and (2) preparation of a comprehensive environmental data base and climatology of the study area.


*Copyright ©2001, ISEH and IAHR*

**Objective 2: Field Studies**

The main objective of this task is the execution of short-term intensive field observational campaigns during meteorological conditions producing poor regional air quality. Such campaigns involve measurement of both meteorological and air quality parameters.

**Objective 3: Modeling Current Conditions**

The main objective of this task is the adaptation and application of appropriate meteorological and air quality model to the study area to increase understanding of air quality problems associated with current levels of regional urbanization. Meteorological, air quality, geographic, and emission data collected to satisfy Objectives 1 and 2 will be used to initialize and evaluate the accuracy of these simulations of current emission patterns. Verification of model results against available meteorological and air quality data will provide confidence limits of the ability of the selected models to carry out the planning simulations using input based on a variety of possible development strategies.

**Objective 4: Modeling Possible Future Conditions**

The main objective of this task is simulation of possible future regional meteorological and air quality patterns using validated models of Objective 3. The models will be applied to a variety of potential urban growth/emission scenarios associated with various urban/industrial development plans supplied by government planning agencies. Results will aid governmental development agencies concerned with regional air quality trends of societal (health and economic) air pollution impacts.

## 3. Accomplishments

**Objective 1: Databases**

**With respect to the new environmental monitoring sites:**

1. Required instruments were selected to be the identical to those used in Israel.
2. Building, exposure, infrastructure, and communications criteria for the three new sites were determined.
3. Three sites fulfilling the above criteria were identified.
4. Instruments were delivered.

**With respect to environmental database and climatology:**

1. The required (for modeling) already processed meteorological, air quality, emissions, and geographic parameters were identified.
2. The required period of data coverage was identified (i.e., planned summer 2002 field study).
3. The locations of the future joint shared databases were determined as the HUJI and ARIJ.
4. Discussions were begun on how to construct the required databases.


*Copyright ©2001, ISEH and IAHR*

**With respect to emission database preparation**

1. The Canadian EMME/2 model was used to estimate the spatial distribution of 1997 and 2000 transportation emissions (Kaplan 1997)[5]. The effort started with GIS distributions of urbanized, industrialized, and roadway areas. These data were then combined with estimates of roadway, population, home, workplace, and fuel usage patterns. Pollutant emission factors were then calculated using observations from concurrent field measurements at highway-tunnel entrances and exits (Tratakovsky et al. 1997)[8] and from California automobile emission factors (Pierson et al. 1996)[7]. Finally, all data sets were input into EMMA/2 to produce both urban-nodal (at urban center points) and highway segment (at midpoint of segment) emission values for an average workday peak activity hour (0800-0900 LST or 0600-0700 UTC). Emission values are thus provided for total organic com-pounds (TOC), carbon monoxide (CO), and nitrogen oxides ($NO_x$) for all points in Israel and the West Bank (Weinroth 2001)[9]. Average vehicle-count data for the latter area were supplied as part of a German sponsored Trilateral Research effort.

2. The first (transportation, stationary, and biogenic) emission inventory for the study area for 1997 was compiled. The first step involved use of the Kaplan transportation data in conjunction with Kleindienst (1992)[6] empirical relationships, derived from chemical chamber measurements. Stationary point-source emissions were tabulated for the following source types: 10 large (electric generators, oil refineries, and cement factories), about 400 medium (factories), and various small (every-thing not in first two categories, and lumped together as area-source emissions). Civilian aircraft takeoff and landing emissions were calculated in a slanted three-dimensional line source along a corridor between Ben Gurion Airport and the Mediterranean coast, where aircraft are above the mixing layer. Area-source biogenic volatile organic compound (VOC) emissions were calculated from GIS vegetation coverage data.

**With respect to climatology**

The report of Dyan (2001)[2] details the following aspects of the air-pollution climatology of the study area: large scale climate forcings, regional air masses, large scale wind and pressure patterns, regional wind flows, seasonal winds, sea-surface, air, and soil temperatures, heat fluxes, relative humidity, and atmospheric stability. The report will be useful in planning various aspects of the proposed field-study measurement programs, e.g., selection of times when different large scale systems should produce ozone episodes at various locations within the study region, locations for the various surface and upper air measurement systems, and the appropriate frequency of the measurements.

**Objective 2: Field Studies**

With respect to the execution of short-term intensive field observational campaigns during periods conducive to the existence of periods with poor regional air quality, the following schedule was originally established and partly carried out:

1. Feb 2000: A successful preliminary field observational study was carried out to estimate the flux of pollutants from Gaza into Israel. This involved deployment of the HUJI mobile laboratory,


*Copyright ©2001, ISEH and IAHR*

equipped with a large variety of in situ surface meteorology and air quality instrumentation, as well as with the remote sensing DOAS system. Results showed that all systems worked properly.

2. June 2000: Another successful similar preliminary field observational study was carried out to estimate the flux of pollutants from Israel into the West Bank. Again the systems worked well.

3. June 2002: The two above preliminary field studies were carried out in preparation for this main study, but additional time will be required to coordinate all the equipment and groups necessary for this larger study. This final campaign will involve measurements of meteorological and air quality parameters by project scientists, as well as by a number of visiting international meteorological and chemical measurement groups who have expressed an interest in joining the study.

**Objective 3: Modeling Current Conditions**

With respect to the adaptation and application of appropriate meteorological and air quality models to the study area to gain an increased understanding of the air quality problems associated with current levels of regional urbanization, the following has been accomplished:

1. The RAMS model was selected as the study meteorological model.
2. The HYPACT Lagrangian particle model was selected to carry out the preliminary air pollutant transport study (Luria et al. 2001)[4].
3. The CAMx photochemical model was selected as the study chemical model.
4. The UAH1D chemical mechanism model was selected to allow for development of new chemical mechanisms tailored for the climate and emission mix of the current study area.
5. Additional state of the art chemical mechanisms developed in Europe have been tested at Stanford (Jacobson 2001). These mechanisms will be inserted into the CAMx photochemical model.
6. The urbanization of MM5, and updating of the PAVE graphics package (based on the NCAR package) and MAPS statistical evaluation package has been carried out at SJSU. The first effort will expand the capabilities of RAMS to better simulate the effects of urban areas on regional flow patters. The latter two packages, supplied by Alpine Geophysics, Inc., will improve the graphical presentation and statistical evaluation opportunities, respectively, for output fields generated by RAMS, CAMX, and HYPACY. MAPS have been expanded under this project, and can now carry out statistical evaluations on arbitrary specified sub-domains. PAVE has likewise been expanded, and is now able to construct vertical cross-sections in arbitrary directions, so that model output can be directly compared to observations.
7.Research scientists at the U.S. EPA Research Triangle Park (RTP), North Carolina re-search center have expressed interest in the application of their new MODELS3 photochemical system to Israel, Gaza, and the West Bank.

**Objective 4: Modeling Possible Future Conditions**

With respect to the final objective, discussions have been carried out with urban planners to identify mechanisms for determination of the emission scenarios to be tested in the models.


*Copyright ©2001, ISEH and IAHR*

## 4. Future Work

### With respect to Objective 1: Data Bases

1. The three monitoring sites will be prepared (i.e., with respect to security, power supply, communications, etc.) for the installation of the instruments.
2. The instruments will be made operational and installed at the three West Bank/ Gaza sites.
3. Meteorological, air quality, emissions, and geographic data required for modeling will continue to be collected.
4. Construction of databases at HUJI and ARIJ will continue.

### With respect to Objective 2: Field Studies

With respect to the execution of short-term intensive field observational campaigns during periods conducive to the existence of poor regional air quality, during June 2002 measurements of the regional transboundary pollutant fluxes will be made. This (final) campaign will involve measurement of both meteorological and air quality parameters by project scientists and students.

### With respect to Objective 3: Modeling Current Conditions

With respect to the adaptation and application of appropriate meteorological and air quality models to the study area to increase understanding of air quality problems associated with current levels of regional urbanization, the following will continue:

1. RAMS meteorological model will be used to simulate additional flow cases
2. HYPACT Lagrangian particle model will be used to simulate additional transport patterns
3. CAMX photochemical model will be tested using output from the above RAMS simulations, a regional first
4. UAH1D chemical mechanism model will be tested, with new routines (appropriate for local climate and emission mixes) developed as needed
5. chemical mechanisms used at Stanford University (Liang and Jacobson 2000)[3] will be tested in the CAMx photochemical model
6. SJSU/Alpine Geophysics urbanization, PAVE graphics, and MAPS statistical evaluation packages will be used to improve the graphical presentation and statistical evaluation capabilities for output from the RAMS, CAMx, and HYPACY models
7. new U.S. EPA MODELS3 photochemical system will be made available via collaboration with the EPA RTP Lab.

### With respect to Objective 4: Modeling Possible Future Conditions

With respect to the simulation of possible future regional meteorological and air quality patterns using the validated models of Objective 3, the following will be done:


*Copyright ©2001, ISEH and IAHR*

1. discussions will continue with transportation planners to identify various possible future regional emission scenarios to be tested in the models during the final project phase
2. planning simulations will study environmental impacts from projected populations during the years 2010 and 2020 (when the regional population will have doubled from its present value).

## 5. References


1. Bornstein, R., et al., 2001: Transbounmdry air-quality effects from urbanization. SJSU report to USAID, 215 pp.

2. Dayan, U., 2001: Air pollution meteorolgy in Israel. Unpublished HUJI report.

3. Liang, J., and M. Jacobson, 2000: Comparison of a 4000-reaction chemical mechanism with the Carbon Bond IV and an adjusted Carbon Bond IV-EX mechanism. Atmos. Environ., 34, 3015-3026.

4. Luria, M., Mahrer, Y., Peleg, M., Rammar, D., Tas, E., Matziev, V., Feitelson, E., Kaplan, J., and Dayan, U., 2001: The impact of coastal transportation emissions on inland air pollution over Israel. Submitted to *Atmos. Environ.*

5. Kaplan J., 1997: Model Structure and Data Requirements. Working Paper for the Trilateral Research Project on GIS Tools for Sustainable Transport in Palestine and Israel.

6. Kleindienst T., et al., 1992:. The Photo-oxidation of automobile emissions -- measurements of the transformation products and their mutagenic activity. *Atmos. Environ.*, **26**, 3039-3053

7. Pierson W., et al., 1996: Real world automobile emissions – Summery of studies in Fort Mc-Henry tunnel. *Atmos. Environ.*, **30**, 2233-2256.

8. Tratakovsky L., et al., 1997:. Estimation of vehicles emission factors in Israel, *Research report – Technion Israel Institute of Technology, Transportation research Institute,* 87 pp.

9. Weinroth, E., 2001: Emission inventory for Israel. Unpublished HUJI report.




*Copyright ©2001, ISEH and IAHR*

6.2

# MIDDLE-EAST TRANSBOUNDARY POLLUTANT TRANSPORT PROJECT

R. Bornstein*, M. Luria+, Y. Mahrer+, M. Peleg+, D. Rammar+, E. Weinroth+, E. Tas+, V. Matziev+, E. Feitelson+, J. Kaplan+, U. Dayan+, J. Issac#, H. Maoh#, M. Ghanayem#, J. Safi0, Y. Einahhal0, A. Bitan^, E. Ben-Dor^, I. Benenson^, Setter%, Y. Levi%

*San Jose State University, San Jose, CA, USA
+The Hebrew University, Jerusalem, Israel
#Applied Research Institute-Jerusalem, Bethlehem, West Bank
0Environmental Protection & Research Institute, Gaza City, Gaza Strip
^Tel Aviv University, Tel Aviv, Israel
%Israel Meteorological Service, Bet Dagan, Israel

## 1. INTRODUCTION

The aim is to generate information required by agencies in Israel and West Bank/Gaza to develop strategies for sustainable development of their coastal areas. The 4 main objectives to achieve the above overall aim are:

### A. Objective 1: Data Bases

The main objectives include: (1) installation of 3 monitoring sites in the Gaza and West Bank and (2) preparation of a comprehensive environmental data base and climatology.

### B. Objective 2: Field Studies

The main objective is execution of short-term intensive observational campaigns during meteorological conditions producing poor regional air quality. Such campaigns involve measurement of both meteorological and air quality parameters.

### C. Objective 3: Modeling Current Conditions

This objective is adaptation and application of appropriate meteorological and air quality models to increase understanding of air quality problems associated with current levels of regional urbanization. Meteorological, air quality, geographic, and emission data collected to satisfy Objectives 1 and 2 will be used to initialize and evaluate the accuracy of these simulations of current emission patterns. Verification of model results against available meteorologyical and air quality data will provide model confidence limits using inputs for a variety of development strategies.

### D. Objective 4: Modeling Future Conditions

The main objective is simulation of possible future regional meteorological and air quality patterns by use of validated models. Models will be applied to a variety of potential growth and emission scenarios associated with various urban/industrial development plans.

* *Corresponding author address:* Robert Bornstein, Department of Meteorology, San Jose State University, San Jose, CA 95192, 408.924.5205, e-mail: pblmodel@hotmail.com

Preprint Vol., 12th Joint AMS/AWMA Joint Conf. on the Applications of Air Pollution Meteorology
20-24 May 2002, Norfolk, VA

## 2. ACCOMPLISHMENTS

### A. Objective 1: Data Bases

**> Environmental monitoring sites**

> Required instruments selected as identical to those used in Israel
> Building, exposure, infrastructure, and communications criteria for new sites determined
> Three sites fulfilling above criteria identified
> Instruments delivered.

**> Environmental data Bases**

> Required meteorological, air quality, emission, and geographic parameters identified
> Required period of data coverage identified (i.e., planned Spring/Summer 2002 field studies)
> Locations of future joint shared data bases determined as HUJI and ARIJ
> Discussions begun on how to construct data-bases.

**> Emissions database**

> EMME/2 (1998) model used to estimate spatial distribution of 1997 and 2000 transportation emissions (Kaplan 1997). Effort started with GIS distributions of urbanized, industrialized, and roadway areas. Data combined with estimates of roadway, population, home, work-place, and fuel usage patterns. Pollutant emission factors calculated from concurrent field measurements at highway-tunnel entrances and exits (Tratakovsky et al. 1997) and from California automobile emission factors (Pierson et al. 1996). Data input into EMMA/2 to produce urban-nodal and highway segment values for workday peak-activity hour (0800-0900 LST or 0600-0700 UTC). Emission values provided for total TOC, CO, and $NO_x$ for Israel and West Bank. Average vehicle-count data for the latter area supplied from German sponsored Trilateral effort.
> First (transportation, stationary, and biogenic) emission inventory for study area for 1997 compiled. First step involved Kaplan transportation data in conjunction with Kleindienst (1992) relationships (from chemical chamber measurements). Stationary point-source emissions tabulated for following source types: 10 large (electric generators, oil refineries, and cement factories), 400 factories, & various small (everything not in first 2 categories) lumped area-sources. Civilian aircraft takeoff and landing emissions calculated in slanted line-source in corridor between Ben Gurion Airport and Mediterranean coast, where air-

301

craft are above the PBL. Area-source biogenic VOC emissions calculated from GIS vegetation data.

> **Climatology**

Dyan (2001) details aspects of the air-pollution climatology of study area: large scale climate forcings, air masses, synoptic wind and pressure patterns, regional wind flows, seasonal winds, sea surface, air, and soil temperatures, heat fluxes, relative humidity, and atmospheric stability. This will be useful in planning the field programs, e.g., times when large scale systems produce ozone episodes within the region, locations for the surface and up-per air measurement systems, and measurement frequency.

### B. Objective 2: Field Studies

With respect to the short-term field campaigns during periods conducive to poor regional air quality, the following schedule was established and partly carried out:
> Feb 2000: A successful preliminary field observational study was carried out to estimate the flux of pollutants from Gaza into Israel. This involved deployment of the HUJI mobile laboratory, equipped with a large variety of in situ surface meteorology and air quality instrumentation, as well as with a DOAS system.
> June 2000: Another successful similar preliminary field observational study was carried out to estimate the flux of pollutants from Israel to the West Bank.
> June 2002: The two preliminary field studies were carried out in preparation for this study, but additional time is required to coordinate for this larger study. This campaign will involve measurements of meteorological and air quality parameters by project scientists and a visiting international measurement groups.

### C. Objective 3: Modeling Current Conditions

With respect to adaptation and application of appropriate models to gain increased understanding of air quality problems associated with current levels of urbanization, the following has been accomplished:
> The RAMS model was selected as the meteorological model for the study.
> The HYPACT Lagrangian particle model was selected to carry out preliminary air pollutant transport studies.
> The CAMx photochemical model was selected for the study.
> The UAH1D chemical mechanism model was selected to allow for development of new chemical mechanisms tailored for the study area.
> Additional chemical mechanisms developed in Europe have been tested at Stanford (Jacobson, 2001) and will be inserted into CAMx.
> Urbanization of MM5, and updating the PAVE graphics package (based on NCAR package) and MAPS statistical evaluation package has been carried out at SJSU. The first effort will allow RAMS to better simulate urban areas. The latter two packages (from Alpine Geophysics, Inc.) will improve graphical presentation and statistical evaluation opportunities. MAPS has been expanded to do statistical evaluations on arbitrary specified sub-domains and PAVE can now construct arbitrary vertical cross-sections.

### D. Objective 4: Modeling Future Conditions

With respect to the final objective, discussions have been carried out with planners to identify mechanisms for determination of emission scenarios to be tested in the models.

## 4. FUTURE WORK

### A. Objective 1: Data Bases

> The 3 monitoring sites will be prepared (i.e., security, power supply, communications, etc.) for the instruments
> Instruments will be made operational at the 3 sites
> Meteorological, air quality, emissions, and geographic data required for modeling will continue to be collected
> Construction of databases at HUJI and ARIJ continues.

### B. Objective 2: Field Studies

Field observational campaigns will be carried out during May-August 2003, with measurements made of regional transboundary pollutant fluxes. This final campaign will involve meteorological and air quality parameters.

### C. Objective 3: Modeling Current Conditions

With respect to the adaptation and application of appropriate meteorological and air quality models to the study area to increase understanding of air quality problems associated with current levels of regional urbanization, the following will continue:
> RAMS meteorological model will simulate additional flow cases
> HYPACT Lagrangian particle model will simulate additional transport patterns
> CAMX photochemical model will be tested using output from the above RAMS simulations, a regional first
> UAH1D chemical mechanism model will be tested, with new routines (appropriate for local climate and emission mixes)
> Chemical mechanisms from Stanford University will be tested in the CAMX photochemical model.
> SJSU/Alpine Geophysics urbanization, PAVE graphics, and MAPS statistical evaluation packages will improve the graphical presentation and statistical evaluation capabilities for RAMS, CAMX, and HYPACT model outputs

### D. Objective 4: Modeling Future Conditions

With respect to the simulation of possible future regional meteorological and air quality patterns using the validated models of Objective 3, the following will be done:
> Discussions will continue with transportation planners to identify possible future regional emission scenarios to be modeled during the final project phase
> Planning simulations will study environmental impacts from projected population conditions during 2010 & 2020 (when regional populations will have doubled)

Preprint Volume
Second Air Quality Management Symposium
Istanbul, Turkey, Sept. 2001

# PRELIMINARY RESULTS FROM THE MIDDLE-EAST TRANSBOUNDARY POLLUTANT TRANSPORT STUDY

**R. Bornstein*, M. Luria[+], Y. Mahrer[+], M. Peleg[+], D. Rammar[+], E. Weinroth[+], E. Tas[+], V. Matziev[+], E. Feitelson[+], J. Kaplan[+], U. Dayan[+], J. Issac[#], H. Maoh[#], M. Ghanayem[#], J. Safi[0], Y. Einabhal[0], A. Bitan^, E. Ben-Dor^, I. Benenson^, Setter[%], Y. Levi[%]**

*San Jose State University, San Jose, CA, USA
[+]The Hebrew University, Jerusalem, Israel
[#]Applied Research Institute-Jerusalem, Bethlehem, West Bank
[0]Environmental Protection & Research Institute, Gaza City, Gaza Strip
^Tel Aviv University, Tel Aviv, Israel
[%]Israel Meteorological Service, Bet Dagan, Israel

## ABSTRACT

The overall aim of this USAID sponsored project is to generate information required by government air quality planning agencies in Israel and West Bank/Gaza to develop strategies for the socially and environmentally sustainable urbanization of their coastal areas. The project re-search team is composed of experts (from Israel, West Bank/Gaza, and U. S.) in meteorology, atmospheric chemistry, pollutant emissions, land use/GIS, (urban and regional) planning, and socio-economic impacts. Specific research objectives include: (1) Installation of environmental monitoring sites and preparation of a comprehensive environmental database and a regional climatology, (2) Intensive field observational campaigns during periods conducive to poor regional air quality, (3) Adaptation and application of the RAMS meteorological model and the CAMx photochemical air quality model to increase understanding of air quality problems. Preliminary results are presented in this paper, while the field campaign is scheduled for July 2001.

**Key Words: Transboundary Transport, Middle East, Ozone, USAID**

## 1. OBJECTIVES

The overall aim of the proposed effort is to generate the information required by government planning agencies in Israel and West Bank/Gaza to develop strategies for the socially and environ-mentally sustainable development of their coastal areas. The four main research objectives instrumental to achievement of the above overall aim are:

### A. Objective 1: Data Bases

The main objectives of this task are: (1) installation of three new environmental monitoring sites in the Gaza and West Bank and (2) preparation of a comprehensive environmental data base and climatology of the study area.

### B. Objective 2: Field Studies

The main objective of this task is the execution of short-term intensive field observational campaigns during meteorological conditions producing poor regional air quality. Such campaigns involve measurement of both meteorological and air quality parameters.

### C. Objective 3: Modeling Current Conditions

The main objective of this task is the adaptation and application of appropriate meteorological and air quality model to the study area to increase understanding of air quality problems associated with current levels of regional urbanization. Meteorological, air quality, geographic, and emission data collected to satisfy Objectives 1 and 2 will be used to initialize and evaluate the accuracy of these simulations of current emission patterns. Verification of model results against available meteorological and air quality data will provide confidence limits of the ability of the selected models to carry out the planning simulations using input based on a variety of possible development strategies.

### D. Objective 4: Modeling Possible Future Conditions

The main objective of this task is simulation of possible future regional meteorological and air quality patterns using validated models of Objective 3. The models will be applied to a variety of potential urban growth and emission scenarios associated with various urban/industrial development plans supplied by government planning agencies. Results will aid governmental development agencies concerned with regional air quality trends of societal (health and economic) air pollution impacts.

## 2. Accomplishments

### A. Objective 1: Data Bases

#### a. With respect to the new environmental monitoring sites:

1. Required instruments were selected to be the identical to those in Israel
2. Building, exposure, infrastructure, and communications criteria for the three new sites were determined
3. Three sites fulfilling the above criteria were identified
4. Instruments were delivered.

#### b. With respect to environmental database and climatology:

1. The required (for modeling) (already processed) meteorological, air quality, emissions, and geographic parameters were identified
2. The required period of data coverage was identified (i.e., planned Summer 2002 field study)
3. The locations of the future joint shared data bases were determined as the HUJI and ARIJ

4. Discussions were begun on how to construct the required databases.

**c. With respect to emission database preparation**

1. The Canadian EMME/2 (1998) model was used to estimate the spatial distribution of 1997 and 2000 transportation emissions (Kaplan 1997). The effort started with GIS distributions of urbanized, industrialized, and roadway areas. These data were then combined with estimates of roadway, population, home, workplace, and fuel usage patterns. Pollutant emission factors were then calculated using observations from concurrent field measurements at highway-tunnel entrances and exits (Tratakovsky et al. 1997) and from California automobile emission factors (Pierson et al. 1996). Finally, all data sets were input into EMMA/2 to produce both urban-nodal (at urban center points) and highway segment (at midpoint of segment) emission values for an average workday peak-activity hour (0800-0900 LST or 0600-0700 UTC). Emission values are thus provided for total organic compounds (TOC), carbon monoxide (CO), and nitrogen oxides ($NO_x$) for all points in Israel and the West Bank. Average vehicle-count data for the latter area were supplied as part of a German sponsored Trilateral Research effort.

2. The first (transportation, stationary, and biogenic) emission inventory for the study area for 1997 was compiled. The first step involved use of the Kaplan transportation data in conjunction with Kleindienst (1992) empirical relationships, derived from chemical chamber measurements. Stationary point-source emissions were tabulated for the following source types: 10 large (electric generators, oil refineries, and cement factories), about 400 medium (factories), and various small (everything not in first two categories, and lumped together as area-source emissions). Civilian aircraft takeoff and landing emissions were calculated in a slanted three-dimensional line source along a corridor between Ben Gurion Airport and the Mediterranean coast, where aircraft are above the mixing layer. Area-source biogenic volatile organic compound (VOC) emissions were calculated from GIS vegetation coverage data.

**d. With respect to climatology**

Dyan (2001) produced a report that details the following aspects of the air-pollution climatology of the study area: large scale climate forcings, regional air masses, large scale wind and pressure patterns, regional wind flows, seasonal winds, sea-surface, air, and soil temperatures, heat fluxes, relative humidity, and atmospheric stability. The report will be useful in planning various aspects of the proposed field-study measurement programs, e.g., selection of times when different large scale systems should produce ozone episodes at various locations within the study region, locations for the various surface and upper air measurement systems, and the appropriate frequency of the measurements.

**B. Objective 2: Field Studies**

With respect to the execution of short-term intensive field observational campaigns during periods conducive to the existence of periods with poor regional air quality, the following schedule was originally established and partly carried out:

1. Feb 2000: A successful preliminary field observational study was carried out to estimate the flux of pollutants from Gaza into Israel. This involved deployment of the HUJI mobile lab-oratory,

equipped with a large variety of in situ surface meteorology and air quality instrumentation, as well as with the remote sensing DOAS system. Results showed that all systems worked properly.

2. June 2000: Another successful similar preliminary field observational study was carried out to estimate the flux of pollutants from Israel into the West Bank. Again the systems worked well.

3. June 2002: The two above preliminary field studies were carried out in preparation for this main study, but additional time will be required to coordinate all the equipment and groups necessary for this larger study. This final campaign will involve measurements of meteorological and air quality parameters by project scientists, as well as by a number of visiting international meteorological and chemical measurement groups who have expressed an interest in joining the study.

**C. Objective 3: Modeling Current Conditions**

With respect to the adaptation and application of appropriate meteorological and air quality models to the study area to gain an increased understanding of the air quality problems associated with current levels of regional urbanization, the following has been accomplished:

1.The RAMS model was selected as the meteorological model to be used in the study.

2.The HYPACT Lagrangian particle model was selected to carry out the preliminary air pollutant transport study.

3.The CAMx photochemical model was selected as the chemical model to be used in the study.

4. The UAH1D chemical mechanism model was selected to allow for development of new chemical mechanisms tailored for the climate and emission mix of the current study area.

5.Additional state of the art chemical mechanisms developed in Europe have been tested at Stanford (Jacobson, 2001). These mechanisms will be inserted into the CAMX photochemical model.

6.The urbanization of MM5, and updating of the PAVE graphics package (based on the NCAR package) and MAPS statistical evaluation package has been carried out at SJSU. The first effort will expand the capabilities of RAMS to better simulate the effects of urban areas on regional flow patters. The latter two packages, supplied by Alpine Geophysics, Inc., will improve the graphical presentation and statistical evaluation opportunities, respectively, for output fields generated by RAMS, CAMX, and HYPACY. MAPS has been expanded under this project, and can now carry out statistical evaluations on arbitrary specified sub-domains. PAVE has likewise been expanded, and is now able to construct vertical cross-sections in arbitrary directions, so that model output can be directly compared to observations.

7.Research scientists at the U.S. EPA Research Triangle Park (RTP), North Carolina re-search center have expressed interest in the application of their new MODELS3 photochemical system to Israel, Gaza, and the West Bank.

### D. Objective 4: Modeling Possible Future Conditions

With respect to the final objective, discussions have been carried out with urban planners to identify mechanisms for determination of the emission scenarios to be tested in the models.

## 4.FUTURE WORK

### A. With respect to Objective 1: Data Bases

1.The three monitoring sites will be prepared (i.e., with respect to security, power supply, communications, etc.) for the installation of the instruments

3.The instruments will be made operational and installed at the three West Bank/ Gaza

4.Meteorological, air quality, emissions, and geographic data required for modeling will continue to be collected

5.Construction of databases at HUJI and ARIJ will continue.

### B. With respect to Objective 2: Field Studies

With respect to the execution of short-term intensive field observational campaigns during periods conducive to the existence of poor regional air quality, during June 2002 measurements of the regional transboundary pollutant fluxes will be made. This (final) campaign will involve measurement of both meteorological and air quality parameters by project scientists and students.

### C. With respect to Objective 3: Modeling Current Conditions

With respect to the adaptation and application of appropriate meteorological and air quality models to the study area to increase understanding of air quality problems associated with current levels of regional urbanization, the following will continue:

1. the RAMS meteorological model will be used to simulate additional flow cases

2.the HYPACT Lagrangian particle model will be used to simulate additional transport patterns

3.the CAMX photochemical model will be tested using output from the above RAMS simulations, a regional first

4.the UAH1D chemical mechanism model will be tested, with new routines (appropriate for local climate and emission mixes) developed as needed

5.the chemical mechanisms used at Stanford University will be tested in the CAMX photochemical model.

6. the SJSU/Alpine Geophysics urbanization, PAVE graphics, and MAPS statistical evaluation packages will be used to improve the graphical presentation and statistical evaluation capabilities for outputs from the RAMS, CAMX, and HYPACY models

7. the new U.S. EPA MODELS3 photochemical system will be made available via collaboration with the EPA RTP Lab

**D. With respect to Objective 4: Modeling Possible Future Conditions**

With respect to the simulation of possible future regional meteorological and air quality pat-terns using the validated models of Objective 3, the following will be done:

1.discussions will continue with transportation planners to identify various possible future regional emission scenarios to be tested in the models during the final project phase

2. the planning simulations will study the environmental impacts from projected population conditions during the years 2010 and 2020 (when the regional population will have doubled from its present value).